AN EXPERIMENTAL AND THEORETICAL STUDY OF THE FLOW ABOUT SPHERES AND DISCS ROTATING SLOWLY IN VISCOELASTIC FLUIDS

by

EUGENE KENNETH CAIRNCROSS

Submitted in fulfilment of the requirements
for the degree of
Doctor of Philosophy
of the
University of Cape Town
September 1974

ABSTRACT

An analysis of the flow about a sphere rotating slowly in a Rivlin-Ericksen fluid contained in a stationary outer concentric sphere is presented. An application of the conformal mapping technique is proposed. The technique is used to obtain the radial and axial velocity components for the flow about a disc rotating within an outer oblate spheroidal shell from the solution to the corresponding problem of the flow about a sphere rotating within an outer spherical shell. The results are compared with an existing rigorous analysis for a disc rotating in an infinite sea of the Third Order fluid. They are also used to estimate wall effects in experimental situations.

Tangential and radial velocity profiles are measured for the flow about a sphere rotating slowly in a Newtonian liquid. Velocities are determined from enlarged streak photographs of aluminium particles moving in a collimated 'sheet' of light, at several planes throughout the flow field. Similar velocity profiles are measured for the flow of a 1,50% Natrosol 250 H solution about two spheres of different diameters rotating in tanks with different dimensions. A set of velocity distributions is also measured for a sphere rotating in a 0,9% Natrosol 250 H solution; a dye tracer study of the flow about a sphere rotating in this liquid is presented as well.

Velocity profiles are presented for the flow of the 1,50% Natrosol solution about a rotating disc and the flow of the 0,9% solution about a second rotating disc of different diameter. Both Natrosol solutions exhibited viscoelastic behaviour in all cases. The Newtonian

fluid study is at a Reynolds number of 1,2; all visco-elastic fluid studies are within the range of Reynolds numbers of 0,05 to 1,24.

The zero shear viscosities of the Natrosol solutions are measured using the falling sphere method. The non-Newtonian material parameters are obtained by fitting the theoretical curves to the measured velocity data. The values of the elastic and shear thinning parameters for the two fluids obtained in the different geometrical and dynamical systems are compared.

ACKNOWLEDGEMENTS

The author wishes to express his gratitude to Dr G.S. Hansford for his help and encouragement during the course of this work.

The author expresses his thanks to Mr K. Wheeler and his assistants, who constructed various pieces of equipment.

It would be impossible to acknowledge the assistance of all those who assisted the author in the final production of this work individually. However, the operating staff at the Computer Centre deserve particular mention. The author is also particularly grateful to Lynette Penning, who interpreted his scrawl and typed the greater part of this thesis, including all the equations, an unenviable task indeed.

Finally, I must acknowledge the many who encouraged and motivated me during the course of this work. I am particularly grateful to my immediate family and friends, who silently chided me whenever my purpose appeared to be dulled.

TABLE OF CONTENTS

TABLE OF FIGURES

INTRODUCTION

An important element in the recent history of the study of non-Newtonian liquids is the search for a constitutive equation which provides a quantitative description of at least some real viscoelastic liquids. Ideally, a successful rheological model would also be relatively simple, contain few material constants and provide a good description of real liquid behaviour for a wide range of flow conditions once these parameters have been determined experimentally. It is important, for practical purposes, that these material parameters be obtainable through the use of one or more well defined experimental procedures [1].

In contrast to the case of Newtonian fluids which satisfy all these conditions to a good degree of approximation, it seems unlikely that a constitutive equation for viscoelastic fluids will be found which is both relatively simple and widely applicable. Thus it is that the usefulness of constitutive equations has to be explored in highly restrictive flow situations. (Pipkin has reviewed the narrow range approximations commonly resorted to [2]). While the principle value of such theoretical and experimental studies lies in their contribution to our understanding of the fundamental nature of viscoelastic liquids, they may well have immediate practical value. The study of the slow flow about discs and spheres in viscoelastic liquids has, for example, provided useful information on the power requirements for mixing these liquids [3] and the effect of their elastic properties on the behaviour of polymerization reactors [4].

A great many equations of state for viscoelastic liquids have been proposed since Oldroyd's pioneering work on the correct formulation of constitutive equations was

published in 1950 [5]. (Historical accounts of the theory and development of constitutive equations are to be found in [6], [7] and [8]). As an immediate test of suitability, these rheological models were analysed in viscometric flow situations in order to evaluate their ability to predict, at least qualitatively, certain well known characteristics of real viscoelastic liquids, such as the Weissenberg effect and shear thinning behaviour. Examples of this approach are the earlier works of Oldroyd [5, 9, 10] and Walters [11].

[The concept of viscometric flows is discussed precisely and rigorously in [7] and [8]. This class of flows includes simple shearing flow, Poiseville flow, torsional flow, Couette flow, cone and plate flow and helical flow. An important sub-class is that of simple viscometric flows [7], characterised by a velocity field whose contravariant components have the form

$$x^1 = 0, \quad x^2 = v(x^1), \quad x^3 = 0$$

in some orthogonal co-ordinate system. Simple viscometric flows have been studied extensively, and are essentially the types of flow present in the majority of viscometers in common usage. Examples are found in [7] and [8], and Truesdell [12] has recently reviewed the subject.]

The next logical step was the construction of suitable experimental devices designed to obtain quantitative data in viscometric flow situations with which the theoretical predictions of the various models could be compared. The theoretical predictions of several Oldroyd-type rheological models were in qualitative agreement [6, 7] with the early experimental work of Oldroyd, Roberts, Toms and others [13, 14, 15]. However, the predicted flow curves were unable to describe the experimental data quantitatively and consequently more complex rheological models were

proposed. (A recent example is that of David [16]). In a parallel development, increasingly sophisticated measuring instruments were constructed to provide more reliable data. Tanner [17], Bogue and Doughty [18], Spriggs et al [19] and Chen and Bogue [20] have reviewed a number of constitutive equations for viscoelastic fluids, with particular reference to their quantitative behaviour in viscometric type flows. The comparatively recent discovery and analysis of problems such as the 'hole effect' [21, 22, 23] and the recent development of instruments employing nearly viscometric flows [24 - 32] testify to the complexity of the problem of obtaining accurate and unambiguous data for viscoelastic liquids.

Beyond the need for a theory able to describe viscometric flow data for viscoelastic liquids adequately lies the problem as to whether that theory is also able to describe non-viscometric flows with some precision. The class of viscometric flow is a highly limited one. It has been shown [8, 33] that viscometric flow behaviour can be completely characterised by three material functions: a viscosity function and two normal stress difference functions. In non-viscometric flows, material functions in addition to the viscometric functions are, in general, required to describe viscoelastic fluid behaviour. Thus the comparison of non-viscometric flow data with available theoretical analyses of such flows is a more demanding test of the suitability of specific constitutive equations. There is a distinct paucity of such quantitative comparisons. The work reported in this thesis is, in large measure, an attempt to provide such non-viscometric flow data and to evaluate the ability of a rather general type of fluid, the Third Order fluid of Coleman and Noll [34]to describe the data. The Rivlin-Eriksen fluid [35]is equivalent in the slow flow situation under consideration.

These introductory remarks would be incomplete without a further mention of the theory of the Simple Fluid or Memory Fluid of Coleman and Noll [34, 35], if only to clarify the terms 'Second Order' and 'Third Order Fluid' used so frequently in the literature review (Section 1A). The Simple Fluid is defined as a continuous material for which the stress at any material point is a functional of the history of the deformation gradient at that point. This formulation is too general for practical use. In practice the functional is approximated by a converging series of multiple integrals or by an expansion in terms of the Rivlin-Ericksen tensors. The above concepts are presented rigorously and more explicitly in [34, 2, 37]. It is sufficient for our purposes to state that the first order approximation to the memory functional yields the Newtonian fluid, defined by the equation

$$T = pI + \alpha_1 A^{(1)};$$

the second order approximation gives the equation for the Second Order fluid:

$$T = -pI + \alpha_1 A^{(1)} + \alpha_2 A^{(2)} + \alpha_3 A^{(1)2};$$

and the Third Order fluid is defined by the equation

$$T = -pI + \alpha_1 A^{(1)} + \alpha_2 A^{(2)} + \alpha_3 A^{(1)2} + \alpha_4 A^{(3)} + \alpha_5 (A^{(1)} A^{(2)} + A^{(2)} A^{(1)}) + \beta_1 (\mathrm{tr} A^{(1)2}) A^{(1)},$$

where T is the stress tensor, p an isotropic pressure, the α_i and β_j are constants and $A^{(1)}$ and $A^{(2)}$ are the first and second Rivlin-Ericksen tensors respectively [12]. The Second Order fluid exhibits non-zero normal stress differences and a constant viscosity in simple shear, whereas the Third Order fluid exhibits both non-zero normal stress differences and a shear dependent viscosity behaviour [12].

The theory of the Simple Fluid has had a tremendous impact on the literature on continuum rheology. An historical perspective of the importance of this theory and its relation to the earlier theories of Oldroyd [5] and Rivlin and Ericksen [36] may be obtained from the review article by Walters [6] and the more recent paper of Stark and Lodge [38].

Chapter 1 of this thesis is a review of relevant theoretical and experimental non-viscometric flow studies. The principle theoretical expositions are contained in Chapter 2. Walters and Waters' analysis of a sphere rotating slowly in an infinite sea of Rivlin-Ericksen fluid [39] was modified by replacing the 'infinite sea' boundary condition with an outer concentric sphere of finite radius. The main purpose of this modification was to estimate the influence of 'wall effects' on measured velocity profiles. The Waters and King [40] analysis of a spheroid rotating slowly in a Third Order fluid is reiterated in brief. The corresponding rotating disc problem is obtainable as a special case of the spheroid. The expression for the stream function obtained by these authors is differentiated in order to give velocity profiles for the rotating disc. A novel application of the conformal mapping technique is also proposed. Using this technique, velocity profiles for a disc rotating within an outer oblate spheroidal shell are obtained from the corresponding problem of a sphere rotating within a concentric spherical outer shell. These velocity profiles are compared with those of the more rigorous analysis of Waters and King.

Chapter 3 contains a description of experimental apparatus used and of experimental procedures adopted. Comprehensive experimental velocity profiles for spheres

and discs rotating in two viscoelastic liquids are presented in Chapter 4. The theoretical curves predicted by the analyses of the flow of the Third Order fluid were compared with the velocity data. The material constants obtained in the different geometries are compared. Chapter 5 contains a discussion of the results presented in Chapter 4 as well as the conclusions and recommendations which flow from this work.

CHAPTER 1

REVIEW OF PREVIOUS WORK

1A REVIEW OF THEORETICAL STUDIES OF FLOWS ABOUT ROTATING DISCS AND SPHERES IN VISCOELASTIC LIQUIDS

Hill [41] and more recently Ide and White [4] have published extensive reviews of laminar flows about rotating bodies. Attention will here be restricted to steady flows about discs and spheres rotating in viscoelastic liquids.

1A.1 Rotating Sphere Studies

Langlois [42] analysed the steady flow of a slightly viscoelastic fluid contained between rotating spheres. This author used perturbation analysis to calculate the disturbance of the Newtonian flow field caused by the viscoelasticity of the fluid. He found that for certain values of the non-Newtonian parameters, a reversal of the secondary flow in a plane through the axis of rotation could occur. However, the validity of this analysis is confined to slightly viscoelastic fluids, since the perturbation quantity used was a tensor polymonial in the Rivlin-Ericksen tensors. The analysis is also restricted by the assumption of negligible inertial forces.

Geisekus [43] investigated the flow around a sphere which was in simultaneous translational and rotational motion, with a common axis of symmetry, in an infinite sea of a Third Order viscoelastic fluid. Expressions for the velocities and the couple on a sphere in pure rotation could be obtained as a special case, but again the analysis is restricted by the assumption of negligible inertial forces. In a subsequent publication [44], Geisekus

considered the case of a sphere rotating in a Second Order viscoelastic liquid, including inertial terms in the analysis, and obtained an expression for the stream function in terms of an elastic parameter $\kappa_o^{(11)}$. His calculations showed that the secondary flow in a plane through the axis of rotation underwent qualitative changes depending on the relative values of inertial forces and normal stresses. At intermediate values of these two forces the flow field splits into an inner region dominated by normal stresses and an outer region dominated by inertial forces. In normal stress-dominated flow, the fluid moved in a direction opposite to that obtaining in inertia-dominated flow.

Thomas and Walters [45] analysed the flow about a sphere rotating slowly in an infinite sea of a Walters B' fluid [11]. They obtained an expression for the stream function, in terms of an elastic parameter m, identical in form to that obtained by Geisekus in his Second Order analysis. They showed, in some detail, that the secondary flow pattern is strongly dependent on the value of m. This result was in complete agreement with that of Geisekus. They also derived expressions for the tangential velocity and the couple on the sphere which included the influence of the elastic parameter. They concluded that couple measurements could be used to estimate the value of this parameter. The Walters B' fluid exhibits elastic effects, but predicts a constant viscosity-shear rate relationship [11]. Thus this conclusion is restricted to real fluids which approximate this behaviour.

Bhatnager and Rajeswari [46] studied the problem of the flow of a Second Order Rivlin-Ericksen fluid contained between two concentric spheres, both in steady rotation about a common axis. They obtained expressions for the stream function, the tangential velocity and the stress distribution in terms of the parameters of the Second

Order fluid. They observed that as long as the spheres rotate in the same direction, only the non-Newtonian fluids were able to exhibit the breaking and reversal of flow in each quadrant for certain values of the non-Newtonian parameters.

Walters and Waters [47] analysed the problem of a sphere rotating within a stationary outer concentric sphere filled with a Walters B' fluid. This study is essentially an extension of the analysis of Thomas and Walters [45] and was undertaken in order to estimate the effect of container walls on the flow field surrounding the inner rotating sphere. They concluded that, provided the ratio of radius of the outer sphere to that of the inner sphere is greater than 12, the couple on the inner sphere is within 1% of that of a sphere rotating in an infinite medium. Like the earlier analysis of Thomas and Walters, these conclusions are strictly valid for fluids which exhibit elastic behaviour, but no shear dependent viscosity behaviour.

Bhatnager, Rajagopalan and Mathur [48] considered the secondary flows induced in a viscoelastic liquid contained between two concentric spheres in arbitrary relative station about a common axis. They studied the behaviour of an Oldroyd four-constant fluid, a Walters' B' fluid and a Second Order Rivlin-Ericksen fluid and concluded that the equation for the stream function is identical for these three fluids if the elastic parameter is properly defined. These authors referred to the earlier analyses of Mohan Rao [49], Thomas and Walters [45] and Bhatnager and Rajeswari [46]. No attempt was made to obtain the tangential velocity component.

Walters and Waters [39], in a paper published in 1964, analysed the problem of the steady flow about a sphere rotating slowly in an infinite sea of an Nth Order

Rivlin-Ericksen fluid. They showed that, under the slow-flow approximation, the constitutive equation reduces to one which is in agreement with that of the Third Order fluid of Coleman and Noll [34, 12]. Their expression for the stream function is identical in form to that obtained from the analyses of the behaviour of a Second Order fluid [44 - 47]. However, their expressions for the tangential velocity and for the couple on the sphere differed from those of earlier analyses in that they contained both an elastic and a shear thinning parameter. This analysis can thus be applied to a wider and more realistic class of fluids and is in agreement with a special case of the Geisekus analysis which disregarded inertial forces [43].

Mow [50], in 1967, published an analysis of the flow about a sphere rotating within an outer concentric sphere filled with an Oldroyd four-constant fluid. This fluid model is capable of exhibiting both elastic and shear thinning behaviour [10]. However, while Mow's expression for the stream function is in agreement with earlier analyses [46, 47], his final expression for the tangential velocity appears to be in error in that it does not satisfy the boundary conditions. Further, his equation for the couple on the inner sphere is not in agreement with that of Walters and Waters [47]. (See Appendix A).

Jones and Lewis [51] proposed a virtual body force technique for predicting the incipient flow pattern around various solids of revolution rotating in a Walters B' fluid. The flow around a sphere rotating within an outer concentric sphere was considered as a special case and the incipient flow was found to be consistent with the steady flow analysis of Thomas and Walters [45].

Kelkar, Mashelkar and Ulbrecht [52] used a somewhat empirical approach to develop expressions for the tangential velocity component and the torque on a sphere rotating in a power law fluid. This analysis ignored secondary flows caused by inertial or elastic forces and is further restricted by the well-known inability of the power law equation to describe very low shear rate behaviour realistically. However, these authors were primarily concerned with correlating their velocity and torque data at relatively high shear rates, and were moderately successful in doing so. This point will be discussed again in Section 1B.

Of the above analyses, that of Walters and Waters [39] for the flow of a Rivlin-Ericksen fluid around a rotating sphere appears to be the most widely applicable, in the sense that the fluid model used incorporates both normal stress or elastic phenomena and shear dependent viscosity behaviour. The validity of this analysis is only restricted by the slow flow condition and by the 'infinite sea of fluid' assumption. While the former condition is easy to realise in practice, the latter can be only approximated experimentally. The analysis of the flow of Second Order type fluids around a sphere rotating within an outer stationary concentric sphere [46, 47] provides a good estimate of the conditions under which the effects of container boundaries on torque and tangential velocity profiles are negligible. However, for liquids which exhibit highly shear dependent viscosities and for situations in which wall effects are significant, the analysis of a Third Order fluid flowing between concentric spheres is required to give precise expressions for the torque on the inner rotating sphere and for the tangential velocity distribution. For this reason, the analysis of the flow of a Third Order type fluid induced by the slow rotation of a sphere within an outer stationary concentric sphere was undertaken, as detailed in Chapter 2.

1A.2 Rotating Disc Studies

Jain [53] used the von Karman approach to analyse the flow near an infinitely large disc rotating in a semi-infinite expanse of non-Newtonian fluid. A similar approach was used by Srivastava [54] for the analysis of the flow of a non-Newtonian fluid between two infinite discs and by Sharma and Sharma [55] in their study of the flow of a Second Order fluid over an enclosed rotating disc. This analytical approach ignores 'edge effects' and remains approximately valid for flow around a finite rotating disc only if the boundary layer is small compared with the disc radius. (See, for example, Schlichting [56]). None of these analyses predict flow reversal due to elastic effects.

Griffiths, Jones and Walters [57] considered the problem of the flow of a Third Order Coleman and Noll fluid between two infinite discs, the one at rest and the other rotating slowly. Their analytical solution to this problem failed to predict flow reversal due to the elasticity of the fluid. They concluded that the flow reversal observed experimentally was in some way due to edge effects. This conclusion was confirmed by their numerical analysis of the problem of a finite disc rotating in a finite bath filled with the Third Order fluid. They were able to predict reverse flow in this geometry.

Waters and King [40], following the work of Jeffrey [58] in 1915, successfully analysed the problem of a spheroid rotating in a Third Order Coleman and Noll fluid. The flow about a finite rotating disc and a rotating sphere can be obtained as special cases of the spheroid. This analysis for the rotating disc problem predicts flow reversal due to the elasticity of the fluid and confirms the earlier numerical analysis of Griffiths et al

[57]. These authors calculated the flow patterns around spheroids of revolution of different shapes and showed that the secondary flow pattern was strongly dependent upon both the elastic parameter and the shape of the body. For example, flow reversal occurred for a lower value of the elastic parameter in the case of the rotating disc than in the case of the rotating sphere. These authors did not, however, obtain a solution for the tangential velocity component or for the couple on the spheroid and in this sense, the solution to this theoretical problem remains, to the author's knowledge, incomplete.

1B REVIEW OF EXPERIMENTAL STUDIES OF NON-VISCOMETRIC FLOWS OF VISCOELASTIC LIQUIDS ABOUT ROTATING BODIES

In this review attention will be concentrated on studies of flow about rotating solids of revolution because these are of particular importance in comparing experimental evidence with theoretical predictions.

In 1963 Geisekus [44] demonstrated the existence of secondary flows induced by the elastic properties of a liquid surrounding a rotating sphere and a rotating cone and plate arrangement. Geisekus used a dye-tracer technique in order to obtain experimental streamlines which were qualitatively in agreement with his theoretical Second Order analyses for the rotating sphere and cone-and-plate systems. Quantitative comparison with theory was not possible both because the experimental rotational speeds were far in excess of the range of applicability of the Second Order theory and because the influence of the bath walls could not be accounted for. A ratio of the length of the sides of the cubical tank to the sphere diameter of approximately four was used and wall effects were certainly of significance. Using the same experimental technique, Geisekus showed that competing inertial

Viscometric measurements were also taken, using a Weissenberg rheogoniometer. The viscometric and non-viscometric measurements differed considerably, even at the lowest shear rates attainable on the rheogoniometer. While the authors explain the difference on the basis that the shear rates were too high for the Second Order analysis to be valid, the fact that torque measurements are insensitive to changes in the elastic parameter [60] is possibly a contributory factor.

Kelkar et al [3] used the Third Order fluid analysis of Geisekus [43] and of Waters and King [40] as a basis for proposing certain dimensionless groups which could be used in correlating power consumption in the mixing of viscoelastic liquids. These authors successfully correlated power consumption data for several spheres, discs and turbine agitators in liquids exhibiting elastic and viscous anomalies, both separately and in combination. Wall effects were not, however, taken into account.

Kelkar et al [52] used a 'three-dimensional particle technique' to measure the primary velocity distribution around a sphere rotating in both Newtonian and non-Newtonian liquids. An expression for the primary velocity distribution in a power law fluid was derived. The derived linear plot was superimposed on the experimental data using a value of the flow index obtained from viscometric measurements in a Weissenberg rheogoniometer. However, while the data for Newtonian liquid were very well represented by the primary flow equation up to a dimensionless radial distance of four, the power law equation is a distinctly poorer representation of the non-Newtonian data. A torque-angular velocity relationship was derived for the sphere and was fitted to the experimental data to give the flow index and the consistency. These values compared well with those obtained

from viscometric data obtained in the rheogoniometer. These authors did not account for 'wall effects' quantitatively, even though the ratio of sphere diameter (5,28 cm) to tank length (34 cm) was approximately 6,3 and wall effects were therefore undoubtedly significant.

Experimental studies of the rotating disc system are confined to dye tracer studies demonstrating the reverse flow phenomenon. Griffiths et al [57] reported a dye tracer study of a disc rotating in a Newtonian liquid, a non-Newtonian liquid showing pronounced elasticity and a slightly elastic liquid. The experimental work constituted a qualitative verification of their theoretical analysis. Hansford and Litt [63] encountered the reverse flow phenomenon at low rotational speeds while doing a mass transfer study in power law liquids. They used a dye study to correlate the failure of their mass transfer predictions based on the power law model with the onset of 'torroidal flow' and 'reverse flow'.

Hill et al [64], in a preliminary study, reported the reverse flow phenomenon in the disc and cylinder system. Hill [41, 65] subsequently measured comprehensive sets of velocity profiles, using streak photography, in this system. He measured tangential and radial velocity profiles in a Newtonian liquid at Reynolds numbers of 0,0616, 24,4 and 97,6 and at 0,0371 for a viscoelastic liquid. Hill compared his experimental work with the analysis of Kramer and Johnson [66] for the disc and cylinder system, who used perturbation analysis and a numerical technique to solve the problem. Hill found that the Newtonian primary flow equations provided a good description of the tangential velocity data for the Newtonian liquid up to the Reynolds number of 24,4 and that significant differences occur at the Reynolds number of 97,6. The Newtonian secondary flow

solution was found to be in fair agreement with the experimental radial velocities up to the Reynolds number of 24,4, but differed from the experimental values by a factor of two or three at the Reynolds number of 97,6. The Newtonian primary flow solution to the disc and cylinder problem was modified by introducing a shear dependent viscosity function and could be made to fit the experimental data to within 20%. Hill used the empirically modified Second Order fluid analysis of Kramer and Johnson [66] to obtain radial velocity profiles which agree with the experimental data to within 40%. Hill also reported a qualitative study of a number of liquids in the disc and cylinder system. The fluids used ranged in behaviour from that of a slightly non-Newtonian liquid to that of a highly viscoelastic liquid.

Hill's work has been summarised in some detail because it was the first attempt to obtain quantitative data in the form of velocity profiles in a non-viscometric flow situation. However, Hill was unable to reconcile theory and experiment in an entirely convincing fashion.

The majority of the experimental studies reviewed above are primarily aimed at establishing the validity of certain theoretical approaches. However, a number of quantitative studies of the practical effects of non-Newtonian fluid behaviour on the mixing of viscoelastic liquids has been reported [67 - 70]. Ulbrecht [71] has recently reviewed this field, and discussed the influence of fluid elasticity and shear thinning behaviour on mixing times and power consumption.

CHAPTER 2

THEORY

The theoretical work presented in this chapter is divided into four sections. Section 2A is an analysis of the flow about a sphere rotating slowly in a Rivlin-Ericksen fluid contained in an outer concentric sphere. The motivation for this analysis was given at the end of Section 1A.1 and it is essentially an extension of the analysis of Walters and Waters [39] in the sense that the outer boundary condition is changed. The method of analysis is that of Thomas and Walters [45] and the nomenclature adopted is similar (though not entirely identical) to that of Walters and Waters [39, 47]. This was done in order to facilitate comparison of the final expressions for the tangential velocity and the couple on the sphere with these earlier analyses.

Section 2B contains a resume of the publication of Waters and King [40] on the flow about a spheroid rotating slowly in the Simple Fluid of Coleman and Noll. The problem is restated briefly and the final expression for the stream function obtained by these authors is quoted. In order to compare this theoretical result with experimental radial velocity measurements, the expression for the stream function was differentiated in order to obtain an explicit equation for the theoretical radial velocity profiles. The special case of a rotating disc is discussed briefly.

In Section 2C a novel application of the conformal mapping technique is proposed. This technique is used to obtain the radial and axial velocity components of flow around the rotating disc from the analytical solu-

tion to the rotating sphere problem. The results are compared with the analytical solutions of Waters and King [40].

Section 2D contains a critical resume of the theory on which the falling sphere viscometer is based. The falling sphere method was used to obtain the zero shear viscosities of the experimental liquids, as reported in Chapters 3 and 4.

2A THE FLOW ABOUT A SPHERE ROTATING SLOWLY IN A RIVLIN-ERICKSEN FLUID CONTAINED IN AN OUTER CONCENTRIC SPHERE

2A.1 Analysis

The constitutive equations defining a Rivlin-Ericksen fluid are expressible in a Cartesian framework as follows:

$$T = -pI + T' \qquad (2A.1)$$

$$T' = f(A^{(1)}, A^{(2)}, \ldots A^{(n)}, \qquad (2A.2)$$

where $T(=[p_{ij}])$ is the stress tensor,

$T'(=[p_{ij}'])$ is the deviatoric stress tensor,

I the unit matrix, p an arbitrary isotropic pressure and f is a polynomial in the Rivlin-Ericksen tensors $A^{(n)}$.

The $A^{(n)}$ are defined by

$$A^{(\gamma)} = [A_{ij}^{(\gamma)}] \qquad (\gamma = 1, 2, \ldots., n). \qquad (2A.3)$$

$$A_{ij}^{(1)} = \frac{\partial v_i}{\partial x_j} + \frac{\partial v_j}{\partial x_i}, \qquad (2A.4)$$

$$A_{ij}^{(\gamma+1)} = \frac{\partial A_{ij}^{(\gamma)}}{\partial t} + v_1 \frac{\partial A_{ij}^{(\gamma)}}{\partial x_1} + A_{mi}^{(\gamma)} \frac{\partial v_m}{\partial x_j} + A_{mj}^{(\gamma)} \frac{\partial v_n}{\partial x_i}, \qquad (2A.5)$$

$$(\gamma = 1, 2, \ldots., n-1)$$

where v_i (i = 1, 2, 3) denote the velocity components in the x_i co-ordinate system [39, 72].

Consider the problem of a sphere of radius a, rotating steadily with angular velocity Ω about a vertical axis within a stationary concentric sphere of radius βa. The space between the spheres is filled by a Rivlin-Ericksen fluid. All physical quantities are defined in terms of spherical polar co-ordinates (r_1, θ, ϕ) with r_1 measured from the centre of the spheres and $\theta = 0$ the axis of rotation of the inner sphere.

Let U, V and W be the physical components of the velocity vector referred to the r_1, θ and ϕ co-ordinates respectively. The boundary conditions are

$$\left.\begin{aligned} &U = V = 0, \quad W = \Omega a \sin\theta \text{ on } r_1 = a \\ &U = V = W = 0 \qquad\qquad \text{on } r_1 = \beta a \end{aligned}\right\} \tag{2A.6}$$

When the velocity vector is independent of ϕ (axial symmetry), Cauchy's equations of motion reduce to

$$\rho\left[U\frac{\partial U}{\partial r_1} + \frac{V}{r_1}\frac{\partial U}{\partial \theta} - \frac{(V^2 + W^2)}{r_1}\right] - \rho g\cos\theta =$$

$$-\frac{\partial p}{\partial r_1} + \frac{1}{r^2}\frac{\partial (r_1^2\, p'_{(r_1 r_1)})}{\partial r_1}$$

$$+\frac{\partial (\sin\theta\, p'_{(r_1\theta)})}{r_1 \sin\theta\, \partial\theta} - \frac{(p'_{(\theta\theta)} + p'_{(\phi\phi)})}{r_1}, \tag{2A.7}$$

$$\rho\left[\frac{U\partial (r_1 V)}{r_1 \partial r_1} + \frac{V}{r_1}\frac{\partial V}{\partial \theta} - \frac{W^2 \cot\theta}{r_1}\right] + \rho g\sin\theta =$$

$$-\frac{1}{r_1}\frac{\partial p}{\partial \theta} + \frac{1}{r^3}\frac{\partial (r_1^3\, p'_{(r\theta)})}{\partial r_1}$$

$$+\frac{1}{r_1 \sin\theta}\frac{\partial (\sin\theta\, p'_{(\theta\theta)})}{\partial \theta} - \frac{\cot\theta}{r_1} p'_{(\phi\phi)} \tag{2A.8}$$

$$\rho\left[\frac{U}{r_1}\frac{\partial(r_1W)}{\partial r_1} + \frac{V}{r_1\sin\theta}\frac{\partial(W\sin\theta)}{\partial\theta}\right] = \frac{1}{r_1^3}\frac{\partial(r_1^3\, p'_{(r_1\phi)})}{\partial r_1} + \frac{1}{r_1\sin^2\theta}\frac{\partial(\sin^2\theta p'_{(\theta\phi)})}{\partial\theta}, \qquad (2A.9)$$

where ρ is the density of the fluid and the $p'_{(ik)}$ are the physical components of the deviatoric stress tensor*. The equation of continuity reduces to

$$\frac{\partial}{\partial r_1}(Ur_1^2\sin\theta) + \frac{\partial}{\partial\theta}(Vr_1\sin\theta) = 0 \qquad (2A.10)$$

It is possible to write equations (2A.7) and (2A.10) in dimensionless form using the substitutions:

$$\left.\begin{aligned} U &= \frac{\alpha_1}{\rho a}u, \quad V = \frac{\alpha_1}{\rho a}v, \quad W = \Omega a w, \quad r_1 = ar, \\ p &= \rho g r_1\cos\theta + \frac{\alpha_1^2}{\rho a^2}p^* \quad \text{and} \\ p'_{(ij)} &= \frac{\alpha_1^2}{\rho a^2}\begin{bmatrix} p''_{(rr)} & p''_{(r\theta)} & \left(\frac{\Omega a^2\rho}{\alpha_1}\right)p''_{(r\phi)} \\ p''_{(r\theta)} & p''_{(\theta\theta)} & \left(\frac{\Omega a^2\rho}{\alpha_1}\right)p''_{(\theta\phi)} \\ \left(\frac{\Omega a^2\rho}{\alpha_1}\right)p''_{(r\phi)} & \left(\frac{\Omega a^2\rho}{\alpha_1}\right)p''_{(\phi\theta)} & p''_{(\phi\phi)} \end{bmatrix} \end{aligned}\right\} \qquad (2A.11)$$

where α_1 is the zero shear viscosity [39]. The equations of motion and continuity now take the form

* Physical components of tensors will be denoted by parentheses around suffixes.

$$u\frac{\partial u}{\partial r} + \frac{v}{r}\frac{\partial u}{\partial \theta} - \frac{v^2}{r} - \frac{Lw^2}{r} = -\frac{\partial p^*}{\partial r}$$

$$+ \frac{1}{r^2}\frac{\partial (r^2 p''_{(rr)})}{\partial r} + \frac{1}{r\sin\theta}\frac{\partial (\sin\theta\, p''_{(r\theta)})}{\partial \theta}$$

$$- \frac{p''_{(\theta\theta)}}{r} - \frac{p''_{(\phi\phi)}}{r}, \qquad (2A.12)$$

$$\frac{u}{r}\frac{\partial (rv)}{\partial r} + \frac{v}{r}\frac{\partial v}{\partial \theta} - \frac{Lw^2\cot\theta}{r} = -\frac{1}{r}\frac{\partial p^*}{\partial \theta}$$

$$+ \frac{1}{r^3}\frac{\partial (r^3 p''_{(r\theta)})}{\partial r} + \frac{1}{r\sin\theta}\frac{\partial (\sin\theta\, p''_{(\theta\theta)})}{\partial \theta}$$

$$- \frac{p''_{(\phi\phi)}\cot\theta}{r}, \qquad (2A.13)$$

$$\frac{u}{r}\frac{\partial (rw)}{\partial r} + \frac{v}{r\sin\theta}\frac{\partial (w\sin\theta)}{\partial \theta} = \frac{1}{r^3}\frac{\partial (r^3 p''_{(r\phi)})}{\partial r}$$

$$+ \frac{1}{r\sin^2\theta}\frac{\partial (\sin^2\theta\, p''_{(\theta\phi)})}{\partial \theta}, \qquad (2A.14)$$

$$\frac{\partial}{\partial r}(ur^2\sin\theta) + \frac{\partial}{\partial \theta}(vr\sin\theta) = 0 \qquad (2A.15)$$

where $L = \left(\frac{\Omega a^2 \rho}{\alpha_1}\right)^2$.

It may be shown that a simple solution (the primary flow solution) to equations (2A.12) to (2A.15) exists when terms of order L are neglected:

$$\left.\begin{aligned} u &= v = 0, \qquad w = \left(\frac{C}{r^2} + Dr\right)\sin\theta \\ p^* &= 0, \quad p''_{(r\phi)} = \frac{-3C\sin\theta}{r^3}, \quad \text{other } p''_{(ij)} = 0, \end{aligned}\right\} \tag{2A.16}$$

where $C = \dfrac{\beta^3}{\beta^3 - 1}$ and $D = \dfrac{1}{1 - \beta^3}$.

Now assume that the velocity components and pressure can be expanded in powers of L as follows:

$$\begin{aligned} u &= Lu + L^2u + \ldots\ldots\ldots \\ v &= Lv + L^2v + \ldots\ldots\ldots \\ w &= \left(\frac{C}{r^2} + Dr\right)\sin\theta + Lw_1 + L^2w_2 + \ldots\ldots \\ p^* &= Lp_1^* + L^2p_2^* + \ldots\ldots\ldots \end{aligned} \tag{2A.17}$$

If only terms up to order L are retained (i.e. terms of order L^2 and higher are ignored), the following expressions for the relevant Rivlin-Ericksen tensors are obtained:

$$A^{(1)} = \begin{bmatrix} A^{(1)}_{r_1r_1} & A^{(1)}_{r_1\theta} & A^{(1)}_{r_1\phi} \\ A^{(1)}_{\theta r_1} & A^{(1)}_{\theta\theta} & A^{(1)}_{\theta\phi} \\ A^{(1)}_{\phi r_1} & A^{(1)}_{\phi\theta} & A^{(1)}_{\phi\phi} \end{bmatrix} \tag{2A.18}$$

where $A^{(1)}_{r_1r_1} = \dfrac{2L\alpha_1}{\rho a}\dfrac{\partial u_1}{\partial r_1}$, $A^{(1)}_{\phi\phi} = \dfrac{2L\alpha_1 r_1\sin^2\theta}{\rho a}(u_1 + v_1\cot\theta)$

$$A^{(1)}_{r_1\theta} = A^{(1)}_{\theta r_1} = \frac{L\alpha_1 r_1}{\rho a}\left(\frac{1}{r_1}\frac{\partial u_1}{\partial\theta} + r_1\frac{\partial}{\partial r_1}\left(\frac{v_1}{r_1}\right)\right),$$

$$A^{(1)}_{r_1\phi} = A^{(1)}_{\phi r_1} = \Omega a r_1 \sin\theta\left(\frac{-3a^2C\sin\theta}{r_1^3} + Lr_1\,\frac{\partial}{\partial r_1}\left(\frac{w_1}{r_1}\right)\right),$$

$$A^{(1)}_{\theta\theta} = \frac{2L\alpha_1 r_1}{\rho a}\left(\frac{\partial v_1}{\partial\theta} + u_1\right),$$

$$A^{(1)}_{\theta\phi} = A^{(1)}_{\phi\theta} = L\Omega a r_1 \sin\theta\left(\frac{\partial w_1}{\partial\theta} - w_1\cot\theta\right);$$

$$A^{(2)} = \begin{bmatrix} A^{(2)}_{r_1r_1} & A^{(2)}_{r_1\theta} & A^{(2)}_{r_1\phi} \\ A^{(2)}_{\theta r_1} & A^{(2)}_{\theta\theta} & A^{(2)}_{\theta\phi} \\ A^{(2)}_{\phi r_1} & A^{(2)}_{\phi\theta} & A^{(2)}_{\phi\phi} \end{bmatrix}; \qquad (2A.19)$$

where $A^{(2)}_{r_1r_1} = \dfrac{18\Omega^2a^6C^2\sin^2\theta}{r_1^6}$,

$$A^{(2)}_{r_1\phi} = A^{(2)}_{\phi r_1} = \frac{-3\Omega L\alpha_1 a^2 C\sin^2\theta}{\rho r_1^2}\left(\frac{\partial u_1}{\partial r_1} + \frac{4v_1\cot\theta}{r_1}\right),$$

$$A^{(2)}_{\theta\phi} = A^{(2)}_{\phi\theta} = \frac{-3\Omega L\alpha_1 a^2 C\sin^2\theta}{\rho r_1^2}\,\frac{\partial u_1}{\partial\theta},$$

$$A^{(2)}_{\theta\theta} = A^{(2)}_{\phi\phi} = A^{(2)}_{r_1\theta} = A^{(2)}_{\theta r_1} = 0$$

and $A^{(\gamma)} = 0$ for $\gamma > 2$. (2A.20)

(See Appendix B1 for details).

Under the restrictions of equations (2A.17) to (2A.20), the constitutive equations (2A.1) and (2A.2) reduce (Walters and Waters [39], [24]) to

$$T = -pI + \left[\alpha_1 + \beta_1 (trA^{(1)2})\right]A^{(1)} + \alpha_2 A^{(2)} + \alpha_3 A^{(1)2} + \alpha_5 (A^{(1)}A^{(2)} + A^{(2)}A^{(1)}), \quad (2A.21)$$

where α_1, α_2, α_3, α_5 and β_1 are constants and the trace of $A^{(1)2}$ is

$$trA^{(1)2} = \frac{18\Omega^2 a^6 C^2 \sin\theta}{r_1^6} .$$

Equation (2A.21) is identical to the equation for a Third Order Coleman and Noll fluid, presented in the Introduction, with $A^{(3)} = 0$.

Substituting (2A.18) and (2A.19) into (2A.21) and using (2A.11) and (2A.17) we obtain

$$p''_{(rr)} = 2L \frac{\partial u_1}{\partial r} + \frac{18L\alpha_2' C^2 \sin^2\theta}{r^6} + \frac{9L\alpha_3' C^2 \sin^2\theta}{r^6} ;$$

$$p''_{(\theta\theta)} = \frac{2L}{r}\left(\frac{\partial v_1}{\partial \theta} + u_1\right) ;$$

$$p''_{(\phi\phi)} = \frac{2L}{r}(u_1 + v_1 \cot\theta) + \frac{9L\alpha_3' C^2 \sin^2\theta}{r^6} ;$$

$$p''_{(r\theta)} = p''_{(\theta r)} = L\left(\frac{1}{r}\frac{\partial u_1}{\partial \theta} + r\frac{\partial}{\partial r}\left(\frac{v_1}{r}\right)\right) ; \quad (2A.22)$$

$$p''_{(\theta\phi)} = p''_{(\phi\theta)} = \frac{L\sin\theta}{r}\frac{\partial}{\partial\theta}\left(\frac{w_1}{\sin\theta} - \frac{3L\alpha_2' C\sin\theta}{r_1^4}\frac{\partial u_1}{\partial\theta}\right) - \frac{3L\alpha_3' C\sin\theta}{r^3}\left(\frac{1}{r}\frac{\partial u_1}{\partial\theta} + r\frac{\partial}{\partial r}\left(\frac{v_1}{r}\right)\right)$$

$$p''_{(r\phi)} = p''_{(\phi r)} = \frac{-3C\sin\theta}{r^3} + Lr\frac{\partial}{\partial r}\left(\frac{w_1}{r}\right) - \frac{54LC^3\sin^3\theta}{r^9}(\alpha_5' + \beta_1') - \frac{3L\alpha_2' C\sin\theta}{r^3}\left(\frac{\partial u_1}{\partial r} + \frac{4v_1\cot\theta}{r}\right) - \frac{6L\alpha_3' C\sin\theta}{r^3}\left(\frac{\partial u_1}{\partial r} + \frac{u_1}{r} + \frac{v_1\cot\theta}{r}\right);$$

where $\alpha_2' = \frac{\alpha_2}{\rho a^2}$, $\alpha_3' = \frac{\alpha_3}{\rho a^2}$, $\alpha_5' = \frac{\alpha_1 \alpha_5}{\rho^2 a^4}$

and $\beta_1' = \frac{\alpha_1 \beta_1}{\rho^2 a^4}$.

From the equation of continuity (2A.15), a stream function χ_1 may be defined by

$$u_1 = -\frac{1}{r^2 \sin\theta} \frac{\partial \chi_1}{\partial \theta}, \quad v_1 = \frac{1}{r \sin\theta} \frac{\partial \chi_1}{\partial r} \tag{2A.23}$$

Substituting (2A.22) and (2A.23) into equations (2A.12) and (2A.13) using (2A.15) and eliminating p* we obtain:

$$\mathcal{L}^2 \chi_1 = 6C \left(\frac{C}{r^5} + \frac{D}{r^2} - \frac{24m'C}{r^7} \right) \sin^2\theta \cos\theta \tag{2A.24}$$

where $\mathcal{L} = \frac{\partial^2}{\partial r^2} + \frac{1}{r^2} \frac{\partial^2}{\partial \theta^2} - \frac{\cot\theta}{r^2} \frac{\partial}{\partial \theta}$ (2A.25)

and $m' = \alpha_2' + \alpha_3'$. (See Appendix B2 for details).

Equation (2A.24) is identical to the differential equation for the stream function obtained by Walters and Waters [47], except for the term $\frac{-24m'C}{r^7}$. They obtained $\frac{-24m'}{r^7}$ instead, due to the earlier erroneous omission of the term C in one of the components of the stress tensor [74]. Equation (2A.24) is also in agreement with the corresponding equations of Bhatnager et al [48] and Mow [50].

The associated boundary conditions are

$$\frac{\partial \chi_1}{\partial r} = \frac{\partial \chi_1}{\partial \theta} = 0 \quad \text{when} \quad r = 1 \quad \text{and} \quad r = \beta \tag{2A.26}$$

The solution of equation (2A.24) subject to these boundary conditions is

$$\chi_1 = \left(\frac{P}{r^2} + Qr^3 + Rr^5 + S + \frac{CD}{2}r^2 - \frac{C^2}{2r} - \frac{2m'C^2}{r^3}\right)\frac{\sin^2\theta\cos\theta}{2} \qquad (2A.27)$$

where $P = \frac{C}{\Delta}[DP_1(\beta) + CP_2(\beta) + m'CP_3(\beta)]$;

$Q = \frac{C}{\Delta}[DQ_1(\beta) + CQ_2(\beta) + m'CQ_3(\beta)]$;

$R = \frac{C}{\Delta}[DR_1(\beta) + CR_2(\beta) + m'CR_3(\beta)]$;

$S = \frac{C}{\Delta}[DS_1(\beta) + CS_2(\beta) + m'CS_3(\beta)]$;

and $\Delta = 1 - \frac{25}{4}\beta^3 + \frac{21}{2}\beta^5 - \frac{25}{4}\beta^7 + \beta^{10}$;

$P_1(\beta) = \frac{\beta^4}{2}\left(1 - \frac{9}{4}\beta + \frac{5}{2}\beta^3 - \frac{9}{4}\beta^5 + \beta^6\right)$;

$P_2(\beta) = \frac{\beta}{4}(1 - 10\beta^3 + 9\beta^4 + 9\beta^5 - 10\beta^6 + \beta^9)$;

$P_3(\beta) = \frac{3}{\beta}(1 - 5\beta^3 + 4\beta^5 + 4\beta^6 - 5\beta^8 + \beta^{11})$;

$Q_1(\beta) = -\frac{3}{4}\left(1 - \frac{10}{3}\beta^2 + \frac{7}{3}\beta^4 + \frac{7}{3}\beta^5 - \frac{10}{3}\beta^7 + \beta^9\right)$;

$Q_2(\beta) = -\frac{5}{8\beta}\left(1 - \frac{12}{5}\beta + \frac{7}{5}\beta^2 + \frac{7}{5}\beta^6 - \frac{12}{5}\beta^7 + \beta^8\right)$;

$Q_3(\beta) = \frac{5}{2\beta^3}\left(1 - \frac{21}{5}\beta^2 + \frac{16}{5}\beta^3 + \frac{16}{5}\beta^7 - \frac{21}{5}\beta^8 + \beta^{10}\right)$;

$R_1(\beta) = \frac{1}{4}(1 - 6\beta^2 + 5\beta^3 + 5\beta^4 - 6\beta^5 + \beta^7)$;

$R_2(\beta) = \frac{3}{8\beta}\left(1 - \frac{8}{3}\beta + \frac{5}{3}\beta^2 + \frac{5}{3}\beta^4 - \frac{8}{3}\beta^5 + \beta^6\right)$;

$R_3(\beta) = -\frac{3}{2\beta^3}(1 - 5\beta^2 + 4\beta^3 + 4\beta^5 - 5\beta^6 + \beta^8)$;

$S_1(\beta) = -\beta^2\left(1 - \frac{15}{8}\beta + \frac{7}{8}\beta^3 + \frac{7}{8}\beta^5 - \frac{15}{8}\beta^7 + \beta^8\right)$;

$S_2(\beta) = \frac{1}{4\beta}(1 - 15\beta^4 + 14\beta^5 + 14\beta^6 - 15\beta^7 + \beta^{11})$;

$S_3(\beta) = -\frac{1}{\beta^3}(1 - 21\beta^5 + 20\beta^6 + 20\beta^7 - 21\beta^8 + \beta^{13})$.

Details of the solution of equation (2A.24) are to be found in Appendix B3. The above solution for χ_1 is in complete agreement with that of Walters and Waters [47] when the omission of the term C is accounted for.

The velocity components obtained from equations (2A.23) and (2A.27) are

$$u = Lu_1 = \frac{L}{2}\left[\left(\frac{P}{r^4} + Qr + Rr^3 + \frac{S}{r^2} + \frac{CD}{2} - \frac{C^2}{2r^3} - \frac{2m'C^2}{r^5}\right)(3\sin^2\theta - 2)\right] \qquad (2A.28)$$

and

$$v = Lv_1 = \frac{L}{2}\left(\frac{-2P}{r^4} + 3Qr + 5Rr^3 + CD + \frac{C^2}{2r^3} + \frac{6m'C^2}{r^5}\right)\sin\theta\cos\theta \qquad (2A.29)$$

The ϕ component of the equations of motion, obtained from equation (2A.14) after substitution from equations (2A.22), (2A.28) and (2A.29), and the use of the equation of continuity (2A.15), is

$$\frac{\partial^2 w_1}{\partial r^2} + \frac{2}{r}\frac{\partial w_1}{\partial r} + \frac{\cot\theta}{r^2}\frac{\partial w_1}{\partial \theta} + \frac{1}{r^2}\frac{\partial^2 w_1}{\partial \theta^2} - \frac{w_1}{r^2\sin^2\theta}$$

$$= \sin\theta\left[\frac{-108m'^2C^3}{r^{10}} + \frac{36m'CP}{r^9} - \frac{8m'C^3}{r^8}\right.$$

$$+ \frac{C}{r^7}(18m'S - P) + \frac{C}{r^5}(S + 18m'CD)$$

$$+ \frac{1}{r^4}(36m'QC - 4PD) + \frac{3C^2D}{2r^3}$$

$$+ \frac{2}{r^2}(2QC + 39m'CR - SD) + 6RC$$

$$+ \; DQr \; + \; 3RDr^3\Big] \; + \; \sin^3\theta\Big[\frac{36m'^2C^3}{r^{10}}$$

$$+ \; \frac{162\sigma'C^3}{r^{10}} \; - \; \frac{15m'CP}{r^9} \; + \; \frac{9m'C^3}{2r^8}$$

$$+ \; \frac{C}{2r^7}\,(P - 36m'S) \; + \; \frac{C^3}{4r^6} - \frac{3C}{2r^5}\,(S + 19m'CD)$$

$$+ \; \frac{5}{r^4}\,(PD - 9m'QC) \; - \; \frac{15C^2D}{4r^3}$$

$$+ \; \frac{3}{2r^2}\,(2DS - 3QC - 52Rm'C) \; + \; \frac{CD^2}{2}$$

$$- \; \frac{13CR}{2} \; - \; 2RDr^3\Big] \qquad (2A.30)$$

where $\sigma' = -2(\alpha_5' + \beta_1')$.

The details involved in obtaining these equations are presented in Appendix B4. If $\sigma' = 0$, equation (2A.30) is identical to the corresponding equation of Walters and Waters [47] when the spurious C terms are accounted for. For $C = 1$ and $D = 0$, the values corresponding to the 'infinite sea' boundary condition, (2A.30) is identical to the corresponding equation in [39].

Equation (2A.30), subject to the boundary conditions $w_1 = 0$ on $r = a$ or $r = \beta a$, may be solved using the method of Thomas and Walters [2]. The solution is

$$w_1 = H_1(r)\,T_1(\theta) + H_3(r)\,T_3(\theta) \qquad (2A.31)$$

where $T_1(\theta) = \sin\theta$; $T_3(\theta) = \sin^3\theta - \frac{4}{5}\sin\theta$;

$$H_1(r) = -\frac{22m'^2C^3}{15r^8} + \frac{12\sigma'C^3}{5r^8} + \frac{3m'CP}{5r^7}$$

$$-\frac{11m'C^3}{70r^6} + \frac{C(6m'S - P)}{30r^5} + \frac{C^3}{50r^4}$$

$$-\frac{C(S + 4m'CD)}{20r^3} - \frac{(QC + SD + 39m'RC)}{5}$$

$$+\frac{(CD^2 + 2RC)}{10}r^2 + \frac{DQ}{10} + \frac{RD}{20}r^5$$

$$+\frac{A_1}{r^2} + A_2 r \,, \qquad \text{(2A.32)}$$

where $A_1 = \frac{\beta^3}{(1 - \beta^3)}\left[-\frac{22m'^2C^3}{15}\left(1 - \frac{1}{\beta^9}\right)\right.$

$$+\frac{12\sigma'C^3}{5}\left(1 - \frac{1}{\beta^9}\right) + \frac{3m'CP}{5}\left(1 - \frac{1}{\beta^8}\right)$$

$$-\frac{11m'C^3}{70}\left(1 - \frac{1}{\beta^7}\right) + \frac{C(6m'S - P)}{30}\left(1 - \frac{1}{\beta^6}\right)$$

$$+\frac{C^3}{50}\left(1 - \frac{1}{\beta^5}\right) - \frac{C(S + 4m'CD)}{20}\left(1 - \frac{1}{\beta^4}\right)$$

$$-\frac{(QC + SD + 39m'RC)}{5}\left(1 - \frac{1}{\beta}\right)$$

$$+\frac{(CD^2 + 2RC)}{10}(1 - \beta) + \frac{DQ}{10}(1 - \beta^2)$$

$$\left.+\frac{RD}{20}(1 - \beta^4)\right]$$

and $A_2 = -A_1 - \left[-\frac{22m'^2C^3}{15} + \frac{12\sigma'C^3}{5} + \frac{3m'CP}{5}\right.$

$$- \frac{11m'C^3}{70} + \frac{C(6m'S - P)}{30} + \frac{C^3}{50} - \frac{C(S + 4m'CD)}{20}$$

$$- \frac{(QC + SD + 39m'RC)}{5} + \frac{(CD^2 + 2RC)}{10} + \frac{DQ}{10} + \frac{RD}{20}\Big] .$$

The equations for $H_1(r)$ are consistent with those obtained by Walters and Waters [47], subject to the conditions mentioned in the discussion of equation (2A.30) above.

$$H_3(r) = \frac{9m'^2C^3}{11r^8} + \frac{81\sigma'C^3}{22r^8} - \frac{m'CP}{2r^7} + \frac{m'C^3}{4r^6} + \frac{C(P - 36m'S)}{16r^5}$$

$$- \frac{C^3}{28r^4}\left(\ell nr + \frac{1}{7}\right) + \frac{C(S + 19m'CD)}{4r^3} - \frac{(DP - 9m'QC)}{2r^2}$$

$$+ \frac{5C^2D}{16r} - \frac{(2SD - 3QC - 52m'RC)}{8} - \frac{(CD^2 - 13CR)}{12}$$

$$- \frac{RD}{9}r^5 + \frac{B_1}{r^4} + B_2r^3,$$

where $B_1 = \frac{\beta^7}{(1 - \beta^7)}\Big[\frac{9m'^2C^3}{11}\left(1 - \frac{1}{\beta^{11}}\right) + \frac{81\sigma'C^3}{22}\left(1 - \frac{1}{\beta^{11}}\right)$

$$- \frac{m'CP}{2}\left(1 - \frac{1}{\beta^{10}}\right) + \frac{m'C^3}{4}\left(1 - \frac{1}{\beta^9}\right)$$

$$+ \frac{C(P - 36m'S)}{16}\left(1 - \frac{1}{\beta^8}\right) - \frac{C^3}{196}\left(1 - \frac{1}{\beta^7} - \frac{7\ell n\beta}{\beta^7}\right)$$

$$+ \frac{C(S + 19m'CD)}{4}\left(1 - \frac{1}{\beta^6}\right) - \frac{(DP - 9m'QC)}{2}\left(1 - \frac{1}{\beta^5}\right)$$

$$+ \frac{5C^2D}{16}\left(1 - \frac{1}{\beta^4}\right) - \frac{(2SD - 3QC - 52m'RC)}{8}\left(1 - \frac{1}{\beta^3}\right)$$

$$- \frac{(CD^2 - 13CR)}{12}\left(1 - \frac{1}{\beta}\right) - \frac{RD}{9}(1 - \beta^2)\Big] ,$$

and $$B_2 = - B_1\Big[- \frac{9m'^2C^3}{11} + \frac{81\sigma'C^3}{22} - \frac{m'CP}{2} + \frac{m'C^3}{4}$$

$$+ \frac{C(P - 36m'S)}{16} - \frac{C^3}{196} + \frac{C(S + 19m'CD)}{4}$$

$$- \frac{(DP - 9m'QC)}{2} + \frac{5C^2D}{16} - \frac{(2SD - 3QC - 52m'RC)}{8}$$

$$- \frac{(CD^2 - 13CR)}{12} - \frac{RD}{9}\Big] .$$

Walters and Waters [39, 47] did not give the equation for $H_3(r)$ explicitly, thus comparison is not possible. The method of solution of the equation for w_1 is detailed in Appendix B5.

The couple Γ on the inner sphere is given by the equation

$$\Gamma = \alpha_1\Omega\Big[\int_0^{\pi} -p''_{(r\phi)}\Big]_{r=1} 2\pi a^3 \sin^2\theta d\theta \qquad (2A.34)$$

Substituting for u_1, v_1 and w_1 (equations (2A.28), (2A.29) and (2A.31) - (2A.33)) in the expression for $p''_{(r\phi)}$, the following equation is obtained:

$$p''_{(r\phi)} = \frac{-3\sin\theta}{r^3} + Lr\Big[- \frac{2m'C^3}{5r^8} + \frac{CP}{5r^7} - \frac{C^3}{10r^6}$$

$$+ \frac{C(S - 2m'CD)}{5r^5} - \frac{21m'CQ}{5r^4} + \frac{(CQ + SD)}{5r^2}$$

$$+ \frac{C(D^2 + 2R)}{10} + \frac{DQ}{5}r + \frac{RD}{5}r^3 - \frac{3A_1}{r^4}\Big] T_1(\theta)$$

$$+ F_3(r)\, T_3(\theta) . \qquad (2A.35)$$

$F_3(r)$ need not be specified as the term $F_3(r)T_3(\theta)$ does not affect the couple on the sphere. Substitution of equation (2A.35) into equation (2A.34) gives the expression for the couple on the inner sphere:

$$\Gamma = 8\Pi\alpha_1\Omega a^3\left\{ C - L\left[- \frac{2m'C^3}{15} + \frac{CP}{15} - \frac{C^3}{30} \right.\right.$$

$$+ \frac{C(S - 2m'CD)}{15} - \frac{7m'CQ}{5} + \frac{(CQ + SD)}{15} + \frac{C(D^2 + 2R)}{30}$$

$$\left.\left. + \frac{DQ}{15} + \frac{RD}{15} - A_1\right]\right\} . \qquad (2A.36)$$

(Details are shown in Appendix B6).

The above equation for the couple on the sphere is consistent with the equations given in [39] and [47]. It should be noted that σ' appears in the expression for the term A_1 and thus Γ is a function of β, m' and σ'.

2A.2 Theoretical Velocity Profiles in a Cylindrical Co-ordinate System

Equations (2A.28), (2A.29) and (2A.31) give the theoretical velocities in a spherical polar co-ordinate system. However the experimental data are obtained more conveniently in terms of cylindrical co-ordinates (see Chapters 3 and 4). It is therefore necessary to obtain expressions for the dimensionless theoretical velocity profiles in terms of this co-ordinate system.

The cylindrical co-ordinate system (r_1', ϕ', z_1) is related to the spherical co-ordinate system (r_1, θ, ϕ) by the equations

$$\begin{aligned} r_1' &= r_1\sin\theta \\ \phi' &= \phi \\ z_1 &= r_1\cos\theta \end{aligned} \qquad (2A.37)$$

Hence the velocity components (u', w', v') in the cylindrical co-ordinate system are related to the velocity components (u, v, w) of the spherical co-ordinate system by the equation

$$\left.\begin{aligned} u' &= u\sin\theta + v\cos\theta \\ v' &= u\cos\theta - v\sin\theta \\ w' &= w \end{aligned}\right\} \qquad (2A.38)$$

(See, for example, Appendix A in [71]).

These equations, ((2A.28), (2A.29) and (2A.31)), and the inverse relations to (2A.37),

$$r_1 = (r_1'^2 + z_1^2)^{\frac{1}{2}}$$
$$\text{and} \quad \theta = \arcsin\left[r_1'/(r_1'^2 + z_1^2)\right] \qquad (2A.39)$$

may be used to obtain complete expressions for the theoretical velocities in the cylindrical co-ordinate system. In practice, however, r_1 and θ are calculated from equation (2A.39). The dimensionless radius $r = r_1/a$ is calculated, and these values for r and θ are inserted into equations (2A.38), (2A.28), (2A.29) and (2A.31) in order to give u', v' and w'. The velocity profiles are calculated at various z positions, where $z = z_1/a$ is the dimensionless axial distance from the equator of the sphere.

2A.3 Presentation and Discussion

The velocity components u' and w' were measured experimentally (Chapters 3 and 4) and it is therefore of interest to observe the influence of the parameters m', σ' and β on these velocity components. Each of the u' and w' curves were calculated at five dimensionless z positions (arbitrarily chosen to coincide with those

used in the experimental work reported in Chapter 4) in order to show theoretical behaviour throughout the flow field. The values of L (= Re^2) and the values of β (where β is the ratio of the radius of the outer sphere to that of the inner sphere) were also chosen to coincide with experimentally encountered values. A β value of 10^4 was used to calculate the curves for "$\beta = \infty$". (See Appendix F). The range of values of m' and σ' was chosen so as to span the experimentally determined values. Thus the theoretical curves presented in Figures 2-1 to 2-9 are illustrative of conditions which may well occur in real situations.

In order to clarify the discussion which follows, it should be recalled that L, m' and σ' are dimensionless parameters, and are related to the material constants in equation (2A.21) by the following equations:

$$L = \left(\frac{a^2\Omega\rho}{\eta_0}\right)^2, \quad m' = \frac{(\alpha_2 + \alpha_3)}{\rho a^2} = \frac{m}{\rho a^2} \quad \text{and}$$

$$\sigma' = -\frac{2(\alpha_5 + \beta_1)\eta_0}{\rho^2 a^4} = \frac{\sigma\eta_0}{\rho^2 a^4},$$

where $\eta_0 = \alpha_1$, the zero shear viscosity. Thus changes in m' and σ' (for constant ρ and η_0) could be due to different non-Newtonian characteristics (m and σ values) or could result from a change in geometry, i.e. a change in the value of the radius a. Furthermore, a change in the radius brings about a relative change in m' and σ' due to their different dependence on a. The value of L depends on both a and the angular velocity Ω.

According to equations (2A.28), (2A.29) and (2A.38) the radial velocity profiles are influenced by m' and β only, for constant L. The curves presented in Figure 2-1

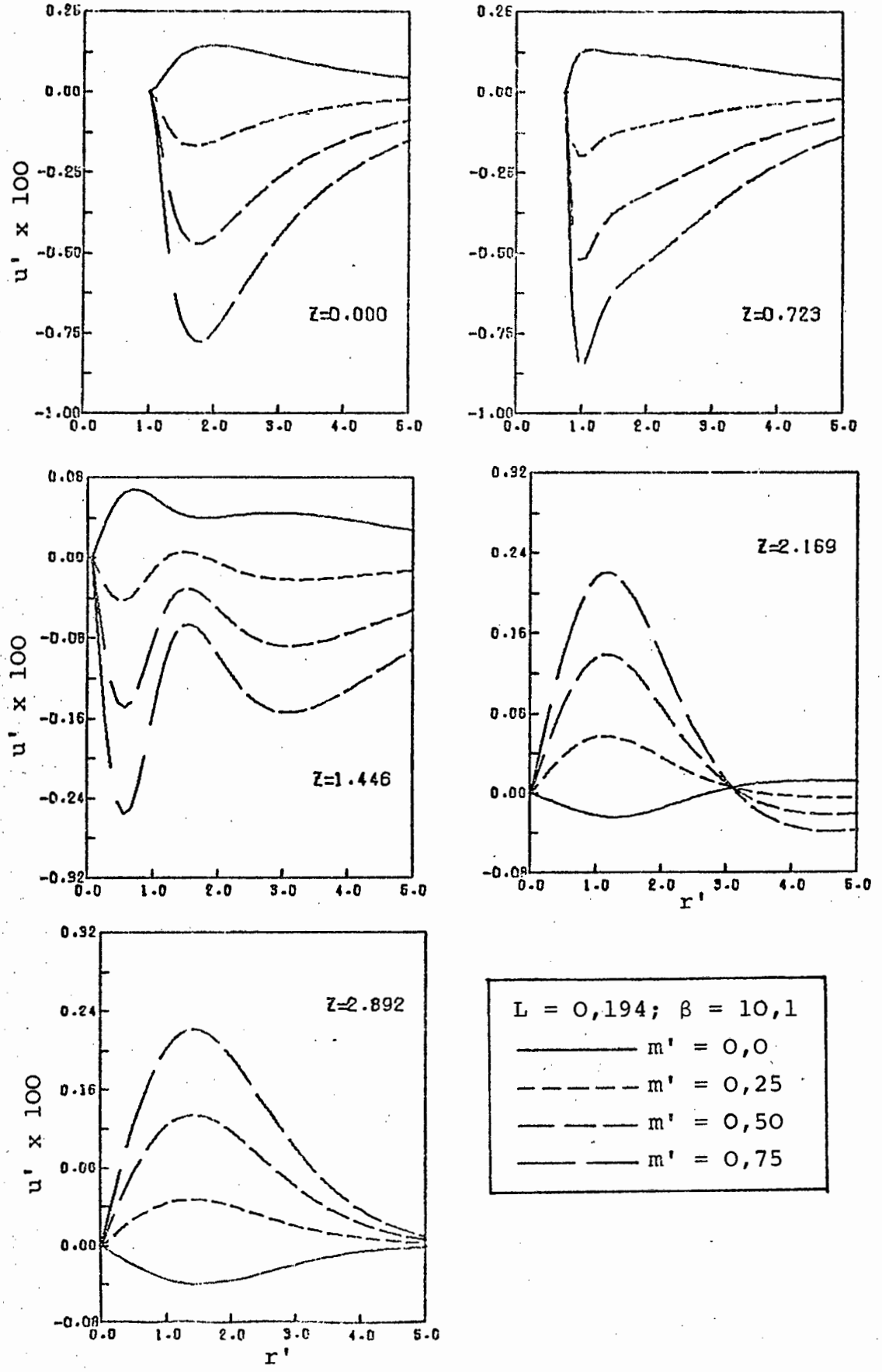

FIGURE 2-1 DIMENSIONLESS RADIAL VELOCITY PROFILES FOR THE ROTATING SPHERE

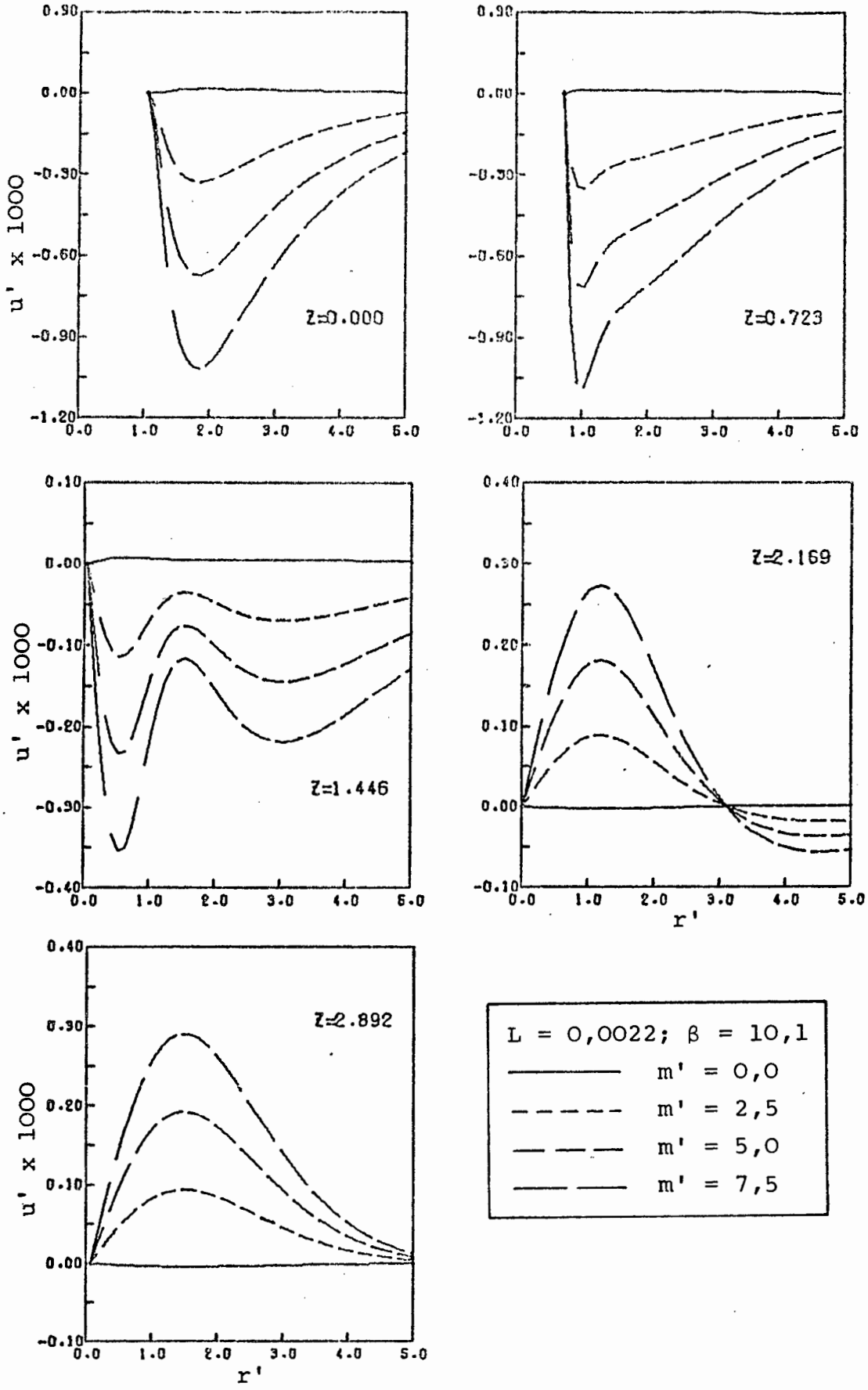

FIGURE 2-2 DIMENSIONLESS RADIAL VELOCITY PROFILES FOR THE ROTATING SPHERE

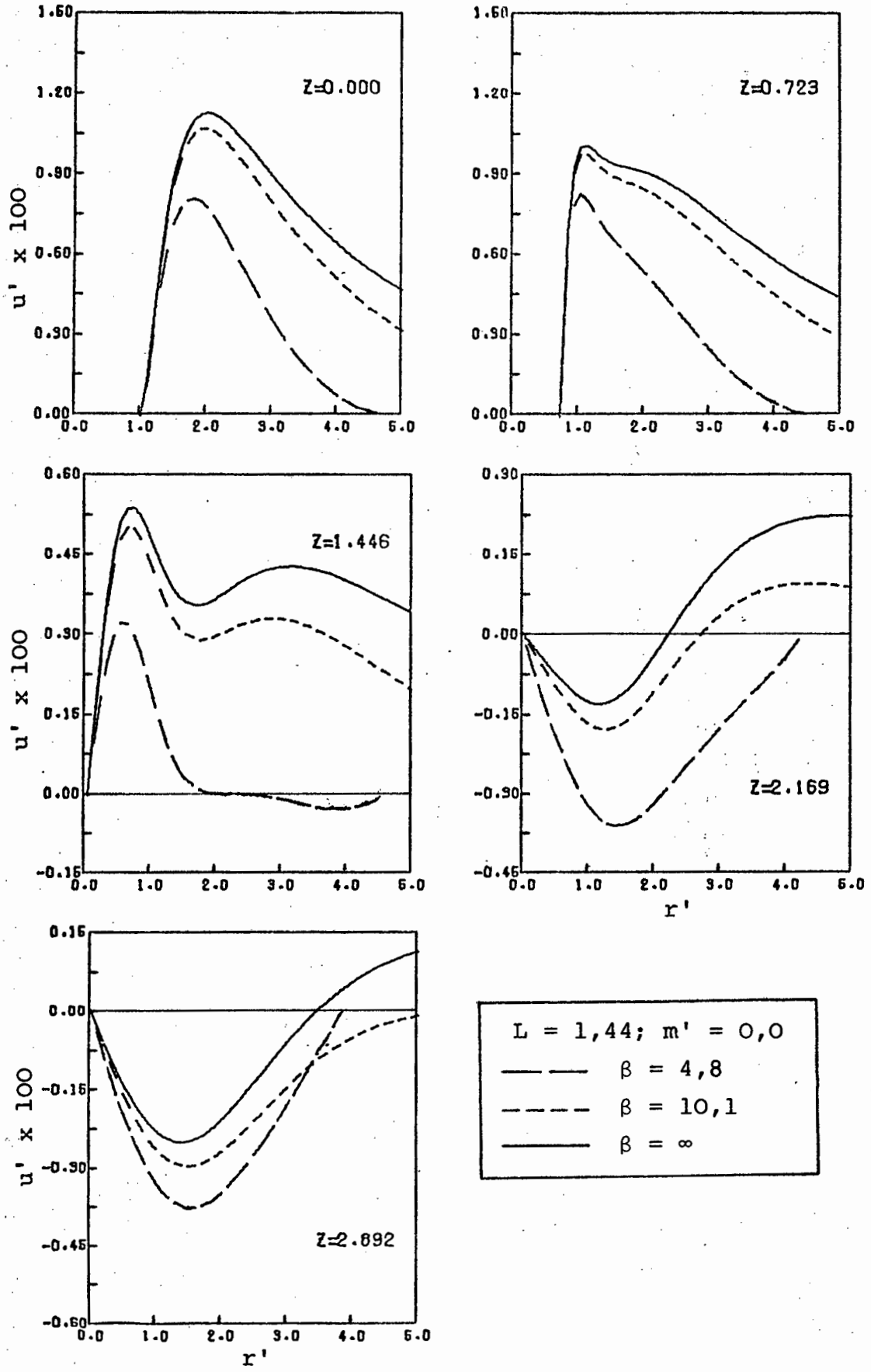

FIGURE 2-3 DIMENSIONLESS RADIAL VELOCITY PROFILES FOR THE ROTATING SPHERE

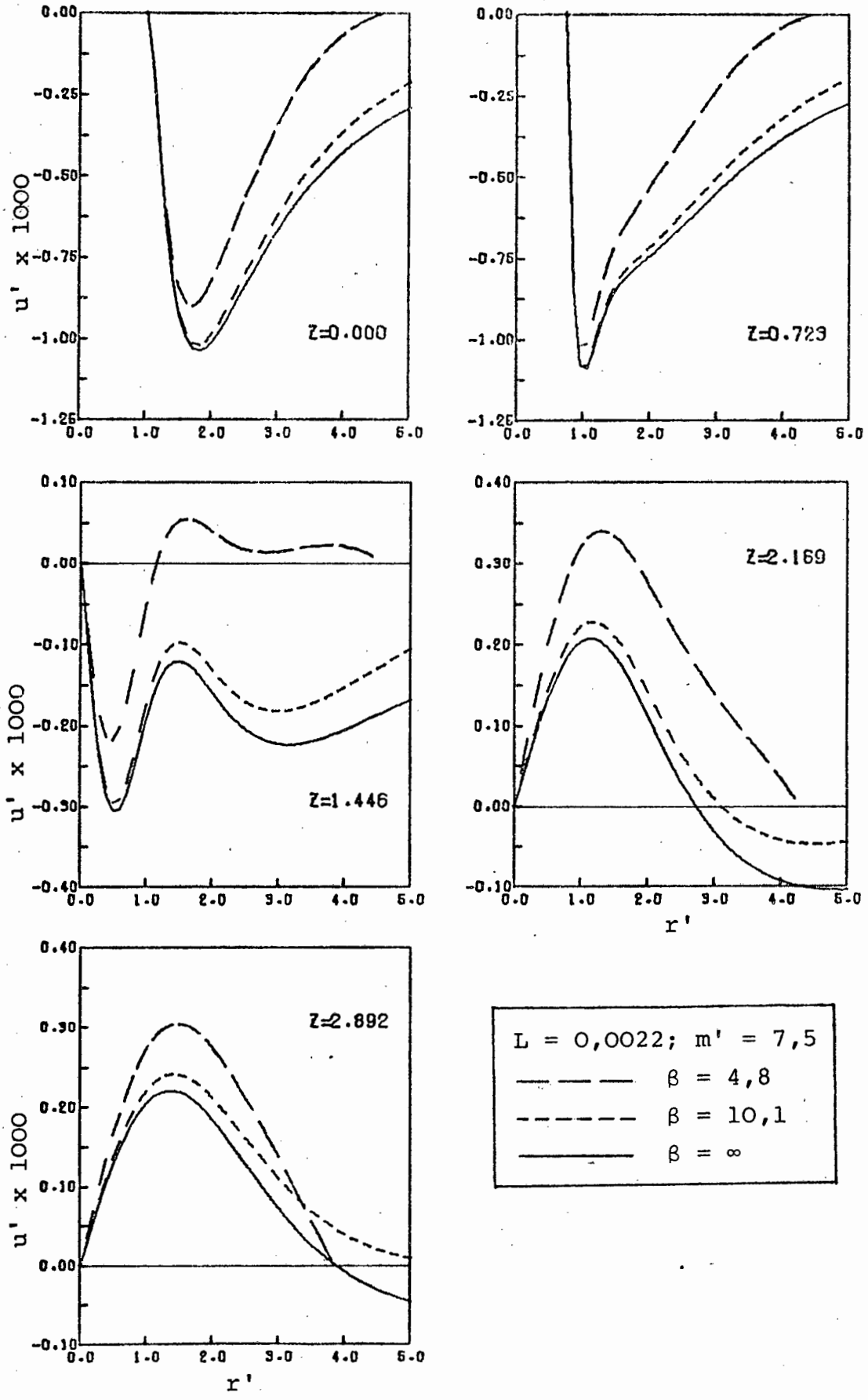

FIGURE 2-4 DIMENSIONLESS RADIAL VELOCITY PROFILES FOR THE ROTATING SPHERE

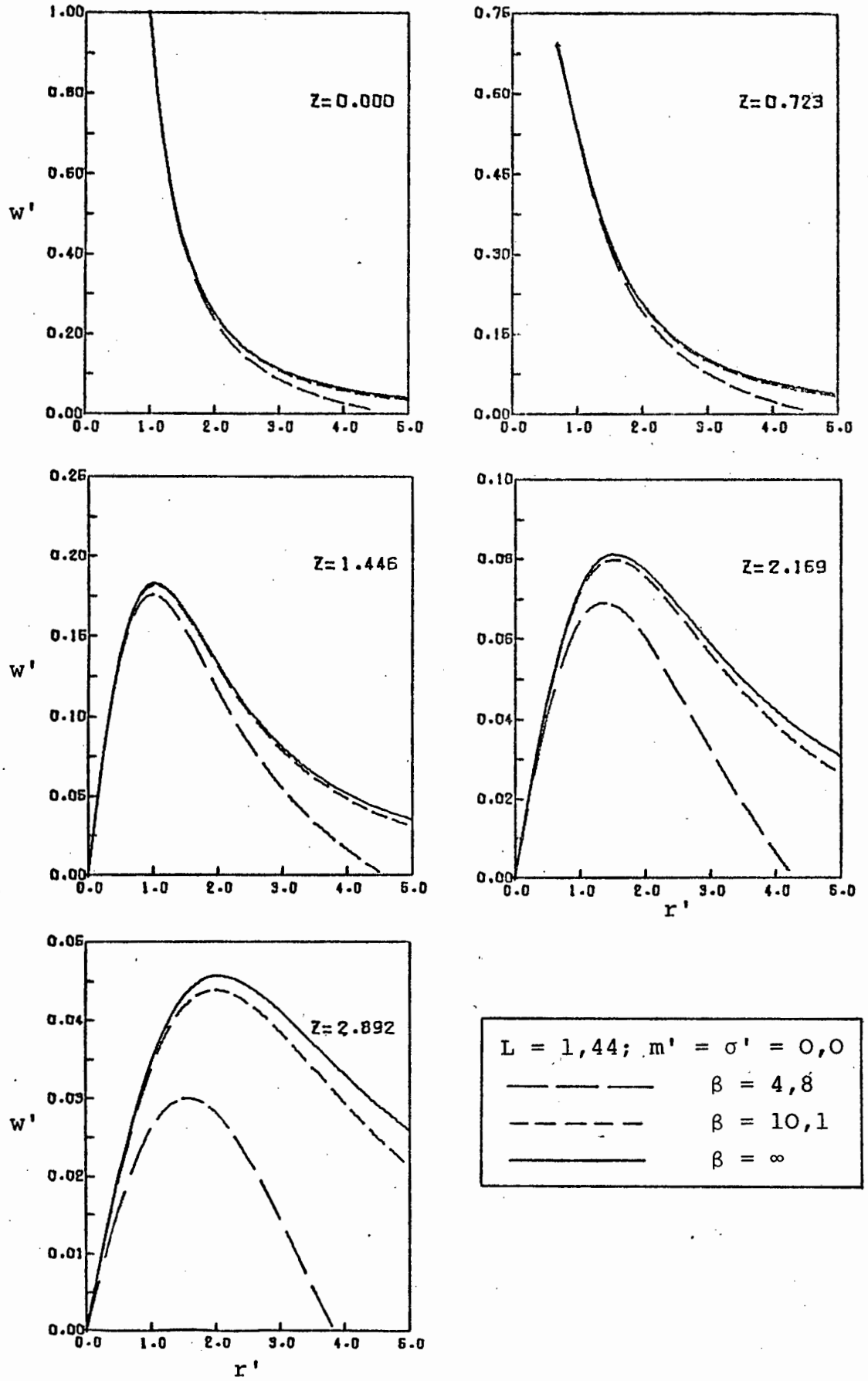

FIGURE 2-5 DIMENSIONLESS TANGENTIAL VELOCITY PROFILES FOR THE ROTATING SPHERE

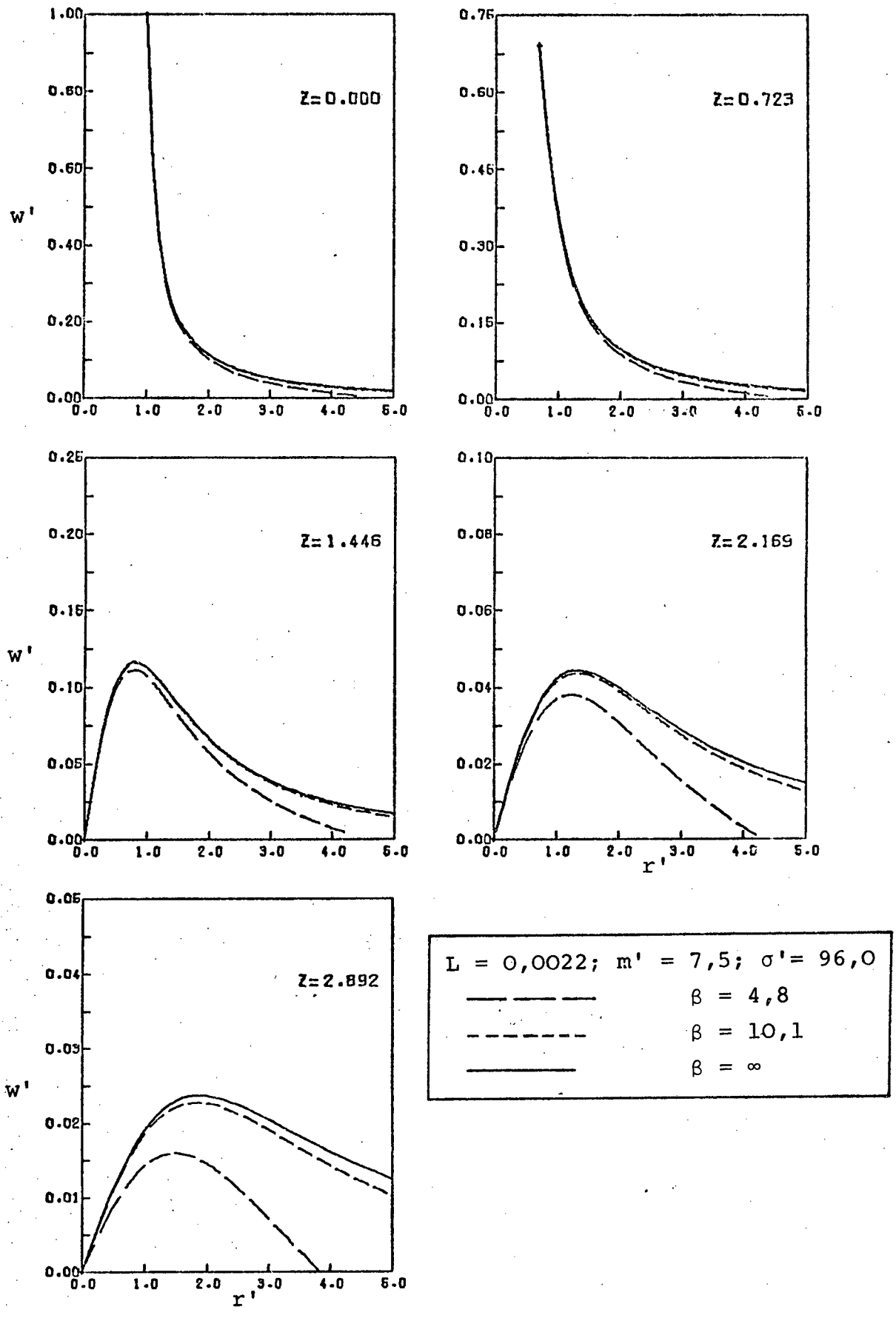

FIGURE 2-6 DIMENSIONLESS TANGENTIAL VELOCITY PROFILES FOR THE ROTATING SPHERE

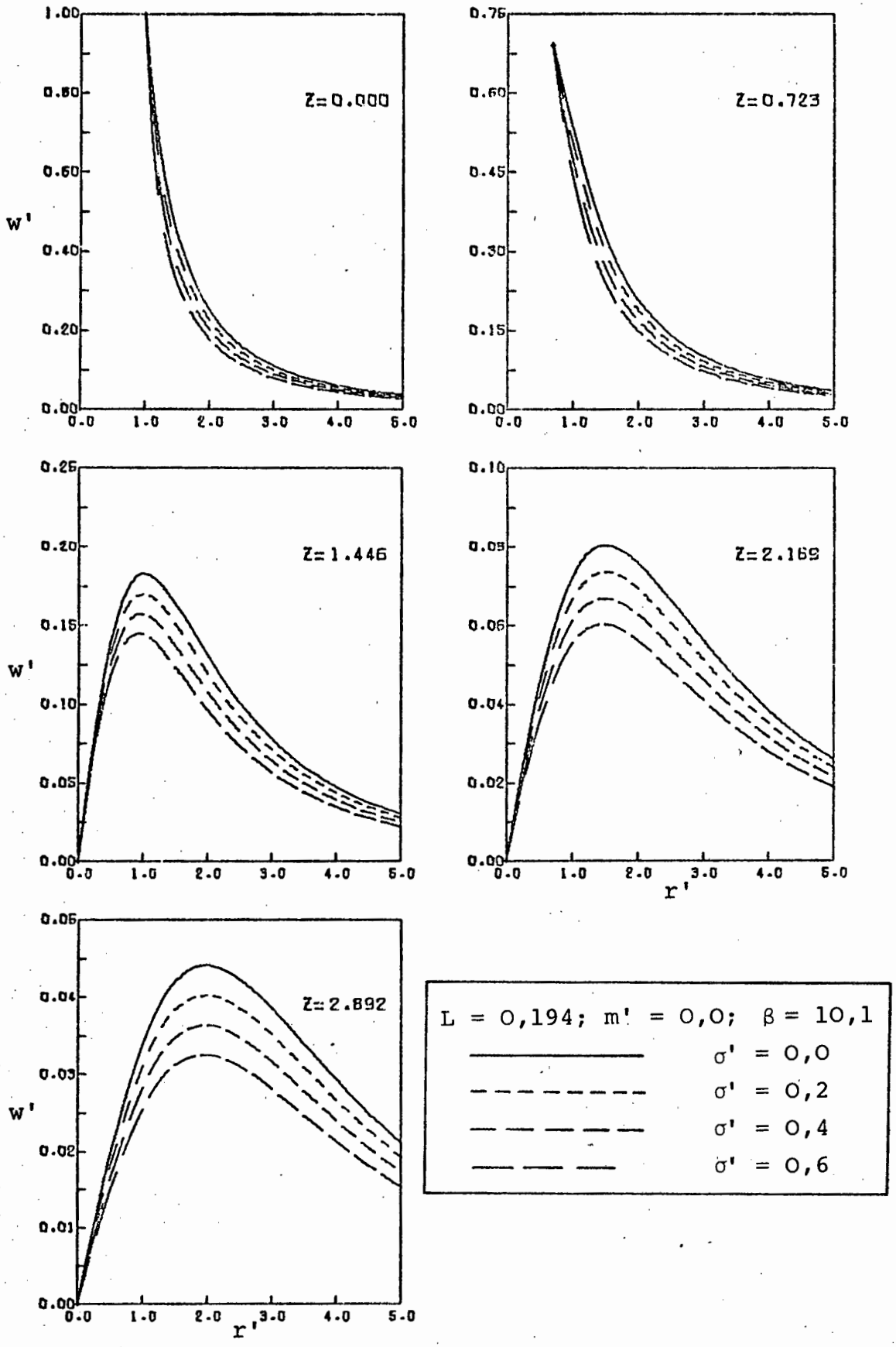

FIGURE 2-7 DIMENSIONLESS TANGENTIAL VELOCITY PROFILES FOR THE ROTATING SPHERE

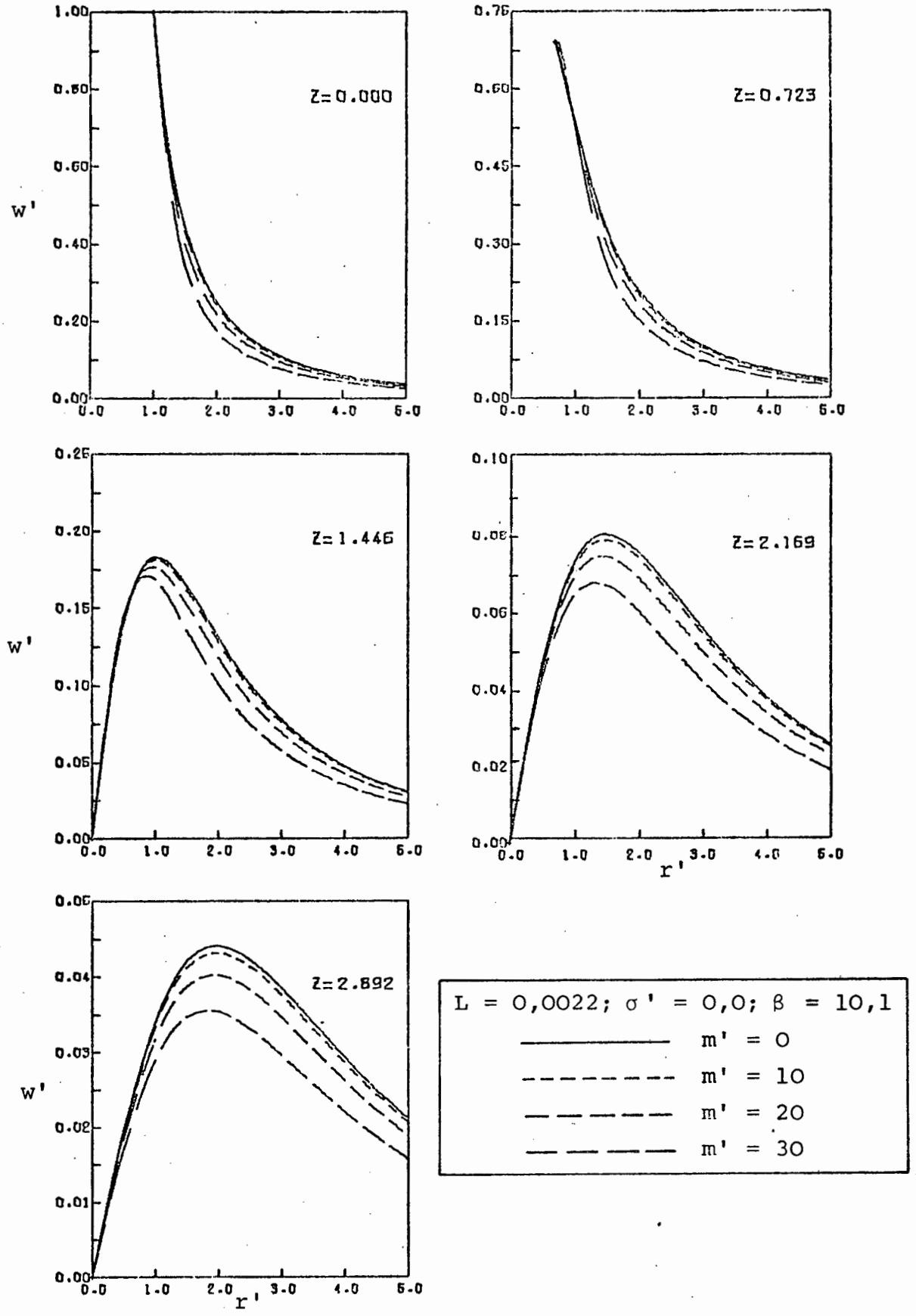

FIGURE 2-8 DIMENSIONLESS TANGENTIAL VELOCITY PROFILES FOR THE ROTATING SPHERE

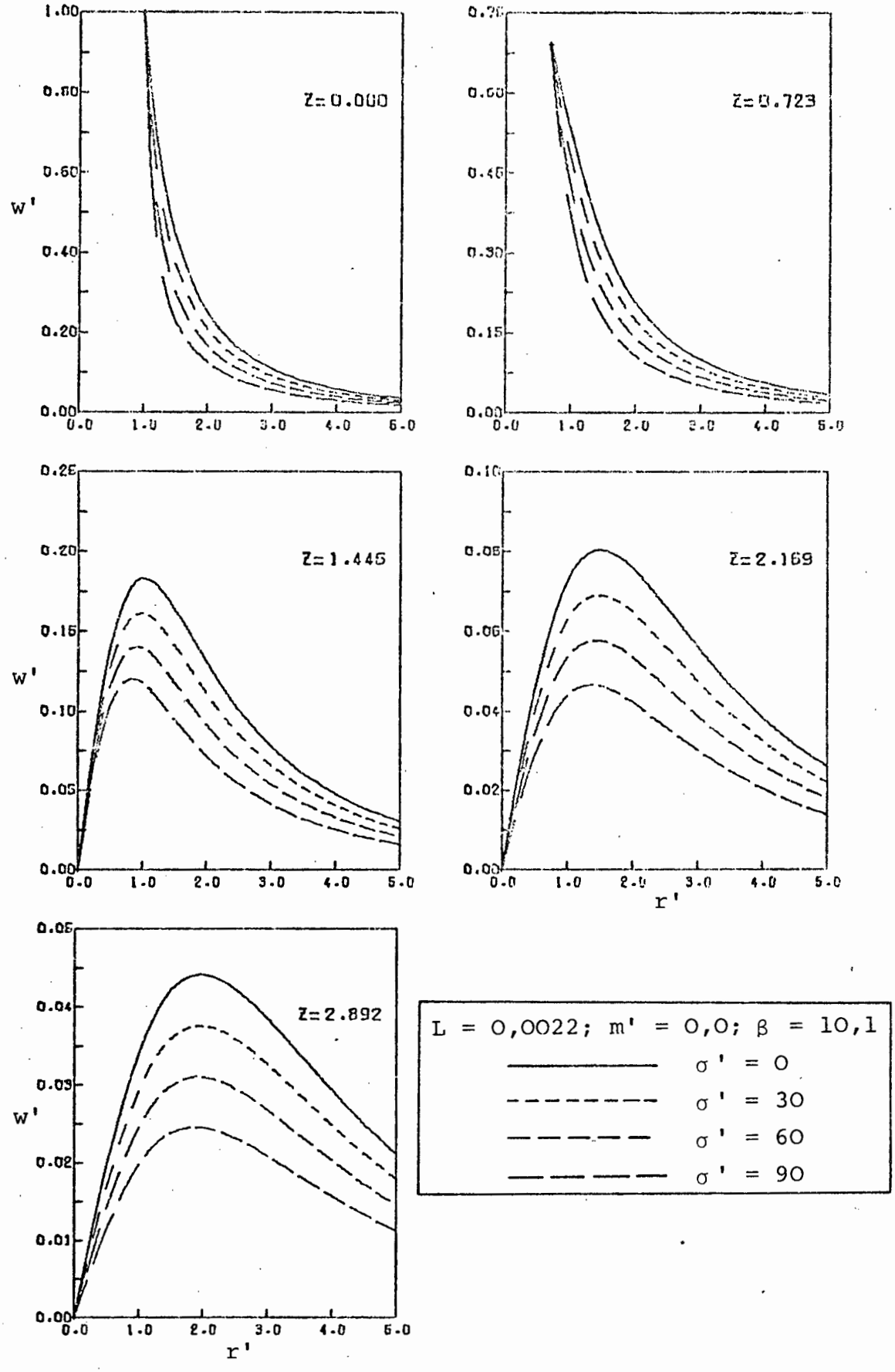

FIGURE 2-9 DIMENSIONLESS TANGENTIAL VELOCITY PROFILES FOR THE ROTATING SPHERE

are for values of L = 0,194 and β = 10,1. The range of m' values is from m' = 0, a Newtonian fluid, to m' = 0,75. The latter value corresponds to a moderately viscoelastic fluid and the curves for m' = 0 show clearly that inertial forces have a significant influence on the secondary flow for these values of L and m'.

The radial velocity profiles shown in Figure 2-2 are for L = 0,0022 and β = 10,1 values. The range of non-zero values of m' shown (m' = 2,5 to m' = 7,5) would occur only in very elastic fluids; the curves for m' = 0 show that inertial forces are negligible, as might be expected from the very low value of L. It is interesting to note that the flow patterns are similar to those of the moderately elastic fluids (Figure 2-1). However, the magnitude of the dimensionless velocities would be an order of magnitude greater if the same value of L (0,194) were used. The magnitude of the secondary velocity components appears to be nearly proportional to m' for m' > 0,25.

Figures 2-3 and 2-4 are sets of curves showing the effect of β on the radial velocity profiles for a Newtonian liquid and a highly viscoelastic liquid respectively. It is clear that, even for the relatively large value of β (10,1), the effect of the outer boundary on the velocity curves is significant. It appears that the influence on the Newtonian curves is somewhat greater than on the curves for a very viscoelastic liquid (m' = 7,5). As might be expected, the curves for β = 4,8 are substantially different from those for $\beta = \infty$ in both types of fluid.

The tangential velocity profiles are, for a given value of L, influenced by the parameters m', σ', and β. Figures 2-5 to 2-9 are presented to illustrate the effect of each of these parameters.

Figure 2-5 shows the effect of the parameter β on tangential velocity profiles for a Newtonian fluid. Figure 2-6 illustrates the effect of this parameter on a non-Newtonian fluid with a large value of σ' (96,0), i.e. strongly shear dependent viscosity behaviour. It is clear that the influence of an outer sphere at β = 10,1 is negligible provided that attention is confined to the region within five sphere radii of the inner sphere. The curves for β = 4,8 show that the relative influence of the outer sphere for the shear thinning non-Newtonian fluid is very similar to that of the Newtonian fluid. The presence of the outer sphere decreases the tangential velocity throughout the flow field.

Figure 2-7 shows the effect of the parameter σ' on the tangential velocity curves, for $\sigma' < 1$ and L = 0,194. Similar curves were drawn for m' values in the range $0 \leq m' \leq 1$ (at L = 0,194) and it was found that this parameter has a negligible influence on the velocity curves over this range of values. These curves are therefore not shown.

The curves shown in Figure 2-8 and 2-9 are for a very low value of L (0,0022). Figure 2-8 illustrates the fact that sufficiently large values of m' ($10 \leq m \leq 30$) have a significant effect on the tangential velocity profiles. While such large values of m' were not encountered in the experimental work reported in this thesis, they certainly appear to be possible [61]. The greater significance of m' relative to σ' for large values (m', $\sigma' >> 1$) is due to the presence of quadratic terms in m' in the equations for the tangential velocity, whereas σ' appears to the first power only. Similar behaviour is found when the expression for the couple on the sphere (Walters and Waters [39]) is examined. When m' = σ'=1,0, the contribution of the m' term is approximately 4% that of the σ' term.

But for $m' = \sigma' = 10,0$ the magnitude of the m' terms in the expression for the couple is approximately 55% that of the σ' terms, and m' becomes dominant for still larger values.

Figure 2-9 shows tangential velocity curves at high σ' values, in the range 0,0 to 90,0. It is clear that sufficiently large values of σ' can produce considerable departure from Newtonian behaviour, even at the low value of L of 0,0022. This point will again be discussed after the presentation of experimental data. Positive σ' values result in a more rapid decrease in the tangential velocity with radial distance than would occur in a Newtonian fluid.

2B.1 Velocity Profiles for the Flow about a Spheroid Rotating Slowly in a Simple Fluid

The analysis of the flow induced by the slow rotation of a finite disc in a viscoelastic liquid presents mathematical difficulties at the edge of the disc. Waters and King [40], following Jeffery [75], approached the problem by considering an ellipsoid of revolution rotating about its axis, then considering the disc as a degenerate case of the ellipsoid. A brief resume of this paper follows, using a similar nomenclature. Velocity profiles are then derived from the stream function.

The equations of state of the Simple Fluid of Coleman and Noll can be written in the form

$$p_{ik} = - pg_{ik} + p'_{ik} \qquad (2B.1)$$

$$p'_{ik}(\underset{\sim}{x},t) = F^{t}[G_{ik}(\underset{\sim}{x},t,t')] \qquad (2B.2)$$

where p'_{ik} is the stress tensor, p an arbitrary isotropic pressure, g_{ik} the metric tensor of a fixed co-ordinate system x^i, and F is an isotropic tensor valued functional.

G_{ik} is the Eulerian component of g_{ik}, also known as the history of the right Cauchy-Green strain tensor with respect to the present configuration. The variable t is the present time and $t' \leq t$.

An oblate spheroidal co-ordinate system (ξ, η, ϕ) may be defined in terms of a cylindrical polar co-ordinate system (r_1', ϕ', z_1) by the equations $z_1 = c \sinh\xi\cos\eta$, $r_1' = c\cosh\xi\sin\eta$. In dimensionless form:

$$z = \frac{z_1}{c} = \sinh\xi\cos\eta; \quad r' = \frac{r_1'}{c} = \cosh\xi\sin\eta \qquad (2B.3)$$

The surfaces ξ = constant are a family of oblate spheroids or ellipsoids of revolution having foci $z_1 = 0$, $r_1' = \pm c$. It is assumed that the oblate spheroid $(\xi = \xi_0)$ rotates slowly about its axis of revolution $(r_1' = 0)$, with angular velocity Ω, in an infinite expanse of the Simple Fluid which is at rest at infinity.

If the physical components of the velocity vector are U, V and W with respect to the oblate spheroidal co-ordinates (ξ, η, ϕ), the boundary conditions are

$$\left.\begin{aligned} U = V = 0, \quad W = \Omega c \cosh\xi\sin\eta \quad &\text{when } \xi = \xi_0 \\ U = V = W = 0 \quad &\text{when } \xi \to \infty \end{aligned}\right\} \qquad (2B.4)$$

Dimensionless velocities u, v and w may be defined by the equations

$$U = \frac{\alpha_1}{\rho c}u, \quad V = \frac{\alpha_1}{\rho c}v \quad \text{and} \quad W = \Omega c w, \qquad (2B.5)$$

where α_1 is the zero shear viscosity and ρ is the density of the fluid. The boundary conditions in terms of the dimensionless variables are

$$\left.\begin{aligned} u = v = 0, \quad w = \cosh\xi\sin\eta \quad &\text{when } \xi = \xi_0 \\ u = v = w = 0 \quad &\text{when } \xi \to \infty \end{aligned}\right\} \qquad (2B.6)$$

For the above boundary conditions the primary flow solution (very slow rotation) of the equations of motion, continuity and the equations of state (2B.1) and (2B.2) is given by

$$u = v = 0, \quad w = \frac{f(\xi)}{f(\xi_0)}\cosh\xi\sin\eta \tag{2B.7}$$

where $f(\xi) = \sinh\xi\,\mathrm{sech}^2\xi - \cot^{-1}(\sinh\xi)$

Waters and King [40] expanded the velocity components and the pressure in terms of L, where

$$L = \left(\frac{\Omega c^2 \rho}{\alpha_1}\right)^2 .$$

They showed that, to first order in L, the equation of state (2B.2) reduces to

$$\begin{aligned} p'_{ik} = {} & 2\alpha_1 e^{(1)}_{ik} + 2\alpha_2 e^{(2)}_{ik} + 4\alpha_3 e^{(1)}_{i}{}^{j} e^{(1)}_{jk} \\ & + 8\beta_1 e^{(1)}_{j}{}^{l} e^{(1)}_{l}{}^{j} e^{(1)}_{ik} + 4\alpha_5 (e^{(1)}_{i}{}^{j} e^{(2)}_{jk} \\ & + e^{(2)}_{i}{}^{j} e^{(1)}_{jk}), \end{aligned} \tag{2B.8}$$

where α_1, α_2, α_3, β_1 and α_5 are material constants; $e^{(1)}_{ik}$ and $e^{(2)}_{ik}$ are the first and second rate-of-strain tensors defined by Oldroyd [5]. Since the Rivlin-Ericksen tensors (defined in Section 2A) are exactly twice the Oldroyd rate of strain tensors, equation (2B.8) is identical to equation (2A.21), the equation for a Rivlin-Ericksen fluid for the slow flow conditions under discussion. (See Kelkar et al [3] for further discussion of this remark; also cf. Walters and Waters [24]).

From the equation of continuity in oblate spheroidal

co-ordinates, a stream function χ may be defined by the equations

$$u = -\frac{1}{h\cosh\xi\sin\eta}\frac{\partial\chi}{\partial\eta}$$
$$v = \frac{1}{h\cosh\xi\sin\eta}\frac{\partial\chi}{\partial\xi} \quad , \tag{2B.9}$$

where $h = \cosh^2\xi - \sin^2\eta$

Waters and King obtained a solution for the stream function, given by the following equations.

$$\chi = L\chi_1 = L\sin^2\eta\cos\eta\{h^2F(\xi) + G(\xi)\} \quad , \tag{2B.10}$$

where F and G are defined as follows.

Let $\mu = \sinh\xi$ and $\mu_0 = \sinh\xi_0$.

$$F(\xi) = F(\sinh^{-1}\mu) = A_1'F_1(\mu) + A_2'F_2(\mu) + F_3(\mu) \tag{2B.11}$$

$$G(\xi) = G(\sinh^{-1}\mu) = B_1' + B_2'F_2(\mu) + H(\mu) \tag{2B.12}$$

where $H(\mu) = A_1'H_1(\mu) + A_2'H_2(\mu) + H_3(\mu) + m'H_4(\mu)$ (2B.13)

and
$$F_1(\mu) = 7\mu^4 + \frac{23}{3}\mu^2 + \frac{16}{15} - \mu(7\mu^4 + 10\mu^2 + 3)\cot^{-1}\mu,$$
$$F_2(\mu) = \mu^2 + \frac{2}{3} - \mu(1+\mu^2)\cot^{-1}\mu,$$
$$F_3(\mu) = \{f(\xi_0)\}^{-2}\{\frac{9}{8}\mu^3 + \mu - \frac{1}{4}(9\mu^4 + 11\mu^2 + 2)\cot^{-1}\mu + \frac{1}{8}\mu(9\mu^4 + 14\mu^2 + 5)(\cot^{-1}\mu)^2\},$$
$$H_1(\mu) = -7\mu^6 - \frac{32}{3}\mu^4 - \frac{46}{15}\mu^2 + \frac{2}{5} + \mu^3(7\mu^4 + 13\mu^2 + 6)\cot^{-1}\mu,$$
$$H_2(\mu) = -2\mu^4 - \frac{4}{3}\mu^2 + \frac{4}{9} + 2\mu^3(1 + \mu^2)\cot^{-1}\mu,$$
$$H_3(\mu) = \mu\{f(\xi_0)\}^{-2}\{-\frac{9}{8}\mu^4 - \frac{13}{8}\mu^2 - \tfrac{1}{2} + \frac{1}{4}\mu(9\mu^4 + 16\mu^2 + 7)\cot^{-1}\mu - \tfrac{1}{8}(9\mu^6 + 19\mu^4 + 11\mu^2 + 1)(\cot^{-1}\mu)^2\}, \tag{2B.14}$$

$$H_4(\mu) = 2\{f(\xi_0)^{-2}\{\mu - (1 + 2\mu^2)\cot^{-1}\mu + \mu(1 + \mu^2)(\cot^{-1}\mu)^2\},$$

$$A_1' = \frac{F_3'(\mu_0)F_2(\mu_0) - F_2'(\mu_0)F_3(\mu_0)}{F_2'(\mu_0)F_1(\mu_0) - F_1'(\mu_0)F_2(\mu_0)}$$

$$A_2' = \frac{F_3'(\mu_0)F_1(\mu_0) - F_1'(\mu_0)F_3(\mu_0)}{F_1'(\mu_0)F_2(\mu_0) - F_2'(\mu_0)F_1(\mu_0)} \qquad (2B.15)$$

$$B_1' = \frac{H'(\mu_0)F_2(\mu_0) - F_2'(\mu_0)H(\mu_0)}{F_2'(\mu_0)}$$

$$B_2' = \frac{-H'(\mu_0)}{F_2'(\mu_0)} \qquad (2B.16)$$

The elastic parameter m' in equation (2B.13) is defined in terms of the coefficients in equations (2B.8):

$$m' = \frac{(\alpha_2 + \alpha_3)}{\rho c^2} .$$

The primes on the functions H, F_1, F_2 and F_3 in equations (2B.15) and (2B.16) denote differentiation with respect to ξ.

In order to compare the results of this theoretical analysis with the experimental radial velocity data for flow around the rotating disc, it is necessary to obtain expressions for the radial velocity component u' in terms of a cylindrical polar co-ordinate system. Equation (2B.6) for the stream function is used as a starting point.

By the definition of the stream function in cylindrical co-ordinates (r', ϕ, z),

$$u' = -\frac{1}{r'}\frac{\partial \chi}{\partial z} . \qquad (2B.17)$$

Since χ is a function of ξ and η and both ξ and η are functions of z, equation (2B.17) becomes

$$u' = -\frac{1}{r'}\left[\frac{\partial\chi}{\partial\xi}\frac{\partial\xi}{\partial z} + \frac{\partial\chi}{\partial\eta}\frac{\partial\eta}{\partial z}\right]. \qquad (2B.18)$$

The terms $\frac{\partial\xi}{\partial z}$ and $\frac{\partial\eta}{\partial z}$ are obtained by differentiating equations (2B.3) implicitly with respect to z:

$$\frac{\partial\xi}{\partial z} = \frac{\cos\eta\,\cosh\xi}{(\cosh^2\xi\cos^2\eta + \sinh^2\xi\sin^2\eta)} \qquad (2B.19)$$

$$\frac{\partial\eta}{\partial z} = \frac{-\sin\eta\sinh\xi}{(\cosh^2\xi\cos^2\eta + \sinh^2\xi\sin^2\eta)} \qquad (2B.20)$$

The $\frac{\partial\chi}{\partial\xi}$ and $\frac{\partial\chi}{\partial\eta}$ terms are obtained by differentiating equation (2B.8) appropriately:

$$\frac{\partial\chi}{\partial\xi} = L\sin^2\eta\cos\eta\left[\frac{\partial(h^2)}{\partial\xi}F(\xi) + h^2F'(\xi) + G'(\xi)\right] \qquad (2B.21)$$

$$\frac{\partial\chi}{\partial\eta} = L\left\{\sin\theta(2 - 3\sin^2\theta)\left[h^2F(\xi) + G(\xi)\right] + \sin^2\eta\cos\eta\frac{\partial}{\partial\eta}(h^2)F(\xi)\right\}, \qquad (2B.22)$$

where $\frac{\partial}{\partial\xi}(h^2) = 2\cosh\xi\sinh\xi$

and $\frac{\partial}{\partial\eta}(h^2) = -2\sin\eta\cos\eta.$

The terms $F'(\xi)$ and $G'(\xi)$ are calculated by a lengthy but straightforward differentiation of equations (2B.11) to (2B.14), and are given in Appendix C. The radial velocity component is thus given by equations (2B.18) to (2B.22), but in terms of the oblate spheroidal co-ordinates.

In order to obtain the radial velocity u' as a function of r' and z (rather than ξ and η) we require ξ and η as functions of r' and z.
From equations (2B.3),

$$\cosh\xi = \frac{r'}{\sin\eta} \quad \text{and} \quad \sinh\xi = \frac{z}{\cos\eta} \qquad (2B.23)$$

The hyperbolic functions are related by the equation

$$\cosh^2\xi - \sin^2\xi = 1 . \qquad (2B.24)$$

Equations (2B.23) and (2B.24) may be solved to give the following expression for $\sin\eta$:

$$\sin\eta = \frac{1}{\sqrt{2}} [1 + r'^2 + z^2 - ((1 + r'^2 + z^2)^2 - 4r'^2)^{\frac{1}{2}}]^{\frac{1}{2}} \qquad (2B.25)$$

The square root signs imply the positive square root. Having determined $\sin\eta$,

$$\cosh\xi = \frac{r'}{\sin\eta} \qquad (2B.26)$$

may be calculated. Thus for a given (r', z), η and ξ may be calculated from equations (2B.25) and (2B.26) and equations (2B.18) to (2B.22) can be used to calculate the radial velocity u'.

The ellipsoid of revolution becomes a disc when $\xi_0 = 0$. In this case $c = a$, the radius of the disc and the theoretical curves for u' can then be compared with experimental data for various values of the elastic parameter m'.

It should be noted that at the edge of the disc, $z = 0$ and $r' = 1$. Hence

$$\sinh\xi = 0, \quad \cosh\xi = 1,$$

$$\sin\eta = 1 \text{ and } \cos\eta = 0.$$

Equations (2B.19) and (2B.20) are therefore not defined as the denominators become zero. However, it can easily be shown that as $\xi \to 0$, $\frac{\partial\xi}{\partial z}$ and $\frac{\partial\eta}{\partial z} \to 0$; thus the singularity can be removed and $u' = 0$ at the edge of the disc.

2B.2 Presentation and Discussion

The theoretical radial velocity curves are shown in Figures 2-10 and 2-11 in order to illustrate the effect of the elastic parameter m'. As was done for the sphere theoretical velocity profiles, the z planes and the L values were chosen to coincide with those used in the experimental investigation and the range of m' values was chosen to span the experimentally determined values. The velocity profiles shown in Figure 2-10 are for L = 0,194 and m' values in the range 0,0 to 0,75 and the profiles shown in Figure 2-11 are for L = 0,018 and m' values in the range 0,0 to 3,0. It should be noted that the curves are valid only for a disc rotating in an infinite sea of fluid. A comparison of Figures 2-10 and 2-1 shows that the radial velocity component for the disc in the z = 0 plane is approximately twice that for the sphere, for the same value of m'. The velocity curves for different m' values are similar in shape (for $m' \geq 0,25$) but the magnitude changes considerably.

2C THE CONFORMAL MAPPING TECHNIQUE

At the start of the work reported in this thesis (1970), no analytical solution to the problem of a finite disc rotating in a viscoelastic fluid had been published. A conformal mapping technique was then proposed in an attempt to obtain the axial and radial velocity components in the disc flow field from the corresponding sphere problem. Comparison of the radial velocity profiles predicted by the conformal map with early experimental results for the rotating disc showed reasonable agreement. However, in August 1971, Waters and King published an analytical solution to the rotating disc problem, which was discussed in the

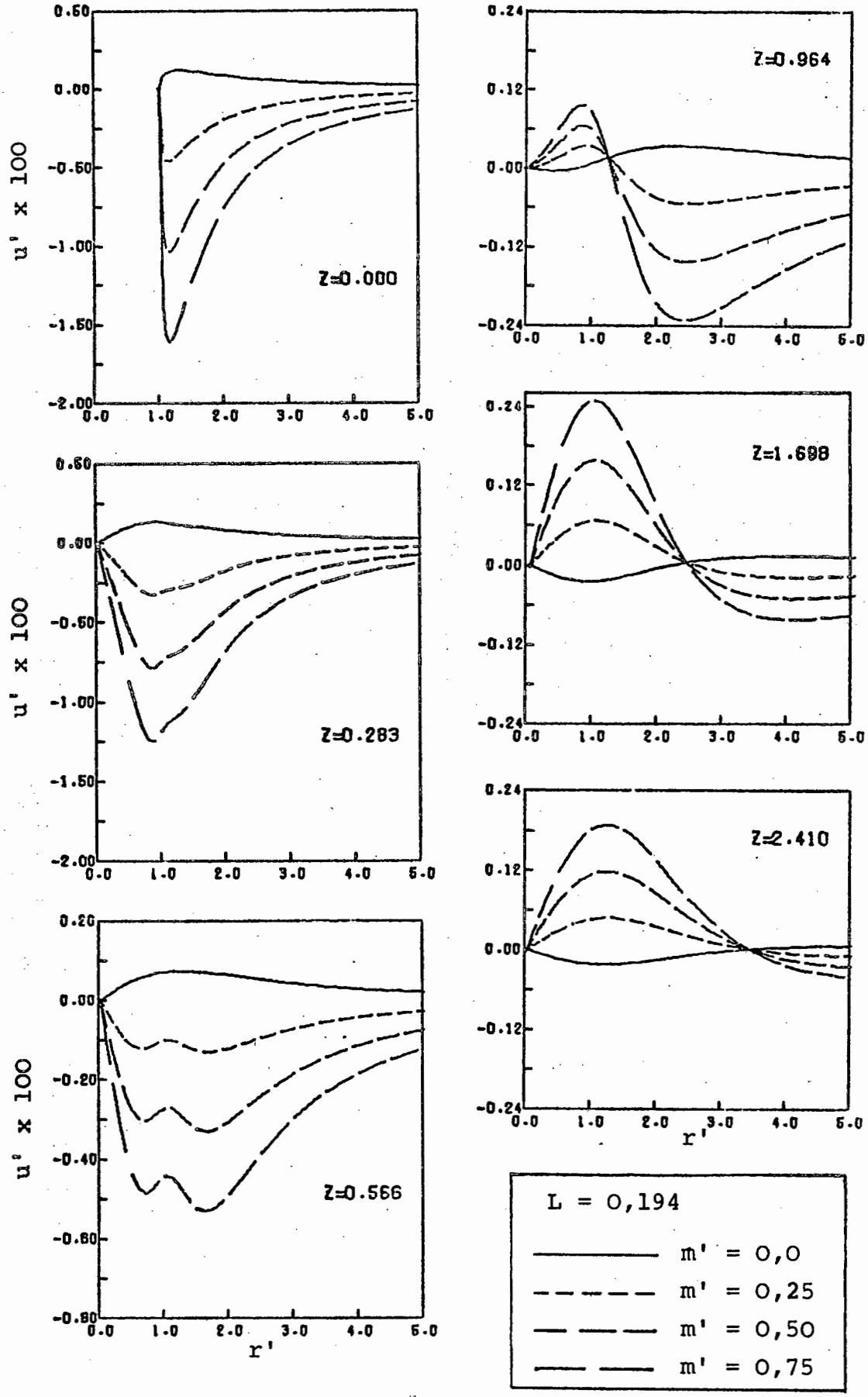

FIGURE 2-10 DIMENSIONLESS RADIAL VELOCITY PROFILES FOR THE ROTATING DISC

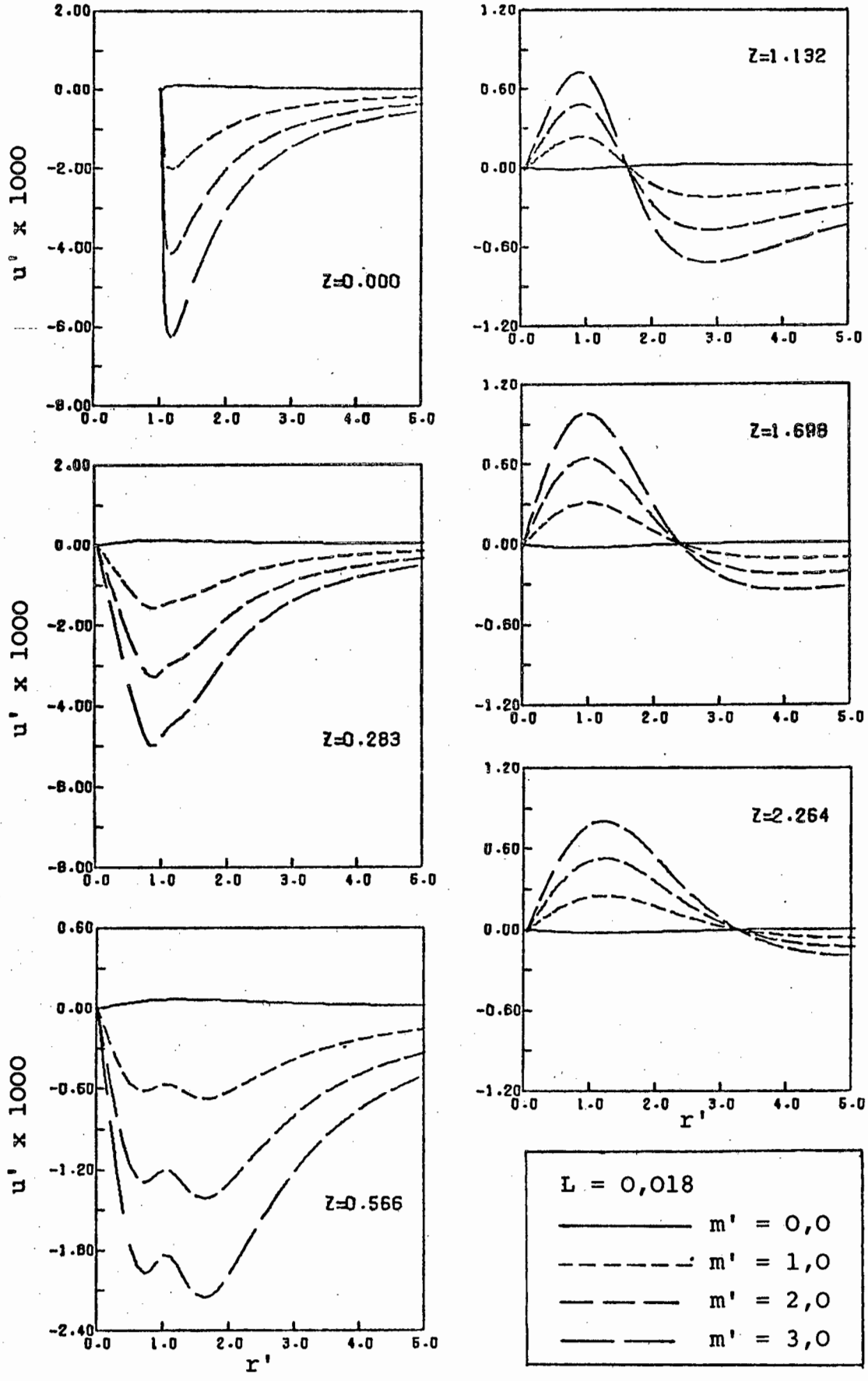

FIGURE 2-11 DIMENSIONLESS RADIAL VELOCITY PROFILES FOR THE ROTATING DISC

previous section. It is thus of interest to compare the results of the two methods.

The classical application of conformal mapping techniques is in the analysis of two dimensional potential or inviscid flows. This approach has practical value in the study, for example, of flow outside the boundary layer of two-dimensional aerofoils at high Reynolds number [76]. In this case it is assumed that, outside of a thin boundary layer, viscous forces are negligible and inertial forces dominate. In the present case of flow around a slowly rotating disc or sphere in a viscoelastic fluid, viscous forces obviously play a large part in the flow field as a whole. However, the secondary flows in a plane through the axes of rotation are generated by inertial and elastic forces. The velocity components in this plane are very much smaller than the tangential velocities, and if the flow in this plane is regarded as independent of the third velocity component, its vorticity is small. This provides a somewhat heuristic argument for regarding the flow in a plane through the axes of rotation is a two dimensional potential flow. However, there are obvious shortcomings in the above argument and the basic test is therefore whether or not the proposed application of the conformal mapping technique provides useful information. It will be shown that the map predicts velocity profiles which are in qualitative agreement with those predicted by the rigorous analysis of Waters and King. Quantitative agreement is good, except in the region near the edge of the disc, and thus the map may be used to estimate 'wall effects' on the velocity profiles.

2C.1 Theoretical Development

We assume the projection of the three dimensional velocity vector onto a plane through the axis of rotation of the sphere or the disc to be a two dimensional potential flow. We also assume the existence of a solution to the rotating sphere problem, thus giving the velocity components U_x and U_y (Cartesian co-ordinates will be used throughout this section) in the plane through the axis of rotation. As a result of the potential flow assumption, a potential function Φ and a stream function Ψ may be postulated, as defined by the equations

$$U_x = \frac{\partial \Phi}{\partial x}, \qquad U_y = \frac{\partial \Phi}{\partial y} \tag{2C.1}$$

$$U_x = \frac{\partial \Psi}{\partial y}, \qquad U_y = -\frac{\partial \Psi}{\partial x} \tag{2C.2}$$

Let $w = x + iy$. The complex potential function

$$F(w) = \Phi(x,y) + i\Psi(x,y) \tag{2C.3}$$

is holomorphic since the Cauchy-Riemann conditions are automatically satisfied by equations (2C.1) and (2C.2).

That is $\frac{\partial \Phi}{\partial x} = \frac{\partial \Psi}{\partial y}$ and $\frac{\partial \Phi}{\partial y} = -\frac{\partial \Psi}{\partial x}$ (2C.4)

Furthermore, the potential flow assumption is also automatically satisfied:

$$\underset{\sim}{\nabla} \times \underset{\sim}{U} = \frac{\partial U_x}{\partial x} - \frac{\partial U_y}{\partial y}$$

$$= \frac{\partial^2 \Phi}{\partial x \partial y} - \frac{\partial^2 \Phi}{\partial y \partial x} = 0, \quad \text{since } \Phi \text{ is by}$$

definition continuous and differentiable.
Thus, for a suitable U_x and U_y, $F(w)$ describes a hypothetical flow net about a 'circle', i.e. the two-dimensional projection of a sphere. It is necessary

to obtain the corresponding velocity components $U_{x'}$ and $U_{y'}$ for the flow about a 'straight line', i.e. the two dimensional projection of the disc.

The conformal transformation

$$\zeta(x',y') = \frac{1 + w}{2w} \qquad (2C.5)$$

maps the upper arc of the unit circle onto a line of length two units. The lower arc is also mapped onto the same line. Figure 2-12 illustrates the mapping.

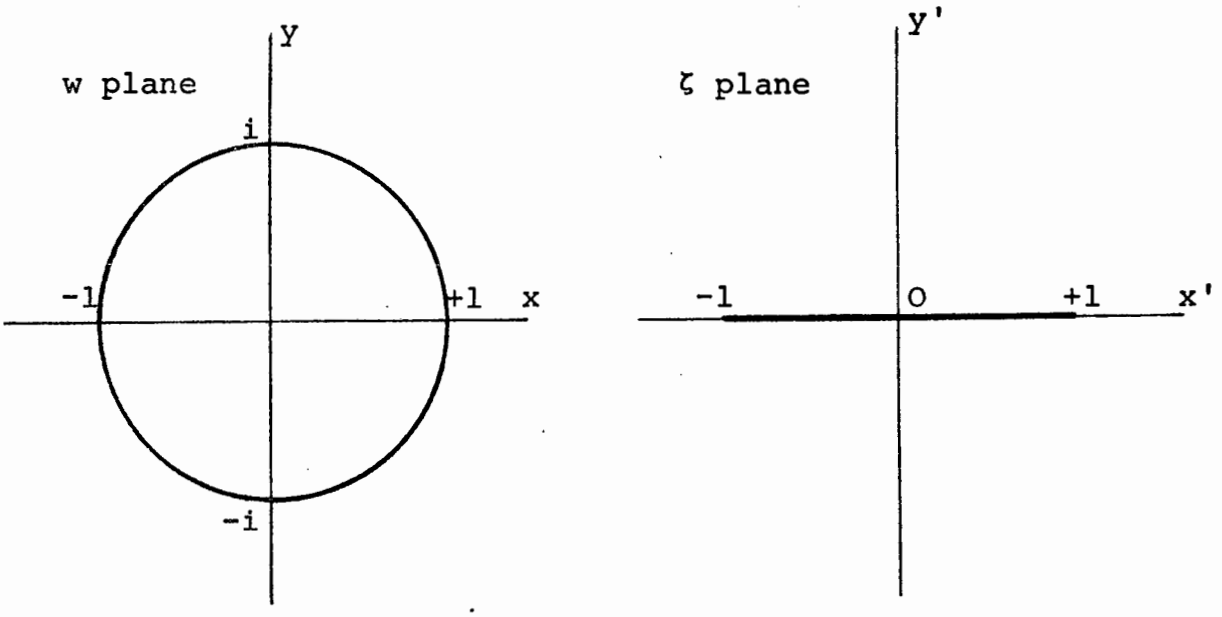

FIGURE 2-12 THE CONFORMAL TRANSFORMATION

The region of the upper half-plane exterior to the unit circle is mapped onto the upper half-plane of the ζ plane. The fixed points are $y = 0$, $x = \pm 1$ and $w = \infty$. The map is symmetrical about both the real and

the imaginary axes [77, 78]. Thus the function ζ transforms the two-dimensional projection of the sphere, the unit circle, onto the two-dimensional projection of the disc, a straight line of length two units and centre at the origin.

It is useful to consider the image of a circle, say $\gamma_c = |\gamma_c|e^{i\theta}$, $|\gamma_c| > 1$, under this mapping. Applying the transformation equation (2C.5), the following expressions are obtained:

$$x' = \tfrac{1}{2}(|\gamma_c| + 1/|\gamma_c|)\cos\theta$$
$$\text{and} \quad y' = \tfrac{1}{2}(|\gamma_c| - 1/|\gamma_c|)\sin\theta \qquad (2C.6)$$

Eliminating θ yields

$$\frac{x'^2}{[\tfrac{1}{2}(|\gamma_c| + 1/|\gamma_c|)]^2} + \frac{y'^2}{[\tfrac{1}{2}(|\gamma_c| - 1/|\gamma_c|)]^2} = 1 \qquad (2C.7)$$

This is the equation of an ellipse, with major axis of length $(|\gamma_c| + 1/|\gamma_c|)$ and minor axis of length $(|\gamma_c| - 1/|\gamma_c|)$. It may easily be shown that the region between the unit circle and the circle of radius $|\gamma_c|$ is mapped onto the region external to the unit circle and bounded by the ellipse defined by equation (2C.7). Thus the mapping, equation (2C.5) may be used to transform the situation of a unit sphere rotating within an outer concentric spherical shell into that of a unit disc rotating within an ellipsoid of revolution.

We would like to obtain the complex potential function, $F'(\zeta) = F'(x' + iy')$ which describes flow around the disc by using equations (2C.3) and (2C.5). The velocity components for the disc are defined by the equations

$$U_{x'} = \frac{\partial\Phi}{\partial x'}, \qquad \text{and} \quad U_{y'} = \frac{\partial\Phi}{\partial y'}, \qquad (2C.8)$$

As we do not have x and y as explicit functions of x' and y', implicit differentiation must be resorted to:

$$U_{x'} = \frac{\partial \Phi(x,y)}{\partial x'} = \frac{\partial \Phi}{\partial x}\frac{\partial x}{\partial x'} + \frac{\partial \Phi}{\partial y}\frac{\partial y}{\partial x'}$$

$$= U_x \frac{\partial x}{\partial x'} + U_y \frac{\partial y}{\partial x'} \qquad (2C.9)$$

Similarly

$$U_{y'} = \frac{\partial \Phi(x,y)}{\partial y'} = U_x \frac{\partial x}{\partial y'} + U_y \frac{\partial y}{\partial y'} \qquad (2C.10)$$

Now $w = x + iy$, thus the following equations may be obtained from equation (2C.5):

$$\left.\begin{aligned} x' &= \tfrac{1}{2}x\left(1 + \frac{1}{x^2 + y^2}\right) \\ y' &= \tfrac{1}{2}y\left(1 - \frac{1}{x^2 + y^2}\right) \end{aligned}\right\} \qquad (2C.11)$$

Differentiation of equations (2C.11) implicitly with respect to x' and solving for $\frac{\partial x}{\partial x'}$, and $\frac{\partial y}{\partial y'}$, yields

$$\left.\begin{aligned} \frac{\partial x}{\partial x'} &= \frac{2\rho^4(\rho^4 - \rho^2 + 2y^2)}{[4x^2y^2 + (\rho^4 + \rho^2 - 2x^2)(\rho^4 - \rho^2 + 2y^2)]} \\ \text{and} \\ \frac{\partial y}{\partial x'} &= \frac{-4\rho^4 xy}{[4x^2y^2 + (\rho^4 + \rho^2 - 2x^2)(\rho^4 - \rho^2 + 2y^2)]} \end{aligned}\right\} \qquad (2C.12)$$

where $\rho^2 = x^2 + y^2$. The expressions for $\frac{\partial x}{\partial y'}$, and $\frac{\partial y}{\partial y'}$, are similarly obtained:

$$\left.\begin{aligned} \frac{\partial x}{\partial y'} &= \frac{4xy\rho^4}{[4x^2y^2 + (\rho^4 + \rho^2 - 2x^2)(\rho^4 - \rho^2 + 2y^2)]} \\ \frac{\partial y}{\partial y'} &= \frac{2\rho^4(\rho^4 + \rho^2 - 2x^2)}{[4x^2y^2 + (\rho^4 + \rho^2 - 2x^2)(\rho^4 - \rho^2 + 2y^2)]} \end{aligned}\right\} \qquad (2C.13)$$

In order to obtain x and y for a given x' and y' (i.e. the pre-image of a point (x',y') in the ζ plane), the following relationships are used:

$$\left.\begin{aligned} \cos\theta &= \frac{x}{\rho} = \frac{2\rho x'}{\rho^2 + 1} \\ \sin\theta &= \frac{y}{\rho} = \frac{2\rho y'}{\rho^2 - 1} \end{aligned}\right] \qquad (2C.14)$$

(cf. equations (2C.11)).

$$\text{Hence } \cos^2\theta + \sin^2\theta = 1 = \left(\frac{2\rho x'}{\rho^2 + 1}\right)^2 + \left(\frac{2\rho y'}{\rho^2 - 1}\right)^2 \qquad (2C.15)$$

By rearranging equation (2C.15), the following equation is obtained

$$\rho^8 - 4(x'^2 + y'^2)\rho^6 + 2(4x'^2 - 4y'^2 - 1)\rho^4 - 4(x'^2 + y'^2)\rho^2 + 1 = 0 \qquad (2C.16)$$

If we let $\rho' = \rho^2$, equation (2C.16) becomes a fourth order polynomial in ρ', which can be solved analytically. Hence the roots of equation (2C.16) can, in principle, be expressed in terms of x' and y'. However, this process is both lengthy and tedious, and a standard numerical technique (IBM's POLRT package) is more convenient to use to calculate the roots of this equation for a given x' and y'. The real roots are then tested against equation (2C.15) to obtain the unique real root ρ_o which satisfies this equation and the inequality $\rho_o > 1$. The pre-image (x,y) of the point (x',y') can then be calculated using equations (2C.14). The velocities U_x and U_y at (x,y) are obtained from the known solution to the rotating sphere problem. Thus equations (2C.9) and (2C.10) are completely determined and may be used to calculate $U_{x'}$ and $U_{y'}$ at any given position (x',y') around the rotating disc. The calcula-

tion procedure is summarised as follows:

(1) At a given position (x',y') calculate the coefficients in equation (2C.16).

(2) Find the real root ρ_o of equation (2C.16) which satisfies equation (2C.15) and the condition $\rho_o > 1$.

(3) Calculate x and y using this root and equation (2C.14)

(4) Use the solution to the rotating sphere problem to obtain U_x and U_y at (x,y)

(5) Calculate $\frac{\partial x}{\partial x'}$, , $\frac{\partial x}{\partial y'}$, , $\frac{\partial y}{\partial x'}$, and $\frac{\partial y}{\partial y'}$, using equations (2C.12) and (2C.13) with $\rho = \rho_o$.

(6) Calculate $U_{x'}$ and $U_{y'}$ using equations (2C.9) and (2C.10).

2C.2 Presentation and Discussion

Radial velocity profiles predicted by the conformal mapping technique are presented in Figure 2-14. The curves shown are for L = 0,018 and m' = 0,0 to 3,0 and may thus be directly compared with the velocity profiles predicted by the analysis of Waters and King (see Section 2B), shown in Figure 2-11. It may be seen that, except for the region near the edge of the disc (z = 0, r' = 1), the shapes of the two sets of curves is remarkably similar. For the region near the edge of the disc, the conformal map predicts velocities which are approximately twice as great as those predicted by the Waters and King analysis. However, for regions distant from the edge, the two sets of curves are in quantitative as well as qualitative agreement. The velocity profiles in Figure 2-13 are for L = 0,194 and the lower range of m' values, m' = 0 to 0,75. The above conclusions are reinforced

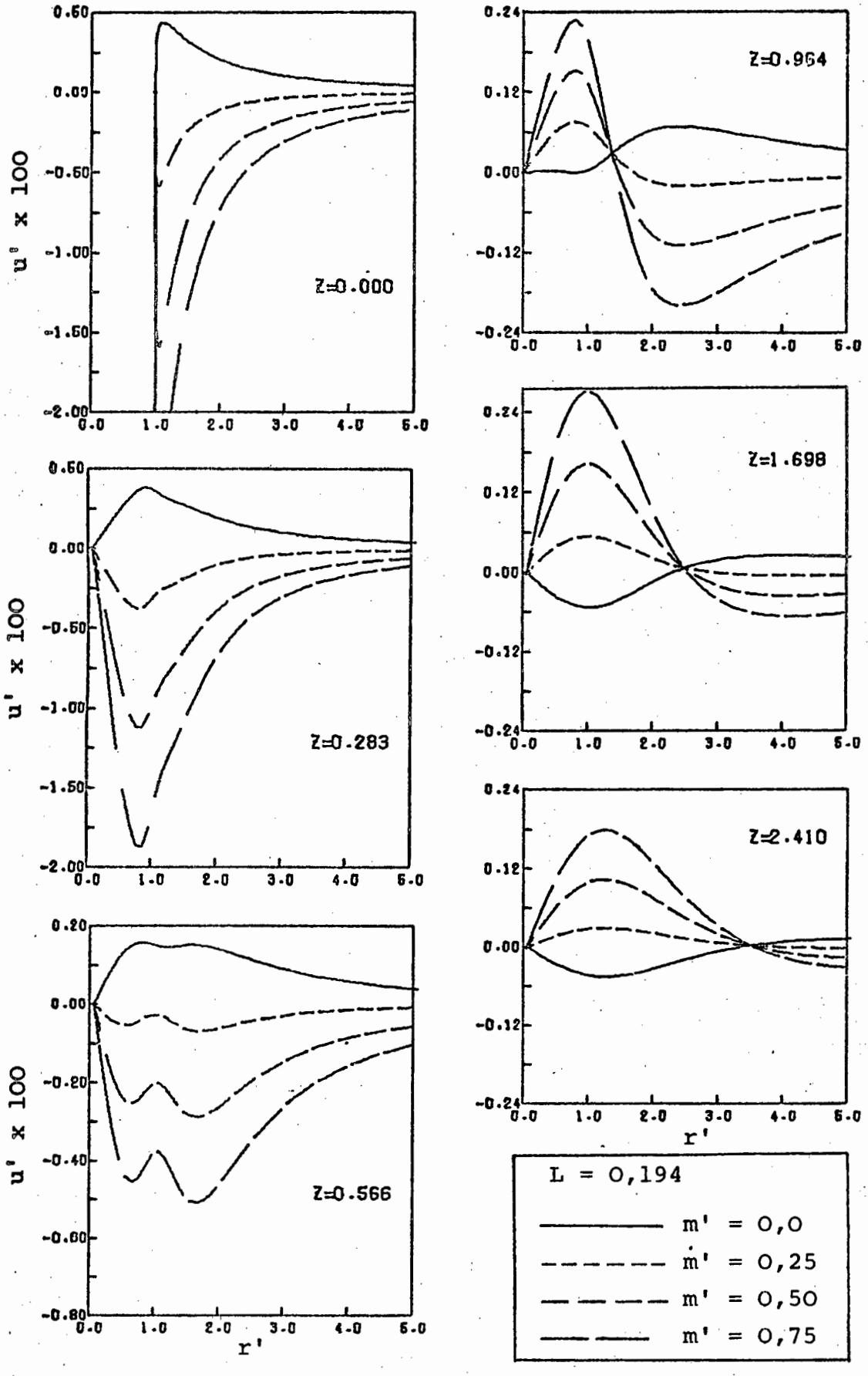

FIGURE 2-13 DIMENSIONLESS RADIAL VELOCITY PROFILES FOR THE ROTATING DISC PREDICTED BY THE CONFORMAL MAP

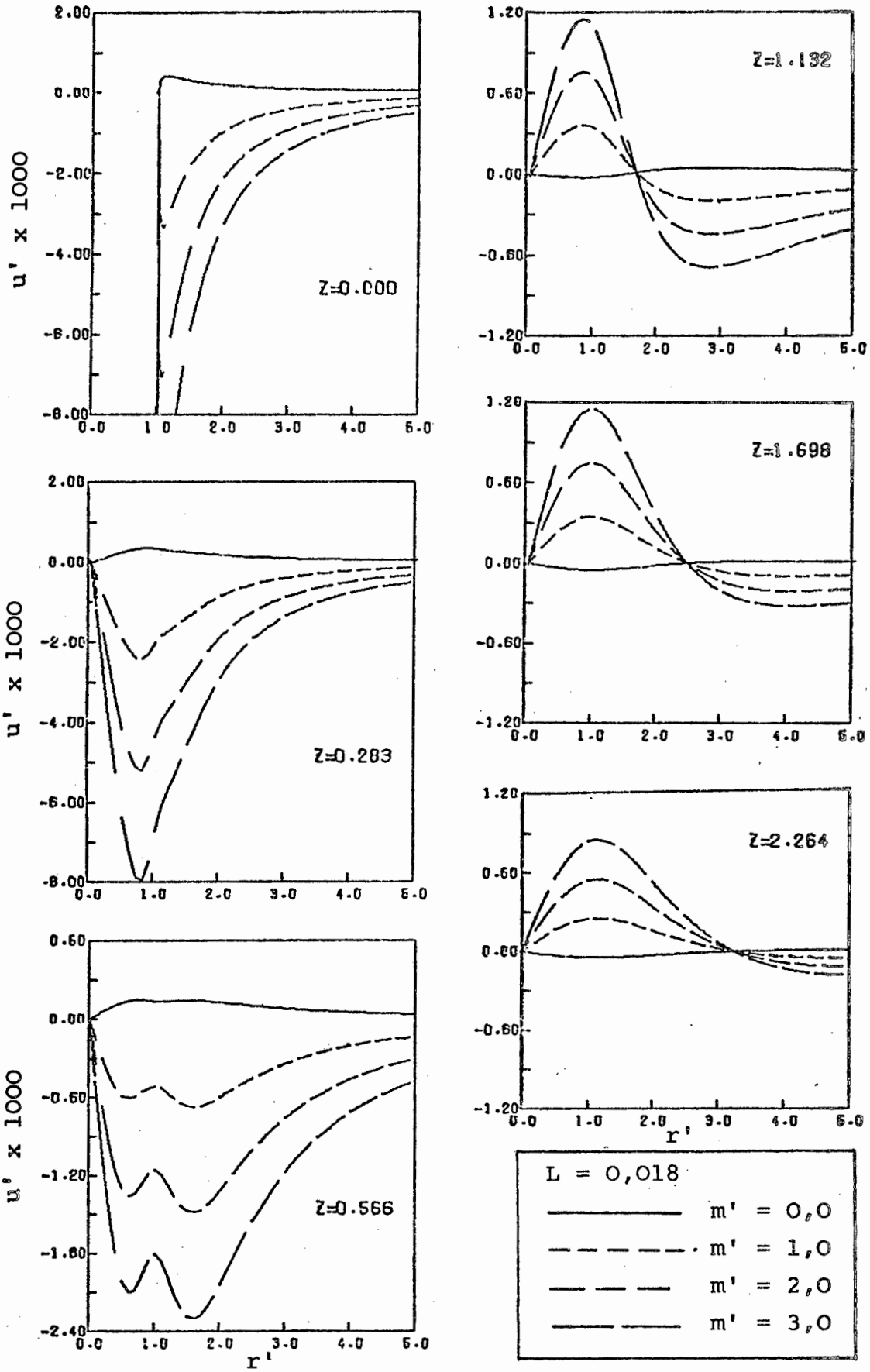

FIGURE 2-14 DIMENSIONLESS RADIAL VELOCITY PROFILES FOR THE ROTATING DISC PREDICTED BY THE CONFORMAL MAP

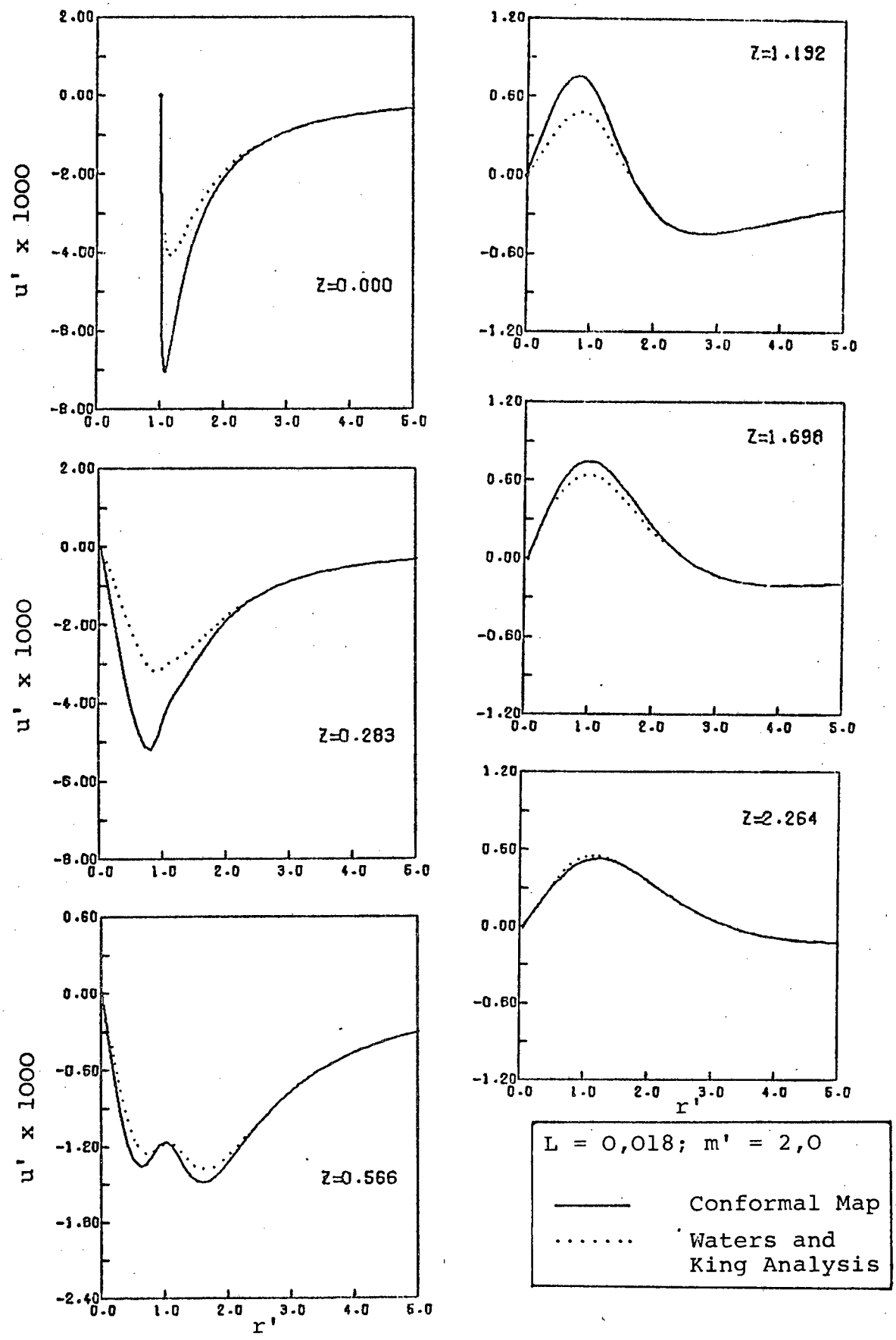

FIGURE 2-15 DIMENSIONLESS RADIAL VELOCITY PROFILES FOR THE ROTATING DISC

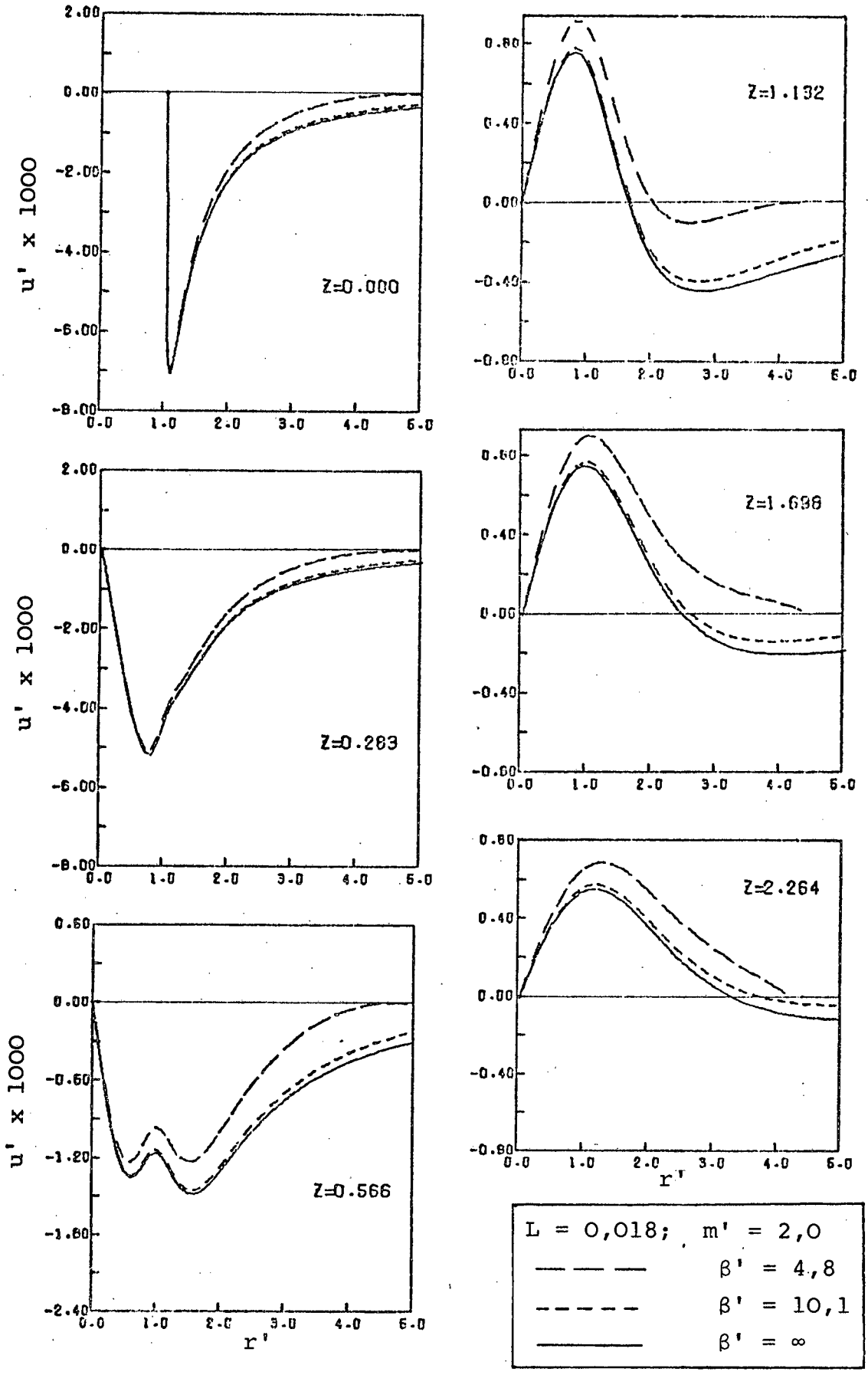

FIGURE 2-16 DIMENSIONLESS RADIAL VELOCITY PROFILES FOR THE ROTATING DISC PREDICTED BY THE CONFORMAL MAP

when these curves are compared with the corresponding set of Figure 2-10. These contentions are best illustrated by comparing the two sets of curves directly, for a single value of m', as is done in Figure 2-15.

The conformal map may be used to estimate the effect of container walls on the velocity curves by assuming that the disc is rotating within an ellipsoid of revolution filled with the viscoelastic fluid (see Section 2C.1). The curves shown in Figure 2-16 show the effect of the presence of an ellipsoid at $\beta' = 4{,}8$; 10,1 and ∞, where β' is the length of the semi-major axis. For these values of β', the ellipsoids are very nearly spherical in shape. The influence on the velocity profiles of container walls at $\beta' = 10{,}1$ is small, but the presence of a solid boundary at $\beta' = 4{,}8$ would clearly result in a significant change in the curves.

2D REVIEW OF THE THEORY OF FALLING SPHERE VISCOMETRY

The material parameter known as the zero shear viscosity invariably appears in any constitutive equation for viscoelastic fluids, yet there is no universally accepted method of measuring this quantity accurately [61, 80]. The method of falling spheres provides a simple and convenient measure of the zero shear viscosity. A very brief review of the theory on which this method is based follows, and serves as a basis for the experimental procedure adopted in Chapter 3 and the extrapolation procedures used in Chapter 4.

Caswell and Schwartz [79] analysed the problem of the slow flow of a Third Order Rivlin-Ericksen fluid past a sphere. In a later publication [62], Caswell considered the effect of finite container boundaries on the motion of the sphere. These analyses, which are

restricted to the inertialess flow regime, yield the following results [80].

$$U_\infty(F) = U_s[1 - \left(\frac{\lambda}{\eta_o}\right)^2 (F/6\pi a^2)^2 + O(F/6\pi a^2)^4] \qquad (2D.1)$$

where F is the net hydrodynamic force on a sphere of radius a, η_o is the zero shear viscosity, λ is a characteristic time which depends on the non-Newtonian fluid properties, U_∞ is the velocity of the sphere falling through an infinite sea of fluid and

$$U_s = F/6\pi a\eta_o \ , \qquad (2D.2)$$

the Stokes velocity of the sphere.
A rearrangement of equations (2D.1) gives

$$\frac{1}{\eta} = \frac{1}{\eta_o} - (\lambda\tau)^2/\eta_o^3 + O(\tau^4) \qquad (2D.3)$$

where the viscosity $\eta = F/6\pi aU_\infty$ and $\tau = F/6\pi a^2$ is a characteristic shear stress. This equation suggests that a plot of $\frac{1}{\eta}$ vs τ^2 should become linear at sufficiently low shear stresses, with intercept $\frac{1}{\eta_0}$ in the limit of zero shear stress.

If the velocity of the sphere, U, is measured at the centre of a tube of radius R, the quantity $U_\infty(F)$ is given by the equation

$$U_\infty(F) = U + (F/6\pi\eta_o R)W(a/R) + O(F/R)^3 \qquad (2D.4)$$

where $W(a/R) = 2{,}1044 - 2{,}0888(a/R)^2 + O(a/R)^4$.

Thus U (and hence η) may be calculated via an iterative procedure by assuming a value for η_o in equation (2D.4), then using a linear plot based on equation (2D.3) to obtain a new value of η_o.

Cygan and Caswell [80] performed a number of careful

experiments to test the validity of the above equations. They concluded that equation (2D.4) describes the effects of container walls very well provided that the correction is less than 10% of the measured velocity U. In contrast, their data contradicted the dependence of the fluidity $\frac{1}{\eta}$ on τ^2 predicted by equation (2D.3). They found instead that a plot of $\frac{1}{\eta}$ vs τ was linear and that Turian's empirical relationship [79], ln η vs τ provided an excellent correlation of their data for values of τ up to approximately 250 [dynes/cm^2]. The zero shear viscosities predicted by the two methods were in excellent agreement. Subbaraman, Mashelkar and Ulbrecht [82] reviewed the extrapolation procedures used in falling sphere viscosity. These authors concluded that an extrapolation procedure based on equation (2D.3) has the best theoretical basis and is thus the most appropriate. However, it appears that they too plot their data on a basis of $\frac{1}{\eta}$ vs τ, rather than τ^2. They also found that η_o values obtained using this method and Turian's empirical method were in close agreement, differing by less than 4% for six different polymer solutions.

In the light of the above discussion, the procedure used to obtain the zero shear viscosity is as follows: U_∞ was calculated from equation (2D.4), using an assumed value of η_o, and was used to calculate η ($\eta = F/6\pi a U_\infty$). Plots of both ln η vs τ (Turian's proposal [81]) and $\frac{1}{\eta}$ vs τ (after Cygan and Caswell [80]) were prepared, straight lines were fitted to the data and extrapolated to zero shear stress. The zero shear viscosities calculated from the intercepts were then inserted in equation (2D.4) and the procedure repeated. Provided that corrections are small, only one or two iterations are necessary.

CHAPTER 3

EXPERIMENTAL

3A EXPERIMENTAL APPARATUS

3A.1 The Velocity Measuring Apparatus

The major experimental apparatus used for obtaining velocity data is shown in the photograph, Figure 3-1 and in the schematic diagram, Figure 3-2:

(i) A and B are two DC electric motors (Bodine Electric Co., Chicago, Illinois) and their solid state variable speed controllers (Minarik Electric Co., Los Angeles, California). The motor A is rated at 1/15 HP and gives a speed range of approximately 25 - 1120 rpm at the shaft C via the pulley system. Motor B is rated at 1/50 HP and is equipped with a 10:1 reduction gearbox. Combined with a 3:1 stepdown pulley system, this motor gives a smooth-running speed range of approximately 12 - 163 rpm at the shaft. The smaller motor was used to rotate the sphere or disc under study. The torque available, even at low speed and in the most viscous experimental liquid used, is considerably in excess of that required to rotate the shaft.

(ii) C is a removable base plate supporting the two adjustable bearings holding the shaft. The construction of the shaft and its attached disc or sphere is to be described later.

(iii) D is a tank containing the experimental fluid. (Water is shown in the picture, for greater clarity.) The tank is constructed of ¼" perspex. The height is 40,6 cm; length and breadth are both 38,1 cm. A smaller cubical perspex tank with sides of 30,5 cm was also used. A graduated strip of masking tape on the left of the tank facilitated the accurate vertical positioning of the light beam. The back and right hand side of the tank were covered with black sheets of cardboard (not shown) to minimise light

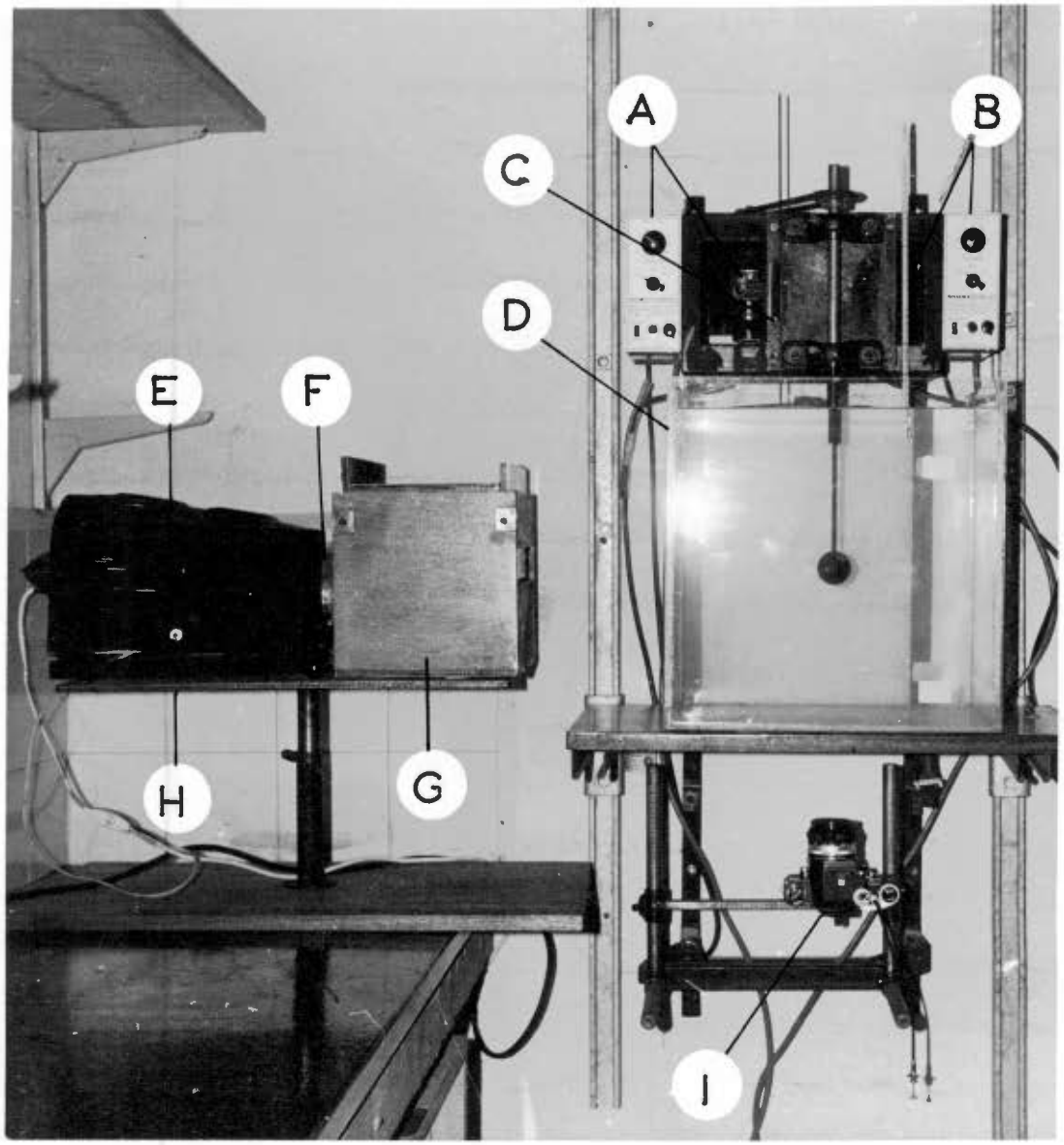

FIGURE 3-1 THE VELOCITY MEASURING APPARATUS

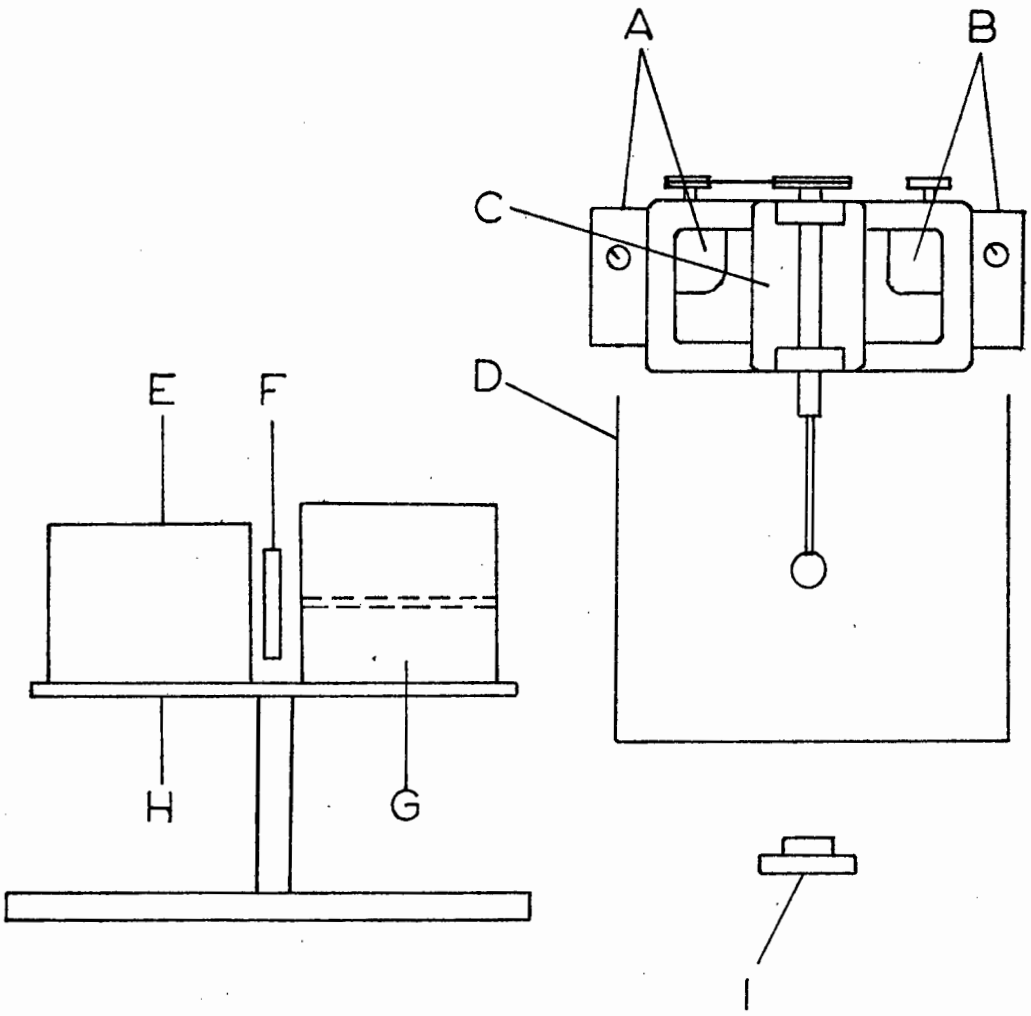

FIGURE 3-2 SCHEMATIC DIAGRAM OF THE VELOCITY MEASURING APPARATUS

A,B Motors and controllers
C Removable base plate
D Tank
E Light source
F Lens
G Collimating system
H Adjustable platform
I Camera

scattering and reflection. The top of the tank was also at times covered with a black sheet of cardboard to provide greater contrast with the aluminium particles in the solution.

(iv) E is a light source consisting of a 500 W quartz-halogen projector lamp which is cooled by a small fan. An aluminium reflector and an ordinary 5½" diameter magnifying lens, shown at F, serve to intensify the light beam. The projector lamp, reflector and cooling fan are housed in the box shown at E.

(v) G is a collimating system. This consists essentially of a wooden box with an adjustable horizontal slit on two sides. The slits are faced with accurately cut 1/16" aluminium sheeting. Generally, slit widths of 2 to 3 mm were used. This system produces a horizontal sheet of light with thickness approximately 5 mm at the centre and 8 mm at the far end of the tank. The adjustable platform H was used to locate the light beam at the desired vertical position.

(vi) I is a Nikon Photomic F 35 mm camera. A 24 mm f2.8 Auto Nikkor wide angle lens was used to obtain most of the data. No distortion was discernible with this lens. A 105 mm f2.5 lens was used for side view photographs in the dye tracer study and a waist level viewfinder was used for convenience when taking bottom view photographs. The camera could be moved to any desired horizontal or vertical position through the adjustable mounting system J. For preliminary studies (Run 7) a Zeiss Contaflex 35 mm camera was used.

3A.2 The Discs and Spheres

The discs and spheres used in the experimental study are shown in Figure 3-3. The larger of the two spheres has a diameter of 6,98 cm. This sphere was manufactured by fixing a solid aluminium block to the ⅝" diameter stainless steel shaft shown. A roughly spherical shape

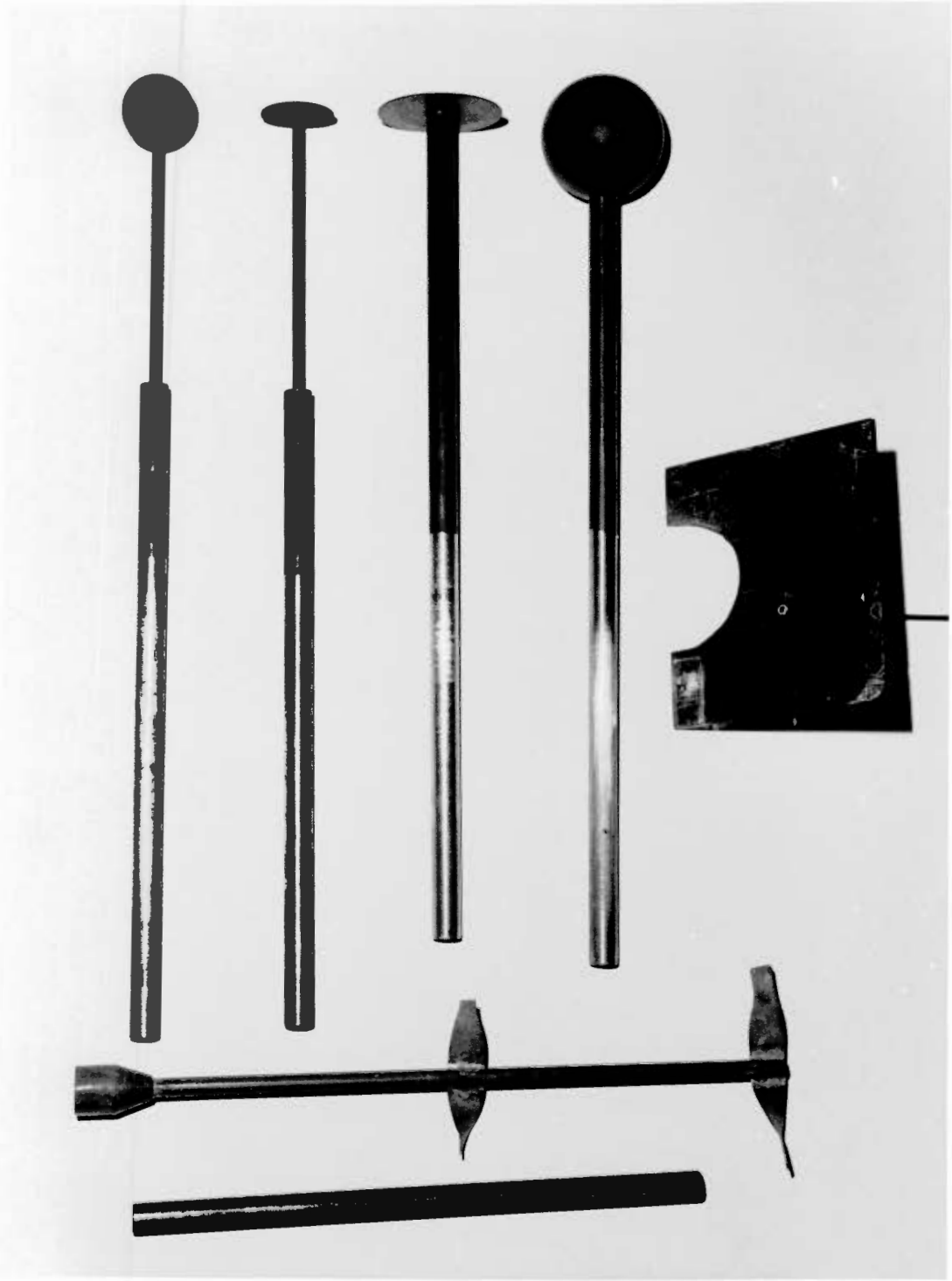

FIGURE 3-3 THE DISCS AND SPHERES

was then cut using an ordinary cutting tool in the lathe. The final shaping of the sphere was done with a specially constructed external radius arm cutting tool.

The smaller sphere shown has a diameter of 4,15 cm. It was manufactured by drilling a billiard ball in a lathe chuck to ensure concentricity. The hole was tapped and the ball screwed onto a ¼" diameter stainless steel rod. The upper end of the rod was inserted into a ⅝" diameter stainless steel shaft, with the exposed part of the rod and the sphere measuring approximately 16 cm in length. The sphere assemblies, mounted on the base plate as shown in Figure 3-1, were sprayed with matt black paint while rotating slowly; this was to ensure an even layer of paint. The sphericity of both spheres was then assessed by making repeated measurements of the diameter using a Kanon vernier callipers graduated to 0,02 mm. In both cases, deviations from the mean sphere diameter were found to be well below 0,1%. (The deviations were of the order of 0,02 - 0,04 mm.)

The small disc shown has a diameter of 4,15 cm and a thickness of 0,8 mm. It was constructed by fixing a ¼" perspex disc to the end of a ¼" stainless steel rod. A special flat-headed brass screw was used. The perspex disc was then turned to the correct diameter in a lathe. The thickness of the disc was reduced to 0,8 mm using a special double edged cutting tool and the brass screw was turned flush with the bottom of the disc. This method of manufacture reduced wobble to less than 0,002", as measured on a dial indicator guage graduated to 0,0005". The other end of the ¼" rod is inserted into a ⅝" diameter stainless steel shaft, the exposed length being approximately 16 cm. The larger disc is 7,07 cm in diameter and 0,8 mm thick. It is manufactured of perspex sheeting in a manner similar to that of the smaller disc, except that it is directly attached to a ⅝" diameter shaft. Final alignment of the discs and spheres took place in the actual experimental apparatus. In all cases, they ran true to

within 0,005". All eccentricities were measured using the dial indicator guage; diameters and thicknesses were measured with the vernier callipers.

The shafts and their attached discs and spheres were sprayed matt black as described earlier. The centres of the discs and spheres were marked with an aluminium paint spot approximately 1 mm in diameter.

A perspex grid was used to obtain the scale of enlargment of photographs, as will be described later. This grid, also sprayed black, is shown. The markings are 1 cm apart and the brass rod is used to position the grid in the tank. The grid is held in position by clamping the brass rod to the base plate, shown at C in Figure 3-1, with a bull clip. Also shown are the stirrer and rod used to mix the solutions.

3B EXPERIMENTAL PROCEDURES

3B.1 Preparation of Solutions

The experimental solutions were prepared by filling the perspex tank to a calibrated mark with water, a volume of 53,7 ℓ in the larger tank shown in Figures 3-1 and 3-2. The amount of Natrosol 250 H (hydroxyethyl cellulose, Hercules Inc., Wilmington, Delaware) powder necessary to give the desired concentration was weighed correct to 0,1 g. The large motor was started with the stirrer turning at approximately 600 rpm and the Natrosol powder was sprinkled into the vortex as rapidly as possible. The controller was then set to give maximum speed (approximately 1000 rpm) and at maximum torque to produce a uniform dispersion of the powder. The Natrosol powder dissolved, with a corresponding viscosity increase, within 30 - 40 minutes. Mixing was continued for a total time of at least 1½ hours to ensure the homogeneity of the solution. At the end of the mixing stage, a clear solution was obtained except for a uniform dispersion of fine air bubbles trapped in the

viscous liquid. The solution was left to stand for 12 - 24 hours to allow the bubbles to rise to the surface. The tank was covered during this period to minimise the formation of a surface skin due to evaporation.

After the complete elimination of air bubbles, the temperature of the Constant Temperature Room, in which all experiments were performed, was raised to 23 - 24°C. The liquid in the tank was stirred at 300 - 400 rpm, both to break up and dissolve any surface skin which might have formed and to speed up heat transfer to the liquid. A fan heater was used to raise the temperature of the polymer solution to the required 25,0°C. All temperatures were measured with a standard thermometer, graduated to 0,1°C. Because of the large heat capacity of the system (54 ℓ of liquid in the tank), it took approximately 3 hours to raise the temperature of the liquid by 4°C. An advantage of the large heat capacity was that the temperature could be maintained at the desired value (25,0°C ±0,1°C) for several hours, provided that the ambient was maintained within 1°C of 25°C. Thorough stirring ensured that the temperature gradient within the tank was negligible (i.e. less than 0,1°C).

At the end of the heating period, 1,2 to 1,5 g of aluminium powder (200 - 300μ) was added to the solution. Stirring was continued until a uniform suspension of the particles was obtained. The settling velocities of these particles are extremely small. In the least viscous solution used the particles took several hours before settling out, and in the more viscous solutions, the majority remained in suspension for 8 - 10 hours. It could thus be concluded that the settling velocities, compared with the measured velocities, are completely negligible.

After the dispersion of the aluminium particles, the stirrer was replaced by a disc or sphere assembly and falling sphere viscosity measurements were taken. The method will be described in section 3B.2.

optimal. A thinner beam of light was unsatisfactory as the alminium particles passed in and out of the light too rapidly to produce satisfactory photographic streaks. A thicker beam increased the uncertainty of the z position of the particle. The horizontal light beam was then centred on the equator of the sphere in preparation for measurements in the z=0 plane. A small degree of weak diffusion of the light beam was evident, but this did not prove troublesome in positioning the beam. In order to provide maximum contrast between the aluminium particles in the light beam and the background, all lights other than the light source were switched off (the room has no windows). The perspex grid shown in Figure 3-3, was lowered into the centre of the light beam and held in a horizontal position by clamping the brass rod to the base plate C shown in Figure 3-1. This was done slowly so as to avoid introducing air bubbles into the liquid.

The camera was loaded with Kodak Tri-X film (ASA 400, 36 exposures) and was mounted as shown in Figure 3-1. It was then focussed on the grid and positioned directly beneath the centre of the sphere, as seen through the lens. It should be noted that great care must be taken to focus correctly as the aperture is often at its maximum, with a corresponding minimal depth of field. This positioning of the camera was necessary in order to eliminate parallax error when finding the centre of the sphere on the photograph. A photograph of the grid was then taken. As described in section 3B.4, this photograph was later used to find the scale of magnification when printing photographs in that particular z plane. The grid was raised to the surface of the liquid and clamped in that position in order to avoid interference with the flow field.

At this stage, the smaller motor was switched on to rotate the shaft and the speed was adjusted to the value of 15,0 rpm at which all experiments were conducted. A Hasler tachometer, graduated to fifths of a revolution per

TABLE 3-1

SPHERE DATA

Diameter [cm]	0,15875	0,23813	0,31750	0,47625
Density [g/cm^3]	7,784	7,786	7,768	7,731

According to the manufacturer's specifications, deviations from the mean sphere diameter are less than 0,00004 cm (less than 0,06%). The densities were measured by weighing a number of spheres accurately and calculating the volumes from the given diameters.

In order to avoid the transfer of large volumes of the highly viscous Natrosol solutions, the falling sphere experiments were conducted without removing the liquid from the tank. The spheres were dropped approximately 6,5 cm from each of two sides of the tank. The fall times between two marks 26,0 cm apart were measured using an Omega stopwatch graduated to 0,1 sec. The upper mark was approximately 6 cm from the surface of the liquid while the lower mark was the same distance from the bottom of the tank. Two corresponding marks on the opposite side of the tank served to minimise errors of parallax. With this arrangement, corrections for the effects of container boundaries were reduced to less than 2% of the measured velocity. (See section 2D for the theoretical justification.) Only two or three readings were taken for each sphere size as the measured fall times were always within 1% of each other.

3B.3 Taking of Photographs

The procedure for taking photographs will be described as applied to the rotating sphere situation only; it is identical for the case of the rotating disc. The sphere was first centred in the tank of experimental liquid, which had been prepared as described in section 3B.1 The collimating system was then adjusted to give a light beam with a mean thickness of 5 mm. This thickness was found to be

When preparing the Natrosol solutions, care must be taken to stir the solution for an extended period of time (at least 1½ hours) to avoid the problem of "incomplete mixing". This manifests itself as an apparently homogeneous solution which has a viscosity less than half that expected for the concentration. Another problem encountered was that of biological degradation of the polymer solutions, usually discernible four to eight days after preparation. This manifests itself as a distinct yellowish discolouration of the liquid and a marked decrease in solution viscosity. Higher ambient temperatures, for example during summer, seem to accelerate the biodegradation. Small quantities of sodium azide or methyl p-hydroxybenzoate were added to the solutions but these did not retard bacterial growth significantly. The probable reason for the failure of small quantities of these antiseptics to reduce biodegradation was the presence of an anaerobic waste treatment experimental plant in the adjacent laboratory which resulted in large quantities of bacteria being continuously present in the air. The use of distilled water did not improve matters, indicating that the bacteria were largely air borne. Rather than use larger amounts of the antiseptics, it was decided to do all experiments on a polymer solution within three days of preparation. Usually, experiments were completed within 48 hours of mixing. The viscosity of the solution was checked at the end of a run and a deviation of less than 2% was regarded as acceptable, this being within the probably error of measurement.

3B.2 Measurement of Zero Shear Viscosity

The falling sphere method of measuring the zero shear viscosity proved simple and satisfactory. The spheres used were stainless steel precision ball bearings. (Ransome Hoffman Pollard Ltd., Chelmsford, Essex). The diameters and densities of the spheres are given in Table 3-1.

minute, was used for this purpose. Readings were reproducible to within one division. A delay of about 20 minutes (i.e. about 300 revolutions) was allowed before taking photographs of the moving aluminium particles so that the system could reach steady state condition.

A series of 10 to 16 photographs of the moving aluminium particles was taken over a range of exposure times of ¼ second to 10 seconds. The number of each photograph, the f stop and the exposure time were recorded. Exposure intervals greater than 1 second were measured with the stopwatch. The shutter speeds of the cameras were calibrated as described in Appendix D. The shorter exposure times of ¼ and ½ second (nominal) were needed to measure the higher velocities of particles close to the moving sphere. The longer exposure times were used to measure the slower velocities farther from the sphere with comparable accuracy. A greater range of velocities was encountered in the higher z planes which cut the rotating sphere than was encountered in the lower z planes. These planes required a larger number of photographs in order to define the velocity distribution accurately. Photographs were only taken when several aluminium particles in the light beam were in a reflecting position. This reduced the number of photographs which had to be printed and analysed in order to obtain the velocity distribution in any one plane. However, enough photographs must be taken to obtain data close to the moving sphere. When a complete series of photographs had been taken in a particular z plane, the light beam was lowered by 1,5 or 2,0 cm, depending on the size of the sphere. The procedure described above was then repeated at the new z position.

Rotational speed was checked at least once during a run, and at the end of a run. It was invariably found to be constant. Both the ambient temperature and the temperature of the experimental liquid were regularly checked. The ambient was kept as close as possible to 25° C so as to maintain the temperature of the experimental liquid at 25,0° C

±0,1°C. Viscosity measurements were repeated at the end of a run.

The photographic films were processed immediately after all the photographs had been taken. Microdol X developer was used at a dilution of 1:3 to give maximum definition. A degree of overdevelopment enhances the contrast of the negatives and makes the analysis of the prints easier. The negatives were carefully examined as soon as possible after processing. If any negatives were spoilt or if more data were desired in specific regions of the flow field, additional photographs were taken. In this case, the viscosity of the solution was measured to check for signs of biodegradation. If no degradation had taken place, the additional data were obtained exactly as in the case of a fresh solution. Otherwise, the run was abandoned and a fresh solution prepared.

3B.4 Printing and Analysis of Photographs

The enlarger (Durst 600) was set up in a horizontal position so that the image could be projected onto a vertically mounted drawing board. The enlarger was aligned to ensure that the light beam was perpendicular to the drawing board. With this arrangement, prints up to 50 x 60 cm in size could be made. The photographic paper used was Kodak SWG 3 and Agfa BH111-5. The hard grades were chosen to give maximum contrast; Kodak D163 paper developer, a 2% acetic acid stopbath and Kodafix fixer were used for processing the prints. The prints were washed and air dried in the normal manner.

In each z plane, the first print made was that of the 1 cm grid. Care was taken not to move the enlarger during subsequent printing so that the grid could be used to calculate the scale of enlargement of all the pictures in that plane. Each print was numbered for identification with the earlier records of exposure times, which were kept when taking the photographs. Prints were made ranging in size

from 25 x 30 cm to 50 x 60 cm. The size depended on whether the region near the sphere was the sole interest or the whole field was required. Approximately 60 to 70 photographs were required to obtain the experimental velocity field in five different z planes. Two typical photographs, although at a lesser enlargement than that used for obtaining the data, are shown in Figures 3-4 and 3-5.

All photographs were pinned to a drawing board to facilitate work. The first step in the analysis of a set of photographs for a particular z plane was the measurement of the enlarged 1 cm grid. The mean of several measurements was taken to obtain the scale factor, usually 3 to 4X full size, for the rest of the photographs in that plane. Enlargements to this scale served to reduce the relative errors in measuring streak lengths and distances from the endpoints of the streaks to the centre.

The velocity measuring technique is based on the assumption that the photographic streaks are images of aluminium particles moving in the light beam throughout the interval during which the camera shutter remains open. Thus, for the correct interpretation of the streaks, their endpoints must be the result of the opening and closing of the shutter and not the result of entering or leaving the light beam during the exposure interval. The former streaks have well defined endpoints. A careful observation of the aluminium particles under experimental conditions reveals that the particles, which are of amorphous shape, appear as bright spots of light only when their orientation is such that they reflect the light toward the camera. Fading edges were thus sometimes due to a change in orientation of the particle. It could also be seen that particles at the edge of the light beam were considerably fainter than those near the centre. As a result of these observations and in order to minimise experimental scatter, only the brightest streaks with well defined endpoints were chosen for measurements. The vast majority of measured streak

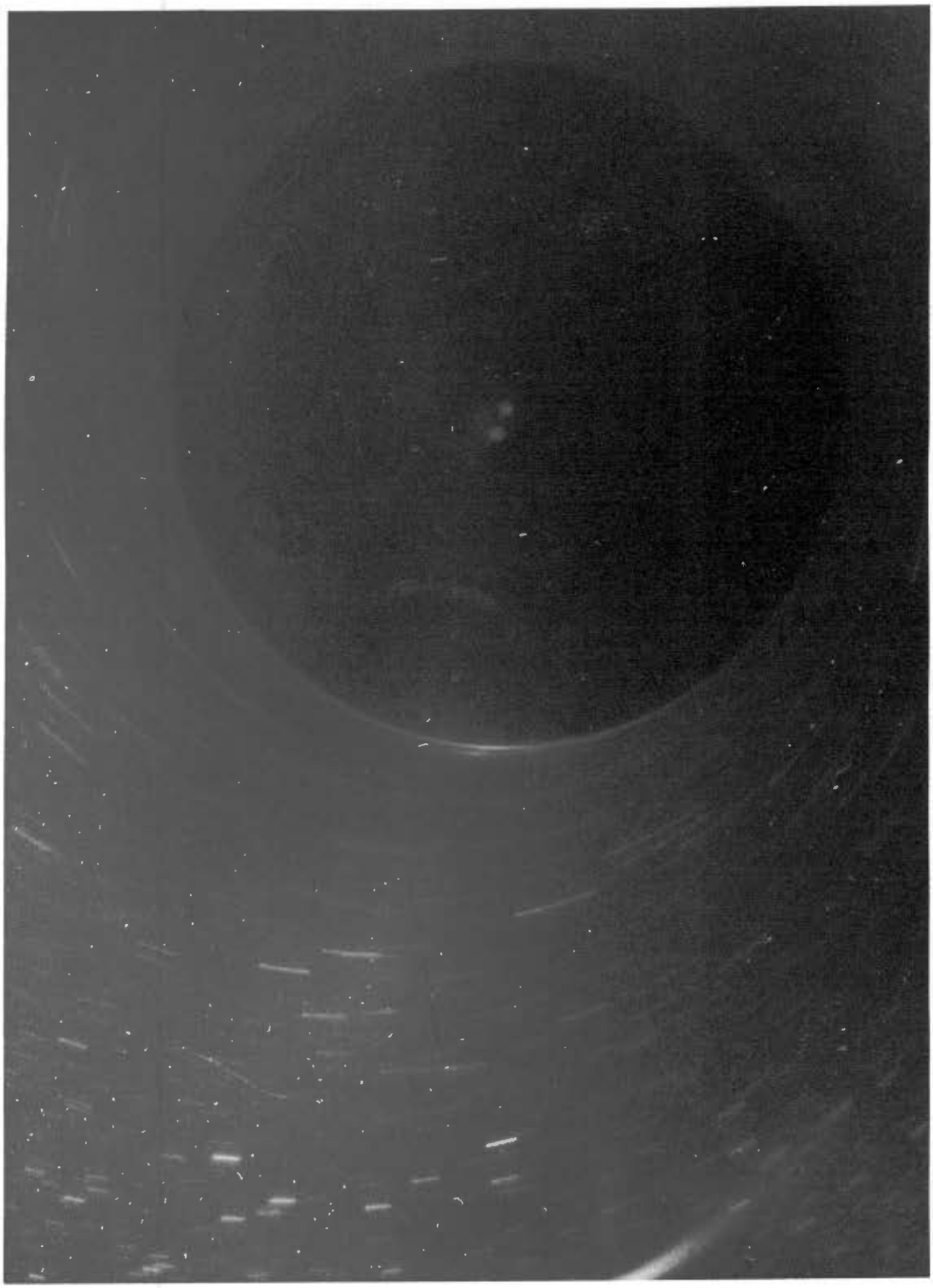

FIGURE 3.5 THE ROTATING DISC, z=0,0; Δt=2,0 SEC

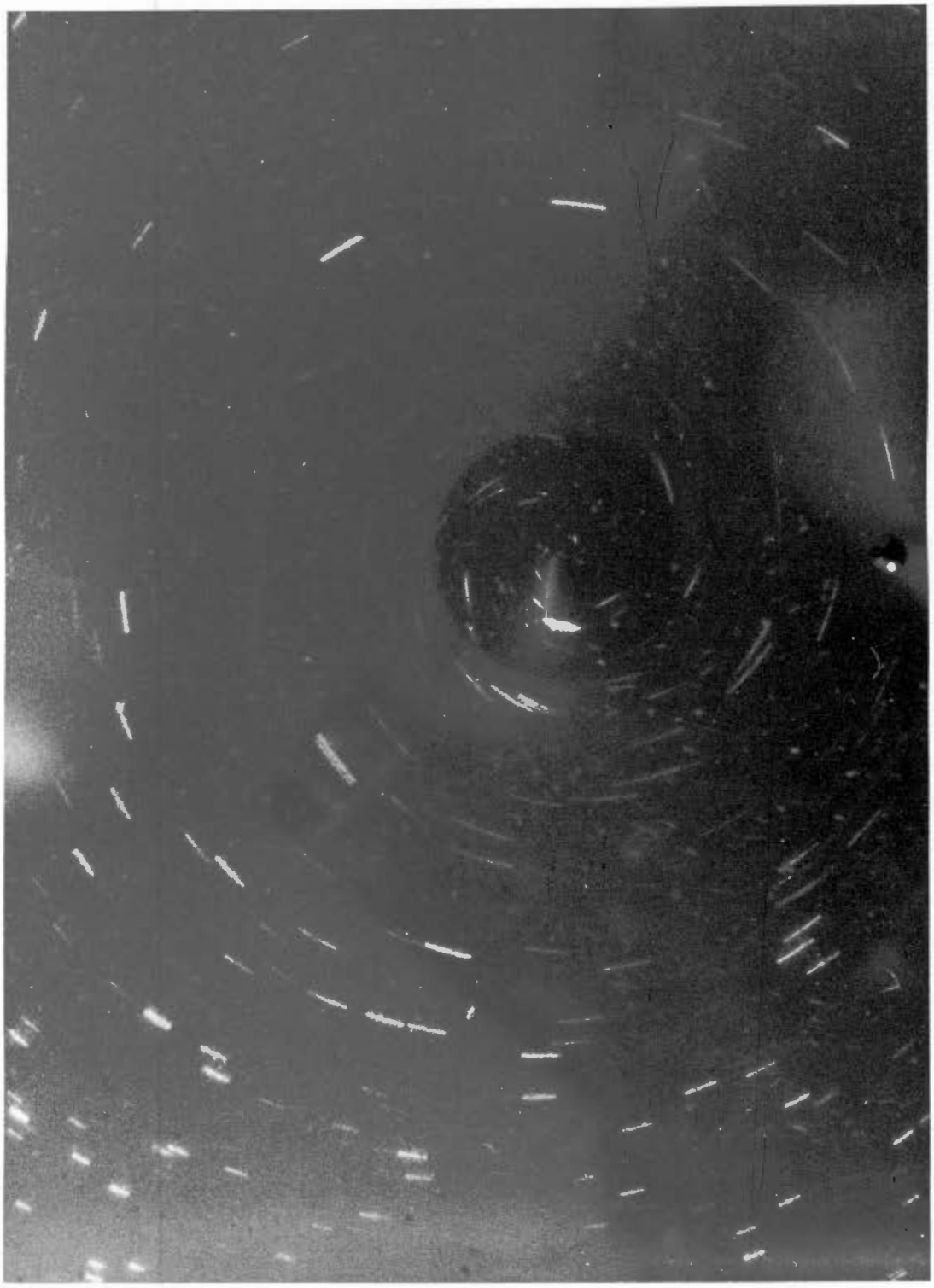

FIGURE 3-6 THE ROTATING SPHERE, z=1,698; Δt=8,0 SEC

lengths were in the range 1 cm to 4 cm, a length of about 3 cm being regarded as optimal. Streaks were usually about 0,5 mm wide.

In the analysis of a photograph, the usable streaks were first identified in accordance with the criteria discussed above. The endpoints of these streaks were then marked to facilitate measurement with the apparatus shown in Figure 3-6. The centre of the sphere was located by the image of the dot of aluminium paint. In the lower Z planes, this dot was, in a few cases, somewhat indistinct. A circular cardboard disc the size of the image of the sphere was then cut. This was fitted over the image and used to locate the centre of the sphere. A test of both methods showed that they agreed to within 1 mm on the enlargement; that is, the difference was less than 0,3 mm full scale.

Once the centre of the sphere had been marked, the centre pin of the measuring instrument was placed on the mark. The perspex base plate and the measuring arm were then placed over the pin, as shown in Figure 3-6. The distances from the endpoints of the streaks on the centre must be measured with the jaws of the measuring instrument closed. The jaws were used to measure streak lengths. All measurements were recorded as correct to 0,01 cm and the measuring arm was always moved in an anti-clockwise direction (i.e. the direction of flow as seen from the bottom of the tank) to obviate confusion. The number of the photograph and the nominal exposure interval were also recorded. Velocity data obtained with the above procedure are given in the next chapter. The errors and limitations of this technique are also discussed in Chapter 5.

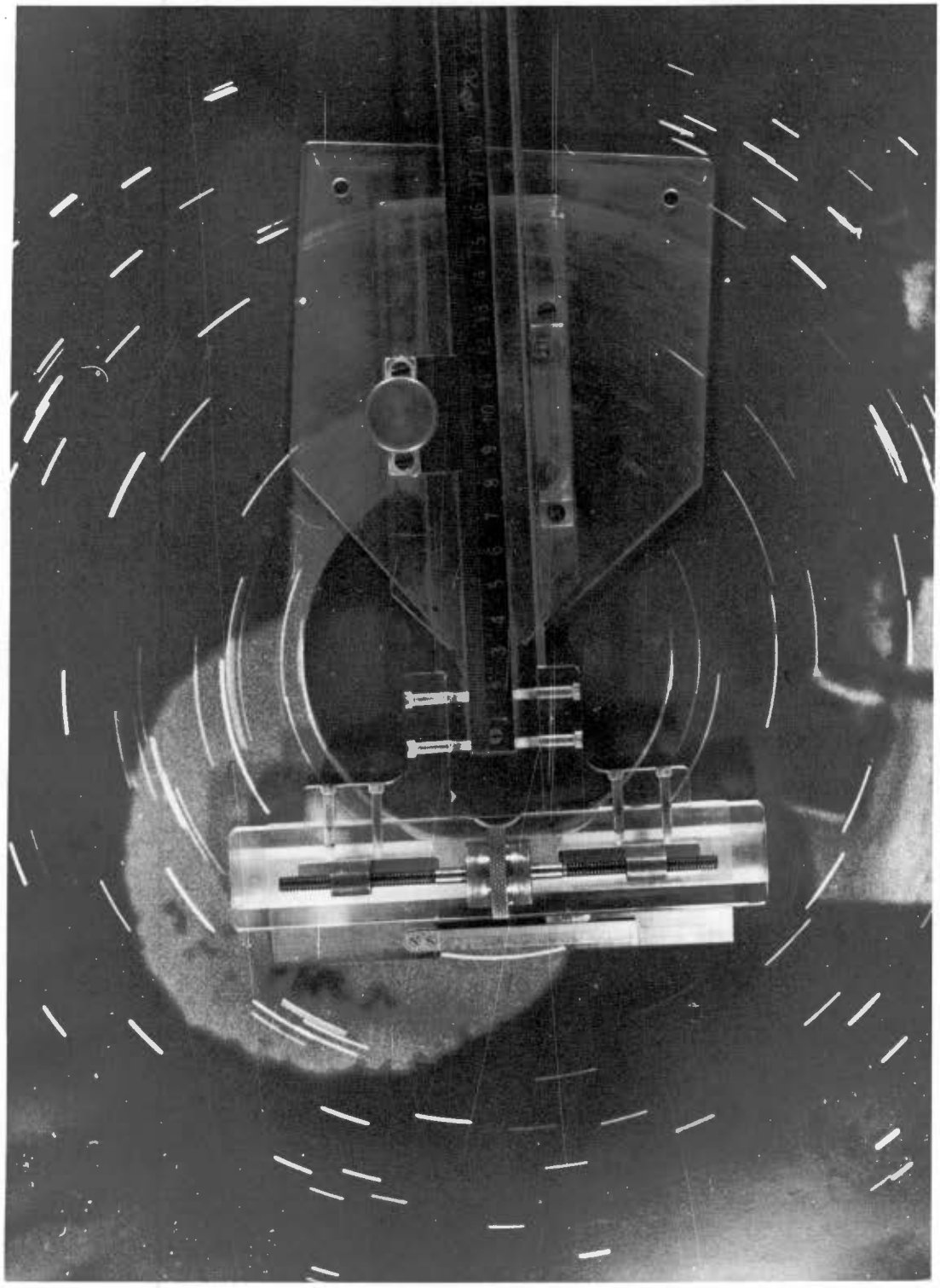

FIGURE 3-6 THE STREAK MEASURING APPARATUS

CHAPTER 4

RESULTS

4A ZERO SHEAR VISCOSITY MEASUREMENTS

For reasons given in the review of the theory pertinent to the measuring of zero shear viscosities by the falling sphere method (Section 2D), two methods of obtaining η_0 are presented. The extrapolation procedures were outlined in Section 2D.

Figures 4-1 and 4-2 represent data for the 0,90% Natrosol 250H solution and Figures 4-3 and 4-4 represent data for the 1,50% solution; both sets of data were obtained at 25° C $\pm$ 0,1°C. The experimental method used is described in Section 3B.2; raw data and calculation procedures are detailed in Appendix E. The zero shear viscosities obtained via the two extrapolation procedures are given in Table 4-1.

TABLE 4-1 ZERO SHEAR VISCOSITIES [POISE]

POLYMER SOLUTION	CASWELL'S PROCEDURE	TURIAN'S PROCEDURE
0,90% Natrosol 250H	15,4	14,0
1,50% Natrosol 250H	145	133

It is clear from Figures 4-1 to 4-4 that the experimental data are well represented by the straight lines. However, Turian's extrapolation procedure gives zero-shear viscosity values which are consistently about 10% lower than those predicted by Caswell's procedure. The viscosity values predicted by the latter method were

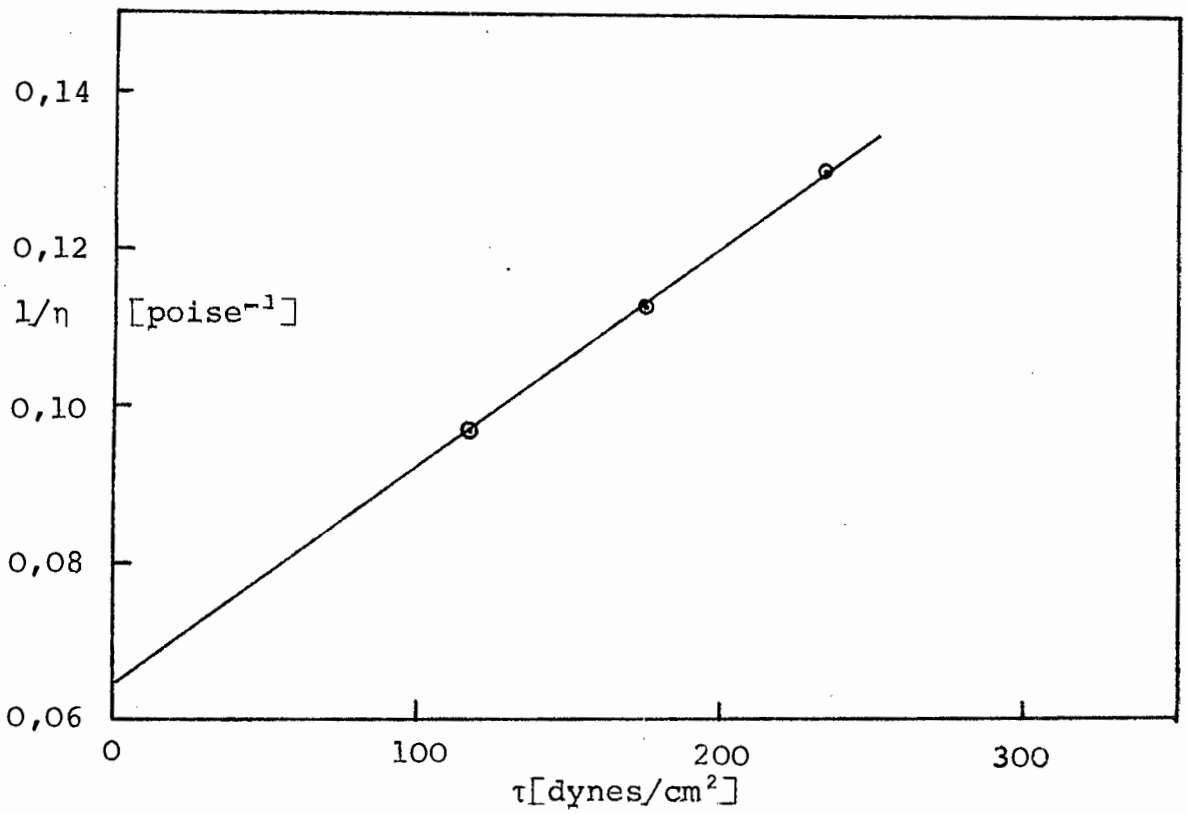

FIGURE 4-1 FLUIDITY VS SHEAR STRESS

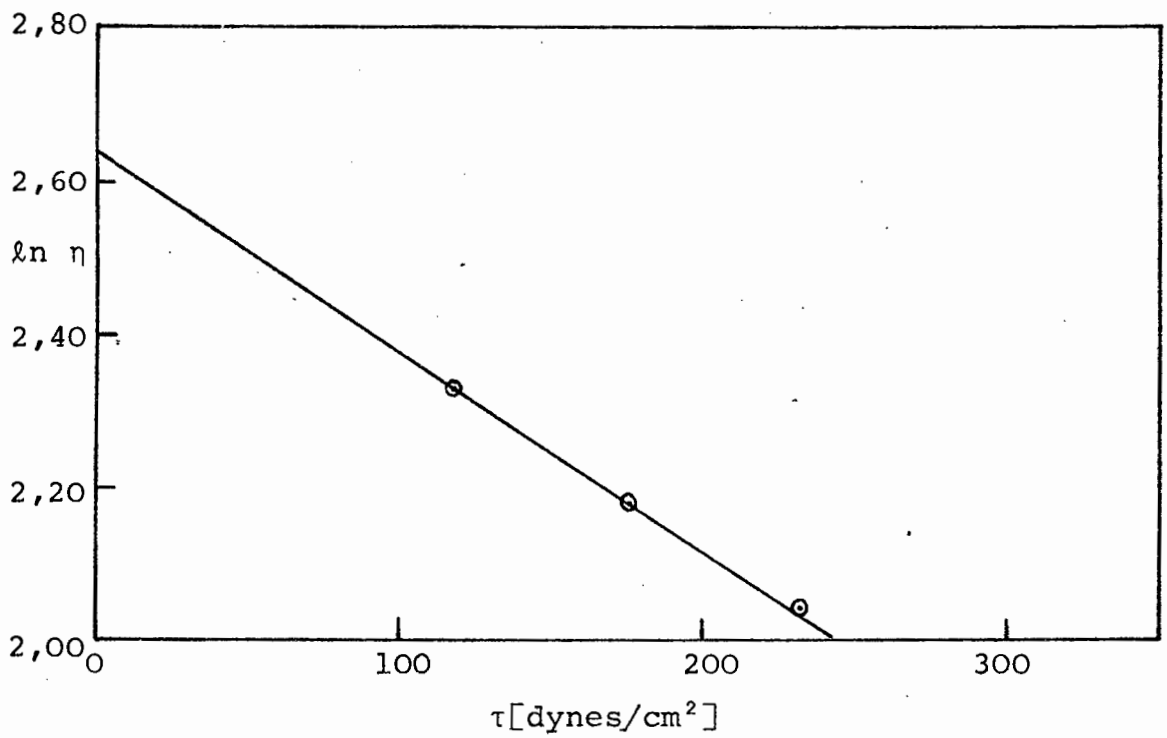

FIGURE 4-2 LOG VISCOSITY VS SHEAR STRESS

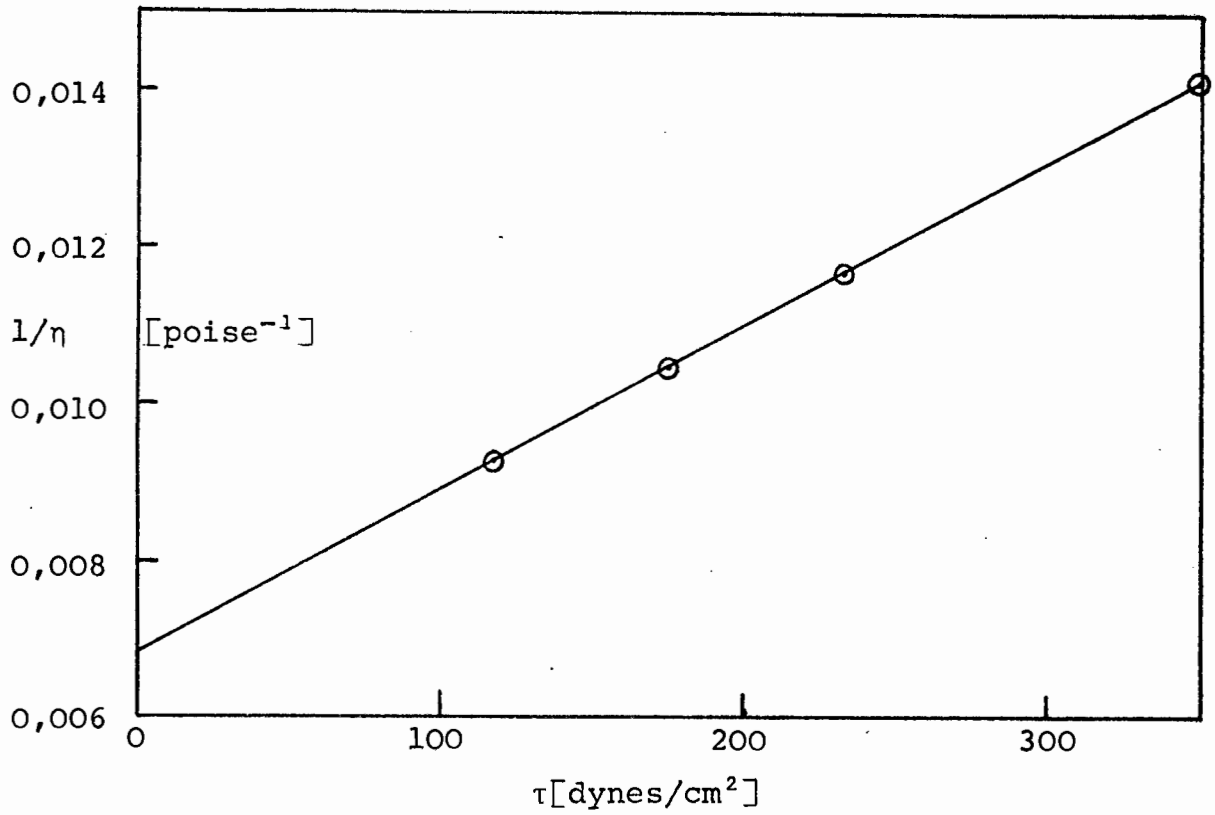

FIGURE 4-3 FLUIDITY VS SHEAR STRESS

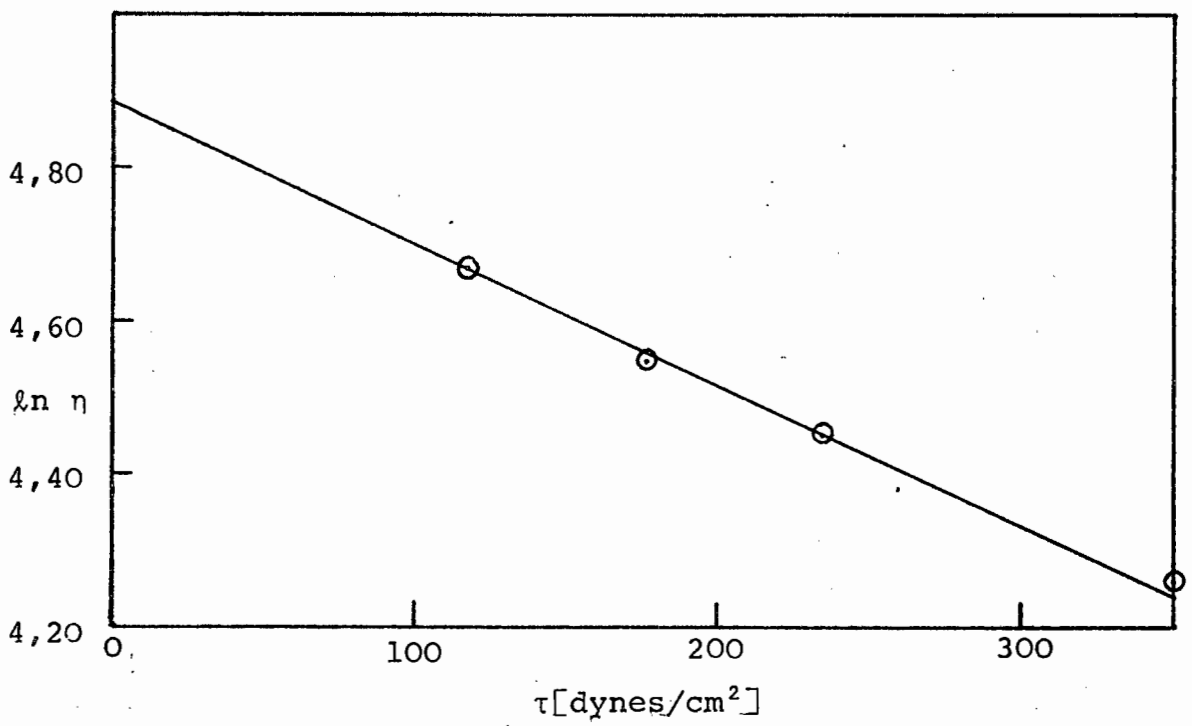

FIGURE 4-4 LOG VISCOSITY VS SHEAR STRESS

used for calculating dimensionless velocities in view of its superior theoretical basis. Huppler [83] also used a 0,9% Natrosol 250H solution in his experimental work, and obtained an η_0 value of 13,7 poise using Turian's procedure. The value of 14,0 obtained in this work compares well with his figure.

4B ANALYSIS OF RAW VELOCITY DATA

Consider the single streak on the schematic 'photograph' show in Figure 4-5. An arrow is superimposed on the streak to show the direction of motion and the measuring arm is shown with jaws opened, as when measuring streak lengths. (See also the typical photograph with the streak measuring instrument in position, Figure 3-6). The circle represents either the sphere or disc, $\Delta\phi$ is the angle in radians subtended at the centre of the circle and R_1' and R_2' are the distances from the end points of the streak to the centre. For clarity, the difference in the lengths R_1' and R_2' are exaggerated in the schematic diagram.

In a cylindrical polar co-ordinate system (r', ϕ, z), the radial and tangential velocity components may be approximated by the equations

$$V_{r'} \simeq \frac{(R_2' - R_1')}{\Delta t} \qquad (4B.1)$$

and

$$V_{\phi} \simeq \frac{(R_1' + R_2')}{2} \frac{\Delta\phi}{\Delta t} , \qquad (4B.2)$$

where Δt is the exposure interval of the camera. These equations are equivalent to replacing the derivatives at a point by their finite difference representations in a neighbourhood of that point. However, Δx rather than $\Delta\phi$ (Figure 4-5) is measured, thus we have to use

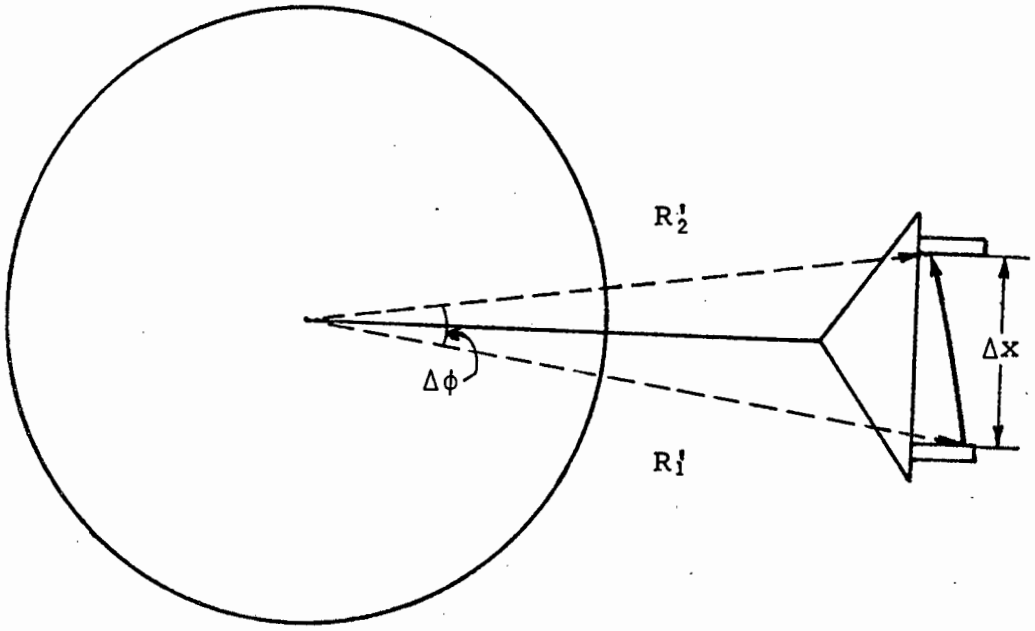

FIGURE 4-5 SCHEMATIC DIAGRAM OF STREAK PHOTOGRAPH

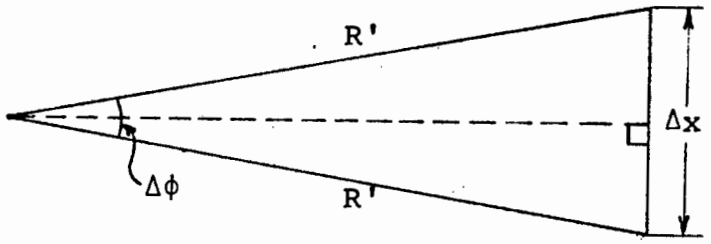

FIGURE 4-6 GEOMETRICAL ANALYSIS OF STREAK PHOTOGRAPH

the geometrical relation

$$\Delta\phi = 2\sin^{-1}\left(\frac{\Delta x}{2R'}\right), \qquad (4B.3)$$

where $R' = (R_2' + R_1')/2.$

This geometrical relation may easily be deduced from the isosceles triangle shown in Figure 4-6; the mean radius R' is used for the length of the two equal sides. Thus

$$V_\phi = \frac{2R'}{\Delta t} \sin^{-1}\left(\frac{2\Delta x}{R'}\right). \qquad (4B.4)$$

Equations (4B.1) and (4B.4) were used to calculate the velocities from actual measurements. The various measured distances R_1', R_2' and Δx were scaled down to allow for the fact that the photographs were enlarged, the scale factor being found by measuring the size of the enlarged 1 cm grid. (The experimental procedure is detailed in Section 3B). Dimensionless velocity components were calculated using the relationships

$$u' = V_{r'}\left(\frac{\rho a}{\eta_0}\right) \qquad (4B.5)$$

$$w = \frac{V_\phi}{\Omega a} \qquad (4B.6)$$

These expressions derive from the theoretical analyses contained in Chapter 2., equations (2A.11) and (2B.5).

All experimental velocity data were obtained at 25,0° C and with the sphere or disc rotating at 15,0 rpm. In the case of the Newtonian fluid (Glycerol), the viscosity was measured using a Brookfield viscometer and was found to be constant over a range of shear rates, as expected. The zero shear viscosities of the non-Newtonian fluids were measured as described in Section 4A, the values obtained from Caswell's extrapolation

procedure being used. All densities were measured using a Baird and Tatlock pyknometer and the radii of the spheres and discs were measured as described in Chapter 3. A computer program was written to calculate the velocity components in dimensionless form, using the appropriate values of the radius, density, zero shear viscosity and angular velocity in equations (4B.5), (4B.6). Raw data and the calculated dimensionless quantities are tabulated in Appendix G. The dimensionless velocity data are presented in graphical form in the next section.

4C PRESENTATION OF EXPERIMENTAL VELOCITY PROFILES, AND COMPARISON WITH THEORY

Experimental radial and tangential velocity profiles for four rotating sphere systems are presented in Figures 4-7 to 4-14 and profiles for two rotating disc systems are presented in Figures 4-15 to 4-18. Sources of error and experimental scatter will be discussed in Chapter 5. It should be noted that the measured radial velocities are about two orders of magnitude smaller than the measured tangential velocities, and are consequently plotted on a much larger scale. The absolute errors are magnified correspondingly.

The theoretical curves presented in Figures 4-7 to 4-14 were calculated using the theory presented in Section 2A, equations (2A.28), (2A.29), (2A.31) and (2A.38). The effect of the tank walls on the velocity data was estimated by using a suitable β value. The choice of a specific β value for a given ratio of tank size to sphere diameter is discussed in Appendix F.

The curves for the Newtonian fluid (Figures 4-7 and 4-8) were calculated with $m' = \sigma' = 0$ in equations

TABLE 4-2 ROTATING SPHERE STUDIES

FIGURES	FLUID	SPHERE DIA-METER	TANK SIZE	β	η_0 [poise]	L	m'	σ'
4-7,8	Glycerol	4,15 cm	38,1 cm	10,1	7,09	1,44	0,0	0,0
4-9,10	1,50% Natrosol	4,15 cm	38,1 cm	10,1	145	0,0022	7,5	96
4-11,12	1,50% Natrosol	6,98 cm	30,5 cm	4,8	145	0,0175	2,3	13,1
4-13,14	0,90% Natrosol	4,15 cm	38,1 cm	10,1	15,4	0,194	0,57	0,33

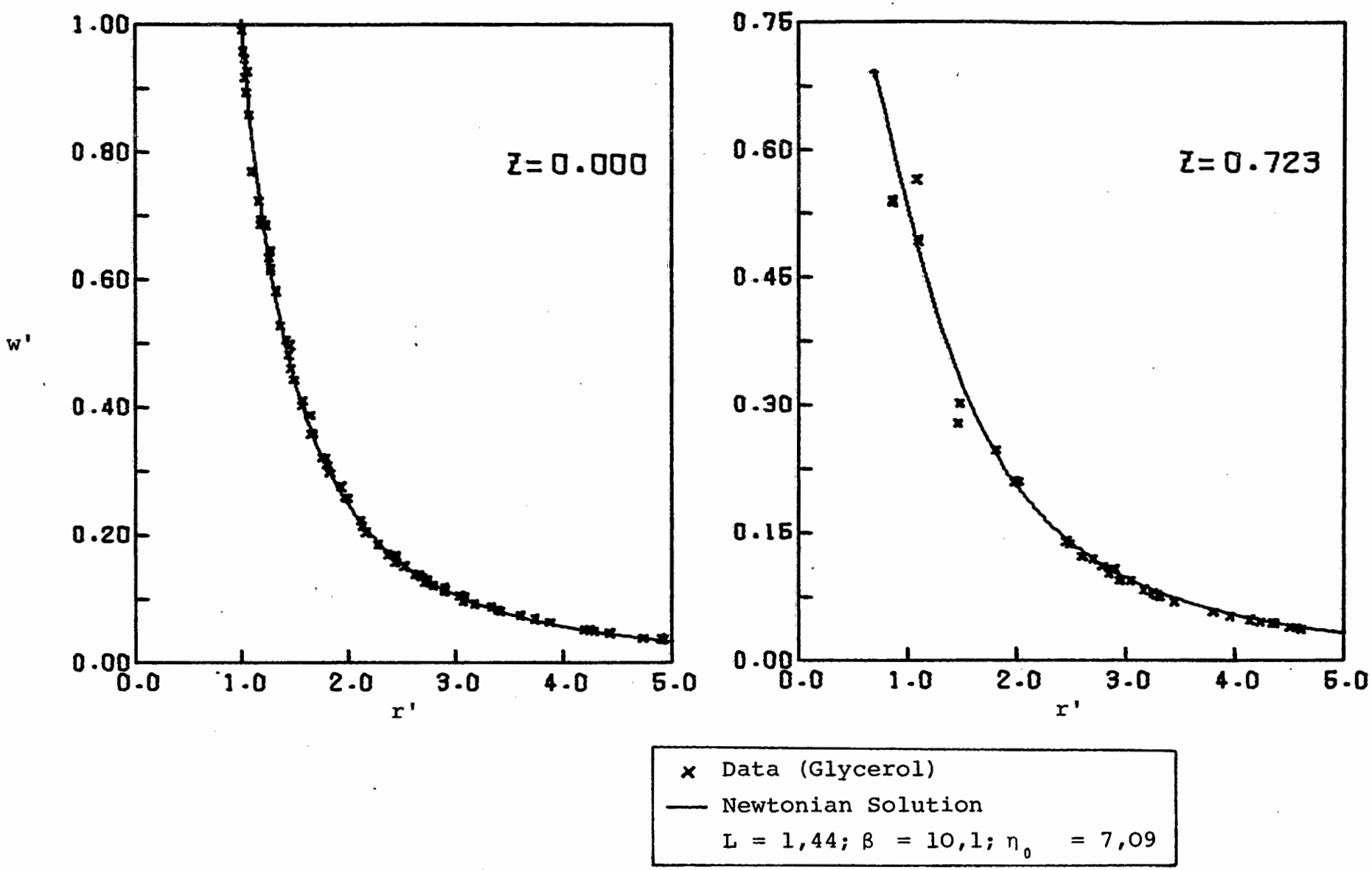

FIGURE 4-7 DIMENSIONLESS TANGENTIAL VELOCITY PROFILES FOR THE ROTATING SPHERE

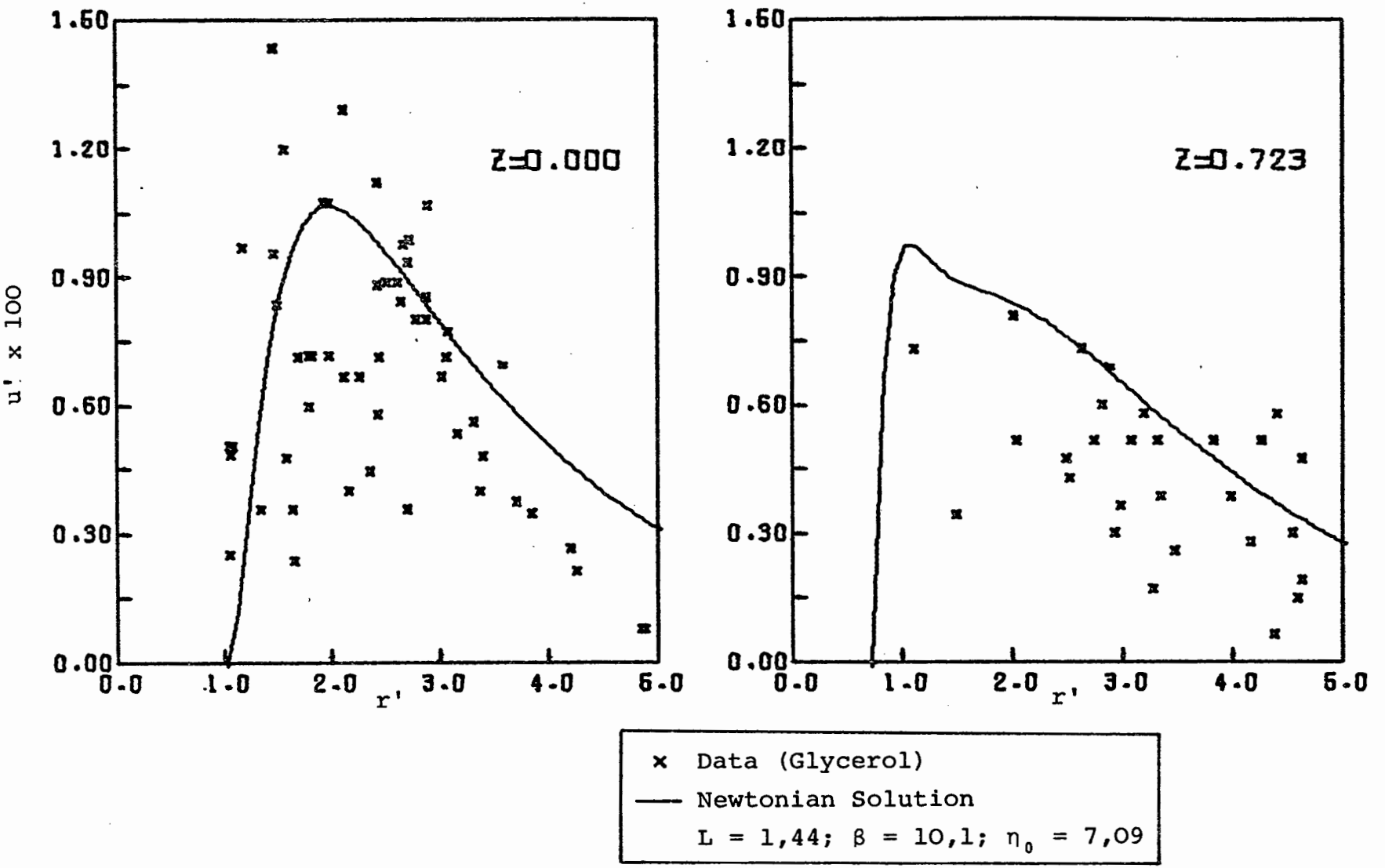

FIGURE 4-8 DIMENSIONLESS RADIAL VELOCITY PROFILES FOR THE ROTATING SPHERE

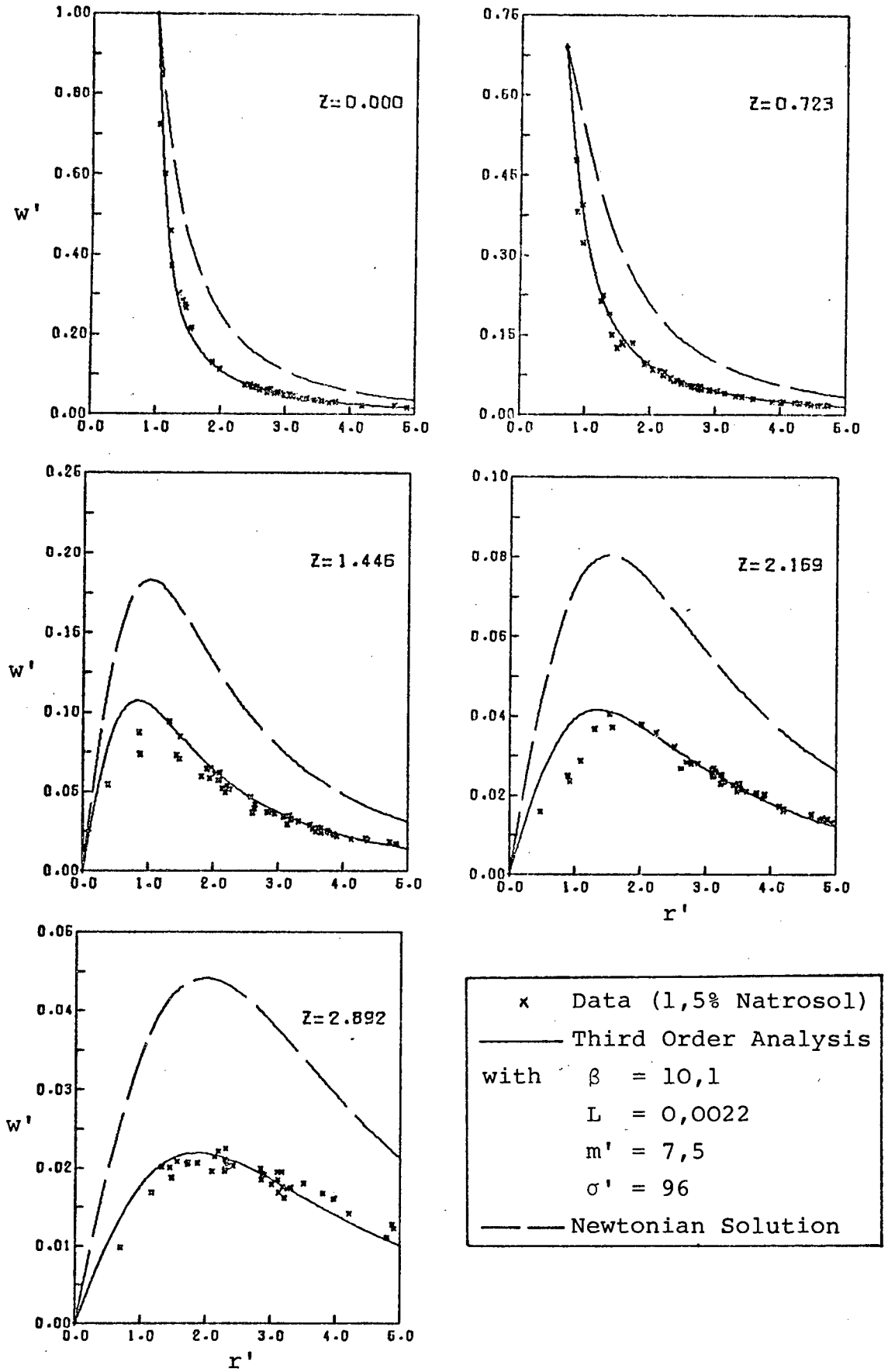

FIGURE 4-9 DIMENSIONLESS TANGENTIAL VELOCITY PROFILES FOR THE ROTATING SPHERE

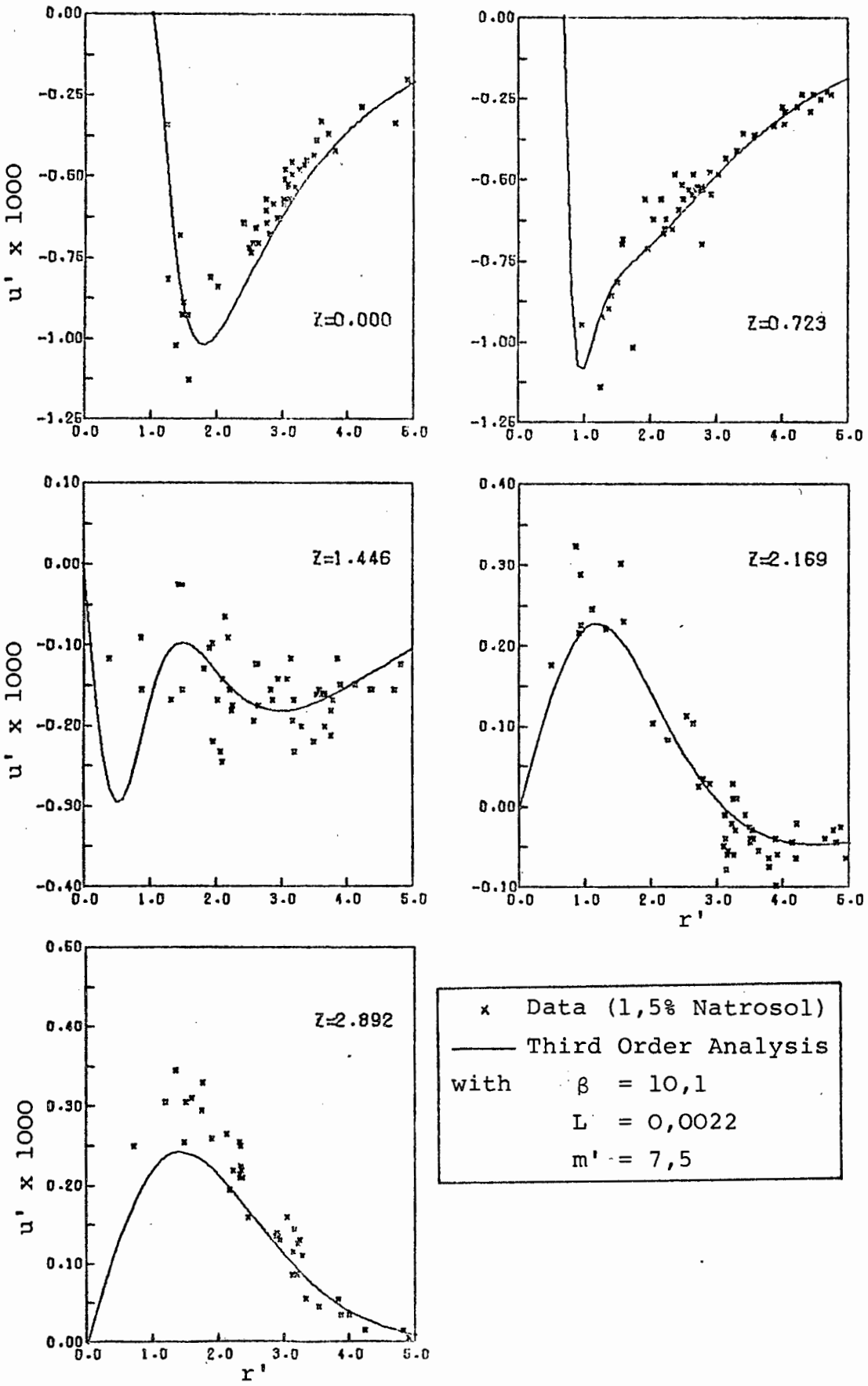

FIGURE 4-10 DIMENSIONLESS RADIAL VELOCITY PROFILES FOR THE ROTATING SPHERE

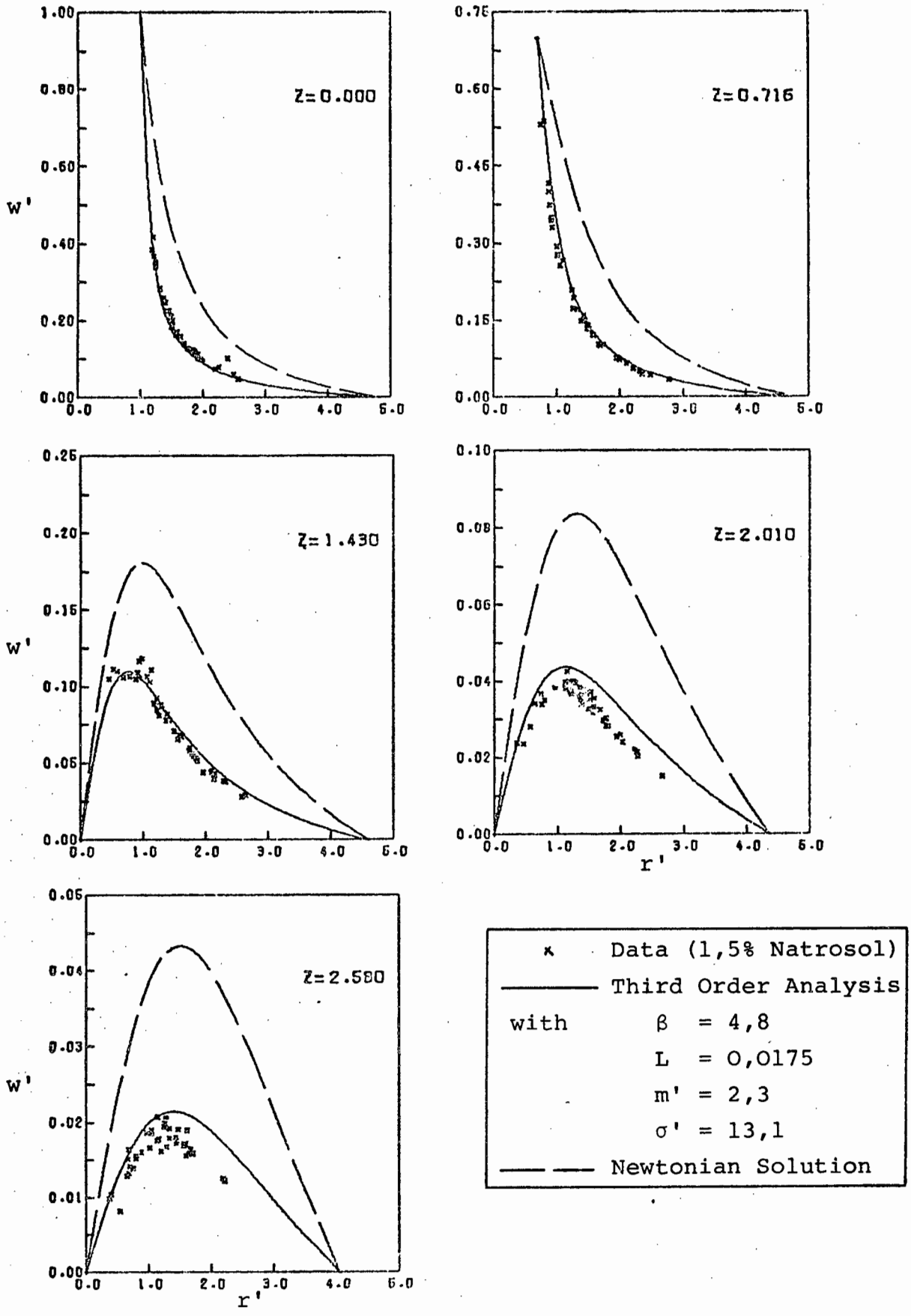

FIGURE 4-11 DIMENSIONLESS TANGENTIAL VELOCITY PROFILES FOR THE ROTATING SPHERE

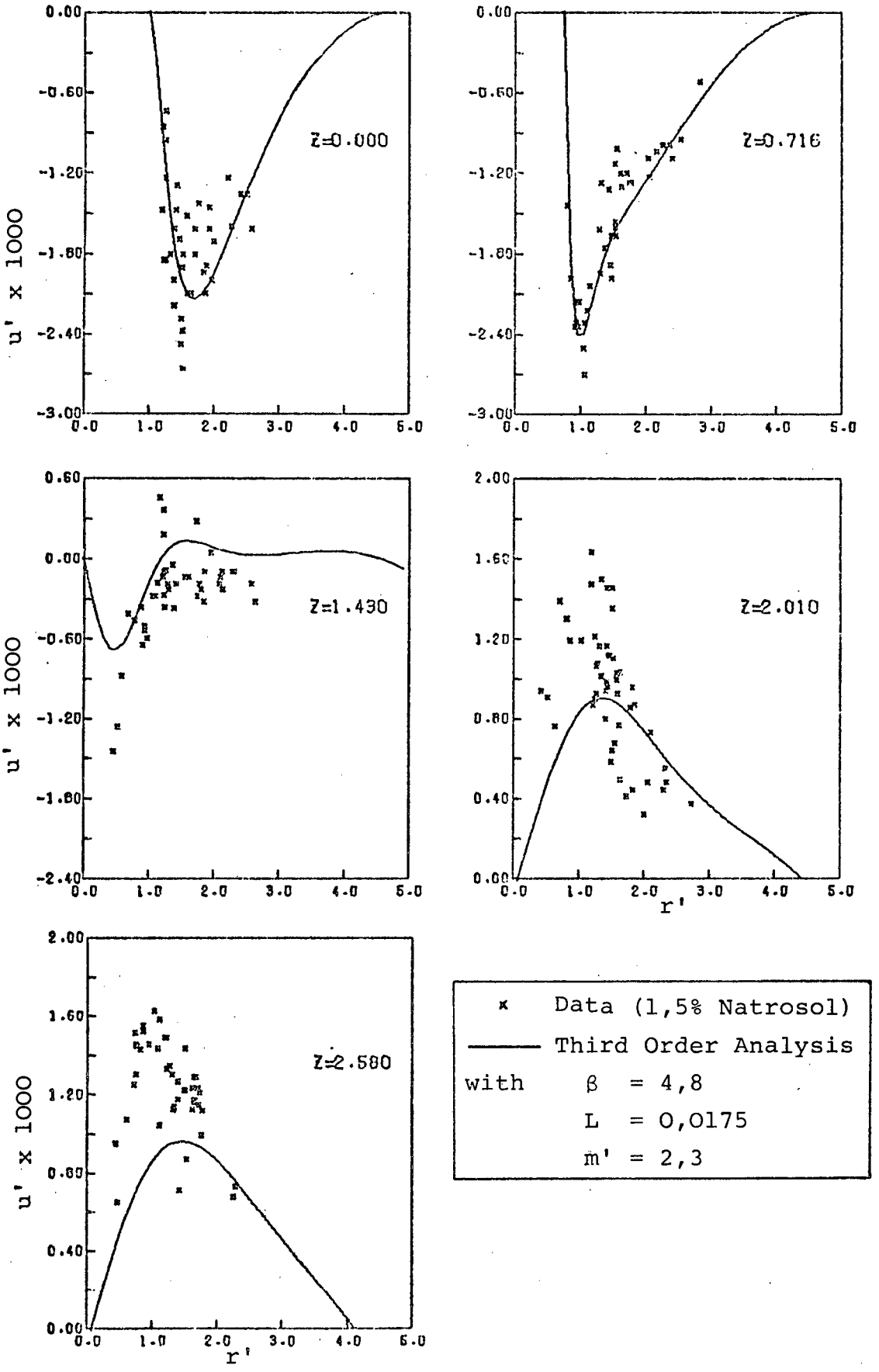

FIGURE 4-12 DIMENSIONLESS RADIAL VELOCITY PROFILES FOR THE ROTATING SPHERE

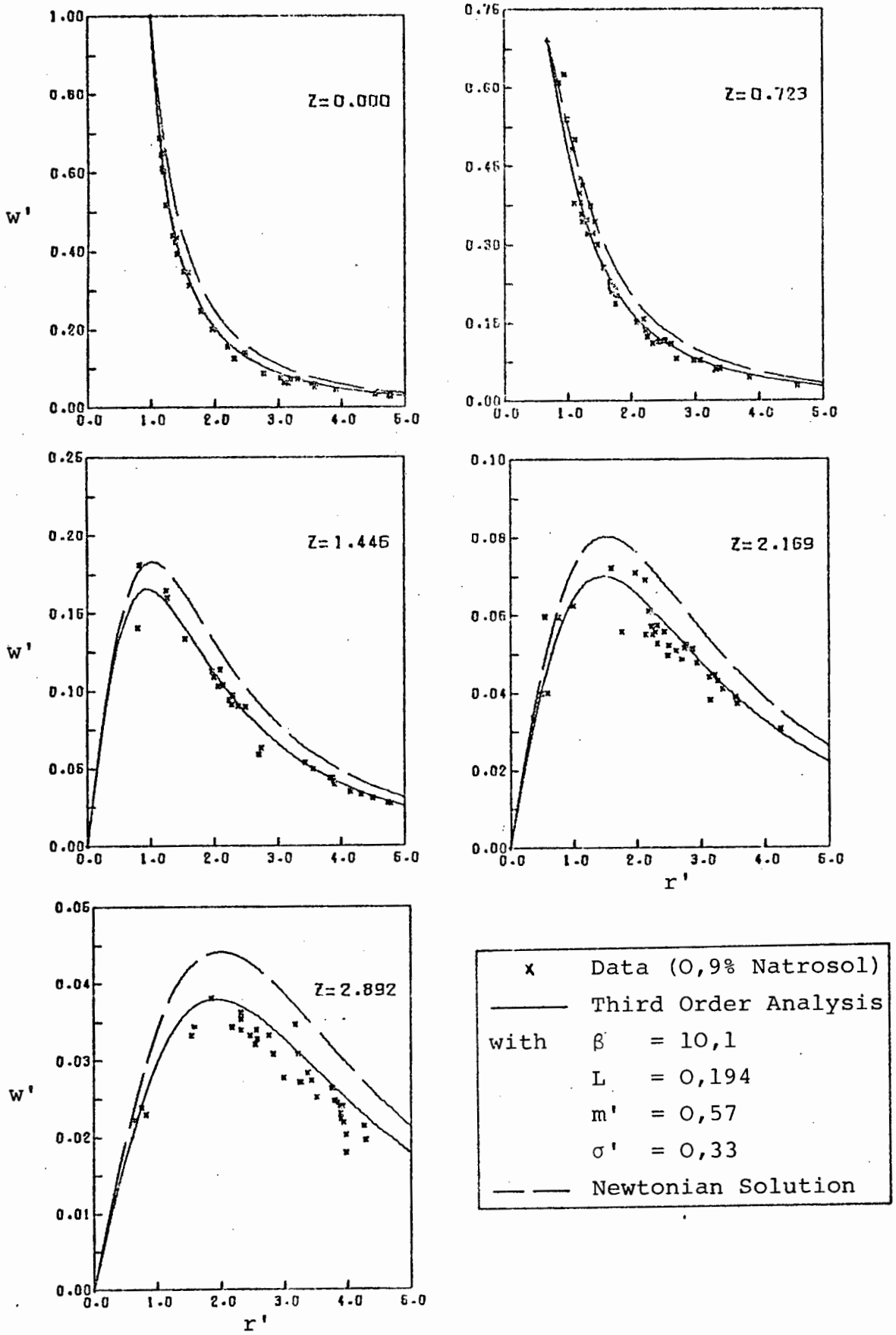

FIGURE 4-13 DIMENSIONLESS TANGENTIAL VELOCITY PROFILES FOR THE ROTATING SPHERE

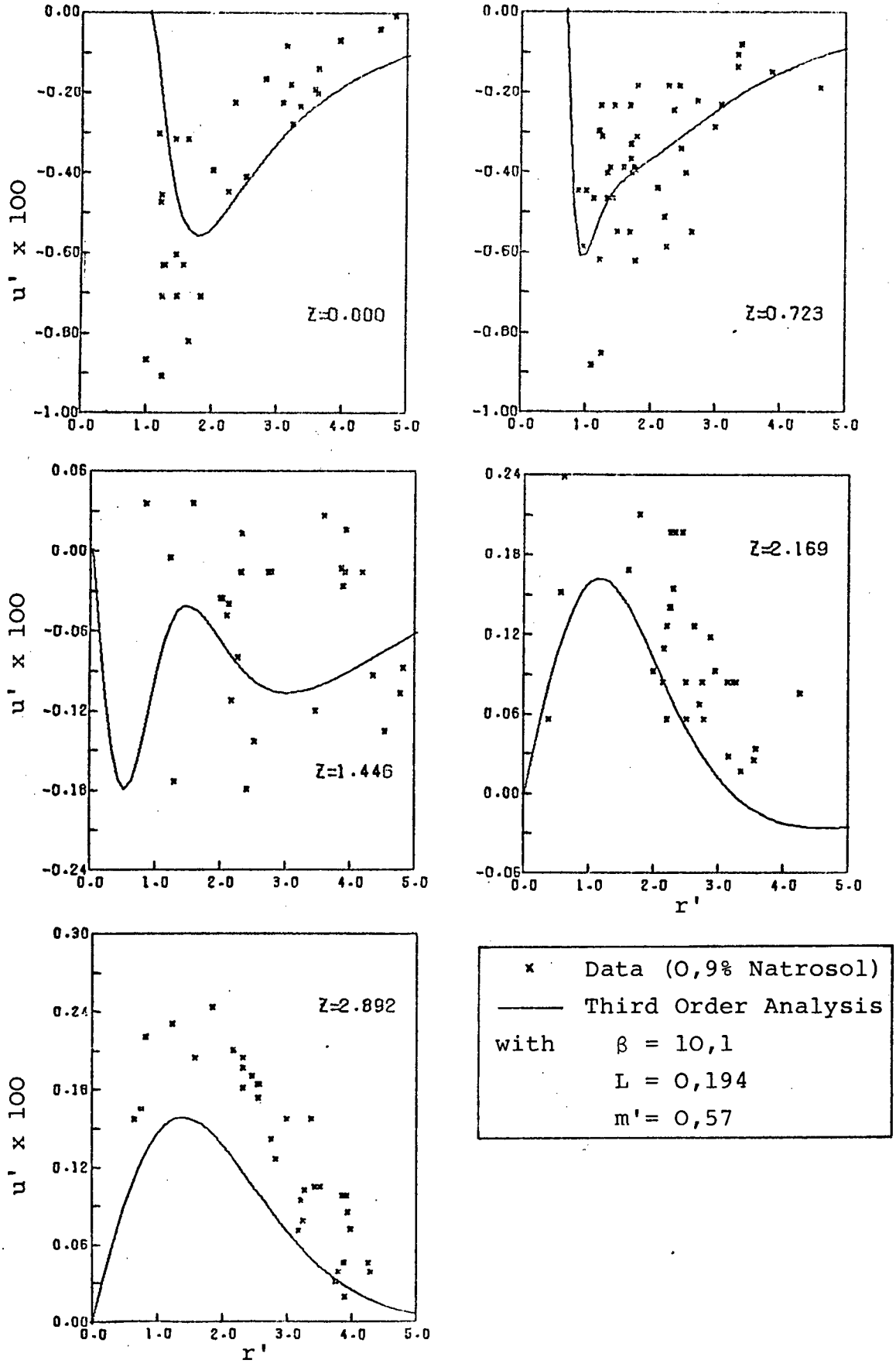

FIGURE 4-14 DIMENSIONLESS RADIAL VELOCITY PROFILES FOR THE ROTATING SPHERE

TABLE 4-3 ROTATING DISC STUDIES

FIGURES	FLUID	DISC DIA-METER	TANK SIZE	η_0[poise]	L	m'
4-15,16	1,50% Natrosol	7,07 cm	30,5 cm	145	0,0179	2,50
4-17,18	0,90% Natrosol	4,15 cm	38,1 cm	15,4	0,194	0,50

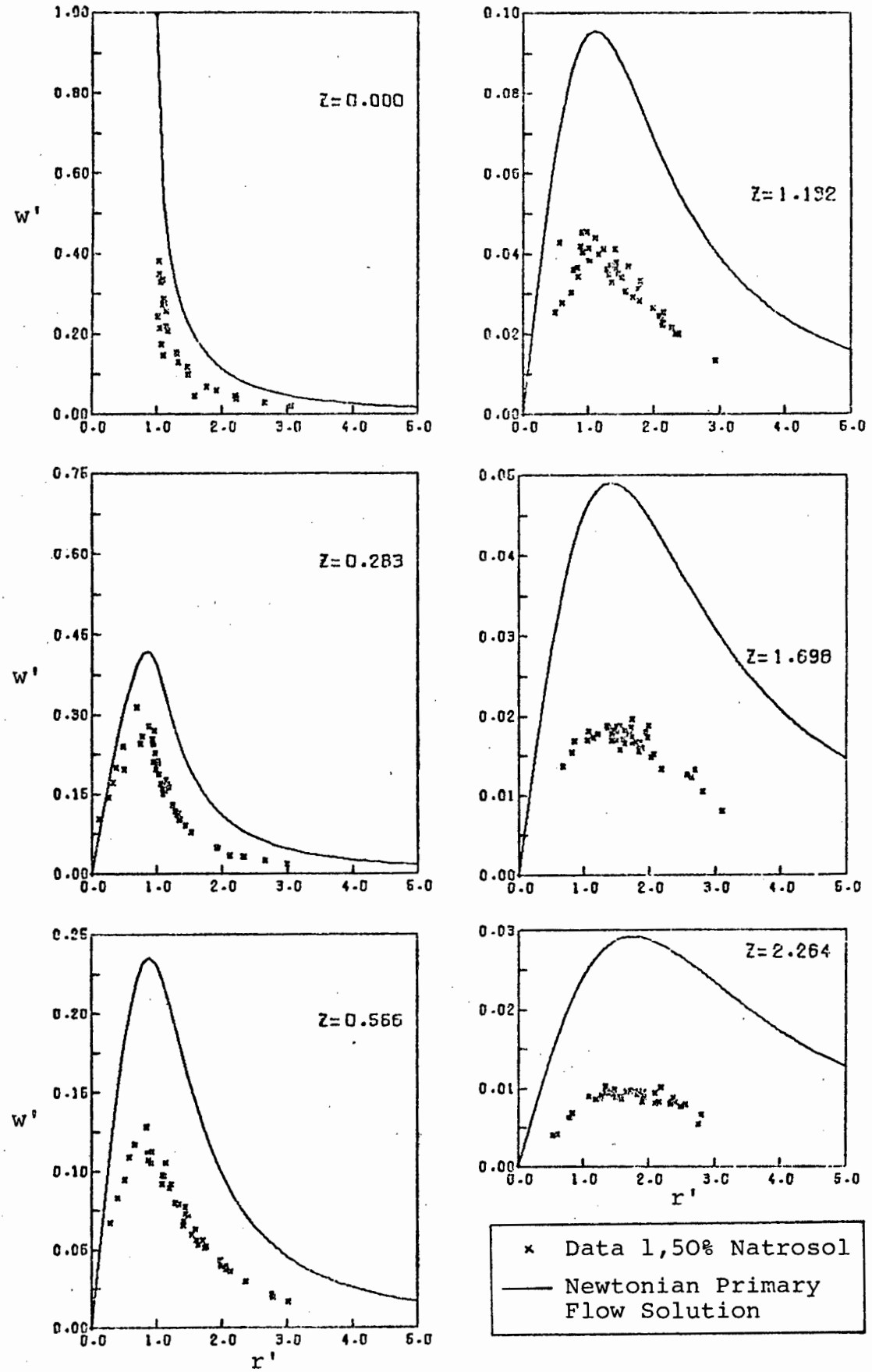

FIGURE 4-15 DIMENSIONLESS TANGENTIAL VELOCITY PROFILES FOR THE ROTATING DISC

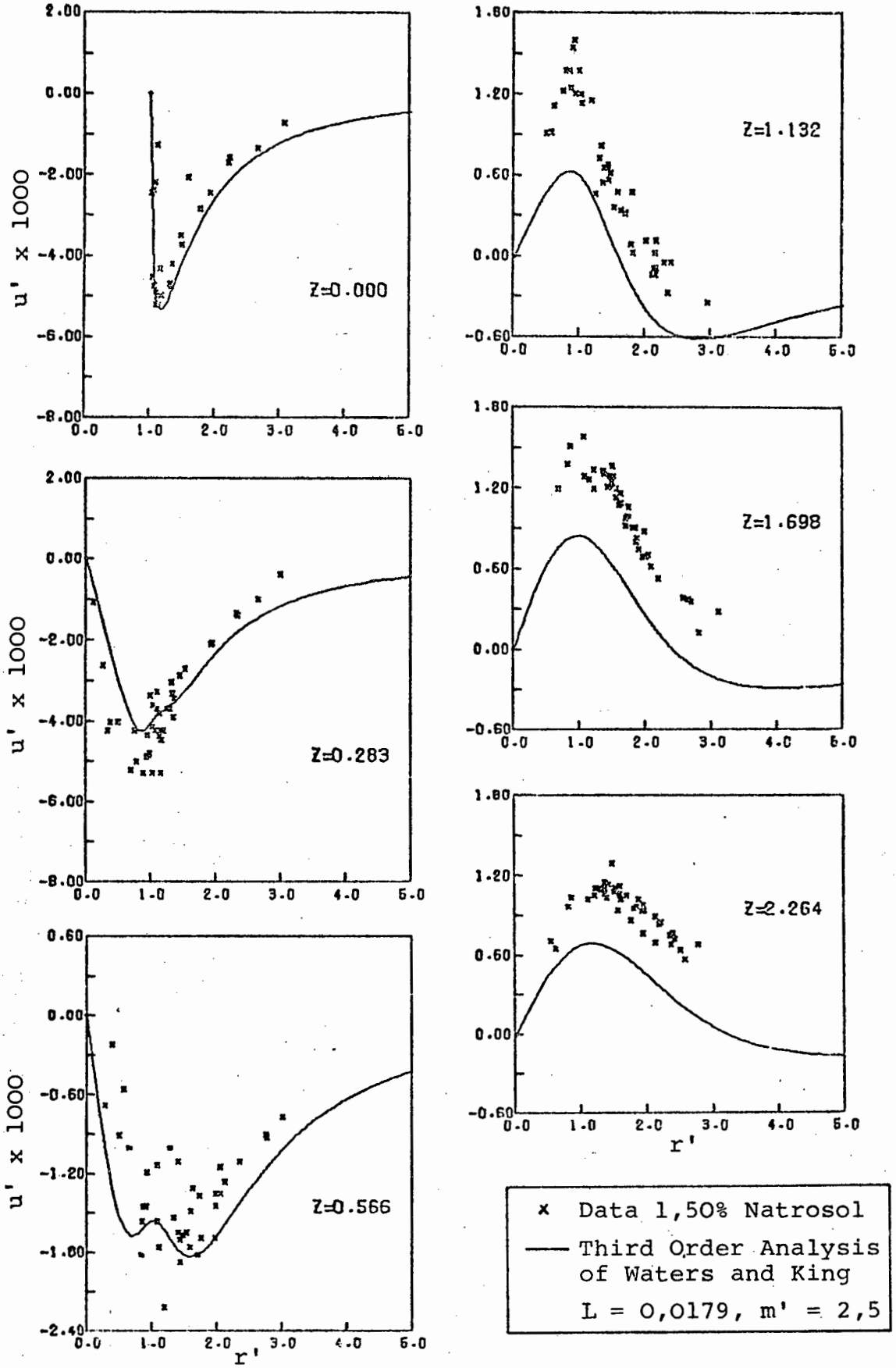

FIGURE 4-16 DIMENSIONLESS RADIAL VELOCITY PROFILES FOR THE ROTATING DISC

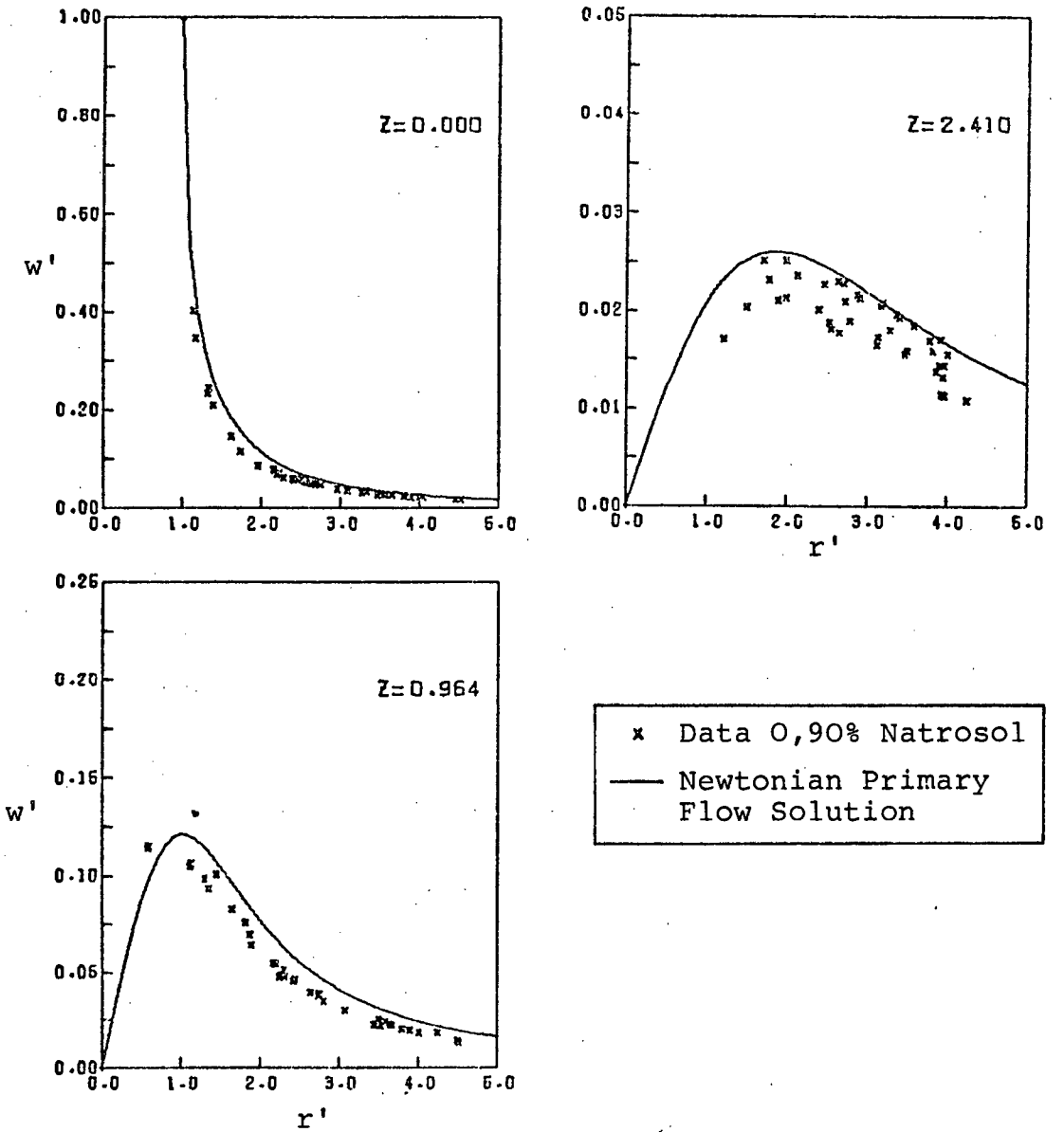

FIGURE 4-17 DIMENSIONLESS TANGENTIAL VELOCITY PROFILES FOR THE ROTATING DISC

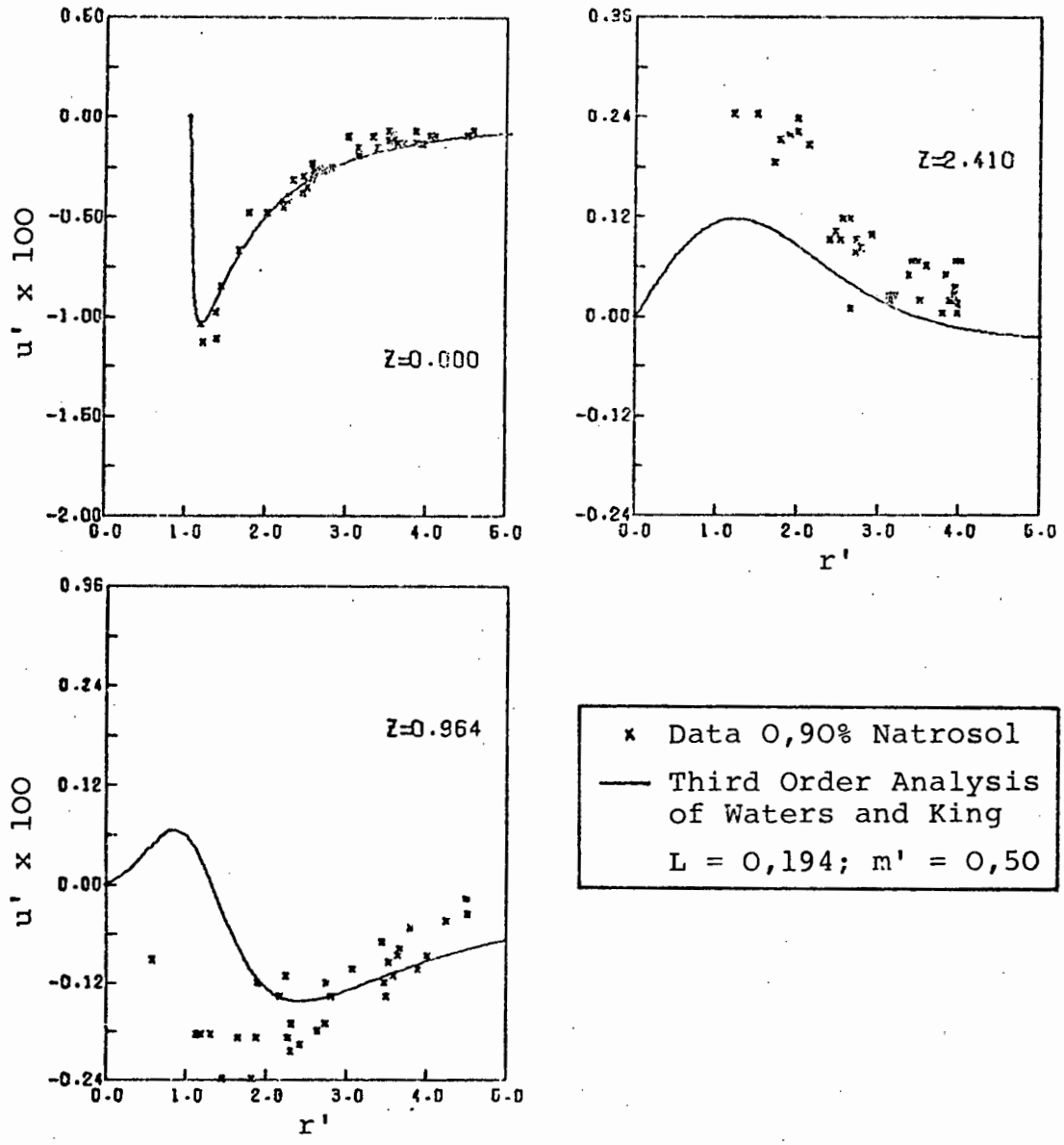

FIGURE 4-18 DIMENSIONLESS RADIAL VELOCITY PROFILES FOR THE ROTATING DISC

(2A.28), (2A.29) and (2A.31). The value of η_0 and the other parameters in these equations were obtained by independent measurement; thus no curve fitting procedure was involved.

The theoretical curves for the viscoelastic fluids were obtained as follows: The equations for the radial velocity profiles (u' vs r') were fitted to the experimental data by doing a least squares regression on the parameter m'. The value of the zero shear viscosity obtained by the falling spheres method was used to calculate L. The data were not weighted in any way and the points for all z planes were fitted simultaneously to give a 'best fit' m' value. The radial velocity curves are a function of m' only, but the tangential velocity curves (w vs r') are a function of both m' and σ'. Thus the 'best fit' m' value based on the u' vs r' data was assumed in the equations for w, and a fit of the tangential velocity data was obtained by doing a least squares regression on σ' only. Again the data were not weighted and all planes were fitted simultaneously. The curves for a Newtonian fluid ($m' = \sigma' = 0$) with viscosity equal to the zero shear viscosity are shown for comparative purposes. Table 4-2 summarises the information relevant to each of Figures 4-7 to 4-14. The significance of these results will be discussed in Chapter 5.

Experimental velocity profiles for the rotating disc are presented in Figures 4-15 to 4-18. The theoretical curves superimposed on the radial velocity data were calculated from the theory for the rotating disc presented in Section 2B. A least squares regression was performed to obtain a best fit value for the parameter m'. The theory is strictly valid for an infinite sea of fluid only and no allowance is made for wall effects.

No theoretical solution for the tangential velocity component of the flow about a disc rotating in a visco-elastic fluid is available and the Newtonian primary flow curves (L = 0) are presented merely for comparison. Table 4-3, on page 105, summarises the information pertinent to Figures 4-15 to 4-18.

4D THE DYE TRACER OBSERVATION

A brief dye tracer study was undertaken, using the 6,98 cm sphere in the 38,1 cm tank filled with a 0,90% Natrosol solution. Some black Indian ink was mixed with a small quantity of the Natrosol solution and an 18 cm hyperdermic needle was used to inject this mixture into the tank at a number of places. The sphere was set in motion at 15,0 rpm and a number of photographs of the developing dye patterns were taken over a period of 2½ hours. A steady dye pattern evolved only about 1¼ hours after the commencement of the run and a fair amount of diffusion had taken place by that time. The photographs shown in Figures 4-19 and 4-20 were taken about 20 minutes and 2¼ hours after the commencement of the run respectively. It is clear that considerable diffusion had taken place at the time that the second photograph was taken, but the nodal positions (following the theory of Thomas and Walters [45]) were still discernible and are as marked. The radii of the nodal positions were measured from this and three similar photographs, all taken 2 to 2½ hours after the injection of the dye to ensure steady state conditions. The dimensionless radii of the nodal positions above and below the equatorial plane are $r^{(n)} = 2,8 \pm 0,2$ and $3,2 \pm 0,2$ respectively. The radii measured in the upper region were consistently smaller than those measured in the lower region. These results will be discussed in Chapter 5.

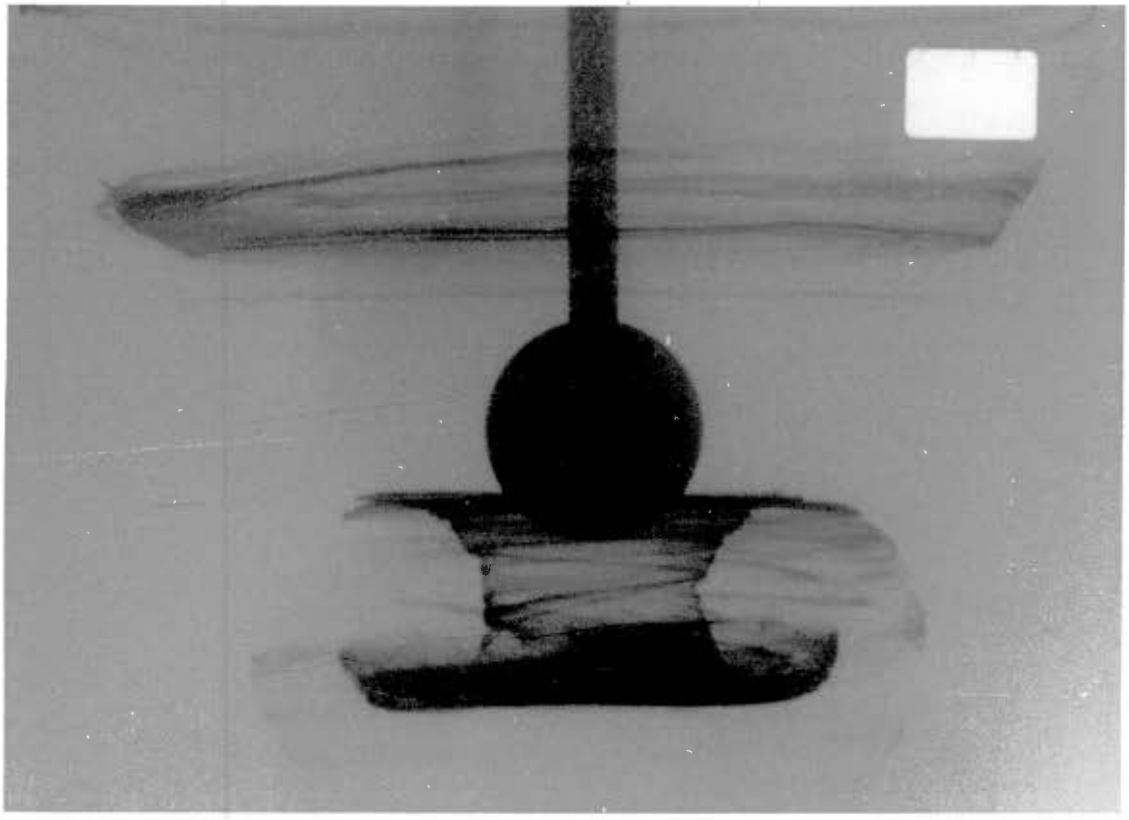

FIGURE 4-19 DEVELOPING DYE PATTERNS

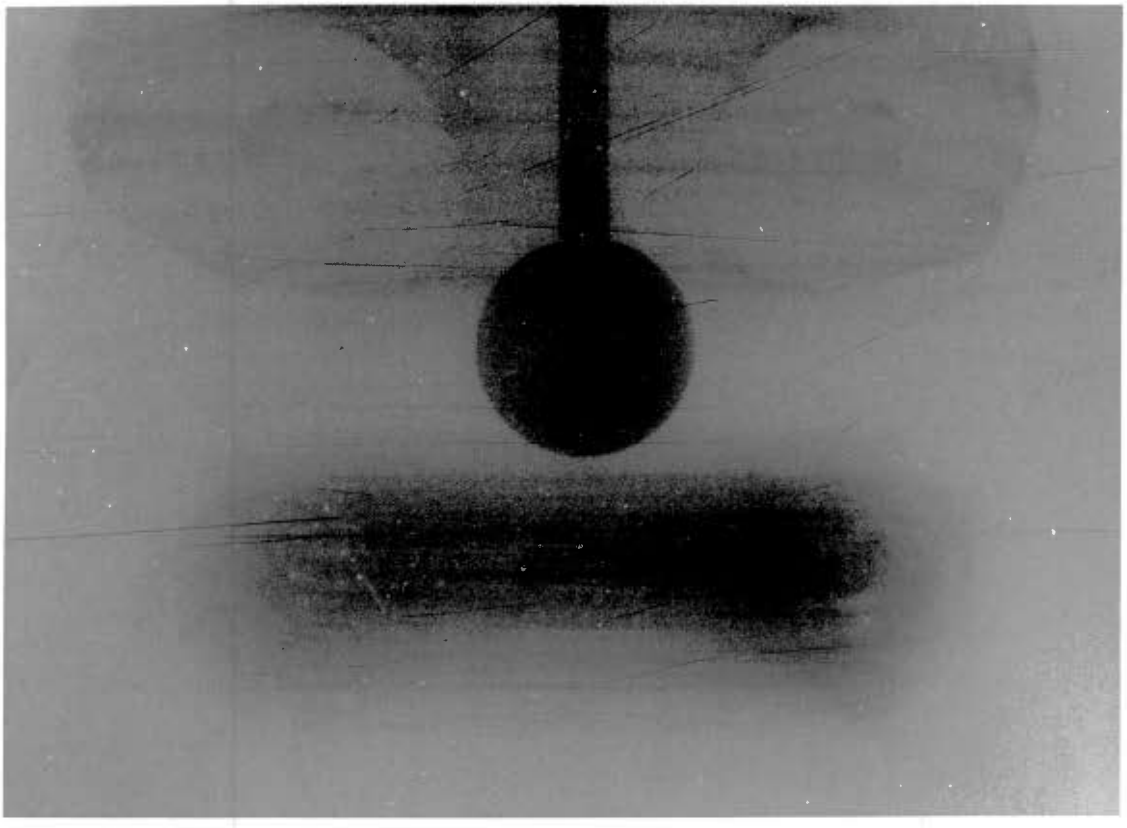

FIGURE 4-20 STEADY STATE DYE PATTERNS

distances greater than 6 cm from the centre, the maximum relative error from this approximation was found to be about 3%. This category includes more than 90% of the data. The average error for these data was certainly less than 1%. For data closer to the centre, the error may be far greater (up to about 40%), but very few data points were taken close to the centre of the sphere or disc.

CHAPTER 5

DISCUSSION OF RESULTS

5A DISCUSSION OF EXPERIMENTAL ERRORS

Following Hill's approach [65] in discussing experimental errors in a very similar system, these errors will be divided into systematic errors, random errors and error generating approximations in the analysis and taking of data.

5A.1 Systematic Errors

The tolerances on the discs and spheres were discussed in Section 3A. The rotational speed of 15,0 rpm used was found to remain constant to within 0,1 rpm during a run, an error limit of less than 1%. Temperature variations during a run were of the order of $0{,}1^{\circ}$ C, as were temperature gradients within the tank. Variations in the velocity field due to temperature changes are thus negligible.

Errors in the location of the centre are of the order of 0,3 - 0,5 mm on an enlarged photograph. More than 90% of the data were taken at distances greater than 6 cms (enlarged photograph) from the centre; thus a maximum error of 1% in the radial position is introduced for these data.

Exposure time intervals of ¼ sec. to 10 sec. were used. For exposure times of 1 sec. and less, the camera speed settings were used. The nominal exposure intervals were calibrated as described in Appendix D, and the maximum deviation from the mean exposure time for each camera setting was found to be less than 2%. Time intervals of 3 sec. to 10 sec. were measured by stop-

watch and the reaction time error is probably about 0,2 sec.

The scale of enlargement of each set of photographs in each z plane was found by measuring the size of the image of a 1 cm grid. The mean of three or four readings was taken and the resulting scale factor is accurate to within 1%. While a 1% error in the scale factor leads to a similar error in the measured velocities, the 1% systematic error in the calculated radial position can lead to a discernible displacement of the experimental data in regions where the velocity profile is very steep. No distortion of the grid was apparent on any photographs, indicating that no optical distortion was present.

5A.2 Random Errors

The principle sources of error in the measuring of streak lengths (and hence tangential velocities) lies in the inevitable diffusion of the edges in an enlarged photograph and the limitations of the measuring instrument. Tests showed that the total maximum error from these sources is 0,2 to 0,4 mm. The shortest streaks measured were approximately 1 cm in length, and therefore the maximum error produced was approximately 4%. However, probably 80% of the data were taken from streaks of lengths 2 cm to 4 cm; thus the average error is about 1%. The error in the measurement of the radial position is of the order of 0,3 mm and may be ascribed to both the error in locating the centre and the error in measuring radial distances. This constitutes a maximum error of about 0,5% for more than 90% of the data.

The radial velocities are measured by taking the difference between the two distances from the end points

of the streak to the centre. The measuring instrument is equipped with a vernier device and radial measurements may be made to within 0,1 mm. A typical streak width is about 0,5 mm and some 30% of the streaks used have widths up to 1,0 mm. Judgment has to be used in locating the centres of the streaks in making radial distance measurements; thus a random error of the order of 0,2 to 0,4 mm may be assumed to be common. The difference in measured radial distances ranged from about 0,2 mm to 5,0 mm, depending on the actual radial velocity and the camera exposure interval. Consequently relative random error in the measured radial velocity ranges from about 8% up to 200%.

5A.3 Approximation Errors

An assumption which is basic to the experimental method is that particles illuminated by the light beam (which is 3 to 8 mm thick) lie in a plane at the centre of the beam. However, errors due to this source are diminished by the fact that only the brightest streaks were chosen for measurements, and these are likely to have been near the centre of the light beam. Furthermore, both the tangential and radial velocities change comparatively slowly with axial direction. No qualitative estimate of this source of error was made, but the smoothness of the tangential velocity data indicates that it is of the order of the other sources of error for this component. Similarly, the relative error in the measured radial velocities due to this source is likely to be small.

Equations (4B.3) and (4B.4) were used to calculate the velocities. These equations approximate the deviations at a point by their finite difference representations in the neighbourhood of that point. For radial

distances greater than 6 cm from the centre, the maximum relative error from this approximation was found to be about 3%. This category includes more than 90% of the data. The average error for these data was certainly less than 1%. For data closer to the centre, the error may be far greater (up to about 40%), but very few data points were taken close to the centre of the sphere or disc.

5B REMARKS ON THE VELOCITY DATA

Velocity profiles were measured for a sphere rotating in Glycerol, a Newtonian fluid, as an independent test of the validity of the experimental method. The theoretical curves which are superimposed on the data in Figure 4-7 are indistinguishable from the primary flow curves and are clearly in excellent agreement with the experimental data. The smoothness of the data validates the error analysis presented in the previous section; the average error in the measured tangential velocity data shown is of the order of 1%. The radial velocity data (Figure 4-8) exhibit considerable scatter, but it is clear that the data are consistent with the theoretical curves.

The tangential velocity profiles shown in Figure 4-9 are for the sphere rotating in a 1,50% Natrosol solution, with β = 10,1. The theoretical curves obtained from the Third Order analysis of Section 2A are in excellent agreement with the experimental data throughout the flow field. That such a good fit is obtainable through the manipulation of a single parameter, σ', is a strong argument for the validity of the theory under the experimental conditions. It is also of interest to note that even for the low value of L of 0,0022, considerable deviation from the Newtonian primary flow curves is apparent. The corres-

ponding radial velocity curves shown in Figure 4-10 are in good agreement with the experimental data, throughout the flow field, within the inherent experimental scatter. The smaller scatter of the radial velocity data, compared with that of the Glycerol data, is due to the fact that the actual velocities are about three times greater and thus relative errors are correspondingly smaller. Therefore the results presented in Figures 4-9 and 4-10 show that the theoretical analysis provides a complete and consistent description of the flow field around the rotating sphere in terms of only two non-Newtonian parameters, m' and σ'. It should also be noted that the value of m' of 7,5 has a negligible effect on the tangential velocity profiles, as can be seen from Figure 2-8. This conclusion is consistent with the work of Kelkar et al [3] and Walters and Savins [60], who found that where both shear dependent viscosity and elastic properties are present in a fluid, the influence of the shear thinning parameter on torque measurements is far greater than that of the elastic parameter.

The theoretical curves shown in Figures 4-11 and 4-12 are also for a sphere rotating in a 1,50% Natrosol solution, but for a β value of 4,8 and $L = 0{,}0175$. The curves for both tangential and radial velocities are in good agreement with the data. However, it can be seen that in the lower z planes, there is a discernible displacement (about 15%) of the theoretical curves relative to the data. The lack of a consistent fit throughout the flow field is due to the fact that wall effects are of great significance at this β value (as can be seen from Figures 2-3 and 2-4) and the presence of the cubical tank is being approximated by an outer concentric sphere. However, if the 'infinite sea' assumption is used (i.e. wall effects are ignored), the theoretical curves would provide a much poorer description of the data. The sum

of squared errors for the best fit to the tangential and radial velocity data increases by 20% and 60% respectively.

The results shown in Figures 4-13 and 4-14 are for the sphere rotating in a 0,9% Natrosol solution, with $L = 0{,}194$ and $\beta = 10{,}1$. The theoretical curves and experimental data are in agreement. The scatter in this set of experimental data is greater than that in corresponding sets of data for the 1,50% Natrosol solutions, but these results nevertheless confirm the earlier conclusions.

The experimental velocity data for the large disc rotating in the small tank (equivalent to $\beta' = 4{,}8$; $L = 0{,}0179$) filled with a 1,50% Natrosol solution are shown in Figures 4-15 and 4-16. Only the Newtonian primary flow curves for the tangential velocity component are available and it can be seen that the displacement of the data relative to these primary flow curves is similar to that observed in the case of the rotating sphere (Figure 4-11). The radial velocity data shown in Figure 4-16 are in good agreement with the theoretical curves predicted by the Third Order analysis of Waters and King in the upper three z planes, but the curves lie distinctly below the data in the lower three planes. This is clearly due to the fact that the theoretical curves are for a disc rotating in an infinite sea of fluid. The conformal map (see Figure 2-16) predicts an increase in the radial velocities in the lower z planes when the disc rotates within an outer nearly spherical container at $\beta' = 4{,}8$. Thus, if wall effects are accounted for, the theoretical curves agree with the data throughout the flow field.

The tangential velocity data shown in Figure 4-17 are for a disc rotating in a 0,9% Natrosol solution, with

β' = 10,1 and L = 0,194. The Newtonian primary flow curves are shown, and again it can be seen that the displacement of the data relative to the primary flow curves is similar to that for the rotating sphere shown in Figure 4-14. Agreement in the z = 0 plane is good, but there is a discernible deviation in the lower z planes. This is only partly ascribalbe to wall effects, as these are small for β' = 10,1. It is possible that an experimental error occurred in the location of the lowest z plane, leading to a systematic displacement of the data.

5C REMARKS ON THE VALUES OF THE MATERIAL PARAMETERS

The theoretical curves shown in Figures 2-3 and 2-4 show that the velocity profiles around a sphere rotating in a tank whose walls are approximately 4,8 radii from the centre are substantially different from those that would occur in a much larger tank in which the wall effects may be neglected. Under these circumstances, no meaningful comparison of the experimental and theoretical velocities can be made unless wall effects are accounted for. However, for β = 10, the error involved in calculating m' and σ' values based on the infinite sea assumption are small, as is illustrated by the following table. The values given are for the sphere rotating in the 1,50% Natrosol solution, with β = 10,1 and L = 0,0022.

TABLE 5-1 VALUES OF m' AND σ' FOR β= 10,1 AND $\beta = \infty$

β	m'	$\Sigma e^2(u')$	σ'	$\Sigma e^2(w')$
10,1	7,5	$0,217 \times 10^{-5}$	96	0,0510
∞	7,1	$0,280 \times 10^{-5}$	97	0,0513

No attempt at a rigorous statistical analysis was made, but it can be seen that the error in the calculated value of σ' incurred by ignoring wall effects is of the order of 1%, whereas the corresponding error in m' is about 5%. This conclusion is consistent with the theory (Figures 2-4 and 2-6) which show that the radial velocities are more sensitive to wall effects than the tangential velocities.

The non-Newtonian parameters of the 1,50% Natrosol solution have been measured in two rotating sphere systems and one rotating disc system. It is of interest to compare the values of m and σ obtained, as distinct from the dimensionless quantities m' and σ' which include geometrical factors, as is done in Table 5-2.

TABLE 5-2 COMPARISON OF NON-NEWTONIAN PARAMETERS FOR 1,50% NATROSOL

System	m'	σ'	m	σ
Sphere 1: L = 0,0022; β = 10,1	7,5	96	32	12,3
Sphere 2: L = 0,0175; β = 4,8	2,3	13,1	28	13,5
Disc: L = 0,0179; β = 4,8	2,5	-	31	-

The values of m and σ calculated from the data obtained in the above three systems are within 10% of each other. Taking into consideration experimental errors and the approximations inherent in the calculation of these quantities, this is a good result.

Following Kelkar et al [3], we can compute a natural time t_n and a characteristic time t_c for this fluid:

$$t_n = \frac{m}{\eta_0} = 0,22 \text{ sec.}$$

$$t_c = \frac{\sigma}{\eta_0} = 0,29 \text{ sec.}$$

The value of t_n is within the range of values determined by Kelkar et al for a number of fluids. The t_c value cannot be compared with their values as it is defined in terms of different material parameters. These values were calculated from the values of m and σ obtained from the first sphere system as these are the most accurate. The Weissenberg number (W_i^*) and Viscosity number (V_i^*) for these systems are

$$W_i^* = t_n \Omega = 0,35$$

and

$$V_i^* = t_c \Omega = 0,46$$

The parameters for the 0,9% Natrosol solution were measured in a rotating sphere and a rotating disc system. The parameter m' was also calculated from the results of the dye tracer study. In this experiment, the 6,98 cm sphere was used in the 38,1 cm tank and wall effects were considerable. Thus equation (2A.29) was used to calculate m' by trial and error, with $\beta = 6,0$; $r = r^{(n)} = 3,2$ (measured) and $\theta = \text{arc.sin } (2/3)$. A value of 0,17 was obtained. The results of the three methods are given in Table 5-3 for comparison.

TABLE 5-3 COMPARISON OF NON-NEWTONIAN PARAMETERS FOR 0,9% NATROSOL

System	m'	σ'	m	σ
Sphere: L = 0,194; β = 10,1	0,57	0,33	2,5	0,40
Disc: L = 0,194; β = 10,1	0,50	-	2,2	-
Sphere: (Dye study) L = 1,55	0,17	-	2,1	-

The values of m obtained from the different systems agree well with each other, despite the amount of scatter in the radial velocity data. The natural time, characteristic time, Weissenberg number and Viscosity number for this fluid are

t_n = 0,16 sec $\quad W_i^*$ = 0,25

t_c = 0,16 sec $\quad V_i^*$ = 0,25 .

5D CONCLUSIONS AND RECOMMENDATIONS

The following are the major conclusions which may be drawn from this work.

(i) The constitutive equations for a Third Order fluid provide a quantitatively correct description of the behaviour of two non-Newtonian experimental fluids, acqueous Natrosol 250 H solutions at concentrations of 0,9% and 1,50% in the non-viscometric flow about a rotating sphere. This conclusion is valid for a range of dynamic situations within the slow flow conditions obtaining in the experimental work, i.e. for values of L less than 1,6.

(ii) The non-Newtonian material parameter m, which arises out of the Third Order fluid analyses, was determined in the geometrically dissimilar non-viscometric flows about discs and spheres and under different dynamic conditions (i.e. different values of L). The values of m determined in the different situations are in agreement with each other (within 10 to 16%), within experimental error and the approximations used in calculating m.

The Third Order fluid parameter σ was measured under two dynamic conditions. The two measured values were within 10% of each other.

It may thus be concluded that true material parameters were obtained in the non-viscometric flows. The values obtained in one experimental system could be used to predict quantitative flow behaviour in a geometrically and dynamically different system providing that conditions were restricted to the slow flow regime.

(iii) The proposed application of the conformal mapping technique predicts velocity profiles for the rotating disc which are in agreement with those predicted by a rigorous analysis, except in the region near the edge of the disc. The map may thus be used to estimate the influence of container walls on the velocity profiles, in the absence of a rigorous analysis of the flow about a disc rotating within a finite container.

(iv) The experimental method used, that of streak photography, is able to provide accurate tangential velocity data in clear fluids. However, radial velocity data cannot be measured with comparable accuracy and a large number of data points are required in order to obtain a statistically meaningful result.

The following recommendations are made.

(i) Kelkar, Mashelkar and Ulbrecht [3] have used discs and spheres rotating in viscoelastic liquids as physical models in the study of the dynamics of the mixing of these liquids by more complicated shaped agitators. Using this approach, and known Third Order fluid analyses, these authors proposed successful correlations for the power consumption in the mixing of viscoelastic liquids in terms of the non-Newtonian material parameters, but excluding the effect of container walls. Using this approach, the analysis presented in Section 2A may be used to propose a correlation which includes the effect of

container walls.

(ii) An attempt should be made at establishing the upper bound to the range of applicability of the Third Order fluid analyses by measuring comprehensive sets of velocity profiles under more rapid flow conditions. The limitations imposed by the perturbation method used in obtaining a mathematical solution must be borne in mind.

Under more rapid flow conditions, shear rates would be higher and may well overlap the lower range of shear rates attainable in commercial viscometers significantly. It would then be possible to make a quantitative comparison of the material parameters measured in the viscometric and the non-viscometric flow situations.

(iii) The experimental method would be considerably improved by the use of small, highly reflecting, particles of uniform size and shape. Uniform aluminium spheres in the size range 200 μ to 250 μ would be ideal, if these could be obtained.

NOMENCLATURE

a	Radius of the sphere or disc, cm
$A^{(n)}$, n=1,2..	Rivlin-Ericksen tensors
$[A^{(n)}_{ij}]$	Matrix representation of the nth Rivlin-Ericksen tensor
$A^{(n)}_{ij}$	Components of the nth Rivlin-Ericksen tensor
$A^{(n)}_{(ij)}$	Physical components of the nth Rivlin-Ericksen tensor
A_1, A_2	Constants in the equation for $H_1(r)$
A'_1, A'_2	Constants in the equation for $F(\xi)$
B_1, B_2	Constants in the equation for $H_3(r)$
B'_1, B'_2	Constants in the equation for $G(\xi)$
c	Radius of the foci of the oblate spheroid, cm
C	Constant defined in equation (2A.16)
D	Constant defined in equation (2A.16)
$e^{(1)}$, $e^{(2)}$	First and second Oldroyd rate-of-strain tensors
F	Function of ξ, defined by equation (2B.11)
F_1, F_2, F_3	Functions of μ, defined by equations (2B.14)
G	Function of ξ, defined by equations (2B.14)
H	Function of μ, defined by equations (2B.13)
H_1, H_2, H_3, H_4	Functions of μ, defined by equations (2B.14)
$H_1(r)$, $H_3(r)$	Functions of r, defined in Section 2A, pages 30 - 32
I	The unit matrix
L	The square of the Reynolds number

m	Elastic parameter defined on page 35
m'	Dimensionless elastic parameter defined on page 26
p	An arbitrary isotropic pressure
p^*	A dimensionless isotropic pressure
$[p_{ij}]$	Matrix representation of the stress tensor
$[p'_{ij}]$	Matrix representation of the deviatoric stress tensor
p'_{ij}	Components of the deviatoric stress tensor
$p'_{(ij)}$	Physical components of the deviatoric stress tensor
$p''_{(ij)}$	Dimensionless physical components of the deviatoric stress tensor
P	A function of β and m', defined on page 27
P_1, P_2, P_3	Functions of β defined on page 27
Q	A function of β and m', defined on page 27
Q_1, Q_2, Q_3	Functions of β defined on page 27
r	Dimensionless radial distance, spherical co-ordinates
r_1	Radial distance in cm,spherical co-ordinates
r'	Dimensionless radial distance, cylindrical co-ordinates
r'_1	Radial distance in cm, cylindrical co-ordnates
S	A function of β and m', defined on page 27
S_1, S_2, S_3	Functions of β, defined on page 27
t_n	Natural time
t_c	Characteristic time

T	Stress tensor
T'	Deviatoric stress tensor
T_1, T_3	Associate Legendre functions, defined on page 29
u	Dimensionless radial velocity in spherical co-ordinates, Section 2A, or Dimensionless ξ velocity component in oblate spheroidal co-ordinates, Section 2B
u'	Dimensionless radial velocity in cylindrical co-ordinates
U_x, U_y	Dimensionless x and y velocity components in Cartesian co-ordinates, Section 2C
$U_{x'}$, $U_{y'}$	Dimensionless x' and y' velocity components in Cartesian co-ordinates, Section 2C
U	Radial physical velocity component in spherical co-ordinates, Section 2A or Physical ξ velocity component in the oblate spheroidal co-ordinate system
v	Dimensionless θ velocity component in spherical co-ordinates, Section 2A or Dimensionless η velocity component in oblate spheroidal co-ordinates, Section 2B
v'	Dimensionless axial velocity in cylindrical co-ordinates
V	Physical θ velocity component in spherical co-ordinates, Section 2A or

	Physical η velocity component in oblate spheroidal co-ordinates, Section 2B
w	Dimensionless tangential velocity component in spherical co-ordinates, Section 2A or Dimensionless tangential velocity component in terms of oblate spheroidal co-ordinates, Section 2B
w'	Dimensionless tangential velocity component in terms of cylindrical co-ordinates
W	Physical tangential velocity component in spherical co-ordinates, Section 2A or Physical tangential velocity component in oblate spheroidal co-ordinates, Section 2B
x	Dimensionless x distance in Cartesian co-ordinates, Section 2C
x'	Dimensionless x' distance in Cartesian co-ordinates, in the ζ plane, Section 2C
y	Dimensionless y distance in Cartesian co-ordinates, Section 2C
y'	Dimensionless y' distance in Cartesian co-ordinates, in the ζ plane, Section 2C
z	Dimensionless axial distance, cylindrical co-ordinates
z_1	Axial distance in cm, cylindrical co-ordinates
α_1 to α_5	Coefficients in the equations for the Third Order fluid
α_2', α_3', α_5'	Dimensionless coefficients in the equations for the Third Order fluid, Page 26

β	Ratio of the radius of the outer sphere to that of the inner sphere, Section 2A
β_1	Coefficient in the equation for the Third Order fluid
β_1'	Dimensionless coefficient in the equation for the Third Order fluid, page 26
Γ	The expression for the couple on the sphere, page 33
Δ	Function of β, defined on page 27
η	Component of the oblate spheroidal co-ordinate system, Section 2B
η	Non-Newtonian viscosity
η_0	Zero shear viscosity
θ	Component of the spherical co-ordinate system
ξ	Component of the oblate spheroidal co-ordinate system
ρ	Fluid density
σ	Shear thinning parameter defined on page 35
τ	Characteristic shear stress, Section 2D
σ'	Dimensionless shear thinning parameter, page 26
ϕ	Component of the spherical, cylindrical and oblate co-ordinate systems
χ	Stream function
Ω	Angular velocity

REFERENCES

1. Middleman, S., "The Flow of High Polymers", Interscience Publishers (1968).

2. Pipkin, A.C., "Approximate constitutive equations", Modern Developments in the Mechanics of Continua, Academic Press (1966).

3. Kelkar, J.V., Mashelkar, K.A. and Ulbrecht, J., "On the rotational viscoelastic flows around simple bodies and agitators", Trans. Instn. Chem. Engrs., 50, 343 (1972).

4. Ide, V. and White, J.L., "Rheological phenomena in polymerisation reactors - Rheological properties and flow patterns around agitators in polystyrene solutions", Report 23/1974 of Department of Chemical and Metallurgical Engineering, University of Tennessee.

5. Oldroyd, J.G., "On the formulation of Rheological equations of state", Proc. Roy Soc., A200, 523 (1950).

6. Walters, K., "Formulation and use of equations of state for elastico-viscous liquids", Nature, 207, 826 (1965).

7. Leigh, D.C., "Nonlinear Continuum Mechanics", McGraw-Hill (1968).

8. Coleman, B.D., Markovitz, H., and Noll, W., "Viscometric Flows of Non-Newtonian Fluids", Springer Tracts in Natural Philosophy, Volume 5 (1966).

9. Oldroyd, J.G., "The motion of an elastico-viscous liquid contained between coaxial cylinders. I", Quart. J. Mech. Appl. Math., 4, 271 (1951).

10. Oldroyd, J.G., "Non-Newtonian effects in steady

motion of some idealized elastico-viscous liquids", Proc. Roy. Soc. A425,278 (1958).

11. Walters, K., "Non-Newtonian effects in some elastico-viscous liquids whose behaviour at small rates of shear is characterised by a general linear equation of state", Quart. J. Mech. Appl. Math., 15, 63 (1962).

12. Truesdell, C., "The meaning of viscometry in fluid dynamics", Annual Review of Fluid Mechanics, Volume 6, Annual Reviews Inc. (1974).

13. Oldroyd, J.G., Strawbridge, D.J. and Toms, B.A. "A Coaxial Cylinder Elastoviscometer", Proc. Phys. Soc. B, 64, 44 (1951).

14. Toms, B.A. and Strawbridge, D.J., "Elastic and viscous properties of dilute solutions of polymethyl methacrylate in organic liquids", Trans. Faraday Soc. 49, 1225 (1953).

15. Jobling, A. and Roberts, J.E., "Goniometry of flow and rupture", Rheology, Theory and Applications, 1, Academic Press (1958).

16. David, J., "On simple-integral viscoelastic fluid models with the rate-of-strain dependent memory function", Rheol. Acta, 11, 333 (1972).

17. Tanner, R.I., "Observations on the use of Oldroyd-type equations of state for viscoelastic liquids", Chem. Engg. Sci., 19, 349 (1964).

18. Bogue, D.C. and Doughty, J.O., "Comparison of constitutive equations for viscoelastic fluids", Ind. Eng. Chem. Fund., 5, 243 (1966).

19. Spriggs, T.W., Huppler, J.D. and Bird, R.B., "An experimental appraisal of viscoelastic models",

Trans. Soc. Rheol., 10, 191 (1966).

20. Chen, I. and Bogue, D.C., "Time-dependent stress in polymer melts and review of viscoelastic theory", Trans. Soc. Rheol., 16, 59 (1972).

21. Broadbent, J.M., Kaye, A., Lodge, A.S. and Vale, D.C., "Possible systematic error in the measurement of normal stress differences in polymer solutions in steady shear flow", Nature, 217, 55 (1968).

22. Tanner, R.I. and Pipkin, A.C., "Intrinsic errors in Pressure-Hole measurements", Trans. Soc. Rheol., 13, 471 (1969).

23. Kearsly, E.A., "Measurement of Normal stress by means of hole pressure", Trans. Soc. Rheol., 17, 617 (1973).

24. Walters, K. and Waters, N.D., "On the use of a rheogoniometer. Part I - Steady shear", Polymer Systems, Macmillan (1968).

25. Walters, K. and Kemp, R.A., "On the use of a rheogoniometer. Part II - Oscillatory shear", Polymer Systems, Macmillan (1968).

26. Walters, K. and Kemp, R.A. "On the use of a rheogoniometer. Part III - Oscillatory shear between parallel plates", Rheol. Acta, 7, 1 (1968).

27. Walters, K., "Rheometrical flow systems. Part I - Flow between concentric spheres rotating about different axes", J. Fluid Mech., 40, 191 (1970).

28. Abbott, T.N.G. and Walters, K., "Rheometrical flow systems. Part 2 - Theory for the orthogonal rheometer, including an exact solution of the Navier-Stokes equations", J. Fluid Mech., 40, 205 (1970).

29. Abbott, T.N.G. and Walters, K. "Rheometrical flow systems. Part 3 - Flow between rotating eccentric cylinders", J. Fluid Mech., 43, 257 (1970).

30. Walters, K. and Jones, T.E.R., "Further studies on the usefulness of the Weissenberg Rheogoniometer", Proc. 5th Int. Congr. Rheol., 4, 337 (1970).

31. Knight, D.G. and Walters, K. "Nearly viscometric flows in the new rheometers", Rheol. Acta, 12, 524 (1973).

32. Payvar, P. and Tanner, R.I., "Velocity lag, axial thrust and edge effects in the eccentric disc rheometer", Trans. Soc. Rheol., 17, 449 (1973).

33. Oldroyd, J.G., "Some steady flows of the general elastico-viscous liquid", Proc. Roy. Soc., A283 (1965).

34. Coleman, B.D. and Noll, W., "An approximation theorem for functionals, with applications in continuum mechanics", Arch. Rat. Mech. Anal., 6, 335 (1960).

35. Noll, W., "A mathematical theory for the behaviour of continuous media", Arch. Rat. Mech. Anal., 2, 197 (1958).

36. Rivlin, R.S. and Ericksen, J.L., "Stress deformation relations for isotropic materials", J. Rat. Mech. Anal., 4, 323 (1955).

37. Markovitz, H., "Nonlinear steady flow behaviour", Rheology, Theory and Applications, Volume 4, Academic Press (1967).

38. Lodge, A.S. and Stark, J.H., "On the description of rheological properties of viscoelastic continua", Rheol. Acta, 11, 119 (1972).

39 Walters, K. and Waters, N.D., "The steady flow of a Rivlin-Ericksen fluid induced by a rotating sphere", Rheol. Acta, 3, 312 (1964).

40. Waters, N.D. and King, M.J., "The steady flow of an elastico-viscous liquid induced by a rotating spheroid", Quart. J. Mech. and Appl. Math, 24, 331 (1971).

41. Hill, C., "Viscoelastic fluid flow in the disc and cylinder system". PhD. Thesis (1969), University of Wisconsin, Madison.

42. Langlois, W.E., "Steady flow of a slightly visco-elastic fluid between rotating spheres", Quart. Appl. Math., 21, 61 (1963).

43. Geisikus, H., "Die simultane Translations und Rotations-beweging einer Kugel in einer elastoviskosen Flussig-keit", Rheol. Acta, 3, 59 (1963).

44. Geisikus, H., "Some secondary flow phenomena in general visco-elastic fluids", Proc. 4th Int. Congr. Rheology, 1, 249 (1963).

45. Thomas, R.H. and Walters, K., "The motion of an elastico-viscous liquid due to a sphere rotating about its diameter", Quart. J. Mech. Appl. Math., 17, 39 (1963).

46. Bhatnager, P.L. and Rajeswari, G.K., "Secondary flow of non-Newtonian fluids between two concentric spheres rotating about an axis", Indian J. Math., 5, 93 (1963).

47. Walters, K. and Waters, N.D., "On the use of a rotating sphere in the measurement of elastico-viscous

parameters", Brit. J. Appl. Phys. 14, 667 (1963).

48. Bhatnager, P.L., Rajagopalan, R. and Mathur, M.N., "Secondary flow of an elastico-viscous fluid between two concentric spheres rotating about a fixed diameter", Indian J. Math., 9, 1 (1967).

49. Mohan Rao, D.K., "Flow of a visco-elastic fluid between two concentric spheres", PhD. Thesis, Indian Inst. Sci., (1964).

50. Mow, V.C., "An asymptomatic solution for an elastico-viscous liquid between rotating spheres", J. Math., Physics, 8, 267 (1968).

51. Jones, J.R. and Lewis, M.K., "Non-Newtonian effects in axially symmetric rotational flows of some elastico-viscous liquids", Proc. Camb. Phil. Soc., 65, 351 (1969).

52. Kelkar, J.V., Mashelkar, R.A. and Ulbrecht, J., "A rotating sphere viscometer", J. Appl. Poly. Sci., 17, 3069 (1973).

53. Jain, M.K., "The flow of a non-Newtonian liquid near a rotating disc", Appl. Sci. Res., A10, 410 (1961).

54. Srivastava, A.C., "Flow of non-Newtonian fluids at small Reynolds number between two infinite discs : one rotating and the other at rest", Quart. J. Mech. Appl. Math., 14, 352 (1961).

55. Sharma, S.K. and Sharma, H.G., "Flow of Second Order fluids over an enclosed rotating disc", Appl. Sci. Res., A15, 278 (1966).

56. Schlichting, H., "Boundary Layer Theory", McGraw-Hill (1960) (Fourth edition).

57. Griffiths, D.F., Jones, D.T. and Walters, K., "A flow reversal due to edge effects", J. Fluid. Mech., 36, 161 (1969).

58. Jeffery, G.B., "On the steady rotation of a solid of revolution in a viscous fluid", Proc. Lond. Math. Soc., 14, 327 (1915).

59. Geisekus, H., "Sekundarstromungen in viskoelastichen Fluissigkeiten bei stationarer und periodischer Beweging", Rheol. Acta, 4, 85, (1965).

60. Walters, K. and Savins, J.G., "A rotating sphere viscometer", Trans. Soc. Rheol., 9, 407 (1965).

61. Mashelkar, R.A., Kale, D.D., Kelkar, J.V. and Ulbrecht, J., "Determination of material parameters of viscoelastic fluids by rotational non-viscometric flows", Chem. Eng. Sci., 27, 973 (1972).

62. Caswell, B., "The effect of finite boundaries on the motion of particles in non-Newtonian fluids", Chem. Engg. Sci., 25, 1167 (1970).

63. Hansford, G.S. and Litt, M., "Mass transport from a rotating disc into power law liquids", Chem. Engg. Sci., 23, 849 (1968).

64. Hill, C.T., Huppler, J.D. and Bird, R.B., "Secondary flows in the disc-and-cylinder system", Chem. Engg. Sci., 21, 815 (1966).

65. Hill, C.T., "Nearly viscometric flow of viscoelastic fluid in the disc and cylinder system. II : Experimental", Trans. Soc. Rheol., 16, 213 (1972).

66. Kramer, J.M. and Johnson, M.W., "Nearly viscometric flow of viscoelastic fluid in the disc and cylinder

system. II : Theoretical", Trans. Soc. Rheol., 16, 197 (1972).

67. Metzner, A.B. and Taylor, J.S., "Flow patterns in agitated vessels", AI Ch EJ., 6, 109 (1960).

68. Smith, J.M., "Secondary flow phenomena in mixing viscous and visco-elastic liquids", The Chemical Engineer (March) CE45 (1970).

69. Peters, D.C. and Smith, J.M., "Mixing in anchor agitated vessels", Can. J. Chem. Eng., 47, 268 (1969).

70. Peters, D.C. and Smith, J.M., "Fluid flow in the region of anchor agitator blades", Trans. Instu. Chem Engrs., 45, 360 (1967).

71. Ulbrecht, J., "Mixing of viscoelastic fluids by mechanical agitation", The Chemical Engineer (June), 347 (1974).

72. Rivlin, R.S., "Solution of some problems in the exact theory of visco-elasticity", J. Rat. Mech. Anal., 5, 179 (1956).

73. Bird, R.B., Stewart, W.E. and Lightfoot, E.N., "Transport Phenomena", Wiley (1966).

74. Waters, N.D., personal communication (1974).

75. Jeffery, G.B., "On the steady rotation of a solid of revolution in a viscous fluid", Proc. Long. Math. Soc., 14, 327 (1915).

76. Piercy, N.A.V., "Aerodynamics", English Universities Press (1937).

77. Kober, H., "Dictionary of Conformal Representations", Dover (1957).

78. Ahlfors, L.V., "Complex Analysis", McGraw-Hill (1953).

79. Caswell, B. and Schwarz, W.H., "The creeping motion of a non-Newtonian fluid past a sphere", J. Fluid. Mech., 13, 417 (1962).

80. Cygan, D.A. and Caswell, B., "Precision falling sphere viscometry", Trans. Soc. Rheol., 15, 663 (1971).

81. Turian, R.M., "An experimental investigation of the flow of aqueous non-Newtonian high polymer solutions past a sphere", AI Ch EJ., 13, 999 (1967).

82. Subbararnan, V., Mashelkar, R.A. and Ulbrecht, J., "Extrapolation procedures for zero shear viscosity with a falling sphere viscometer", Rheol. Acta, 10, 429 (1971).

83. Huppler, J.D., "The Secondary Normal Stress Difference", PhD. Thesis, University of Wisconsin (1965).

84. Wylie, C.R., "Advanced Engineering Mathematics", McGraw-Hill (1960).

85. Mow, V.C.S., "The secondary flow about a sphere rotating in an elastico-viscous fluid", PhD. Thesis, Rensselaer Polytechnic Institute (1966).

86. Sutterby, J.L., "Falling sphere viscometry. II. End effects in short tubes", Trans. Soc. Rheol. 17, 575 (1973).

87. Sutterby, J.L., "Falling sphere viscometry. I. Wall and inertial corrections to Stokes' law in long tubes", Trans. Soc. Rheol. 17, 559 (1973).

88. King, M.J., Personal Communication (1972).

APPENDICES

APPENDIX A

CRITICISM OF MOW'S ANALYSIS

Mow [50] considered the problem of a sphere rotating in an Oldroyd four-constant fluid contained in a concentric and coaxially rotating sphere. He obtained an expression for the tangential velocity given by the equations (in his nomenclature)

$$w = w^{(0)} + Rw^{(1)},$$

where $w^{(0)} = (K\zeta + \frac{L}{\zeta^2})\sin\theta,$

R is the square of the Reynolds number, ζ is the dimensionless radius and K and L are constants related to the ratio of the radius of the outer sphere to the inner sphere and to the angular velocities of the two spheres. Mow's final equation for $w^{(1)}$ is reproduced below.

$$\begin{aligned} w^{(1)} = \frac{P_1^1(\theta)}{30}\Big\{ & m(1-\gamma)L^2\Big[\frac{3C_1}{\zeta^5} + \frac{9C_2}{\zeta^7} - 117C_4 - \frac{9K}{\zeta^3} - \frac{45L}{7\zeta^6} \\ & - \frac{44mL}{\zeta^3}\Big(1 - \gamma - \frac{18}{11}\epsilon\Big)\Big] + L^2\Big[-\frac{3}{4}\frac{C_1}{\zeta^3} - \frac{1}{2}\frac{C_2}{\zeta^5} - 3C_3 + 3C_5\zeta^2 \\ & + \frac{3}{5}\frac{L}{\zeta^4} + \frac{12}{7}\frac{m(1-\gamma)L}{\zeta^7}\Big] + KL\Big[-3C_1 + \frac{3}{2}C_3\zeta^3 + \frac{3}{4}C_5\zeta^5 \\ & + 3K\zeta^2 + \frac{3m(1-\gamma)L}{\zeta^3}\Big]\Big\} + \frac{P_3^1(\theta)}{30}\Big\{m(1-\gamma)L^2\Big[\frac{9}{2}\frac{C_1}{\zeta^5} + \frac{C_2}{\zeta^7} \\ & - \frac{9C_3}{\zeta^3} - 13C_4 - \frac{11K}{\zeta^3} - \frac{5}{3}\frac{L}{\zeta^6} - \frac{36m}{11\zeta^3}\Big(1 - \gamma + \frac{9}{2}\epsilon\Big)L\Big] \\ & + L^2\Big[-\frac{C_1}{2\zeta^3} - \frac{C_2}{3\zeta^5} - \frac{3}{4}C_3 - \frac{13}{6}C_5\zeta^2 + \frac{L}{7}\frac{\ln\zeta}{\zeta^4} + \frac{2m(1-\gamma)L}{3\zeta^6}\Big] \\ & + KL\Big[\frac{C_1}{2} + \frac{C_2}{\zeta^2} + \frac{2}{9}C_5\zeta^5 + \frac{K\zeta^2}{3} - \frac{5}{4}\frac{L}{\zeta} - \frac{8m(1-\gamma)L}{\zeta^3}\Big]\Big\}, \end{aligned}$$

This equation is reproduced from [50]. The equation given by Mow in [85] is identical.
Here $P_1^1(\theta)$ and $P_3^{(1)}(\theta)$ are associate Legendre functions;

m, γ and ε are dimensionless material constants and the C_i are functions of the geometry and of m and γ only. The above expression for $w^{(1)}$ should satisfy the boundary conditions. In particular, at the inner sphere,

$$w^{(1)}(1,0) = 0$$

However, if $\zeta = 1$ is substituted in the equation for $w^{(1)}$, it is found that $w^{(1)}(1,0) \neq 0$. This point is most easily illustrated by examining the terms containing ε. We have

$$-44mL - \frac{18}{11}\varepsilon - \frac{36m}{11}\frac{9}{2}\varepsilon L \neq 0$$

Thus Mow's solution appears to contain an error.

APPENDIX B

APPENDICES TO THE ANALYSIS CONTAINED IN SECTION 2A

B1 The Rivlin-Ericksen Tensors in Spherical Polar Co-ordinates, to First Order in L

In a general curvilinear co-ordinate system, the Rivlin-Ericksen tensors may be defined by the equations:

$$A_{ij}^{(1)} = v_{i,j} + v_{j,i} \quad (i,j = 1, 2, 3) \tag{B1.1}$$

$$A_{ij}^{(\gamma+1)} = v^k \frac{\partial A_{ij}^{(\gamma)}}{\partial x^k} + A_{ik}^{(\gamma)} \frac{\partial v^k}{\partial x^j} + A_{kj}^{(\gamma)} \frac{\partial v^k}{\partial x^i} \tag{B1.2}$$

$$(i,j = 1, 2, 3; \quad \gamma = 1, 2, \ldots N)$$

where v_i and v^i $(i = 1, 2, 3)$ represent respectively the covariant and contravariant velocity components in the x^i co-ordinate system and the commas denote covariant differentiation [42]. That is,

$$v_{i,j} = \frac{\partial v_i}{\partial x^j} - \left\{ \begin{matrix} k \\ ij \end{matrix} \right\} v_i \,, \tag{B1.3}$$

where $\left\{ \begin{matrix} i \\ jk \end{matrix} \right\}$ is the Christoffel symbol [1].

The physical components of a tensor (generally of mixed order), denoted here by affixes in parentheses, are related to its components in an orthogonal curvilinear co-ordinate system by the equation

$$A^{(ij\ldots)}_{(rs\ldots)} = \frac{h_i h_j \ldots}{h_r h_s} A^{ij\ldots}_{rs\ldots} \tag{B1.4}$$

where $h_i^2 = g_{ii}$ $(i = 1, 2, 3)$.

For a second order tensor A^{ij}, A_{ij}

$$A^{(ij)} = h_i h_j A^{ij} \qquad \text{(contravariant tensor)} \qquad \text{(B1.5)}$$

and $$A_{(ij)} = \frac{hA_{ij}}{h_i L_j} \qquad \text{(covariant tensor)} \qquad \text{(B1.6)}$$

Thus in a spherical co-ordinate system (r_1, θ, ϕ) the physical components of the velocity vector $\nu_{(r_1)}$, $\nu_{(\theta)}$, $\nu_{(\phi)}$ are related to is covariant and contravariant components by the equations

$$\begin{aligned} \nu_{(r_1)} &= \nu^1 = \nu_1 \\ \nu_{(\theta)} &= r_1\nu^2 = \nu_2/r_1 \\ \nu_{(\phi)} &= r_1\sin\theta\nu^3 = \nu_3/r_1\sin\theta \end{aligned} \qquad \text{(B1.7)}$$

The only non-vanishing components of the Christoffel symbols are

$$\left\{\begin{matrix} r_1 \\ \theta\theta \end{matrix}\right\} = -r_1, \qquad \left\{\begin{matrix} r_1 \\ \phi\phi \end{matrix}\right\} = -r_1\sin^2\theta ,$$

$$\left\{\begin{matrix} \theta \\ r_1\theta \end{matrix}\right\} = \left\{\begin{matrix} \theta \\ \theta r_1 \end{matrix}\right\} = \left\{\begin{matrix} \phi \\ r_1\phi \end{matrix}\right\} = \left\{\begin{matrix} \phi \\ \phi r_1 \end{matrix}\right\} = \frac{1}{r_1} , \qquad \text{(B1.8)}$$

$$\left\{\begin{matrix} \theta \\ \phi\phi \end{matrix}\right\} = \sin\theta\cos\theta, \quad \left\{\begin{matrix} \phi \\ \theta\phi \end{matrix}\right\} = \left\{\begin{matrix} \phi \\ \phi\theta \end{matrix}\right\} = \cot\theta$$

and the scale factors are given by

$$h_1 = 1, \quad h_2 = r_1, \quad h_3 = r_1\sin\theta \qquad \text{(B1.9)}$$

Thus, for example, equations (B1.1) and (B1.3) give

$$A_{11}^{(1)} = 2\left[\frac{\partial\nu_1}{\partial x^1} - \left(\left\{\begin{matrix} 1 \\ 11 \end{matrix}\right\}\nu_1 + \left\{\begin{matrix} 2 \\ 11 \end{matrix}\right\}\nu_2 + \left\{\begin{matrix} 3 \\ 11 \end{matrix}\right\}\nu_3\right)\right]$$

By equations (B1.8), $\left\{ {1 \atop 11} \right\} = \left\{ {2 \atop 11} \right\} = \left\{ {3 \atop 11} \right\} = 0$, hence

$$A^{(1)}_{11} = 2 \frac{\partial \nu_1}{\partial x'} \quad ;$$

equations (B1.6) and (B1.9) give

$$A^{(1)}_{r_1 r_1} = 2 \frac{\partial \nu(r_1)}{\partial r_1}$$

Similarly the rest of the components and physical components of the first Rivlin-Ericksen tensor $A^{(1)}$ may be obtained.

The components of the second Rivlin-Ericksen tensor are obtained from equation (B1.2) and a knowledge of the components of $A^{(1)}$. For example

$$A^{(2)}_{r\phi} = A^{(2)}_{13} = \nu' \frac{\partial A^{(1)}_{13}}{\partial x'} + \nu^2 \frac{\partial A^{(1)}_{13}}{\partial x^2} + \cancel{\nu^3 \frac{\partial A^{(1)}_{13}}{\partial x^3}}$$

$$+ \cancel{A^{(1)}_{11} \frac{\partial \nu'}{\partial x^3}} + \cancel{A^{(1)}_{12} \frac{\partial \nu^2}{\partial x^3}} + \cancel{A^{(1)}_{13} \frac{\partial \nu^3}{\partial x^3}}$$

$$+ A^{(1)}_{13} \frac{\partial \nu'}{\partial x'} + \cancel{A^{(1)}_{23} \frac{\partial \nu^2}{\partial x'}} + A^{(1)}_{33} \frac{\partial \nu^3}{\partial x'}$$

The first four terms crossed out are zero by axial symmentry and the fifth is of order L^2 and therefore neglected. After substitution from the expressions for the components of $A^{(1)}$, use of equation (B1.7) and the expressions for the dimensionless velocity components (equations (2A.17), Chapter 2), the following equation, to first order in L, is obtained:

$$A^{(2)}_{r_1\phi} = \frac{-3\Omega L \alpha_1 a^2 C \sin^2\theta}{\rho r_1^2} \left(\frac{\partial u_1}{\partial r_1} + \frac{4 v_1 \cot\theta}{r_1} \right)$$

The other components for the second Rivlin-Ericksen tensor are similarly obtained. The third (and consequently all subsequent) Rivlin-Ericksen tensor vanishes as all the components are of order L^2 or higher.

B2 The Differential Equation for χ_1

Substituting from equations (2A.22), the equations for the dimensionless physical components of the stress tensor, into equation (2A.12), the r component of the equations of motion, and discarding terms of order L^2 and higher, we obtain:

$$-\frac{L}{r}\left(\frac{C}{r^2}+Dr\right)^2\sin^2\theta = -\frac{\partial p^*}{\partial r}+\frac{L}{r^2}\frac{\partial}{\partial r}\left[r^2\left(\frac{2\partial u_1}{\partial r}+\frac{18\alpha_2'C^2\sin^2\theta}{r^6}+\frac{9\alpha_3'C^2\sin^2\theta}{r^6}\right)\right]$$

$$+\frac{L}{r\sin\theta}\frac{\partial}{\partial\theta}\left[\sin\theta\left(\frac{1}{r}\frac{\partial u_1}{\partial\theta}+r\frac{\partial}{\partial r}\left(\frac{v_1}{r}\right)\right)\right]$$

$$-\frac{L}{r}\left[\frac{2}{r}\left(\frac{\partial v_1}{\partial\theta}+u_1\right)+\frac{2}{r}(u_1+v_1\cot\theta)+\frac{9\alpha_3'C^2\sin^2\theta}{r^6}\right]$$

A stream function χ_1 is defined by the equations

$$u_1 = -\frac{1}{r^2\sin\theta}\frac{\partial\chi_1}{\partial\theta};\quad v_1 = \frac{1}{r\sin\theta}\frac{\partial\chi_1}{\partial r}$$

Hence $$-\frac{L}{r}\left(\frac{C}{r^2}+Dr\right)^2\sin^2\theta = -\frac{\partial p^*}{\partial r}$$

$$+\frac{L}{r^2}\frac{\partial}{\partial r}\left[\frac{4}{r\sin\theta}\frac{\partial\chi_1}{\partial\theta}-\frac{2}{\sin\theta}\frac{\partial^2\chi_1}{\partial r\partial\theta}\right]$$

$$- \frac{36C^2\sin^2\theta(2\alpha_2' + \alpha_3')}{r^7} - \frac{9L\alpha_3'C^2\sin^2\theta}{r^7}$$

$$+ \frac{L}{r\sin\theta}\frac{\partial}{\partial\theta}\left[\frac{\cot\theta}{r^3}\frac{\partial\chi_1}{\partial\theta} - \frac{1}{r^3}\frac{\partial^2\chi_1}{\partial\theta^2} - \frac{2}{r^2}\frac{\partial\chi_1}{\partial r}\right.$$

$$\left. + \frac{1}{r}\frac{\partial^2\chi_1}{\partial r^2}\right] - L\left[\frac{-2\cos\theta}{r^3\sin^2\theta}\frac{\partial\chi_1}{\partial r} + \frac{2}{r^3\sin\theta}\frac{\partial^2\chi_1}{\partial\theta\partial r}\right.$$

$$\left. - \frac{4}{r^4\sin\theta}\frac{\partial\chi_1}{\partial\theta} + \frac{2\cos\theta}{r^3\sin^2\theta}\frac{\partial\chi_1}{\partial\theta}\right].$$

This equation may be simplified by differentiating the second term on the R.H.S. with respect to r and collecting like terms to give the following equation:

$$-\frac{L}{r}\left(\frac{C}{r^2} + Dr\right)^2\sin^2\theta = -\frac{\partial p^*}{\partial r} + \frac{L}{\sin\theta}\frac{\partial}{\partial\theta}\left[\frac{\cot\theta}{r^4}\frac{\partial\chi_1}{\partial\theta}\right.$$

$$\left. - \frac{1}{r^4}\frac{\partial^2\chi_1}{\partial\theta^2} - \frac{1}{r^2}\frac{\partial^2\chi_1}{\partial r^2}\right] - \frac{C^2\sin^2\theta}{r^7}(72\alpha_2' + 45\alpha_3') \quad \text{(B2.1)}$$

Similarly, equation (2A.13) for the θ component of the equations of motion becomes

$$-\frac{L}{r}\left(\frac{C}{r^2} + Dr\right)^2\sin\theta\cos\theta = -\frac{1}{r}\frac{\partial p^*}{\partial\theta} + \frac{L}{r\sin\theta}\frac{\partial}{\partial r}\left[\frac{\partial^2\chi_1}{\partial r^2}\right.$$

$$\left. + \frac{1}{r^2}\frac{\partial^2\chi_1}{\partial\theta^2} - \frac{\cot\theta}{r^2}\frac{\partial\chi_1}{\partial\theta}\right] - \frac{9L\alpha_3'C\sin\theta\cos\theta}{r^7}. \quad \text{(B2.2)}$$

The quantity p* is eliminated from the problem by cross-differentiating equations (B2.1) and (B2.2):

Dividing equation (B2.1) by L and differentiating with respect to θ gives

$$-\frac{2}{r}\left(\frac{C}{r^2}+Dr\right)^2\sin\theta\cos\theta = -\frac{1}{L}\frac{\partial^2 p^*}{\partial\theta\partial r} - \frac{1}{r^2\sin\theta}\frac{\partial^2}{\partial\theta^2}\left[\frac{\partial^2\chi_1}{\partial r^2}\right.$$
$$\left.+\frac{1}{r^2}\frac{\partial^2\chi_1}{\partial\theta^2}-\frac{\cot\theta}{r^2}\frac{\partial^2\chi_1}{\partial\theta}\right] + \frac{\cot\theta}{r^2\sin\theta}\frac{\partial}{\partial\theta}\left[\frac{\partial^2\chi_1}{\partial r^2}\right.$$
$$\left.+\frac{1}{r^2}\frac{\partial^2\chi_1}{\partial\theta^2}-\frac{\cot\theta}{r^2}\frac{\partial\chi_1}{\partial\theta}\right] - \frac{2C^2\sin\theta\cos\theta(72\alpha_2' + 45\alpha_3')}{r^7} \qquad \text{(B2.3)}$$

Dividing equation (B2.2) by rL and differentiating with respect to r gives

$$-2\left(\frac{C}{r^2}+Dr\right)\left(\frac{-2C}{r^3}+D\right)\sin\theta\cos\theta = -\frac{1}{L}\frac{\partial^2 p^*}{\partial r\partial\theta}$$
$$+\frac{1}{\sin\theta}\frac{\partial^2}{\partial r^2}\left[\frac{\partial^2\chi_1}{\partial r^2}+\frac{1}{r^2}\frac{\partial^2\chi_1}{\partial\theta^2}-\frac{\cot\theta}{r^2}\frac{\partial\chi_1}{\partial\theta}\right]$$
$$+\frac{54\alpha_3' C\sin\theta\cos\theta}{r^7} \,. \qquad \text{(B2.4)}$$

Now $\frac{\partial^2 p^*}{\partial r\partial\theta} = \frac{\partial^2 p^*}{\partial\theta\partial r}$ by the continuity of p*.

Thus, subtracting (B2.4) from (B2.3), we obtain equation (2A.24):

$$\mathcal{L}^2\chi_1 = \left(\frac{6C^2}{r^5}+\frac{6CD}{r^2}-\frac{144C^2m'}{r^7}\right)\sin^2\theta\cos\theta, \qquad \text{(B2.5)}$$

where the operator

$$\mathcal{L} = \frac{\partial^2\chi_1}{\partial r^2}+\frac{1}{r^2}\frac{\partial^2\chi_1}{\partial\theta^2}-\frac{\cot\theta}{r^2}\frac{\partial\chi_1}{\partial\theta} \,.$$

B3 The Solution to the Differential Equation For χ

The stream function χ is defined by the equations

$$u_1 = -\frac{1}{r^2\sin\theta}\frac{\partial\chi_1}{\partial\theta}\ ; \quad v_1 = \frac{1}{r\sin\theta}\frac{\partial\chi_1}{\partial r}\ , \tag{B3.1}$$

where $\chi = L\chi_1$. The boundary conditions are:

$$u_1 = v_1 = 0 \text{ on } r = 1 \text{ and on } r = \beta \tag{B3.2}$$

Using equations (B3.1), the boundary conditions become

$$\chi_1(1,\theta) = \chi_1(\beta,\theta) = 0. \tag{B3.3}$$

Try a solution to equation (B2.5) of the form

$$\chi_1 = f(r)\sin^2\theta\cos\theta,$$

where $f(r)$ is a polynomial in r, say r^n [85].

Thus $\mathcal{L}\chi_1 = \frac{\partial^2\chi_1}{\partial r^2} + \frac{1}{r^2}\frac{\partial^2\chi_1}{\partial\theta^2} - \frac{\cot\theta}{r^2}\frac{\partial\chi_1}{\partial\theta}$

$$= [n(n-1)r^{n-2} - 6r^{n-2}]\sin^2\theta\cos^2\theta$$

and

$$\mathcal{L}^2\chi_1 = n(n-5)(n-3)(n+2)r^{n-4}\sin^2\theta\cos\theta \tag{B3.4}$$

Considering the polynomial $f(r)$ to have terms of the form $\alpha_n r^n$ and comparing equation (B3.4) with equation (B2.5), we obtain the following particular integral:

$$\chi_{1p} = \left(\frac{CD}{4}r^2 - \frac{C^2}{4r} - \frac{C^2m'}{r^3}\right)\sin^2\theta\cos\theta.$$

In order to obtain the complementary function, we consider the homogeneous equation

$$\mathcal{L}^2\chi_1 = 0$$

It is clear that this equation is satisfied by equation (B3.4) for $n = 0$, 5, 3 and -2. Thus the complementary

function is

$$\chi_{1c} = (C_1 + C_2 r^5 + C_3 r^3 + C_4 r^{-2}) \sin^2\theta\cos\theta .$$

In the nomenclature of Walters and Waters [47], this equation becomes

$$\chi_{1c} = \left(\frac{P}{r^2} + Qr^3 + Rr^5 + S \right) \frac{\sin^2\theta\cos\theta}{2}$$

A complete solution is thus

$$\chi_1 = \left(\frac{P}{r^2} + Qr^3 + Rr^5 + S + \frac{CD}{2} r^2 - \frac{C^2}{2r} - \frac{2m'C^2}{r^3} \right) \frac{\sin^2\theta\cos\theta}{2} .$$

The boundary conditions are:

BC1 : $\chi_1 = 0$ on $r = 1$.

BC2 : $\chi_1 = 0$ on $r = \beta$.

BC3 : $\frac{\partial \chi_1}{\partial r} = 0$ on $r = 1$ and $r = \beta$.

BC4 : $\frac{\partial \chi_1}{\partial \theta} = 0$ on $r = 1$ and $r = \beta$.

Hence

$$P + Q + R + S = \frac{C^2}{2} + 2m'C^2 - \frac{CD}{2} \qquad \text{(i)}$$

$$\frac{P}{\beta^2} + Q\beta^2 + R\beta^5 + S = \frac{C^2}{2\beta} + \frac{2m'C^2}{\beta^3} - \frac{CD\beta^2}{2} \qquad \text{(ii)}$$

$$-2P + 3Q + 5R = -\frac{C^2}{2} - 6m'C^2 - CD \qquad \text{(iii)}$$

$$-\frac{2P}{\beta^3} + 3Q\beta^2 + 5R\beta^4 = -\frac{C^2}{2\beta^2} - \frac{6m'C}{\beta^4} - CD\beta \qquad \text{(iv)}$$

These four equations in the unknowns P, Q, R and S may be reduced to three equations in P, Q and R by eliminating S from equations (i) and (ii). P, Q and R may then be found by using Cramer's rule [84] and S is obtained by substitution in equation (i). The solution equations are as given in the text, Section 2A.

B4 The Differential Equation For w_1

Equations (2A.22) for the physical components of the stress tensor and the expansion given by equations (2A.17), to first order L, were used in order to obtain the following expressions for the various terms in the ϕ component of the equations of motion, equation (2A.14):

$$\frac{u}{r}\frac{\partial}{\partial r}(rw) = Lu_1\left(-\frac{C}{r^2} + 2Dr\right)\sin\theta$$

$$\frac{v}{r\sin\theta}\frac{\partial(w\sin\theta)}{\partial\theta} = 2Lv_1\left(\frac{C}{r^3} + D\right)\cos\theta$$

$$\frac{1}{r^3}\frac{\partial(r^3p''_{(r\phi)})}{\partial r} = 4L\frac{\partial}{\partial r}\left(\frac{w_1}{r}\right) + Lr\frac{\partial^2}{\partial r^2}\left(\frac{w_1}{r}\right) - \frac{162L\sigma'C^3\sin^3\theta}{r^{10}}$$
$$- \frac{3L\alpha_2'C\sin\theta}{r^3}\left(\frac{\partial^2u_1}{\partial r^2} + 4\cot\theta\frac{\partial}{\partial r}\left(\frac{v_1}{r}\right)\right)$$
$$- \frac{6L\alpha_3'C\sin\theta}{r^3}\left(\frac{\partial^2u_1}{\partial r^2} + \frac{\partial}{\partial r}\left(\frac{u_1}{r}\right) + \cot\theta\frac{\partial}{\partial r}\left(\frac{v_1}{r}\right)\right)$$

and

$$\frac{1}{r\sin^2\theta}\frac{\partial}{\partial\theta}(\sin^2\theta p''_{(\theta\phi)}) = \frac{L\cot\theta}{r^2}\frac{\partial w_1}{\partial\theta} - \frac{L\cot^2\theta w_1}{r^2}$$
$$+ \frac{L}{r^2}\frac{\partial w_1}{\partial\theta^2} + \frac{Lw_1}{r} - \frac{3Lm'C}{r^5}\left(3\cos\theta\frac{\partial u_1}{\partial\theta} + \sin\theta\frac{\partial^2u_1}{\partial\theta^2}\right)$$
$$- \frac{3LC\alpha_3'}{r^3}\left(3\cos\theta\frac{\partial}{\partial r}\left(\frac{v_1}{r}\right) + \sin\theta\frac{\partial^2}{\partial\theta\partial r}\left(\frac{v_1}{r}\right)\right)$$

Equation (2A.14) then becomes, after letting $\alpha_2' + \alpha_3' = m'$ and some simplification

$$\frac{Lu_1}{r}\left(-\frac{C}{r^2} + 2Dr\right)\sin\theta + 2Lv_1\left(\frac{C}{r^3} + D\cos\theta\right)$$
$$= \frac{L\partial^2w_1}{\partial r^2} + \frac{2L}{r}\frac{\partial w_1}{\partial r} + \frac{L\cot\theta}{r^2}\frac{\partial w_1}{\partial\theta}$$

$$+ \frac{L}{r^2}\frac{\partial^2 w_1}{\partial\theta^2} - \frac{Lw_1}{r^2\sin^2\theta} - \frac{162L\sigma'C^3\sin^3\theta}{r^{10}}$$

$$- \frac{3Lm'C\sin\theta}{r^3}\frac{\partial^2 u_1}{\partial r^2} - \frac{12Lm'C\cos\theta}{r^3}\frac{\partial}{\partial r}\left(\frac{v_1}{r}\right)$$

$$- \frac{3Lm'C}{r^5}\left(3\cos\theta\frac{\partial u_1}{\partial\theta} + \sin\theta\frac{\partial^2 u_1}{\partial\theta^2}\right) + [\text{terms A}], \qquad \text{(B4.1)}$$

where [terms A] $= - \frac{3L\alpha_3 C}{r^3}\left[\sin\theta\left(\frac{\partial^2 u_1}{\partial r^2} + \frac{2\partial}{\partial r}\left(\frac{u_1}{r}\right)\right)\right.$

$$\left. + \cos\theta\frac{\partial}{\partial r}\left(\frac{v_1}{r}\right) + \sin\theta\frac{\partial^2}{\partial\theta\partial r}\left(\frac{v_1}{r}\right)\right]$$

The continuity equation, equation (2A.15), is

$$\sin\theta\frac{\partial}{\partial r}(u_1 r^2) + r\frac{\partial}{\partial\theta}(v_1\sin\theta) = 0$$

i.e. $\sin\theta\left(r^2\frac{\partial u_1}{\partial r} + 2ru_1\right) + r\left(\sin\theta\frac{\partial v_1}{\partial\theta} + v_1\cos\theta\right) = 0$

Multiplying by $\frac{1}{r^2}$ and differentiating partially with respect to r, this equation becomes

$$\sin\theta\left(\frac{\partial^2 u_1}{\partial r^2} + 2\frac{\partial}{\partial r}\left(\frac{u_1}{r}\right)\right) + \sin\theta\frac{\partial^2}{\partial r\partial\theta}\left(\frac{v_1}{r}\right) + \cos\theta\frac{\partial}{\partial r}\left(\frac{v_1}{r}\right) = 0$$

Thus [term A] $= 0$, since $\frac{\partial^2}{\partial r\partial\theta}\left(\frac{v_1}{r}\right) = \frac{\partial^2}{\partial\theta\partial r}\left(\frac{v_1}{r}\right)$

Dividing throughout by L and grouping terms in w_1, equation (B4.1) becomes

$$\frac{\partial^2 w_1}{\partial r^2} + \frac{2}{r}\frac{\partial w_1}{\partial r} + \frac{\cot\theta}{r^2}\frac{\partial w_1}{\partial\theta} + \frac{1}{r^2}\frac{\partial^2 w_1}{\partial\theta^2} - \frac{w_1}{r^2\sin^2\theta}$$

$$= \frac{u_1}{r}\left(\frac{-C}{r^2} + 2Dr\right)\sin\theta + 2v_1\left(\frac{C}{r^3} + D\right)\cos\theta$$

$$+\frac{162\sigma'C^3\sin^3\theta}{r^{10}} + \frac{3m'C\sin\theta}{r^3}\frac{\partial^2 u_1}{\partial r^2}$$

$$+\frac{12m'C\cos\theta}{r^3}\frac{\partial}{\partial r}\left(\frac{v_1}{r}\right)+\frac{3m'C}{r^5}\left(3\cos\theta\frac{\partial u_1}{\partial\theta}+\sin\theta\frac{\partial^2 u_1}{\partial\theta^2}\right) \quad \text{(B4.2)}$$

The differential equation for w_1, equation (2A.30) is obtained after substitution for u_1 and v_1 from equations (2A.28) and (2A.29) respectively.

B5 The Solution to the Differential Equation for w_1

The method of solution of the differential equation for w_1, equation (2A.30), follows that of Thomas and Walters [45].

Equation (2A.30) may be written in the form

$$\begin{aligned}N(w_1) = T_1(\theta)\Bigg[&\frac{-396m'^2C^3}{5r^9}+\frac{648\sigma'C^3}{5r^9}+\frac{24m'CP}{r^8}\\&-\frac{22m'C^3}{5r^7}+\frac{C(18m'S-3P)}{5r^6}+\frac{C^3}{5r^5}-\frac{C(S+4m'CD)}{5r^4}\\&+\frac{2(QC+SD+39m'CR)}{5r}+\frac{2(CD^2+2)}{5}r\\&+DQr^2+\frac{7RD}{5}r^4\Bigg]+T_3(\theta)\Bigg[\frac{36m'C^3}{r^9}+\frac{162\sigma'C^3}{r^8}\\&-\frac{15m'CP}{r^8}+\frac{9m'C^3}{2r^7}+\frac{C(P-36m'S)}{2r^6}+\frac{C^3}{4r^5}\\&-\frac{3C(S+19m'CD)}{2r^4}+\frac{5(PD-9m'QC)}{r^3}-\frac{15C^2D}{4r^2}\\&+\frac{3(2DS-3QC-52Rm'C)}{2r}+\left(\frac{CD^2-13CR}{2}\right)r\\&-2RDr^4\Bigg],\end{aligned} \quad \text{(B5.1)}$$

where $T_1(\theta) = \sin\theta$, $T_3(\theta) = \sin^3\theta - \frac{4}{5}\sin\theta$ and the operator N is defined by

$$N(\psi) = \frac{\partial^2(r\psi)}{\partial r^2} + \frac{1}{r}\frac{\partial}{\partial\theta}\left[\frac{1}{\sin\theta}\frac{\partial(\psi\sin\theta)}{\partial\theta}\right] \qquad (B5.2)$$

It is clear that $N(w_1)$ = r x L.H.S. of equation (2A.30). For convenience, rewrite equation (B5.1) as

$N(w_1) = T_1(\theta)f_1(r) + T_3(\theta)f_3(r)$, where f_1 and f_3 represent the appropriate terms in the square brackets.

Let $\psi = H(r)T(\theta)$ and consider the homogeneous equation

$$N(\psi) = N(H(r)T(\theta)) = 0 \qquad (B5.3)$$

The variables may be separated:

$$N(\psi) = T\frac{\partial^2(rH)}{\partial r^2} + \frac{H}{r}\frac{\partial}{\partial\theta}\frac{1}{\sin\theta}\left[\frac{\partial(T\sin\theta)}{\partial\theta}\right] = 0$$

Multiplying this equation by $\frac{r}{HT}$:

$$r\frac{\partial^2(rH)}{\partial r^2} = \frac{1}{T}\frac{\partial}{\partial\theta}\left[\frac{1}{\sin\theta}\frac{\partial(T\sin\theta)}{\partial\theta}\right] \qquad (B5.4)$$

Each term in equation (B5.4) is independent of both r and θ, hence each may be equated to a constant, say k. Thus

$$\frac{d^2(rH)}{dr^2} - k\frac{H}{r} = 0 \qquad (B5.5)$$

and

$$\frac{d}{d\theta}\left[\frac{1}{\sin\theta}\frac{d(T\sin\theta)}{\partial\theta}\right] + kT = 0 \qquad (B5.6)$$

(Total derivatives are used since each term has only one independent variable).

It is convenient to let $k = n(n + 1)$ where n is an integer. Equation (B5.6) becomes

$$\frac{d}{d\theta}\left[\frac{1}{\sin\theta}\frac{d(T\sin\theta)}{d\theta}\right] + n(n+1)T = 0$$

A well known solution to an equation of this form is

T_n = constant x $\frac{dP_n}{d\theta}$, where P_n is the Legendre polynomial of order n [84].

Hence $T_1(\theta) = \sin\theta$

and $T_3(\theta) = \sin^3\theta - \frac{4}{5}\sin\theta$ (B5.7)

It follows that a solution to equation (B5.1) is of the form

$$w_1 = H_1(r)T_1(\theta) + H_3(r)T_3(\theta) \quad \text{(B5.8)}$$

Substituting (B5.7) into (B5.1) and separating T_1 and T_3 :

$N(H_1T_1 + H_3T_3) = N(H_1T_1) + N(H_3T_3)$ (N is linear)

$= T_1[f_1(r)] + T_3[f_3(r)]$, i.e. the terms on the R.H.S. of equation (B5.1).

Thus from equations (B5.1) and (B5.5) for n = 1 :

$$\frac{d^2(rH_1)}{dr^2} - \frac{2H_1}{r} = f_1(r) \quad \text{(B5.9)}$$

and for n = 3 :

$$\frac{d^2(rH_3)}{dr^2} - \frac{12H_3}{r} = f_3(r) \quad \text{(B5.10)}$$

The homogeneous equation

$$\frac{d^2(rH_1(r))}{dr^2} - \frac{2H_1(r)}{r} = 0$$

may be solved by the method of Euler. The solution is

$y = rH_1(r) = \frac{A_1}{r} + A_2r^2$ where A_1 and

A_2 are arbitrary constants. To solve the non-homogeneous equation (B5.9), we require a particular integral Y. The method of variation of parameters may be used:

Postulate $Y = \mu_1(r)y_1 + \mu_2(r)y_2$ as a solution to equation (B5.9), where $y_1 = r^{-1}$ and $y_2 = r^2$.

$$\frac{d\mu_1}{dr} = \frac{-y_2}{y_1y_2' - y_2y_1'} f_1(r)$$

$$= -\frac{r^2}{3} f_1(r)$$

$$\mu_1 = -\frac{1}{3}\left[\frac{66m'^2C^3}{5r^6} - \frac{108\sigma'C^3}{5r^6} - \frac{24m'CP}{5r^5}\right.$$

$$- \frac{11m'C^3}{10r^4} - \frac{C(18m'S - 3P)}{15r^3} - \frac{C^3}{10r^2}$$

$$+ \frac{C(S + 4m'CD)}{5r} + \frac{(QC + SD + 39m'CR)}{5} r^2$$

$$\left. + \frac{(CD^2 + 2RC)}{10} r^4 + \frac{DQr^5}{5} + \frac{RDr^7}{5}\right]$$

$$\frac{d\mu_2}{dr} = \frac{y_1}{y_1y_2' - y_2y_1'} f_1(r)$$

$$= \frac{1}{3r} f_1(r)$$

$$\mu_2 = \frac{1}{3}\left[\frac{44m'^2C^3}{5r^9} - \frac{72\sigma'C^3}{5r^9} - \frac{3m'CP}{r^8} + \frac{22m'C^3}{35r^7}\right.$$

$$- \frac{C(6m'S - P)}{10r^6} - \frac{C^3}{25r^5} + \frac{C(S + 4m'CD)}{20r^4}$$

$$- \frac{2(QC + SD + 39m'CR)}{5r} + \frac{2(CD^2 + 2RC)}{5} r$$

$$\left. + \frac{DQr^2}{2} + \frac{7RDr^4}{20}\right]$$

Thus we have a complete solution to equation (B5.9):

$$y = rH_1(r) = \mu_1 y_1 + \mu_2 y_2 + A_1 y_1 + A_2 y_2$$

The arbitrary constants A_1 and A_2 are determined from the boundary conditions:

$$H_1 = 0 \text{ on } r = 1 \quad \text{i.e.} \quad y = 0 \text{ on } r = 1$$
$$\text{and } H_1 = 0 \text{ on } r = \beta \quad \text{i.e.} \quad y = 0 \text{ on } r = \beta$$

Hence equation (2A.32) for $H_1(r)$ is obtained. The expression for $H_1(r)$, equation (2A.33), is obtained in identical fashion.

B6 The Equation for the Couple on the Inner Sphere

If we let $m' = \alpha_2' + \alpha_3'$ and $\sigma' = -2(\alpha_5' + \beta_1')$, the equation for $p''_{(r\phi)}$ in equations (2A.22) can be re-written in the form

$$p''_{(r\phi)} = -\frac{3C\sin\theta}{r^3} + Lr\frac{\partial}{\partial r}\left(\frac{w_1}{r}\right) + \frac{27LC^3\sigma'\sin^3\theta}{r^9}$$
$$-\frac{3LC\sin\theta}{r^3}\left\{3m'\frac{\partial u_1}{\partial r} + 4m'\frac{u_1}{r}\right.$$
$$\left. + (2\alpha_2' + \alpha_3')\left(\frac{2v_1\cot\theta}{r} - \frac{\partial u_1}{\partial r} - 2\frac{u_1}{r}\right)\right\} \qquad \text{(B6.1)}$$

Equation (B6.1) is simplified by invoking the Weissenberg hypothesis, i.e. $2\alpha_2' + \alpha_3' = 0$ and thus the terms $\{\ \} = 0$. If we now substitute for u_1, v_1 and w_1 from equations (2A.28), (2A.29) and (2A.31), equation (2A.35) is obtained.

Note that the term $F_3(r)T_3(\theta)$ in equation (2A.35) does not affect the couple on the sphere since

$$\int_0^\pi T_3(\theta)\sin^2\theta d\theta = 0 ,$$

by the orthogonality condition on $T_3(\theta)$ [84]. This term may also be shown to be zero by direct evaluation of the integral.

APPENDIX C

THE DERIVATIVE OF $F(\xi)$ AND $G(\xi)$

The functions $F(\xi)$ and $G(\xi)$ are expressed more simply as functions of μ, where $\mu = \sinh\xi$, as was done in Section 2B. The derivatives are also obtained in a more convenient form by using the chain rule:

$$F(\xi) = F(\sinh^{-1}\mu) = A_1' F_1(\mu) + A_2' F_2(\mu) + F_3(\mu)$$

$$\frac{dF(\xi)}{d\xi} = \frac{dF}{d\mu}\frac{d\mu}{d\xi}$$

$$= \cosh\xi \left(A_1' \frac{dF_1(\mu)}{d\mu} + A_2' \frac{dF_2(\mu)}{d\mu} + \frac{dF_3(\mu)}{d\mu}\right)$$

The derivatives in the brackets are obtained from the expressions for F_1, F_2 and F_3 in Section 2B, and are as follows:

$$\frac{dF_1(\mu)}{d\mu} = 28\mu^3 + \frac{46}{3}\mu - (35\mu^4 + 30\mu^2 + 3)\cot^{-1}\mu + \mu(7\mu^4 + 10\mu^2 + 3)/(1 + \mu^2),$$

$$\frac{dF_2(\mu)}{d\mu} = 2\mu - (1 + 3\mu^2)\cot^{-1}\mu + \mu ,$$

$$\frac{dF_3(\mu)}{d\mu} = \left[f(\xi_0)\right]^{-2} \left[\frac{27}{8}\mu^2 + 1 - \frac{1}{4}(36\mu^3 + 22\mu)\cot^{-1}\mu + \frac{1}{4}(9\mu^4 + 11\mu^2 + 2)/(1 + \mu^2) - \frac{\mu}{8}(9\mu^4 + 14\mu^2 + 5).2.\cot^{-1}\mu(1 + \mu^2) + \tfrac{1}{8}(45\mu^4 + 42\mu^2 + 5)(\cot^{-1}\mu)^2\right].$$

The function $G(\xi)$ is defined by the equations:

$$G(\xi) = B_1' + B_2' F_2(\mu) + H(\mu)$$

where $H(\mu) = A_1' H_1(\mu) + A_2' H_2(\mu) + H_3(\mu) + m' H_4(\mu)$

Thus $$\frac{dG(\xi)}{d\xi} = \frac{d\mu}{d\xi} \cdot \frac{dG}{d\mu}$$

$$= \cosh\xi \cdot \frac{dG}{d\mu} ;$$

$$\frac{dG}{d\mu} = B_2' \frac{dF_2(\mu)}{d\mu} + \frac{dH(\mu)}{d\mu} ;$$

$$\frac{dH(\mu)}{d\mu} = A_1' \frac{dH_1(\mu)}{d\mu} + A_2' \frac{dH_2(\mu)}{d\mu} + \frac{dH_3(\mu)}{d\mu} + \frac{dH_4(\mu)}{d\mu} .$$

H_1, H_2, H_3 and H_4 were defined in Section 2B, and the above derivatives are given by

$$\frac{dH_1(\mu)}{d\mu} = -42\mu^5 - \frac{128}{3}\mu^3 - \frac{92}{15}\mu + (49\mu^6 + 65\mu^4 + 18\mu^2)\cot^{-1}\mu - \mu^3(7\mu^4 + 13\mu^2 + 6)/(1 + \mu^2) ,$$

$$\frac{dH_2(\mu)}{d\mu} = -8\mu^3 - \frac{8}{3}\mu + 2(3\mu^2 + 5\mu^4)\cot^{-1}\mu - 2\mu^3 ,$$

$$\frac{dH_3(\mu)}{d\mu} = [f(\xi_0)]^{-2}[-\frac{45}{8}\mu^4 - \frac{39}{8}\mu^2 - \tfrac{1}{2} + \frac{1}{4}(54\mu^5 + 64\mu^3 + 14\mu)\cot^{-1}\mu - \frac{1}{4}\mu^2(9\mu^4 + 16\mu^2 + 7)/(1 + \mu^2) - \tfrac{1}{8}(63\mu^6 + 95\mu^4 + 33\mu^2 + 1)(\cot^{-1}\mu)^2 + \tfrac{1}{8}\mu(9\mu^6 + 19\mu^4 + 11\mu^2 + 1).2.\cot^{-1}\mu/(1 + \mu^2)] ,$$

$$\frac{dH_4(\mu)}{d\mu} = 2[f(\xi_0)]^{-2}[(1 + 4\mu\cot^{-1} + (1 + 2\mu^2)/(1 + \mu^2)) + (1 + 3\mu^2)(\cot^{-1}\mu)^2 - 2\mu\cot^{-1}\mu].$$

APPENDIX D

CALIBRATION OF THE CAMERAS

Two cameras were used to obtain velocity data, a Zeiss Contaflex and a Nikon Photomic F. The nominal exposure settings of ¼ sec., ½ sec. and 1 sec. were calibrated, both to obtain the true exposure interval under experimental conditions (i.e. at 25°C) and to assess variations in the exposure interval for a given setting.

The cameras were calibrated by photographing a large (9,5 cm) black disc rotating at a known rotational speed. The disc was marked with a thin silver strip placed in the radial direction. Rotational speeds in the range 20 to 40 rpm were used, and were measured correct to 0,1 rpm. A number of exposures were made at ¼ sec., ½ sec. and 1 sec. (nominal). The angle through which the silver strip rotates during the exposure could be clearly seen on the resulting photograph. These angles (in the range 60° to 180°) were measured with a large protractor, graduated to 0,5°, and used in conjunction with a knowledge of the rotational speed to calculate the true exposure interval.

A total of five calibration runs were performed (three for the Zeiss and two for the Nikon camera) over a period of several months, with six or seven measurements of each exposure setting for each calibration. The results from the various calibrations were consistent, within the experimental error, and thus the readings were combined to calculate the averages given below. The maximum deviation from the mean in all calibrations was less than 2%. Variations about the mean are probably as much a reflection of errors in the calibration method

as a reflection of changes inherent in the camera mechanisms.

Results for Zeiss Contaflex:

Nominal Exposure interval [sec]	¼	½	1
Actual Exposure interval [sec]	0,314	0,604	1,19

Results for Nikon Photomic F:

Nominal Exposure interval [sec]	¼	½	1
Actual Exposure interval [sec]	0,275	0,528	1,116

APPENDIX E

RAW DATA AND CALCULATIONS FOR ZERO SHEAR VISCOSITY MEASUREMENTS

The data obtained from the falling sphere experiments are presented in Table E-1.

TABLE E-1 FALLING SPHERE DATA

SPHERE DIAMETER [cm]	FALL TIMES [sec]	MEAN VELOCITY, U [cm/sec]
0,90% Natrosol 250 H solution		
0,15875	29,0; 29,0	0,897
0,23813	11,1; 11,0; 11,1	2,34
0,31750	5,3; 5,5; 5,5	4,78
1,50% Natrosol 250 H solution		
0,15875	303,0; 300,0	0,0862
0,23813	119,6; 119,0	0,218
0,31750	60,8; 60,4	0,429
0,47625	22,7; 22,5	1,15

According to the theory reviewed in Section 2D, the wall effect correction factor to the velocity of a sphere of radius a falling at the centre of a tube of radius R is given by

$$U_c = (F/6\pi\eta_0 R)W(a,R),$$

where F is the net hydrodynamic force. The initial value of η_0 must be assumed. The net hydrodynamic force is given by

$$F = (\rho_s - \rho_f)(4\pi a^3/3)g,$$

where ρ_s is the density of the sphere, ρ_f is the density of the fluid and g is the acceleration due to gravity. In the experimental procedure used, the spheres were dropped 6,5 cm from each of two of the tank walls. The effect of these two walls on the velocity of the sphere was estimated by assuming a value of 6,5 for R and using half the correction velocity, since the two far walls have a negligible effect.

In order to use Turian's [79] extrapolation procedure, it is necessary to calculate a characteristic shear stress τ, defined by

$$\tau = F/6\pi a^2.$$

The viscosity is calculated from the equation

$$\eta = F/6\pi a U_\infty,$$

where U_∞ is the corrected velocity. The final corrections and calculated values are shown in Table E-2. As can be seen from this table, the largest correction ($U_c/2$) is less than 3% of the measured velocity. The values of η and τ shown in this table were used to obtain the plots shown in Figures 4-1 to 4-4.

No top or bottom corrections were applied as Sutherby [86] suggests that these are negligible under the experimental conditions used. In all cases but one, the Reynolds numbers of the falling spheres were less than 0,06 and inertial corrections were thus negligible [87].

In the exceptional case, that of the 0,3175 cm sphere falling in the 0,9% solution, the inertial correction was not negligible, but was ignored as it was certainly smaller than the uncertainty in the measured fall velocity.

TABLE E-2 FINAL CORRECTIONS AND CALCULATED VALUES

SPHERE DIAMETER [cm]	U[cm/sec]	U_c[cm/sec]	$U_\infty = U + U_c/2$ [cm/sec]	$\eta = F/6\pi a U_\infty$	τ[dynes/cm^2]	$Re = \frac{2aU\rho f}{\eta}$
0,90% Natrosol 250 H solution						
0,15875	0,897	0,015	0,905	10,3	117,3	0,015
0,23813	2,34	0,052	2,37	8,85	176,1	0,06
0,31750	4,78	0,123	4,84	7,66	234,1	0,2
1,50% Natrosol H solution						
0,15875	0,0862	0,0016	0,0870	107	117,3	<0,005
0,23813	0,218	0,0055	0,221	94,9	176,1	<0,005
0,31750	0,429	0,0129	0,435	85,4	234,1	<0,005
0,47625	1,15	0,044	1,17	71,1	349,3	0,007

APPENDIX F

NOTES ON THE COMPUTATION OF THE THEORETICAL VELOCITY PROFILES

F1 Computation of the Quantities P, Q, R, S and Δ in Section 2A

The computation of the variable P will be used as an example. P is given by

$$P = \frac{C}{\Delta}\left[DP_1(\beta) + CP_2(\beta) + m'CP_3(\beta)\right],$$

where P_1, P_2, P_3 and Δ are as given in Section 2A, and are all of order β^{10} for $\beta > 1$. Thus if we compute P_1, P_2, P_3 and Δ individually and then compute P according to the above equation, the answer is swamped by the round-off error in the calculation of these four quantities, particularly for large β. Thus it is necessary to calculate $P_1(\beta)/\Delta$, etc. by dividing both quantities by β^{10}. For example

$$\frac{P_1(\beta)}{\Delta} = \frac{\frac{1}{2}(\beta^{-6} - 2{,}25\beta^{-5} + 2{,}5\beta^{-3} - 2{,}25\beta^{-1} + 1)}{(\beta^{-10} - 6{,}25\beta^{-7} + 10{,}5\beta^{-5} - 6{,}25\beta^{-3} + 1)}.$$

Q, R and S are calculated in similar fashion.

F2 The Computation of F(ξ) and G(ξ) in Section 2B

The functions F and G are defined in terms of functions $F_1(\mu)$ etc., as given in Section 2B. However, the expressions for $F_1(\mu)$, ... , $H_1(\mu)$ .... given in equations (2B.14) are not suitable for computation when μ is large [88]. The difficulty may be illustrated with $F_1(\mu)$ as an example:

If $\mu = 10$, and F_1 is calculated from equation (2B.14), then

$$F_1(10) = 7 \times 10^4 + \frac{23}{8} \times 10^2 + \frac{16}{15} - 10[7 \times 10^4 \times 10^2 + 3]\cot^{-1}(10);$$

terms of order greater than 10^{-4} will cancel. In computing the above equation, eight significant figures are included in the range 10^{-4} to 10^4. Thus, for the ordinary nine digit precision on the UNIVAC 1106, only one significant figure will be accurate. The problem may be overcome by using double precision (18 digits).

In earlier work (prior to mid-1972) only an IBM 1130 computer was available. This machine was capable of six digit precision only, thus the calculation of F on ordinary precision resulted in completely spurious answers, even at μ values of 4 or 5. The difficulty may be obviated as follows.

For $\mu^2 > 1$, we may expand $\cot^{-1}\mu$ in a power series and thus rewrite the expression for $F_1(\mu)$ in the following form

$$F_1(\mu) = \delta_1\mu^{-4} + \delta_2\mu^{-6} + \ldots\ldots$$

(King [88]). An expression of this form may be calculated accurately, even on a low precision instrument. However, with the availability of the higher precision UNIVAC computer, the original expressions can be used, certainly for $\mu < 6$.

F3 The Use of Specific β Values in the Estimation of Wall Effects on Experimental Data

The problem encountered in using a specific β value is that the sphere rotates in the centre of a cubical tank in the experimental situation, but the analysis presented in Section 2A is for a sphere rotating within

an outer concentric sphere. If the influence of the tank walls is approximated by an outer concentric sphere with diameter equal to the length of the tank walls, the effect of these walls on the velocity profiles is clearly over estimated, particularly in the lower z planes. On the other hand, if the diameter of the outer sphere is calculated on the basis of the volume of liquid in the tank (i.e. diameter = 1,21 x tank length), the effect of the walls on the velocity profiles is under estimated, particularly in the z planes near the equator. Thus, as a somewhat arbitrary compromise, wall effects were estimated by replacing the cubical tank with an outer sphere with diameter equal to 1,1 x tank length. The value of β was then calculated.

APPENDIX G

TABULATION OF VELOCITY DATA

The measured quantities R_1, R_2 and Δx are tabulated together with the calculated dimensionless variables R (radius), VR (radial velocity) and V PHI (tangential velocity). Table G1 summarises the relevant information.

TABLE G1 INFORMATION FOR THE TABULATED VELOCITY DATA

Run	Pages	System	Diameter [cm]	Tank Size [cm]	Fluid
12S	G2-G3	Sphere	4,15	38,1	Glycerol
15S	G4-G8	Sphere	4,15	38,1	1,5% Natrosol
7S	G9-G13	Sphere	6,98	30,5	1,5% Natrosol
9S	G14-G18	Sphere	4,15	38,1	0,9% Natrosol
7D	G19-G23	Disc	7,07	30,5	1,5% Natrosol
16D	G25-G27	Disc	4,15	38,1	0,9% Natrosol

Z DISTANCE .000
SCALE FACTOR 2.72

RUN 12S

	R1	R2	DELX	R	V PHI	VR
DEL T= .275						
	6.65	6.65	1.67	1.178	.6868	.000
	6.20	6.20	1.87	1.099	.7699	.000
	5.89	5.90	2.17	1.044	.8952	.492-02
	6.55	6.57	1.76	1.162	.7241	.984-02
	5.69	5.69	2.40	1.008	.9918	.000
	5.78	5.78	2.32	1.024	.9581	.000
DEL T= .528						
	5.83	5.84	4.20	1.034	.9178	.256-02
	5.81	5.83	4.33	1.031	.9478	.513-02
	6.03	6.05	3.95	1.070	.8596	.513-02
	7.09	7.09	2.95	1.256	.6348	.000
	6.70	6.70	3.22	1.187	.6947	.000
	7.69	7.69	2.46	1.363	.5278	.000
	7.18	7.18	2.88	1.272	.6195	.000
	5.99	5.97	4.25	1.060	.9282	-.513-02
	6.97	6.97	3.18	1.235	.6854	.000
	8.14	8.14	2.25	1.442	.4822	.000
	7.19	7.19	3.00	1.274	.6456	.000
	7.19	7.19	2.86	1.274	.6151	.000
	8.02	8.02	2.36	1.421	.5060	.000
	9.40	9.40	1.68	1.665	.3594	.000
DEL T=1.116						
	8.17	8.29	4.85	1.458	.4976	.146-01
	9.24	9.27	3.81	1.640	.3879	.364-02
	8.86	8.90	4.02	1.573	.4099	.485-02
	10.09	10.15	3.17	1.793	.3217	.728-02
	10.86	10.95	2.72	1.932	.2756	.109-01
	11.18	11.24	2.53	1.986	.2563	.728-02
	11.09	11.18	2.56	1.973	.2593	.109-01
	7.50	7.53	5.62	1.332	.5822	.364-02
	9.33	9.35	3.52	1.655	.3579	.243-02
	8.39	8.46	4.34	1.493	.4437	.849-02
	9.84	9.97	3.17	1.755	.3218	.158-01
	8.77	8.92	3.96	1.567	.4037	.182-01
	8.21	8.29	4.51	1.462	.4617	.970-02
	10.28	10.34	2.93	1.827	.2971	.728-02
	10.13	10.18	3.06	1.799	.3105	.606-02
DEL T=3.000						
	8.68	8.95	.00	1.562	.0000	.122-01
	15.70	15.88	3.20	2.798	.1205	.812-02
	16.28	16.46	2.97	2.900	.1118	.812-02
	11.86	12.15	5.64	2.127	.2141	.131-01
	15.02	15.24	3.58	2.681	.1349	.993-02
	17.09	17.24	2.78	3.041	.1046	.677-02
	17.90	18.02	2.45	3.182	.0922	.541-02
	15.26	15.34	3.36	2.711	.1266	.361-02
	12.74	12.89	4.89	2.271	.1850	.677-02
	12.14	12.23	5.39	2.159	.2043	.406-02
	13.68	13.81	4.18	2.435	.1578	.587-02
	9.48	9.64	.00	1.694	.0000	.722-02
	11.88	12.03	5.88	2.118	.2234	.677-02
	14.13	14.33	4.00	2.521	.1509	.902-02
	14.67	14.87	3.69	2.617	.1391	.902-02
	14.90	15.09	3.69	2.657	.1391	.857-02
	17.29	17.45	2.57	3.078	.0967	.722-02
	13.30	13.40	4.48	2.365	.1692	.451-02
	13.73	13.89	4.43	2.447	.1673	.722-02

DEL T=5.000

13.58	14.00	.00	2.443	.0000	.114-01
15.20	15.55	5.65	2.724	.1282	.948-02
15.30	15.67	5.72	2.744	.1298	.100-01
16.19	16.51	5.00	2.897	.1132	.866-02
19.22	19.40	3.62	3.421	.0818	.487-02
21.83	21.96	2.83	3.879	.0639	.352-02
24.17	24.25	2.25	4.290	.0508	.217-02
21.04	21.18	3.04	3.740	.0686	.379-02
27.77	27.80	1.62	4.923	.0366	.812-03
26.72	26.70	1.73	4.732	.0390	-.541-03
23.69	23.70	2.35	4.198	.0530	.271-03
19.08	19.23	3.72	3.394	.0841	.406-02
20.22	20.48	3.28	3.606	.0741	.704-02
16.19	16.59	5.21	2.904	.1180	.108-01
13.62	13.95	.00	2.442	.0000	.893-02
17.30	17.59	4.56	3.091	.1032	.785-02
18.76	18.97	3.85	3.342	.0870	.569-02
23.90	24.00	2.31	4.243	.0521	.271-02
27.65	27.68	1.68	4.902	.0379	.812-03
24.98	24.98	2.07	4.426	.0467	.000

Z DISTANCE .723
SCALE FACTOR 2.86

	R1	R2	DELX	R	V PHI	VR
DEL T= .528						
	6.40	6.43	2.76	1.081	.5652	.731-02
	5.10	5.09	2.63	.859	.5405	-.244-02
	5.09	5.15	2.62	.863	.5383	.146-01
DEL T=1.114						
	6.56	6.51	5.00	1.101	.4932	-.577-02
	10.70	10.70	2.57	1.803	.2476	.000
	11.71	11.78	2.18	1.979	.2099	.807-02
	8.73	8.73	3.13	1.471	.3025	.000
DEL T=3.000						
	15.99	16.11	3.33	2.705	.1193	.515-02
	18.00	18.12	2.64	3.043	.0945	.515-02
	17.13	17.20	3.00	2.892	.1074	.300-02
	11.88	12.00	5.84	2.012	.2110	.515-02
	8.60	8.68	7.55	1.456	.2794	.343-02
	16.84	17.00	2.87	2.851	.1027	.687-02
	14.50	14.61	3.90	2.453	.1399	.472-02
	14.70	14.80	3.84	2.485	.1377	.429-02
	16.46	16.60	3.10	2.785	.1110	.601-02
DEL T=6.000						
	25.74	25.77	2.44	4.340	.0436	.644-03
	27.03	27.10	2.20	4.561	.0393	.150-02
	17.41	17.58	5.24	2.948	.0940	.365-02
	20.37	20.49	3.88	3.443	.0695	.257-02
	26.68	26.82	2.20	4.508	.0393	.300-02
	22.43	22.67	3.23	3.800	.0578	.515-02
	15.26	15.60	6.80	2.600	.1226	.729-02
	18.65	18.92	4.65	3.165	.0834	.579-02
	19.37	19.61	4.28	3.284	.0767	.515-02
	19.56	19.74	4.25	3.311	.0761	.386-02
	25.00	25.24	2.57	4.233	.0460	.515-02
	25.80	26.07	2.46	4.370	.0440	.579-02
	27.22	27.44	2.13	4.605	.0381	.472-02
	19.22	19.30	4.40	3.245	.0788	.172-02
	23.39	23.57	2.96	3.957	.0530	.386-02
	24.48	24.61	2.70	4.136	.0483	.279-02
	27.27	27.36	2.11	4.603	.0377	.193-02

Z DISTANCE .000
SCALE FACTOR 3.19

RUN 15S

	R1	R2	DELX	R	V PHI	VR
DEL T= .275						
	6.81	6.83	2.06	1.030	.7232	.327-02
	8.23	8.18	1.06	1.240	.3710	-.818-03
	7.39	7.39	1.72	1.116	.6029	.000
DEL T= .528						
	8.08	8.04	2.51	1.218	.4591	-.341-02
	9.40	9.32	1.55	1.414	.2827	-.682-03
	9.02	8.90	1.65	1.354	.3010	-.102-02
DEL T=1.116						
	9.88	9.86	3.09	1.476	.2674	-.887-03
	9.79	9.56	3.17	1.462	.2744	-.927-03
	10.47	10.19	2.50	1.561	.2160	-.113-02
DEL T=3.000						
	20.14	19.82	1.50	3.018	.0481	-.480-02
	16.06	15.63	2.30	2.394	.0738	-.645-03
	16.63	16.15	2.27	2.476	.0728	-.720-02
	19.65	19.23	1.68	2.937	.0539	-.630-03
	20.12	19.78	1.56	3.014	.0500	-.510-02
	20.59	20.21	1.56	3.082	.0500	-.570-03
	17.49	17.02	1.95	2.607	.0625	-.705-02
	17.00	16.53	2.15	2.533	.0690	-.705-03
	20.03	19.65	1.50	2.997	.0481	-.570-02
	16.78	16.29	2.13	2.498	.0699	-.735-03
	10.56	9.94	6.53	1.549	.2131	-.930-02
	17.23	16.79	2.06	2.570	.0661	-.660-03
	18.33	17.90	1.91	2.737	.0613	-.645-02
	18.60	18.15	1.91	2.776	.0613	-.675-03
	18.94	18.55	1.68	2.832	.0539	-.585-02
	20.27	19.89	1.55	3.034	.0497	-.570-03
	12.76	12.22	4.03	1.887	.1298	-.810-02
	13.50	12.94	3.56	1.997	.1145	-.840-03
	18.19	17.81	1.82	2.719	.0584	-.570-02
DEL T=6.000						
	25.33	24.77	1.95	3.784	.0313	-.420-02
	19.62	18.78	3.42	2.901	.0549	-.630-03
	20.17	19.39	3.16	2.988	.0507	-.585-02
	20.63	19.92	2.92	3.063	.0468	-.532-03
	20.92	20.31	2.82	3.114	.0452	-.457-02
	23.40	22.88	2.20	3.496	.0353	-.390-03
	23.86	23.42	2.06	3.571	.0330	-.330-02
	32.45	32.18	1.13	4.882	.0181	-.202-03
	27.93	27.55	1.42	4.191	.0228	-.285-02
	21.00	20.34	2.90	3.123	.0465	-.495-03
	21.30	20.69	2.85	3.164	.0457	-.532-02
	23.17	22.59	2.32	3.457	.0372	-.435-03
	21.74	21.10	2.80	3.236	.0417	-.480-02
	22.42	21.82	2.52	3.342	.0404	-.450-03
	24.66	24.17	1.85	3.688	.0297	-.367-02
	22.22	21.60	2.37	3.310	.0380	-.465-03
	31.30	30.85	1.36	4.695	.0218	-.337-02
	18.43	17.62	3.48	2.723	.0559	-.607-03
	20.59	19.89	2.97	3.058	.0477	-.525-02

Z DISTANCE .723
SCALE FACTOR 3.16

	R1	R2	DELX	R	V PHI	VR
DEL T=.275						
	5.67	5.59	1.35	.859	.4778	-.132-02
DEL T= .528						
	5.87	5.68	2.06	.881	.3808	-.163-02
	6.35	6.24	1.75	.960	.3228	-.946-03
	6.29	6.09	2.14	.944	.3955	-.172-02
DEL T=1.116						
	8.28	8.00	2.44	1.241	.2131	-.114-02
	9.97	9.77	1.44	1.505	.1254	-.814-03
	9.07	8.85	2.18	1.366	.1901	-.395-03
	9.38	9.17	1.73	1.415	.1507	-.855-03
	11.49	11.24	1.53	1.733	.1350	-.102-02
DEL T=3.000						
	15.48	15.05	2.13	2.328	.0690	-.651-03
	14.79	14.38	2.30	2.223	.0745	-.651-03
	16.15	15.78	1.98	2.433	.0641	-.590-03
	19.37	19.01	1.42	2.927	.0463	-.545-03
	18.23	17.88	1.55	2.754	.0502	-.530-03
	18.49	18.14	1.50	2.793	.0486	-.530-03
	10.63	10.19	4.09	1.587	.1332	-.681-03
	13.11	12.84	3.00	1.984	.0973	-.712-03
	15.69	15.37	2.00	2.368	.0648	-.484-03
	12.82	12.45	2.96	1.927	.0900	-.560-03
	14.63	14.19	2.34	2.198	.0758	-.666-03
	17.49	17.13	1.65	2.640	.0534	-.545-03
	16.48	16.14	1.83	2.497	.0593	-.515-03
	17.74	17.39	1.62	2.679	.0524	-.530-03
	14.89	14.48	2.47	2.240	.0800	-.621-03
	13.65	13.24	2.63	2.050	.0862	-.621-03
	10.57	10.11	4.18	1.577	.1362	-.696-03
	8.71	8.10	6.76	1.282	.2251	-.924-03
	14.32	13.95	2.60	2.156	.0843	-.560-03
	18.49	18.03	1.66	2.785	.0537	-.696-03
	17.15	16.80	1.74	2.589	.0563	-.530-03
DEL T=6.000						
	18.55	17.86	3.03	2.776	.0491	-.522-03
	23.70	23.22	1.93	3.578	.0312	-.363-03
	26.44	26.02	1.42	4.005	.0230	-.273-03
	28.39	28.08	1.32	4.306	.0214	-.235-03
	30.84	30.64	1.17	4.680	.0178	-.227-03
	30.21	29.80	1.16	4.582	.0188	-.250-03
	31.27	30.96	1.13	4.745	.0193	-.235-03
	20.20	19.56	2.73	3.032	.0442	-.484-03
	16.78	16.04	3.70	2.503	.0600	-.560-03
	19.42	18.79	2.92	2.914	.0473	-.477-03
	22.01	21.47	2.36	3.316	.0366	-.409-03
	27.89	27.53	1.43	4.226	.0231	-.273-03
	26.74	26.36	1.53	4.049	.0256	-.298-03
	29.27	28.89	1.40	4.433	.0227	-.288-03
	17.59	17.05	3.44	2.643	.0558	-.484-03
	22.64	22.17	2.10	3.417	.0340	-.356-03
	25.63	25.19	1.63	3.870	.0264	-.333-03
	26.67	26.24	1.44	4.033	.0233	-.326-03
	29.50	29.19	1.17	4.473	.0189	-.235-03
	18.12	17.43	3.27	2.711	.0530	-.522-03
	20.94	20.37	2.52	3.150	.0408	-.432-03

Z DISTANCE 1.446
SCALE FACTOR 3.08

	R1	R2	DELX	R	V PHI	VR
DEL T=6.000						
	18.93	18.71	2.17	2.945	.0300	-.171-03
	26.57	26.34	1.03	4.139	.0204	-.179-03
	23.59	23.34	1.46	3.672	.0242	-.194-03
	12.52	12.37	3.52	1.947	.0586	-.117-03
	16.77	16.59	2.21	2.609	.0367	-.148-03
	25.12	24.89	1.33	3.913	.0221	-.179-03
	11.79	11.59	3.89	1.823	.0597	-.155-03
	14.56	14.29	3.10	2.257	.0516	-.210-03
	21.32	21.01	1.97	3.312	.0316	-.241-03
	18.27	18.03	2.36	2.840	.0375	-.188-03
	20.44	20.14	2.09	3.175	.0347	-.233-03
	23.30	23.05	1.63	3.626	.0271	-.194-03
	23.55	23.30	1.60	3.663	.0249	-.194-03
	20.66	20.36	2.00	3.205	.0332	-.280-03
	28.20	27.96	1.20	4.394	.0199	-.186-03
	24.79	24.61	1.33	3.865	.0229	-.140-03
	24.38	24.12	1.47	3.794	.0244	-.202-03
	23.59	23.28	1.66	3.667	.0276	-.241-03
	22.50	22.16	1.74	3.494	.0289	-.264-03
	24.24	23.91	1.66	3.767	.0257	-.256-03
	24.21	23.96	1.56	3.766	.0249	-.217-03
	22.74	22.43	1.62	3.533	.0269	-.194-03
	20.54	20.23	1.93	3.194	.0324	-.202-03
	19.84	19.62	2.06	3.087	.0340	-.171-03
	30.29	30.06	1.13	4.721	.0188	-.186-03
	30.95	30.76	1.06	4.823	.0176	-.148-03
	27.97	27.73	1.26	4.356	.0209	-.186-03
	20.18	20.00	1.77	3.143	.0294	-.140-03
	17.07	16.80	2.52	2.650	.0419	-.210-03
	14.04	13.90	2.93	2.186	.0496	-.109-03
	17.00	16.81	2.40	2.643	.0399	-.148-03
	18.46	18.19	2.26	2.867	.0375	-.202-03
	23.04	22.80	1.50	3.586	.0249	-.186-03
	2.55	2.46	1.00	.392	.0541	-.140-03
	5.58	5.51	2.60	.862	.0871	-.109-03
	12.60	12.43	1.93	1.958	.0651	-.264-03
	13.78	13.73	1.67	2.152	.0822	-.777-04
	14.28	14.18	1.42	2.225	.0538	-.196-03
	8.56	8.43	2.83	1.329	.0944	-.202-03
	13.53	13.42	1.70	2.108	.0365	-.171-03
	5.71	5.59	2.20	.884	.0735	-.186-03
	13.52	13.33	1.86	2.101	.0618	-.295-03
	9.20	9.18	2.20	1.438	.0732	-.311-04
	12.24	12.16	1.93	1.909	.0642	-.124-03
	13.38	13.20	1.73	2.079	.0575	-.280-03
	14.44	14.30	1.54	2.248	.0512	-.217-03
	9.61	9.45	2.05	1.484	.0849	-.186-03
	13.03	12.90	1.84	2.029	.0611	-.202-03
	14.20	14.06	1.57	2.212	.0522	-.186-03
	16.59	16.44	1.41	2.584	.0468	-.233-03
	9.49	9.47	2.13	1.483	.0709	-.311-04

Z DISTANCE 2.169
SCALE FACTOR 3.04

	R1	R2	DELX	R	V PHI	VR
DEL T=3.000						
	9.50	9.73	1.20	1.524	.0404	.362-03
DEL T=8.000						
	19.62	19.62	1.96	3.110	.0247	.000
	20.74	20.76	1.86	3.289	.0235	.118-04
	22.43	22.36	1.70	3.549	.0215	-.472-04
	22.94	22.83	1.67	3.628	.0211	-.649-04
	20.70	20.64	1.87	3.277	.0236	-.354-04
	20.32	20.38	1.83	3.226	.0231	.354-04
	20.03	19.92	2.04	3.167	.0257	-.649-04
	14.05	14.22	2.83	2.241	.0358	.100-03
	22.16	22.08	1.81	3.507	.0228	-.472-04
	23.96	23.83	1.80	3.788	.0202	-.767-04
	20.34	20.30	2.00	3.221	.0252	-.236-04
	19.68	19.60	2.13	3.114	.0269	-.472-04
	18.12	18.18	2.23	2.877	.0281	.354-04
	19.66	19.64	2.08	3.115	.0263	-.118-04
	22.10	22.01	1.78	3.496	.0225	-.531-04
	21.98	21.93	1.87	3.481	.0211	-.295-04
	7.97	8.42	2.83	1.299	.0366	.266-03
	17.62	17.59	2.42	2.783	.0280	.413-04
	2.80	3.16	1.25	.472	.0159	.212-03
	6.60	7.10	2.27	1.086	.0288	.295-03
	12.64	12.85	3.00	2.020	.0379	.124-03
	19.88	19.78	2.08	3.142	.0263	-.708-04
	20.57	20.45	2.00	3.251	.0252	-.708-04
	21.60	21.58	1.80	3.423	.0227	-.118-04
	24.68	24.48	1.53	3.897	.0201	-.118-03
	24.69	24.57	1.61	3.905	.0203	-.766-04
	26.57	26.53	1.32	4.209	.0167	-.236-04
	30.68	30.63	1.10	4.860	.0139	-.295-04
	30.26	30.17	1.12	4.790	.0141	-.531-04
	30.00	29.94	1.08	4.751	.0136	-.354-04
	29.22	29.14	1.20	4.626	.0151	-.472-04
	24.53	24.45	1.54	3.882	.0194	-.472-04
	26.50	26.37	1.38	4.191	.0161	-.767-04
	22.30	22.24	1.81	3.530	.0228	-.354-04
	19.88	19.72	1.93	3.139	.0250	-.944-04
	9.66	10.13	2.94	1.509	.0372	.277-03
	31.20	31.07	1.03	4.936	.0130	-.767-04
	5.39	5.83	1.98	.889	.0251	.260-03
	16.43	16.64	2.12	2.621	.0268	.124-03
	17.07	17.12	2.25	2.710	.0284	.295-04
	20.63	20.63	1.85	3.270	.0233	.000
	20.39	20.41	1.82	3.234	.0230	.118-04
	23.95	23.80	1.62	3.785	.0204	-.885-04
	26.12	26.03	1.37	4.134	.0173	-.531-04
	5.58	6.04	1.87	.921	.0237	.271-03
	15.80	16.03	2.55	2.523	.0322	.136-03
	19.53	19.43	2.10	3.088	.0265	-.590-04
	19.60	19.58	2.02	3.106	.0255	-.118-04

Z DISTANCE 2.892
SCALE FACTOR 3.00

	R1	R2	DELX	R	V PHI	VR
DEL T=8.000						
	11.43	11.95	1.61	1.878	.0206	.311-03
	19.70	19.87	1.52	3.178	.0194	.102-03
	30.38	30.38	1.00	4.881	.0128	.598-05
	24.70	24.77	1.25	3.973	.0160	.419-04
	19.29	19.46	1.52	3.112	.0194	.102-03
	14.17	14.62	1.63	2.312	.0208	.269-03
	14.25	14.69	1.63	2.324	.0208	.263-03
	14.11	14.53	1.65	2.300	.0211	.251-03
	13.47	13.91	1.73	2.199	.0221	.263-03
	8.96	9.57	1.46	1.488	.0187	.365-03
	17.98	18.24	1.43	2.909	.0191	.155-03
	12.84	13.37	1.53	2.105	.0196	.317-03
	18.68	19.00	1.40	3.027	.0179	.191-03
	19.28	19.51	1.45	3.118	.0185	.138-03
	13.15	13.54	1.67	2.144	.0214	.233-03
	17.72	18.00	1.45	2.869	.0185	.167-03
	17.82	18.08	1.50	2.884	.0192	.161-03
	23.93	24.00	1.73	3.850	.0221	.419-04
	30.53	30.53	.96	4.904	.0123	.000
	26.21	26.24	1.11	4.213	.0142	.179-04
	21.86	21.95	1.41	3.519	.0180	.538-04
	23.69	23.80	1.31	3.814	.0167	.658-04
	9.46	10.08	1.63	1.569	.0209	.371-03
	7.90	8.59	1.57	1.324	.0201	.413-03
	8.86	9.37	1.56	1.464	.0200	.305-03
	10.49	11.15	1.62	1.738	.0207	.395-03
	14.07	14.68	1.53	2.301	.0196	.305-03
	19.34	19.63	1.32	3.130	.0169	.173-03
	19.77	20.02	1.37	3.196	.0175	.150-03
	14.11	14.54	1.65	2.301	.0198	.257-03
	20.58	20.69	1.36	3.315	.0174	.658-04
	29.84	29.87	.67	4.796	.0111	.179-04
	4.08	4.58	.77	.696	.0099	.299-03
	14.99	15.31	1.58	2.434	.0202	.191-03
	14.36	14.78	1.57	2.341	.0201	.251-03
	14.19	14.69	1.56	2.320	.0200	.299-03
	14.19	14.61	1.75	2.313	.0225	.251-03
	17.63	17.90	1.56	2.864	.0199	.161-03
	19.90	20.16	1.26	3.218	.0161	.155-03
	20.17	20.39	1.25	3.258	.0173	.132-03
	7.03	7.64	1.32	1.178	.0169	.365-03
	10.46	11.05	1.60	1.728	.0205	.353-03

Z DISTANCE .000
SCALE FACTOR 4.19

RUN 7S

	R1	R2	DELX	R	V PHI	VR
DEL T= .312						
	17.45	17.37	2.75	1.191	.3841	-.148-02
	18.21	18.11	2.51	1.242	.3505	-.185-02
	17.90	17.80	2.63	1.221	.3673	-.185-02
	18.27	18.23	2.46	1.248	.3435	-.739-03
	20.47	20.39	1.78	1.397	.2485	-.148-02
	20.77	20.70	1.63	1.418	.2275	-.129-02
DEL T= .606						
	20.21	20.04	3.53	1.376	.2539	-.162-02
	18.32	18.19	4.77	1.248	.3437	-.124-02
	19.41	19.22	3.92	1.321	.2821	-.181-02
	20.26	20.03	3.44	1.378	.2474	-.219-02
	22.22	21.94	2.72	1.510	.1955	-.266-02
	23.13	22.97	2.28	1.576	.1639	-.152-02
	22.13	21.93	2.56	1.507	.1840	-.190-02
	24.84	24.67	1.93	1.693	.1387	-.162-02
	21.78	21.54	2.90	1.481	.2085	-.228-02
	20.22	20.01	3.62	1.376	.2604	-.200-02
	21.98	21.78	2.93	1.496	.2106	-.190-02
	27.45	27.23	1.68	1.870	.1207	-.209-02
	24.15	23.93	2.20	1.644	.1581	-.209-02
	17.57	17.48	5.76	1.198	.4157	-.856-03
	22.19	21.94	2.78	1.509	.1998	-.238-02
	21.82	21.56	2.94	1.483	.2114	-.247-02
	20.19	20.02	3.49	1.375	.2510	-.162-02
	18.33	18.23	4.72	1.250	.3400	-.951-03
	25.63	25.48	1.78	1.748	.1279	-.143-02
	28.29	28.12	1.42	1.929	.1020	-.162-02
	22.26	22.07	2.61	1.516	.1876	-.181-02
	23.25	23.03	2.36	1.582	.1696	-.209-02
	29.22	29.04	1.34	1.992	.0963	-.171-02
	28.90	28.69	1.40	1.969	.1006	-.200-02
	24.98	24.79	1.96	1.702	.1408	-.181-02
	20.36	20.13	3.43	1.384	.2467	-.219-02
	32.20	32.07	1.03	2.198	.0740	-.124-02
	37.72	37.55	.66	2.574	.0474	-.162-02
DEL T=1.190						
	21.56	21.21	6.18	1.462	.2269	-.169-02
	28.20	27.90	3.02	1.918	.1105	-.145-02
	27.60	27.21	3.20	1.874	.1171	-.189-02
	27.03	26.63	3.44	1.835	.1259	-.194-02
	33.16	32.83	2.12	2.256	.0776	-.160-02
	35.27	34.99	2.78	2.402	.1017	-.136-02
	36.78	36.50	1.63	2.506	.0596	-.136-02

Z DISTANCE .716
SCALE FACTOR 4.30

	R1	R2	DELX	R	V PHI	VR
DEL T= .312						
	15.34	15.19	2.02	1.017	.2749	-.270-02
	18.71	18.62	1.54	1.244	.2094	-.162-02
	13.90	13.78	2.53	.922	.3445	-.216-02
	13.26	13.14	2.94	.880	.4006	-.216-02
	13.91	13.78	2.57	.923	.3499	-.234-02
	13.99	13.86	2.54	.928	.3458	-.234-02
	12.20	12.09	3.94	.809	.5381	-.198-02
	14.03	13.91	2.42	.931	.3295	-.216-02
	13.17	13.04	3.05	.873	.4156	-.234-02
	11.28	11.20	3.88	.749	.5302	-.144-02
DEL T= .606						
	13.58	13.33	5.32	.897	.3749	-.232-02
	15.38	15.13	3.96	1.017	.2780	-.232-02
	25.17	25.04	1.48	1.673	.1036	-.120-02
	22.84	22.73	1.90	1.518	.1330	-.102-02
	21.63	21.45	2.15	1.435	.1506	-.167-02
	23.55	23.42	1.74	1.565	.1218	-.120-02
	20.02	19.83	2.46	1.328	.1723	-.176-02
	18.95	18.74	2.48	1.256	.1737	-.195-02
	21.73	21.55	2.12	1.442	.1485	-.167-02
	16.00	15.76	3.64	1.058	.2554	-.222-02
	15.33	15.06	4.17	1.013	.2928	-.250-02
	16.76	16.54	3.77	1.109	.2645	-.204-02
	23.95	23.81	1.73	1.591	.1211	-.130-02
	22.61	22.43	2.00	1.501	.1401	-.167-02
DEL T=1.190						
	26.17	25.90	2.90	1.735	.1034	-.127-02
	19.20	18.93	5.45	1.270	.1950	-.127-02
	22.34	22.10	3.90	1.481	.1392	-.113-02
	29.27	29.17	2.13	1.947	.0759	-.472-03
	31.89	31.67	1.85	2.118	.0660	-.104-02
	30.24	29.98	2.05	2.006	.0731	-.123-02
	29.94	29.71	2.08	1.987	.0742	-.109-02
	21.71	21.29	4.44	1.433	.1586	-.198-02
	41.72	41.61	.95	2.776	.0339	-.519-03
	22.37	22.04	3.76	1.480	.1342	-.156-02
	25.54	25.27	2.84	1.693	.1013	-.127-02
	22.38	22.04	3.78	1.480	.1349	-.160-02
	35.50	35.27	1.26	2.358	.0449	-.109-02
	37.48	37.28	1.23	2.491	.0438	-.944-03
	33.43	33.22	1.56	2.221	.0556	-.991-03
	34.96	34.75	1.39	2.323	.0496	-.991-03
	20.97	20.69	4.18	1.388	.1493	-.132-02

Z DISTANCE= 1.430
SCALE FACTOR 4.41

	R1	R2	DELX	R	V PHI	VR
DEL T= .606						
	18.86	18.90	1.26	1.227	.0860	.361-03
	18.89	18.91	1.25	1.228	.0853	.181-03
	X 22.12	21.14	1.04	1.405	.0710	X -.885-02
	17.44	17.42	1.62	1.132	.1106	-.181-03
	14.38	14.32	1.54	.932	.1052	-.542-03
	18.04	18.09	1.30	1.174	.0888	.452-03
	19.14	19.10	1.26	1.242	.0860	-.361-03
	19.36	19.35	1.18	1.258	.0806	-.903-04
	13.57	13.53	1.53	.880	.1045	-.361-03
	8.24	8.10	1.63	.531	.1114	-.126-02
	7.13	6.97	1.53	.458	.1046	-.145-02
	19.00	18.97	1.23	1.234	.0840	-.271-03
DEL T=1.190						
	11.99	11.89	3.05	.776	.1063	-.460-03
	10.66	10.57	3.03	.690	.1057	-.414-03
	14.49	14.38	3.35	.938	.1167	-.506-03
	18.90	18.88	2.48	1.227	.0863	-.920-04
	18.73	18.70	2.65	1.216	.0922	-.138-03
	19.90	19.86	2.52	1.292	.0877	-.184-03
	24.80	24.77	1.94	1.610	.0675	-.138-03
	27.43	27.39	1.62	1.781	.0563	-.184-03
	32.15	32.11	1.26	2.088	.0438	-.184-03
	32.76	32.74	1.22	2.128	.0424	-.920-04
	33.09	33.04	1.20	2.148	.0417	-.230-03
	35.75	35.73	1.09	2.322	.0379	-.920-04
	28.55	28.48	1.53	1.853	.0532	-.322-03
	21.38	21.30	2.36	1.387	.0821	-.368-03
	23.62	22.58	2.03	1.501	.0706	-.478-02
	14.13	13.99	3.12	.914	.1087	-.644-03
	9.18	8.99	3.15	.590	.1100	-.874-03
	16.33	16.27	3.06	1.059	.1065	-.276-03
	24.07	24.04	1.89	1.563	.0657	-.138-03
	27.93	27.88	1.56	1.813	.0542	-.230-03
	32.96	32.91	1.14	2.140	.0396	-.230-03
	26.83	26.89	1.66	1.745	.0577	.276-03
	15.10	14.97	3.40	.977	.1184	-.598-03
	20.03	19.98	2.46	1.300	.0856	-.230-03
	21.77	21.73	2.24	1.413	.0779	-.184-03
	26.91	26.85	1.72	1.746	.0598	-.276-03
	32.33	32.30	1.29	2.100	.0448	-.138-03
	17.00	16.94	2.96	1.103	.1030	-.276-03
	21.08	21.07	2.23	1.369	.0775	-.460-04
	24.30	24.30	1.97	1.579	.0685	.000
	35.33	35.31	1.11	2.295	.0386	-.920-04
	18.68	18.65	2.52	1.213	.0877	-.138-03
	28.67	28.65	1.47	1.862	.0511	-.920-04
	30.14	30.15	1.25	1.959	.0435	.460-04
	39.74	39.70	.81	2.581	.0282	-.184-03
	40.72	40.65	.83	2.643	.0289	-.322-03

Z DISTANCE= 2.010
SCALE FACTOR 4.52

	R1	R2	DELX	R	V PHI	VR
DEL T=1.190						
	8.84	9.01	.83	.566	.0282	.763-03
	11.68	11.97	1.00	.750	.0339	.130-02
	21.27	21.53	1.04	1.357	.0353	.117-02
	23.83	24.06	1.10	1.518	.0373	.103-02
	24.62	24.73	1.05	1.564	.0356	.494-03
	19.02	19.26	1.08	1.213	.0366	.108-02
	18.50	18.78	1.12	1.179	.0380	.898-03
	22.51	22.64	1.03	1.431	.0349	.583-03
	5.49	5.70	.70	.355	.0238	.943-03
	10.06	10.37	1.01	.648	.0343	.139-02
	11.55	11.84	1.08	.741	.0366	.130-02
	18.41	18.68	1.18	1.176	.0400	.121-02
	19.64	19.90	1.18	1.253	.0400	.117-02
	21.19	21.40	1.13	1.350	.0383	.943-03
	21.32	21.54	1.06	1.358	.0360	.987-03
	21.79	22.04	1.09	1.389	.0370	.112-02
	21.88	22.13	1.12	1.395	.0380	.112-02
DEL T=3.000						
	6.92	7.43	1.75	.455	.0236	.908-03
	17.27	18.19	2.83	1.124	.0381	.164-02
	19.65	20.49	2.73	1.272	.0368	.150-02
	22.34	23.10	2.68	1.440	.0361	.135-02
	22.28	23.10	2.62	1.438	.0353	.146-02
	17.22	18.05	2.95	1.118	.0397	.148-02
	28.09	28.58	2.11	1.796	.0284	.872-03
	35.49	35.80	1.60	2.260	.0215	.552-03
	22.74	23.36	2.66	1.461	.0358	.110-02
	26.96	27.44	2.20	1.724	.0296	.855-03
	35.07	35.32	1.64	2.231	.0221	.445-03
	19.77	20.34	2.93	1.271	.0395	.101-02
	23.86	24.38	2.76	1.529	.0371	.926-03
	31.33	31.60	1.93	1.995	.0260	.481-03
	20.97	21.42	2.70	1.344	.0363	.801-03
	17.88	18.37	3.17	1.149	.0427	.872-03
	41.86	42.07	1.13	2.660	.0152	.374-03
	21.12	21.94	2.73	1.365	.0367	.146-02
	21.29	23.01	2.53	1.404	.0341	.306-02
	24.58	25.16	2.46	1.577	.0331	.103-02
	27.50	28.04	2.10	1.760	.0283	.961-03
	31.99	32.40	1.78	2.041	.0239	.730-03
	35.68	35.95	1.51	2.270	.0203	.481-03
	23.70	24.26	2.60	1.520	.0350	.997-03
	14.83	15.50	2.84	.961	.0383	.119-02
	18.62	19.22	2.76	1.199	.0372	.107-02
	21.30	21.84	2.52	1.367	.0339	.961-03
	24.34	24.77	2.36	1.557	.0818	.766-03
	12.30	12.97	2.61	.801	.0352	.119-02
	18.74	19.26	2.78	1.204	.0374	.926-03
	22.70	23.06	2.75	1.450	.0370	.641-03
	23.22	23.60	2.43	1.484	.0327	.677-03
	26.14	26.37	2.42	1.664	.0326	.409-03
	27.71	27.96	2.24	1.765	.0301	.445-03
	30.40	30.58	1.90	1.933	.0256	.320-03

Z DISTANCE 2.580
SCALE FACTOR 4.63

	R1	R2	DELX	R	V PHI	VR
DEL T=4.000						
	25.10	26.09	1.72	1.584	.0169	.129-02
	25.47	26.46	1.92	1.607	.0189	.129-02
	26.20	27.08	1.61	1.649	.0159	.115-02
	10.14	11.30	1.53	.663	.0151	.151-02
	12.20	13.39	1.54	.792	.0152	.155-02
	15.03	16.28	1.89	.969	.0186	.163-02
	22.82	23.92	1.78	1.446	.0175	.143-02
	12.17	13.34	1.58	.789	.0156	.153-02
	13.78	14.90	1.62	.887	.0160	.146-02
	16.02	17.12	1.68	1.025	.0166	.143-02
	18.90	19.93	1.64	1.202	.0162	.134-02
	25.10	26.00	1.74	1.581	.0171	.117-02
	25.20	26.09	1.73	1.587	.0170	.116-02
	25.40	26.30	1.58	1.600	.0156	.117-02
	35.08	35.60	1.27	2.187	.0125	.678-03
	27.12	27.98	1.61	1.705	.0159	.112-02
	35.64	36.20	1.23	2.223	.0121	.730-03
	10.15	11.11	1.30	.658	.0128	.125-02
	18.22	19.24	1.80	1.159	.0177	.133-02
	21.00	21.97	1.82	1.330	.0179	.126-02
	22.83	23.77	1.75	1.442	.0172	.123-02
	18.06	19.00	1.83	1.147	.0180	.123-02
	6.22	6.72	1.05	.400	.0104	.652-03
	16.55	17.35	1.87	1.049	.0184	.104-02
	23.43	24.10	1.94	1.471	.0191	.873-03
DEL T=5.000						
	19.90	20.98	2.53	1.265	.0199	.113-02
	20.13	21.22	2.62	1.279	.0207	.114-02
	20.97	22.10	2.43	1.333	.0192	.118-02
	19.42	20.67	2.46	1.241	.0194	.130-02
	17.90	19.33	2.62	1.152	.0207	.149-02
	26.29	27.45	2.10	1.663	.0166	.121-02
	25.87	27.05	2.00	1.638	.0158	.123-02
	10.46	11.71	2.07	.686	.0163	.130-02
	5.65	6.56	1.24	.378	.0098	.949-03
	10.34	11.74	1.68	.683	.0133	.146-02
	10.52	11.91	1.80	.694	.0142	.145-02
	16.21	17.73	2.40	1.050	.0189	.159-02
	17.57	19.00	2.23	1.132	.0176	.149-02
	8.28	9.31	1.04	.544	.0082	.107-02
	11.49	12.86	1.77	.753	.0140	.143-02
	20.60	20.83	2.12	1.282	.0167	.240-03
	24.46	25.64	2.18	1.550	.0172	.123-02
	24.63	25.71	2.13	1.558	.0168	.113-02
	26.95	27.90	2.01	1.697	.0158	.991-03

Z DISTANCE .000
SCALE FACTOR 3.25

RUN 9S

	R1	R2	DELX	R	V PHI	VR
DEL T= .275						
	8.09	8.03	1.76	1.195	.6054	-.907-02
	7.69	7.67	2.00	1.139	.6885	-.302-02
	9.48	9.44	1.26	1.403	.4329	-.605-02
	7.94	7.91	1.78	1.175	.6123	-.454-02
	9.09	9.00	1.28	1.341	.4398	-.136-01
DEL T= .528						
	8.08	7.96	3.61	1.189	.6510	-.945-02
	13.28	13.23	1.12	1.966	.2003	-.394-02
	8.16	8.08	3.36	1.204	.6051	-.630-02
	10.74	10.70	1.93	1.590	.3455	-.315-02
	10.21	10.13	1.95	1.508	.3492	-.630-02
	8.09	8.00	3.40	1.193	.6125	-.709-02
	12.07	11.98	1.38	1.783	.2469	-.709-02
	9.33	9.29	2.36	1.381	.4231	-.315-02
	7.86	7.80	3.58	1.161	.6458	-.473-02
	8.37	8.29	2.88	1.235	.5175	-.630-02
	9.56	9.47	2.20	1.411	.3942	-.709-02
DEL T=1.116						
	16.75	16.64	1.64	2.476	.1388	-.410-02
	10.90	10.68	3.68	1.600	.3128	-.820-02
	14.91	14.79	1.85	2.202	.1566	-.447-02
	15.58	15.52	1.48	2.306	.1252	-.224-02
DEL T=3.000						
	26.38	26.33	1.47	3.908	.0463	-.693-03
	24.24	24.14	1.88	3.587	.0592	-.139-02
	21.60	21.40	2.24	3.188	.0705	-.277-02
	21.38	21.25	1.98	3.161	.0623	-.180-02
	20.84	20.78	2.07	3.086	.0652	-.832-03
	30.53	30.50	1.05	4.525	.0330	-.416-03
	32.00	32.01	.91	4.746	.0286	.139-03
DEL T=5.000						
	24.17	23.93	2.80	3.566	.0529	-.200-02
	23.93	23.70	3.23	3.531	.0610	-.191-02
	22.41	22.13	3.95	3.302	.0747	-.233-02
	20.59	20.32	4.04	3.033	.0764	-.225-02
	32.16	32.15	1.65	4.768	.0312	-.832-04
	32.15	32.15	1.48	4.767	.0279	.000
	18.72	18.52	4.68	2.761	.0886	-.166-02

Z DISTANCE .723
SCALE FACTOR 3.30

	R1	R2	DELX	R	V PHI	VR
DEL T= .275						
	6.79	6.76	1.59	.989	.5388	-.447-02
	7.38	7.38	1.42	1.078	.4808	.000
	5.98	5.95	1.80	.871	.6109	-.447-02
	8.14	8.12	1.18	1.187	.3993	-.298-02
	7.68	7.69	1.48	1.122	.5011	.149-02
DEL T= .528						
	8.47	8.43	1.95	1.234	.3441	-.310-02
	8.50	8.39	2.35	1.233	.4151	-.853-02
	8.39	8.36	2.03	1.223	.3583	-.233-02
	9.58	9.52	1.82	1.395	.3210	-.465-02
	8.36	8.23	2.16	1.211	.3814	-.101-01
	7.56	7.50	2.15	1.100	.3799	-.465-02
	9.00	8.94	1.97	1.310	.3476	-.465-02
	11.47	11.44	1.25	1.673	.2202	-.233-02
	10.80	10.75	1.45	1.574	.2555	-.388-02
	8.33	8.25	2.43	1.211	.4294	-.620-02
	9.77	9.74	1.95	1.425	.3439	-.233-02
	9.30	9.25	2.12	1.355	.3741	-.388-02
	12.13	12.09	1.22	1.769	.2149	-.310-02
	11.86	11.81	1.25	1.728	.2202	-.388-02
DEL T=1.116						
	17.40	17.29	1.41	2.533	.1175	-.404-02
	14.39	14.27	1.82	2.093	.1517	-.440-02
	12.07	11.90	2.48	1.750	.2070	-.624-02
	11.49	11.34	2.75	1.667	.2297	-.550-02
	11.65	11.54	2.51	1.693	.2095	-.404-02
	11.53	11.44	2.60	1.677	.2171	-.330-02
	15.49	15.44	1.48	2.258	.1233	-.183-02
	11.54	11.44	2.60	1.678	.2171	-.367-02
	16.65	16.60	1.37	2.428	.1142	-.183-02
	9.04	8.93	3.83	1.312	.3215	-.404-02
	10.17	10.02	3.58	1.474	.2998	-.550-02
	12.23	12.18	2.43	1.782	.2028	-.183-02
	6.59	6.43	7.10	.951	.6256	-.587-02
	15.14	15.00	1.89	2.201	.1576	-.514-02
	18.06	17.91	1.33	2.627	.1108	-.550-02
	15.38	15.22	1.63	2.234	.1359	-.587-02
DEL T=3.000						
	23.24	23.18	2.00	3.390	.0620	-.819-03
	22.83	22.73	2.00	3.327	.0620	-.137-02
	16.93	16.68	3.72	2.454	.1155	-.341-02
	21.13	20.96	2.52	3.073	.0781	-.232-02
	12.20	11.91	6.00	1.760	.1879	-.396-02
	26.42	26.31	1.46	3.850	.0453	-.150-02
	18.67	18.40	4.41	2.707	.0822	-.221-02
	22.83	22.70	3.30	3.325	.0614	-.106-02
	16.17	15.87	5.98	2.340	.1118	-.246-02
	20.54	20.19	4.17	2.974	.0777	-.287-02
	31.59	31.36	1.58	4.597	.0294	-.188-02

Z DISTANCE 1.446
SCALE FACTOR 3.38

	R1	R2	DELX	R	V PHI	VR
DEL T=1.116						
	5.56	5.60	1.72	.796	.1405	.143-02
	10.84	10.85	1.64	1.546	.1335	.358-03
	13.82	13.81	1.38	1.970	.1123	-.358-03
	17.48	17.44	1.10	2.489	.0895	-.143-02
	5.73	5.74	2.21	.818	.1809	.358-03
	8.77	8.67	2.02	1.243	.1647	-.358-02
	14.00	13.99	1.34	1.995	.1090	-.358-03
	16.69	16.64	1.11	2.376	.0903	-.179-02
DEL T=3.000						
	8.89	8.76	5.20	1.258	.1597	-.173-02
	27.13	27.17	1.45	3.871	.0439	.533-03
	26.87	26.86	1.45	3.830	.0439	-.133-03
	24.13	24.04	1.78	3.434	.0539	-.120-02
	16.05	16.06	3.20	2.289	.0970	.133-03
	14.73	14.70	3.74	2.098	.1135	-.400-03
	24.96	24.98	1.63	3.560	.0493	.267-03
	27.02	27.00	1.45	3.851	.0439	-.267-03
	30.35	30.28	1.09	4.322	.0330	-.933-03
	33.29	33.21	.93	4.741	.0281	-.107-02
DEL T=5.000						
	15.93	15.91	5.02	2.270	.0915	-.160-03
	19.20	19.18	3.46	2.736	.0629	-.160-03
	27.31	27.33	2.18	3.895	.0396	.160-03
	29.07	29.05	1.93	4.143	.0350	-.160-03
	33.59	33.48	1.49	4.781	.0271	-.880-03
	31.67	31.50	1.70	4.503	.0309	-.136-02
	15.03	14.89	5.66	2.133	.1034	-.112-02
	14.50	14.44	5.65	2.063	.1032	-.480-03
	15.74	15.64	5.17	2.237	.0943	-.800-03
	18.96	18.94	3.25	2.702	.0591	-.160-03
	27.24	27.22	2.27	3.883	.0412	-.160-03

Z DISTANCE 2.169
SCALE FACTOR 3.21

	R1	R2	DELX	R	V PHI	VR
DEL T=3.000						
	11.70	11.85	1.75	1.768	.0558	.211-02
	14.52	14.61	1.92	2.187	.0612	.126-02
	14.90	15.04	1.73	2.247	.0551	.196-02
	16.09	16.23	1.75	2.426	.0558	.196-02
	10.58	10.70	2.26	1.597	.0721	.168-02
	6.54	6.77	1.96	.999	.0627	.323-02
	14.18	14.24	2.17	2.133	.0692	.842-03
	14.85	14.95	1.79	2.237	.0571	.140-02
	3.22	3.41	1.24	.498	.0397	.267-02
	18.24	18.30	1.62	2.743	.0516	.842-03
	20.83	20.89	1.38	3.132	.0440	.842-03
	14.92	15.02	1.91	2.247	.0609	.140-02
	15.41	15.55	1.65	2.324	.0526	.196-02
	16.52	16.58	1.56	2.485	.0497	.842-03
	14.57	14.61	1.92	2.190	.0612	.561-03
	15.21	15.32	1.75	2.292	.0558	.154-02
	3.93	4.10	1.25	.603	.0400	.239-02
	16.60	16.64	1.64	2.495	.0523	.561-03
	18.40	18.44	1.65	2.765	.0526	.561-03
	20.94	20.96	1.20	3.145	.0382	.281-03
	15.36	15.50	1.80	2.317	.0574	.196-02
	2.46	2.50	1.05	.372	.0337	.561-03
DEL T=5.000						
	23.76	23.80	1.94	3.570	.0371	.337-03
	21.69	21.79	2.25	3.264	.0430	.842-03
	19.46	19.57	2.50	2.930	.0478	.926-03
	17.89	17.97	2.54	2.692	.0486	.674-03
	13.12	13.23	3.70	1.978	.0710	.926-03
	35.23	35.25	.98	5.291	.0187	.168-03
	4.92	5.25	3.06	.763	.0594	.278-02
	14.26	14.39	2.88	2.151	.0551	.109-02
	17.31	17.46	2.66	2.610	.0509	.126-02
	19.02	19.16	2.68	2.866	.0513	.118-02
	21.43	21.53	2.32	3.225	.0444	.842-03
	23.55	23.58	2.03	3.538	.0388	.253-03
	28.22	28.31	1.60	4.244	.0306	.758-03
	22.23	22.25	2.14	3.339	.0409	.168-03
	3.64	3.82	3.03	.560	.0596	.152-02

Z DISTANCE 2.892
SCALE FACTOR 3.43

	R1	R2	DELX	R	V PHI	VR
DEL T=5.000						
	5.28	5.49	1.33	.757	.0239	.165-02
	16.37	16.60	1.90	2.316	.0340	.181-02
	20.03	20.19	1.72	2.826	.0308	.126-02
	23.29	23.42	1.52	3.281	.0272	.102-02
	22.85	22.97	1.72	3.219	.0308	.946-03
	16.41	16.66	2.02	2.323	.0362	.197-02
	16.32	16.58	1.98	2.311	.0354	.205-02
	18.11	18.33	1.90	2.560	.0340	.173-02
	4.52	4.72	1.24	.649	.0223	.158-02
	19.53	19.71	1.86	2.757	.0333	.142-02
	23.03	23.13	1.52	3.243	.0272	.788-03
	22.57	22.66	1.94	3.177	.0347	.709-03
	26.69	26.73	1.47	3.753	.0263	.315-03
	11.11	11.37	1.92	1.579	.0344	.205-02
	10.94	11.00	1.86	1.541	.0333	.473-03
	5.72	6.00	1.28	.823	.0229	.221-02
	26.97	27.02	1.38	3.793	.0247	.394-03
DEL T=6.000						
	12.96	13.33	2.55	1.847	.0381	.243-02
	15.33	15.65	2.30	2.176	.0343	.210-02
	24.90	25.06	1.69	3.510	.0252	.105-02
	28.31	28.42	1.20	3.985	.0179	.722-03
	28.31	28.42	1.36	3.985	.0203	.722-03
	27.94	28.07	1.47	3.935	.0219	.854-03
	27.57	27.64	1.61	3.879	.0240	.460-03
	21.18	21.42	1.86	2.993	.0277	.158-02
	23.87	24.11	1.90	3.371	.0283	.158-02
	27.29	27.44	1.64	3.845	.0245	.985-03
	17.39	17.68	2.23	2.464	.0333	.190-02
	17.93	18.21	2.15	2.539	.0321	.184-02
	30.28	30.35	1.44	4.259	.0215	.460-03
	24.36	24.52	1.84	3.434	.0274	.105-02
	27.87	28.02	1.61	3.926	.0240	.985-03
	27.62	27.77	1.55	3.891	.0231	.985-03
	18.17	18.45	2.20	2.573	.0328	.184-02
	27.71	27.74	1.50	3.895	.0224	.197-03
	30.47	30.53	1.31	4.285	.0195	.394-03

RUN NUMBER 700

SCALE FACTOR 3.43
Z DISTANCE .000

RUN 7D

R1	R2	DELX	R	V THETA	VR
DELTA T .312 SEC					
13.240	13.010	1.970	1.0902	.3342	-.005218
13.680	13.450	1.630	1.1267	.2764	-.005218
12.630	12.430	2.250	1.0408	.3818	-.004538
12.670	12.360	2.060	1.0395	.3495	-.007033
14.290	14.070	1.220	1.1778	.2068	-.004991
12.900	12.690	1.940	1.0628	.3291	-.004764
DELTA T .606 SEC					
12.400	12.190	2.770	1.0212	.2422	-.002453
13.300	13.190	1.680	1.1001	.1467	-.001285
16.060	15.650	1.730	1.3169	.1510	-.004789
14.050	13.680	2.930	1.1516	.2561	-.004322
17.860	17.560	1.360	1.4710	.1187	-.003504
13.560	13.130	3.300	1.1085	.2887	-.005023
14.070	13.700	2.520	1.1533	.2202	-.004322
13.360	12.940	3.120	1.0923	.2729	-.004906
16.290	15.930	1.490	1.3381	.1301	-.004205
DELTA T 1.190 SEC					
12.870	12.470	4.820	1.0524	.2155	-.002379
13.080	12.710	3.930	1.0711	.1753	-.002201
19.250	18.900	1.030	1.5844	.0458	-.002082
21.580	21.100	1.560	1.7725	.0693	-.002855
18.140	17.510	2.230	1.4806	.0992	-.003747
DELTA T 2.000 SEC					
16.420	15.090	5.870	1.3086	.1561	-.004707
26.960	26.510	1.490	2.2206	.0394	-.001593
23.410	22.720	2.260	1.9158	.0598	-.002442
26.730	26.250	1.700	2.2003	.0450	-.001699
32.080	31.700	1.130	2.6488	.0299	-.001345
36.920	36.720	.750	3.0583	.0198	-.000708

RUN NUMBER 701

SCALE FACTOR 3.68
Z DISTANCE .283

R1	R2	DELX	R	V THETA	VR
DELTA T .312 SEC					
12.450	12.220	1.330	.9550	.2102	-.004864
14.970	14.720	1.030	1.1493	.1627	-.005287
4.950	4.760	1.260	.3759	.1996	-.004018
1.470	1.420	.650	.1119	.1036	-.001057
6.620	6.430	1.240	.5052	.1962	-.004018
11.550	11.300	1.770	.8845	.2799	-.005287
13.380	13.130	1.340	1.0262	.2118	-.005287
12.660	12.430	1.710	.9712	.2703	-.004864
4.400	4.200	1.080	.3329	.1711	-.004229
DELTA T .606 SEC					
14.320	13.980	1.980	1.0955	.1612	-.003702
14.750	14.400	1.920	1.1284	.1563	-.003811
6.520	6.150	2.920	.4904	.2396	-.004028
16.860	16.520	1.430	1.2921	.1163	-.003702
17.530	17.170	1.250	1.3432	.1017	-.003919
3.500	3.260	1.740	.2617	.1431	-.002613
12.420	12.020	2.980	.9461	.2430	-.004355
12.980	12.670	2.400	.9929	.1955	-.003375
15.290	14.880	2.070	1.1679	.1685	-.004464
13.300	12.920	2.570	1.0150	.2094	-.004137
15.290	14.880	2.070	1.1679	.1685	-.004464
13.300	12.920	2.570	1.0150	.2094	-.004137
14.010	13.620	2.090	1.0695	.1701	-.004246
13.530	13.200	2.300	1.0347	.1873	-.003593
14.340	14.040	1.850	1.0986	.1506	-.003266
12.270	11.820	3.110	.9325	.2536	-.004899
9.930	9.540	3.000	.7537	.2450	-.004246
16.300	15.960	1.580	1.2488	.1286	-.003702
10.310	9.850	3.180	.7804	.2597	-.005008
15.040	14.650	2.170	1.1493	.1766	-.004246
9.200	8.720	3.830	.6937	.3139	-.005226
15.620	15.230	2.010	1.1942	.1636	-.004246
12.930	12.490	2.800	.9840	.2282	-.004790
DELTA T 1.190 SEC					
25.080	24.700	1.150	1.9269	.0476	-.002107
15.090	14.300	4.000	1.1377	.1662	-.004380
17.810	17.190	2.480	1.3548	.1028	-.003437
17.230	16.680	2.700	1.3126	.1119	-.003049
18.910	18.390	2.180	1.4439	.0903	-.002883
20.040	19.550	1.910	1.5325	.0791	-.002717
17.430	16.830	2.730	1.3262	.1132	-.003327
17.400	16.800	2.730	1.3239	.1132	-.003327
DELTA T 2.000 SEC					
29.060	25.540	1.380	2.1135	.0340	-.011612
25.270	24.640	2.000	1.9320	.0493	-.002078
30.210	29.800	1.340	2.3229	.0330	-.001353
30.400	29.980	1.340	2.3373	.0330	-.001386
34.390	34.090	1.060	2.6508	.0261	-.000990
38.740	38.620	.780	2.9945	.0192	-.000396

RUN NUMBER 702

SCALE FACTOR 3.58
Z DISTANCE .566

I R1	I R2	I DELX	I R	I V THETA	I VR I
DELTA T .606 SEC					
11.620	11.490	1.260	.9196	.1054	-.001455
8.420	8.330	1.400	.6665	.1172	-.001007
7.330	7.280	1.300	.5813	.1088	-.000560
16.240	16.150	.960	1.2888	.0803	-.001007
5.130	5.110	.990	.4075	.0829	-.000224
13.850	13.710	1.170	1.0966	.0978	-.001567
11.100	10.970	1.280	.8782	.1071	-.001455
11.030	10.890	1.340	.8722	.1121	-.001567
DELTA T 1.190 SEC					
18.300	18.000	1.810	1.4444	.0771	-.001710
15.390	15.000	2.100	1.2092	.0895	-.002223
15.640	15.210	2.160	1.2275	.0920	-.002451
14.190	13.880	2.280	1.1169	.0972	-.001767
17.850	17.560	1.530	1.4090	.0652	-.001653
19.500	19.210	1.400	1.5403	.0596	-.001653
11.950	11.740	2.630	.9426	.1122	-.001197
14.370	14.400	2.470	1.1448	.1053	.000171
17.010	16.740	1.850	1.3429	.0788	-.001539
20.770	20.540	1.250	1.6437	.0532	-.001311
21.650	21.330	1.320	1.7102	.0562	-.001824
22.030	21.790	1.200	1.7436	.0511	-.001368
6.490	6.330	2.210	.5101	.0946	-.000912
10.820	10.500	3.000	.8483	.1281	-.001824
13.900	13.700	2.150	1.0982	.0916	-.001140
DELTA T 3.000 SEC					
26.280	25.080	2.340	2.0675	.0395	-.001356
18.630	17.800	4.320	1.4496	.0731	-.001876
22.630	21.880	3.060	1.7711	.0517	-.001695
25.420	24.820	2.360	1.9991	.0399	-.001356
27.100	26.540	2.130	2.1344	.0360	-.001266
29.890	29.400	1.760	2.3592	.0297	-.001108
38.210	37.870	.980	3.0273	.0166	-.000769
3.820	3.520	3.780	.2921	.0671	-.000678
19.010	18.270	4.230	1.4834	.0716	-.001673
20.440	19.660	3.740	1.5956	.0633	-.001763
25.400	24.760	2.420	1.9959	.0409	-.001447
25.180	24.430	2.540	1.9740	.0429	-.001695
18.050	17.560	4.050	1.4169	.0685	-.001108
20.660	20.000	3.320	1.6179	.0561	-.001492
26.160	25.650	2.190	2.0615	.0370	-.001153
35.240	34.830	1.160	2.7881	.0196	-.000927
35.000	34.600	1.260	2.7694	.0213	-.000904

RUN NUMBER 703

SCALE FACTOR 3.56
Z DISTANCE 1.132

I R1 I	R2 I	DELX I	R I	V THETA I	VR I
DELTA T 1.190 SEC					
13.780	13.790	1.030	1.1032	.0441	.000057
12.170	12.410	1.060	.9835	.0454	.001375
10.950	11.220	.980	.8871	.0420	.001547
11.160	11.440	1.060	.9043	.0454	.001605
11.160	11.440	1.060	.9043	.0454	.001605
10.360	10.600	.850	.8387	.0364	.001375
9.560	9.800	.840	.7747	.0360	.001375
12.490	12.700	.970	1.0080	.0415	.001204
15.420	15.500	.960	1.2372	.0411	.000458
6.940	7.100	1.000	.5618	.0428	.000917
DELTA T 3.000 SEC					
5.930	6.330	1.500	.4906	.0255	.000909
7.180	7.670	1.640	.5942	.0279	.001114
9.030	9.570	1.790	.7443	.0304	.001228
10.370	10.920	2.020	.8519	.0344	.001250
12.500	13.000	2.250	1.0204	.0383	.001137
16.200	16.560	2.050	1.3109	.0348	.000818
16.650	16.890	2.190	1.3421	.0372	.000546
19.490	19.700	1.800	1.5682	.0306	.000477
26.900	26.860	1.340	2.1512	.0228	-.000091
29.240	29.120	1.180	2.3352	.0200	-.000273
16.900	17.190	1.940	1.3641	.0330	.000659
26.660	26.670	1.310	2.1340	.0222	.000023
21.040	21.180	1.720	1.6894	.0292	.000318
26.130	26.070	1.450	2.0887	.0246	-.000136
28.380	28.360	1.280	2.2704	.0217	-.000045
17.590	17.890	2.420	1.4197	.0411	.000682
20.040	20.190	2.180	1.6098	.0370	.000341
22.500	22.510	1.950	1.8010	.0331	.000023
17.800	18.050	2.230	1.4345	.0379	.000568
22.000	22.040	1.840	1.7622	.0313	.000091
24.800	24.850	1.550	1.9867	.0263	.000114
11.230	11.760	2.380	.9199	.0405	.001205
17.580	17.870	2.140	1.4185	.0364	.000659
22.240	22.450	1.660	1.7882	.0282	.000479
14.200	14.710	2.350	1.1568	.0400	.001159
18.070	18.340	2.060	1.4569	.0350	.000614
18.860	19.020	2.010	1.5157	.0342	.000364
26.720	26.660	1.350	2.1360	.0229	-.000136
26.840	26.890	1.500	2.1500	.0255	-.000114
29.710	29.690	1.180	2.3768	.0200	-.000045
36.730	36.580	.800	2.9334	.0136	-.000341
26.500	26.460	1.450	2.1191	.0246	-.000091
15.920	16.240	2.130	1.2869	.0362	.000727
				.0362	.000727

RUN NUMBER 704

SCALE FACTOR 3.53
Z DISTANCE 1.698

R1	R2	DELX	R	V THETA	VR
DELTA T 3.000 SEC					
18.440	19.000	1.060	1.5109	.0182	.001284
12.810	13.500	.990	1.0617	.0170	.001582
9.870	10.470	.900	.8208	.0154	.001376
10.340	11.000	.980	.8612	.0168	.001513
8.170	8.690	.800	.6804	.0137	.001192
13.130	13.690	1.060	1.0823	.0182	.001284
21.350	21.780	1.150	1.7405	.0197	.000986
24.530	24.830	1.100	1.9919	.0188	.000688
18.960	19.480	1.100	1.5512	.0188	.001192
16.580	17.160	1.100	1.3615	.0188	.001330
DELTA T 5.000 SEC					
16.510	17.460	1.810	1.3708	.0186	.001307
17.240	18.120	1.730	1.4269	.0178	.001211
19.410	20.190	1.660	1.5980	.0171	.001073
21.880	22.540	1.640	1.7925	.0169	.000908
25.000	25.510	1.450	2.0383	.0149	.000702
25.480	25.930	1.480	2.0746	.0152	.000619
34.770	34.860	1.020	2.8099	.0105	.000124
31.750	32.030	1.230	2.5738	.0126	.000385
17.580	18.520	1.770	1.4568	.0182	.001293
19.760	20.600	1.620	1.6287	.0167	.001156
38.300	38.500	.780	3.0992	.0080	.000275
18.130	19.120	1.820	1.5032	.0187	.001362
24.240	24.880	1.680	1.9822	.0173	.000880
32.640	32.910	1.190	2.6452	.0122	.000371
33.200	33.460	1.280	2.6900	.0132	.000358
21.200	21.970	1.610	1.7421	.0165	.001059
17.890	18.800	1.750	1.4806	.0180	.001252
18.110	18.990	1.650	1.4971	.0170	.001211
19.710	20.500	1.770	1.6226	.0182	.001087
22.490	23.150	1.580	1.8418	.0162	.000908
27.000	27.380	1.300	2.1945	.0134	.000523
18.890	19.710	1.540	1.5577	.0158	.001128
13.750	14.670	1.680	1.1469	.0173	.001266
20.720	21.430	1.740	1.7009	.0179	.000977
14.730	15.600	1.730	1.2239	.0178	.001197
20.690	21.360	1.730	1.6969	.0178	.000922
21.180	21.950	1.700	1.7405	.0175	.001059
20.950	21.670	1.810	1.7199	.0186	.000990
24.000	24.500	1.750	1.9572	.0180	.000688
22.860	23.460	1.630	1.8692	.0168	.000825
23.240	23.780	1.560	1.8975	.0160	.000743
22.600	23.180	1.510	1.8474	.0155	.000798
14.560	15.530	1.730	1.2143	.0178	.001334
17.340	18.220	1.650	1.4350	.0170	.001211

RUN NUMBER 705

SCALE FACTOR 3.50
Z DISTANCE 2.264

I R1 I	R2 I	DELX I	R I	V THETA I	VR I
DELTA T 5.000 SEC					
16.790	17.610	.910	1.4001	.0094	.001138
14.250	15.010	.830	1.1909	.0086	.001054
21.120	21.740	.950	1.7444	.0098	.000860
13.060	13.800	.870	1.0932	.0090	.001027
9.920	10.670	.660	.8380	.0068	.001041
16.170	17.000	.990	1.3500	.0103	.001152
16.160	16.960	.910	1.3480	.0094	.001110
16.170	16.940	.910	1.3476	.0094	.001068
17.450	18.380	.890	1.4583	.0092	.001290
23.180	23.890	.920	1.9158	.0095	.000985
26.590	27.200	.980	2.1893	.0102	.000846
29.240	29.760	.800	2.4013	.0083	.000721
28.300	28.840	.780	2.3256	.0081	.000749
28.950	29.500	.860	2.3789	.0089	.000763
20.190	20.950	.920	1.6744	.0095	.001054
17.980	18.780	.860	1.4961	.0089	.001110
25.530	26.170	.910	2.1042	.0094	.000888
26.320	26.920	.800	2.1669	.0083	.000832
22.340	23.080	.930	1.8486	.0096	.001027
23.370	24.050	.850	1.9300	.0088	.000943
23.030	23.700	.800	1.9019	.0083	.000930
28.610	29.100	.800	2.3488	.0083	.000680
30.380	30.840	.740	2.4917	.0077	.000638
33.600	34.090	.530	2.7550	.0055	.000680
18.690	19.370	.870	1.5490	.0090	.000943
23.270	23.820	.870	1.9166	.0090	.000763
16.500	17.250	.930	1.3736	.0096	.001041
17.840	18.620	.960	1.4839	.0100	.001082
15.420	16.210	.880	1.2873	.0091	.001096
15.300	16.100	.840	1.2780	.0087	.001110
9.400	10.100	.600	.7937	.0062	.000971
6.240	6.750	.390	.5287	.0040	.000708
18.880	19.690	.870	1.5698	.0090	.001124
18.900	19.670	.870	1.5698	.0090	.001068
19.140	19.880	.830	1.5881	.0086	.001027
22.100	22.800	.890	1.8274	.0092	.000971
14.440	15.240	.830	1.2080	.0086	.001110
25.620	26.120	.790	2.1058	.0082	.000694
7.120	7.590	.400	.5987	.0041	.000652
21.560	22.250	.920	1.7831	.0095	.000957
31.260	31.670	.760	2.5613	.0079	.000569
34.540	34.300	.640	2.8018	.0066	-.000333

Z DISTANCE .000
SCALE FACTOR 2.72

RUN 16D

	R1	R2	DELX	R	V PHI	VR
DEL T= .528						
	6.73	6.61	1.62	1.182	.3469	-.113-01
	6.50	6.39	1.88	1.142	.4031	-.104-01
DEL T=1.116						
	7.62	7.40	2.31	1.331	.2344	-.979-02
	9.26	9.11	1.46	1.627	.1477	-.668-02
	7.99	7.80	2.08	1.399	.2108	-.846-02
	7.68	7.43	2.42	1.339	.2457	-.111-01
DEL T=3.000						
	11.24	10.95	2.26	1.966	.0851	-.480-02
	15.05	14.89	1.37	2.652	.0515	-.265-02
	12.37	12.10	2.05	2.168	.0772	-.447-02
	14.26	14.12	1.55	2.514	.0583	-.232-02
	12.98	12.79	1.68	2.283	.0632	-.315-02
	12.58	12.33	1.87	2.207	.0704	-.414-02
	13.66	13.43	1.60	2.400	.0602	-.381-02
	13.94	13.73	1.62	2.451	.0609	-.348-02
	12.72	12.48	1.93	2.232	.0723	-.397-02
	15.60	15.45	1.28	2.751	.0481	-.248-02
	14.43	14.27	1.47	2.543	.0553	-.265-02
DEL T=6.000						
	16.83	16.71	2.00	2.971	.0376	-.994-03
	12.46	11.95	4.13	2.162	.0780	-.422-02
	13.79	13.43	3.10	2.411	.0584	-.298-02
	14.40	14.03	3.00	2.519	.0565	-.306-02
	15.32	15.00	2.58	2.686	.0486	-.265-02
	14.48	14.13	3.04	2.535	.0573	-.290-02
	14.69	14.37	2.85	2.574	.0537	-.265-02
	15.40	15.09	2.71	2.701	.0510	-.257-02
	18.90	18.72	1.78	3.333	.0335	-.149-02
	19.95	19.82	1.60	3.523	.0301	-.108-02
	22.06	21.90	1.22	3.894	.0229	-.132-02
	20.67	20.52	1.45	3.649	.0273	-.124-02
	21.52	21.44	1.35	3.806	.0254	-.662-03
	22.93	22.81	1.20	4.052	.0226	-.994-03
	25.23	25.12	.97	4.460	.0182	-.911-03
	10.07	9.49	6.13	1.733	.1172	-.480-02
	14.98	14.85	2.88	2.623	.0505	-.257-02
	14.55	14.24	2.78	2.550	.0523	-.257-02
	17.54	17.31	1.95	3.087	.0367	-.190-02
	17.57	17.39	1.89	3.097	.0355	-.149-02
	20.21	20.06	1.43	3.568	.0269	-.124-02
	21.58	21.43	1.27	3.810	.0239	-.124-02
	22.58	22.47	1.16	3.991	.0218	-.911-03
	25.60	25.52	.95	4.529	.0179	-.662-03
	18.51	18.39	1.73	3.269	.0325	-.994-03
	19.91	19.81	1.54	3.519	.0290	-.828-03
	19.68	19.54	1.92	3.474	.0286	-.116-02
	19.64	19.56	1.47	3.473	.0276	-.662-03

Z DISTANCE .964
SCALE FACTOR 2.66

	R1	R2	DELX	R	V PHI	VR
DEL T=1.116						
	6.58	6.54	1.27	1.189	.1315	-.182-02
	6.28	6.24	1.03	1.134	.1066	-.182-02
	6.18	6.18	1.01	1.120	.1045	.000
	3.27	3.27	1.11	.592	.1156	.000
	3.25	3.23	1.10	.587	.1142	-.911-03
	7.25	7.21	.95	1.310	.0983	-.182-02
DEL T=3.000						
	10.43	10.32	1.80	1.880	.0693	-.186-02
	10.15	10.01	1.97	1.826	.0759	-.237-02
	10.50	10.43	1.67	1.896	.0643	-.119-02
	12.81	12.69	1.34	2.310	.0515	-.203-02
	15.20	15.13	1.02	2.748	.0392	-.119-02
	8.15	8.01	2.60	1.464	.1004	-.237-02
	9.17	9.06	2.15	1.651	.0829	-.186-02
	12.23	12.08	1.41	2.202	.0542	-.254-02
	12.84	12.74	1.25	2.317	.0481	-.169-02
	12.02	11.94	1.43	2.170	.0550	-.135-02
	7.59	7.43	2.43	1.361	.0938	-.271-02
DEL T=6.000						
	13.55	13.32	2.37	2.434	.0456	-.195-02
	15.60	15.44	1.82	2.812	.0350	-.135-02
	19.40	19.24	1.33	3.500	.0256	-.135-02
	17.01	16.89	1.58	3.071	.0304	-.102-02
	24.92	24.88	.70	4.511	.0135	-.339-03
	15.22	15.02	1.99	2.739	.0381	-.169-02
	21.54	21.42	1.02	3.892	.0196	-.102-02
	22.20	22.10	.95	4.013	.0183	-.847-03
	19.50	19.39	1.14	3.523	.0219	-.931-03
	20.11	20.01	1.17	3.634	.0225	-.847-03
	13.63	13.34	2.43	2.443	.0468	-.246-02
	12.50	12.37	2.49	2.253	.0479	-.110-02
	12.69	12.47	2.56	2.279	.0493	-.186-02
	20.95	20.89	1.04	3.790	.0200	-.508-03
	19.07	18.99	1.17	3.448	.0225	-.677-03
	24.84	24.82	.75	4.499	.0144	-.169-03
	23.43	23.38	.97	4.240	.0186	-.423-03
	19.21	19.07	1.19	3.468	.0229	-.119-02
	19.86	19.73	1.28	3.586	.0246	-.110-02
	20.26	20.17	1.18	3.662	.0227	-.762-03
	14.70	14.49	2.07	2.644	.0398	-.178-02

Z DISTANCE 2.410
SCALE FACTOR 2.60

DEL T=10,0 sec

R1	R2	DELX	R	V PHI	VR
9.04	9.40	2.13	1.709	.0252	.187-02
13.24	13.44	1.92	2.473	.0227	.104-02
14.60	14.78	1.77	2.723	.0209	.936-03
17.08	17.13	1.73	3.171	.0204	.260-03
18.11	18.21	1.67	3.366	.0197	.520-03
19.16	16.26	1.53	3.283	.0181	-.151-01
21.12	21.17	1.45	3.919	.0171	.260-03
21.58	21.71	1.32	4.012	.0156	.676-03
15.60	15.79	1.80	2.909	.0213	.988-03
14.12	14.35	1.95	2.639	.0230	.120-02
10.54	11.00	2.13	1.996	.0252	.239-02
16.90	16.94	1.47	3.136	.0174	.208-03
21.03	21.07	1.22	3.902	.0144	.208-03
14.94	15.10	1.61	2.784	.0190	.832-03
20.43	20.44	1.44	3.788	.0170	.520-04
17.16	17.21	1.76	3.185	.0208	.260-03
19.30	19.42	1.57	3.589	.0185	.624-03
18.29	18.42	1.64	3.402	.0194	.676-03
20.56	20.66	1.35	3.820	.0159	.520-03
15.92	15.08	1.83	2.873	.0216	-.437-02
14.52	14.67	1.93	2.705	.0228	.780-03
11.32	11.72	2.00	2.135	.0236	.208-02
9.44	9.85	1.96	1.788	.0232	.213-02
21.38	21.41	1.22	3.966	.0144	.156-03
16.77	16.82	1.40	3.113	.0165	.260-03
13.57	13.75	1.60	2.532	.0189	.936-03
18.85	18.89	1.35	3.498	.0159	.208-03
20.84	20.88	1.17	3.867	.0138	.208-03
6.37	6.84	1.44	1.224	.0170	.244-02
7.84	8.31	1.72	1.497	.0203	.244-02
10.00	10.42	1.78	1.892	.0210	.218-02
10.51	10.94	1.80	1.988	.0213	.224-02
13.64	13.87	1.54	2.550	.0182	.120-02
18.64	18.77	1.32	3.467	.0156	.676-03
21.27	21.40	1.12	3.958	.0132	.676-03
21.41	21.42	.96	3.969	.0113	.520-04
21.19	21.26	.97	3.934	.0114	.364-03
21.19	21.26	.97	3.934	.0114	.364-03
22.88	22.88	.92	4.241	.0109	.000
14.31	14.33	1.51	2.654	.0178	.104-03
12.84	13.02	1.70	2.397	.0201	.936-03

S = 0